1997

THE INTEGRATION OF CLOUD SATELLITE IMAGES WITH PREDICTION OF ICY CONDITIONS ON DEVON'S ROADS

CLARK, ROBIN TRISTAN

http://hdl.handle.net/10026.1/1844

http://dx.doi.org/10.24382/1362
University of Plymouth

THE INTEGRATION OF CLOUD SATELLITE IMAGES WITH PREDICTION OF ICY CONDITIONS ON DEVON'S ROADS

by

ROBIN TRISTAN CLARK

A thesis submitted to the University of Plymouth
in partial fulfilment for the degree of

DOCTOR OF PHILOSOPHY

Institute of Marine Studies
Faculty of Science

In collaboration with
Devon County Council

October 1997

THE INTEGRATION OF CLOUD SATELLITE IMAGES WITH PREDICTION OF ICY CONDITIONS ON DEVON'S ROADS

Robin Clark BSc. (Hons)

Abstract

The need for improved cloud parameterisations in a road surface temperature model is demonstrated.

Case studies from early 1994 are used to investigate methods of tracking cloud cover using satellite imagery and upper level geostrophic flow. Two of these studies are included in this thesis. Errors encountered in cloud tracking methods were investigated as well as relationships between cloud height and pixel brightness in satellite imagery.

For the first time, a one dimensional energy balance model is developed to investigate the effects of erroneous cloud forecasts on surface temperature. The model is used to determine detailed dependency of surface freezing onset time and minimum temperature on cloud cover.

Case studies from the 1995/96 winter in Devon are undertaken to determine effects of differing scenarios of cloud cover change. From each study, an algorithm for predicting road surface temperature is constructed which could be used in future occurrences of the corresponding scenario of the case study. Emphasis is strongly placed on accuracy of predictions of surface freezing onset time and minimum surface temperature.

The role of surface and upper level geostrophic flow, humidity and surface wetness in temperature prediction is also investigated. In selected case studies, mesoscale data are also analysed and compared with observations to determine feasibility of using mesoscale models to predict air temperature.

Finally, the algorithms constructed from the 1995/96 studies are tested using case studies from the 1996/97 winter. This winter was significantly different from its preceding one which consequently meant that the algorithm from only one scenario of the 1995/96 winter could be tested. An algorithm is also constructed from a 1996/97 winter case study involving a completely different scenario.

Recommendations for future research suggest testing of existing algorithms with guidance on additional scenarios.

Contents

List of tables:-

List of figures:-

ACKNOWLEDGEMENTS

I gratefully acknowledge Devon County Council's Environment Department for the funding for this project without which the research would not have been possible.

I would like to thank Dr. Len Wood as my main project supervisor for his excellent support in keeping me on track as well as Professor Roger Motte. Andy Ackerman of Devon County Council arranged the essential computer links supplying meteorological data from the network of Devon road weather stations. Anthony Astbury supplied mesoscale data from the UK Meteorological office whilst Pauline Framingham drew the map in Appendix 2 of Devon's road weather stations. I also appreciate the help which I have received from various members of staff at the University of Plymouth whenever my computer had a mind of its own.

Finally, I am indebted to my family and friends around Europe for their support and encouragement during the three years of this project.

DATA SOURCES

Road weather station data:

Devon County Council network of stations

NOAA Infrared satellite imagery:

Dundee Satellite Receiving Station (via *http://www.sat.dundee.ac.uk*)

NPM NERC Image Analysis unit, Plymouth (via *http://www.npm.ac.uk/rsdas*)

Meteosat imagery:

Local Dartcom receiving station, Plymouth

Surface pressure and geopotential height analyses:

European Meteorological Bulletin, Germany

Radiosonde data:

European Meteorological Bulletin, Germany

Plymouth Weather Centre (via UK Meteorological Office)

Mesoscale model data:

UK Meteorological Office, Birmingham

AUTHOR'S DECLARATION

At no time during the registration for the degree of Doctor of Philosophy has the author been registered for any other University award.

This study was financed with the aid of a studentship from Devon County Council and carried out in collaboration with the Environment Department of the County Council.

A programme of advanced study was undertaken, which included courses in statistics.

Relevant scientific seminars and conferences were attended including an international conference at which work was presented and published. External institutions were visited for consultation purposes including the 'Road and Bridge Research Institute' in Warsaw, Poland.

Publications:

Clark, R. T and Wood, N. L. H. (1996) The Sensitivity of a Surface Energy Balance Model to Cloud Variation. SIRWEC (Standing International Road Weather Conference) proceedings, pp. 82-95

Presentations:

"Sensitivity of a Surface Energy Balance Model to Cloud Variation" at the SIRWEC April 1996 conference at Birmingham, England.

Poster competition (winner), July 1996, Institute of Marines Studies,
University of Plymouth, England.

External Contacts:

Mr. Andy Ackerman,
Environment Department,
Devon County Council,
Lucombe House,
County Hall,
Topsham Road,
Exeter,
EX2 4QW

Mr. Jerzy Szymonski,
Instytut Badawczy Drog i Mostow
ul. Jagiellonska 80,
Warsaw,
PL 03-301,
Poland

Signed........RLC...............

Date...18...2...98.............

Nomenclature

ALBEDO	see page 67
AMS	American Meteorological Society
c	Specific heat of ground in Roadsurf
N	Cloud cover
cl	Climate (a ground layer in Roadsurf)
CMW	Cloud motion wind
d	Deep (a ground layer in the Roadsurf model)
DEC	Declination of sun
deg. C	*Change* of temperature
D1,D2,D3	Thickness of ground layers in Roadsurf model
DJF	December, January and February period
DPLUS	See page 67
DALR	Dry adiabatic lapse rate
DWB	Depression of wet bulb temperature
DWD	Deutscher Wetterdienst
ELR	Environment lapse rate
EMB	European Meteorological Bulletin
EXXO	Parameter related to Richardson number of stability (see page 194)
fFT	Fast Fourier transform
g	Acceleration due to gravity
gph	Geopotential height
H	Sensible heat flux
IR	Infrared
KCLOUD	See page 67
M	Mass of ground layers in Roadsurf
MORIPM	UK Meteorological Office Road Ice Prediction Model
obs	Observations
R	Fraction of Earth-sun distance
Rn	Net radiation
RST	Road surface temperature
s	Surface
S	Solar radiation
SALR	Saturated adiabatic lapse rate
SRHF	Surface wetness factor
TA	Atmospheric temperature
Tcl	cl layer temperature in Roadsurf model
Td	d layer temperature in Roadsurf model
tff	Time filter factor
Ts	Surface temperature in Roadsurf model

TH	Ground temperature in Surftemp model
TW	Wet bulb temperature
U_1, U_2	Wind speed at heights Z_1 and Z_2 respectively
U_3	3m Wind speed
UKMO	UK Meteorological Office
UTC	Universal co-ordinated time (=GMT=Z time)
var	Variable
Vg	Geostrophic wind
XLAT	Latitude
Za	Damping Depth
$\partial z/\partial n$	Change of height with horizontal distance
$\partial T/\partial z$	Sub-surface lapse rate
$\partial T/\partial t$	Change of temperature with time
ϕ	Latitude
Ω	Angular velocity of Earth
κ	Thermal conductivity
ρ	Density
σ	Stefan-Boltzmann constant
ε	Combined emissivity of surface and sky

Chapter 1 Introduction

Winter road maintenance presents a major problem for Devon County Council. Marginal situations of icy/ice free conditions occur regularly from November to March. Whilst Plymouth may be relatively mild, valleys in East Devon could be experiencing cold air drainage, severe enough to cause frost and freezing fog. Meanwhile, roads on Dartmoor following evening showers, can be treacherous with black ice.

The average number of days on which frost occurs in winter, shown in Figure 1.1 highlights clearly the wide range of conditions across Devon which present difficulties to road maintenance engineers. A relationship between height above sea level and the number of frost days can be seen by comparing Figures 1.1 and 1.2, though at Hartland Point, and along most of the coastline, proximity to the sea and prevailing wind direction is a greater influence on frequency of frost.

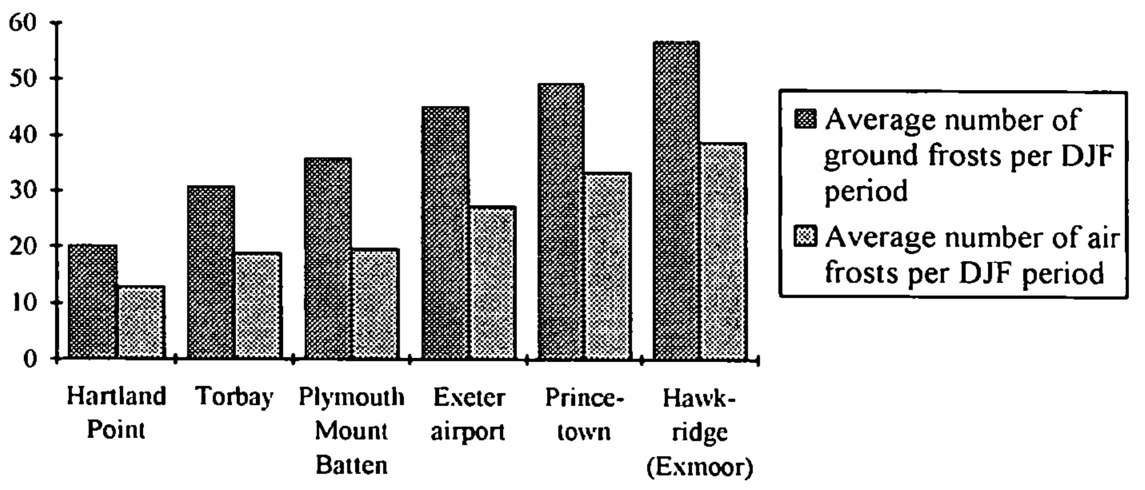

Figure 1.1 Accumulated days of frost in Devon for an average DJF (December, January and February) period compiled from UK Meteorological Office data reproduced in "West Country Weather Guide" by Craig Rich, 1980. Averages from period 1941 to 1970.

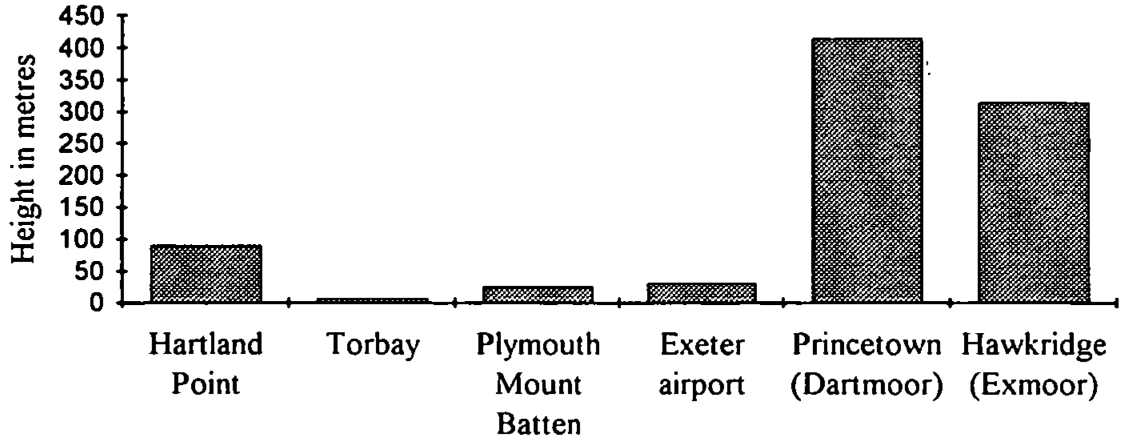

Figure 1.2 Height above mean sea level

Perry (1997) noted that coastal proximity greatly influences average minimum air temperature. The average minimum temperature for mid-winter ranges from 4.5 °C along the coast to 0.7 °C at Princetown on Dartmoor. Ratsey (1975) commented that Slapton on the South Devon coast is the mildest location in Devon during mid-winter. January is on average the coldest month at inland locations, whereas February is coldest at coastal stations since sea temperatures are at their lowest values in late February, rather than in January.

Most air frosts in Devon are caused by radiational cooling, especially in valleys, but along the coast, air frosts are more likely to occur only with very cold polar continental air advection from the east.

Compared to most of England, Devon (Plymouth) is mild between November and March as shown by Figure 1.3 of average minimum temperature. Extreme cold spells however *have* occurred in Devon, most notably during January 1987 and February 1991 when air temperatures at Plymouth fell below -6° C, though they rarely last more than 5 days. Perry (1997) noted in particular that the maximum air temperature at Okehampton on January 12th 1987 did not exceed -8.5 °C. The air temperature across the whole of Devon including the coast, stayed below 0 °C on that particular day.

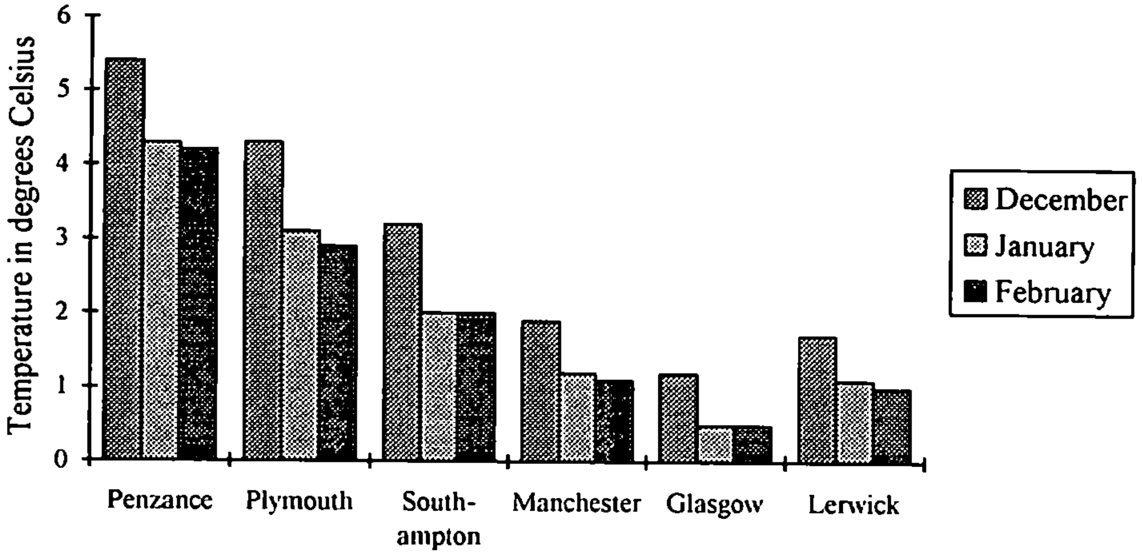

Figure 1.3 Average minimum air temperature at locations of increasing distance from Penzance in Cornwall and Plymouth in Devon. Plymouth and Southampton averages are from period 1951 to 1980. All other averages are from period 1961 to 1990.

During exceptionally cold spells, the milder coastal effects mentioned above are of less significance, for example on January 23rd 1958 when Exeter, a mere 16 km from the sea recorded a minimum air temperature of -15 °C. Other cold spells occurred during the winters of 1962, '63 and '86 as clearly shown in Figure 1.4 of the mean DJF (December, January and February) temperatures recorded at Plymouth Mount Batten. The cold years are clearly those when the mean DJF temperature for the year was lower than the lower standard deviation limit of 5.19° C. It is interesting to note that the 5th coldest winter (1986) since 1874 occurred during a decade in which global temperatures were rising. Even more peculiar was the occurrence of the two warmest winters of the century just 3 years later (1989 and 1990). Patterns of consecutively warmer winters followed by short periods of cooling winters have occurred 3 times since 1960 (1961 to 1970, 1972 to 1980 and 1986 to 1991). These trends are not reliable means of predicting the coming winter.

As mentioned above, it is the marginality of Devon's climate which causes problems to Devon County Council. Rapidly changing conditions due to shifts in wind direction and front passage have great effects on air temperature in Devon. An overcast night with 11° C

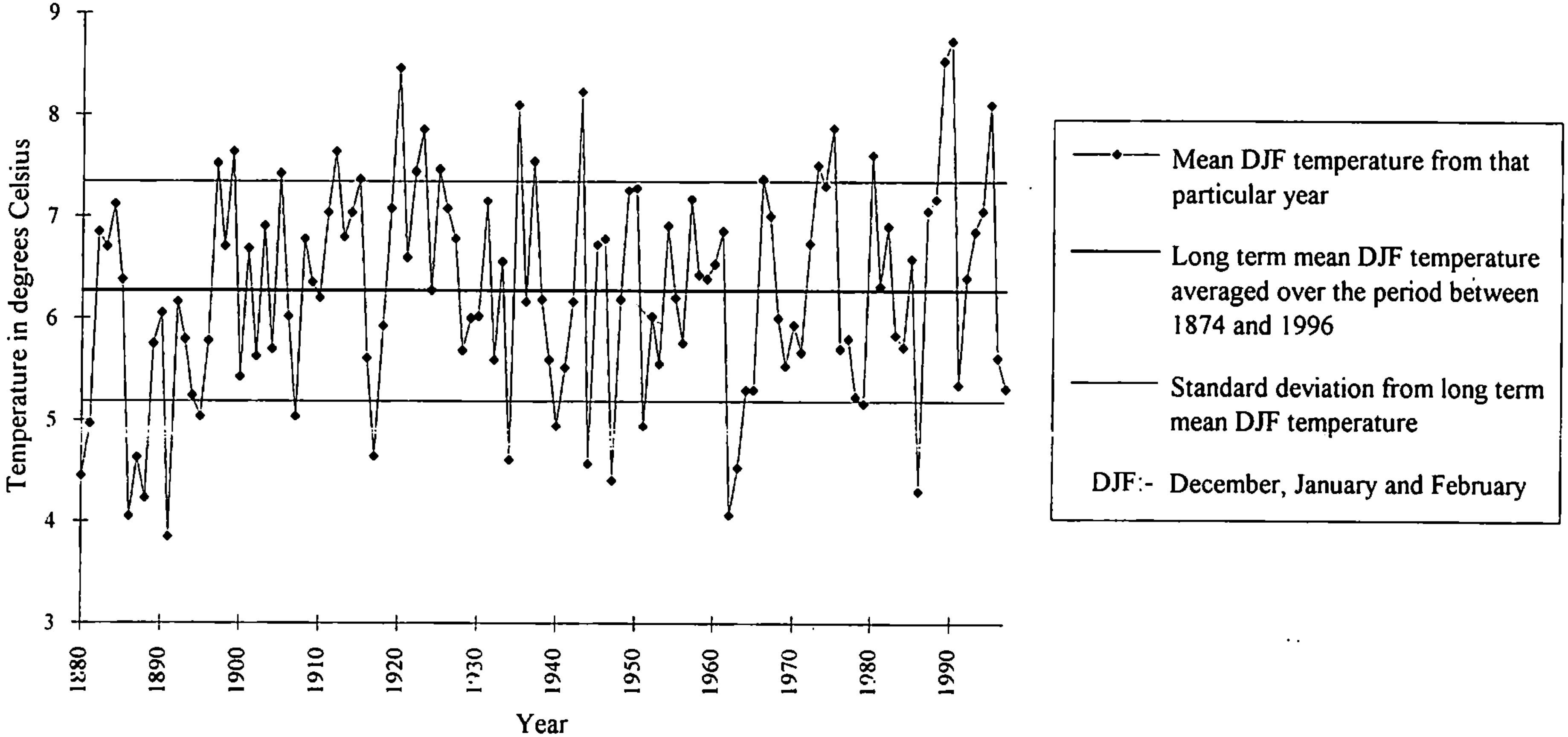

Figure 1.4 Winter air temperatures from Plymouth Mount Batten between 1880 and 1996

can quite easily be followed by a clear night with frost simply as a result of a passing cold front and vice versa due to warm fronts. There are frequent possibilities of snow with warm fronts introducing precipitation into cold air, but usually the marginality and range of relief of Devon means although there will be rain at most locations, on Dartmoor, Exmoor and in East Devon, there can be heavy snow before it turns to rain.

If road maintenance officers are too late in sending out gritters, motorists face the consequences of icy roads, reducing safety and occasionally even blocking the access routes which gritting vehicles need to use.

Furthermore, Devon has one of the longest road networks of any county in Britain (over 14,000 km) so salting every road would be an operation too costly and massive. A significant proportion of salting operations are not required and a waste of public money. For example, during a 13 day period of the 1996/97 winter, the costs of salt alone spread on Devon's roads amounted to £200,000. A complete salting of Devon's roads is about £30,000 per night including labour costs. Therefore even if eight unnecessary salting operations per winter could be cancelled, Devon County Council would save £240,000.

Figure 1.5 shows the amount of salt used by DCC between 1979 and 1994. Whilst severe winters still require large amounts of salt, savings of salt during milder winters have been made.

Additional reasons for cancelling unnecessary salting operations arise because of environmental concerns. For example, a close proximity of most roads to water courses presents problems due to excess salting, polluting the water after being washed off road surfaces by rain or melting snow and ice. Furthermore, corrosion of expensive metal body work of vehicles by precipitation is accelerated greatly by salt spray.

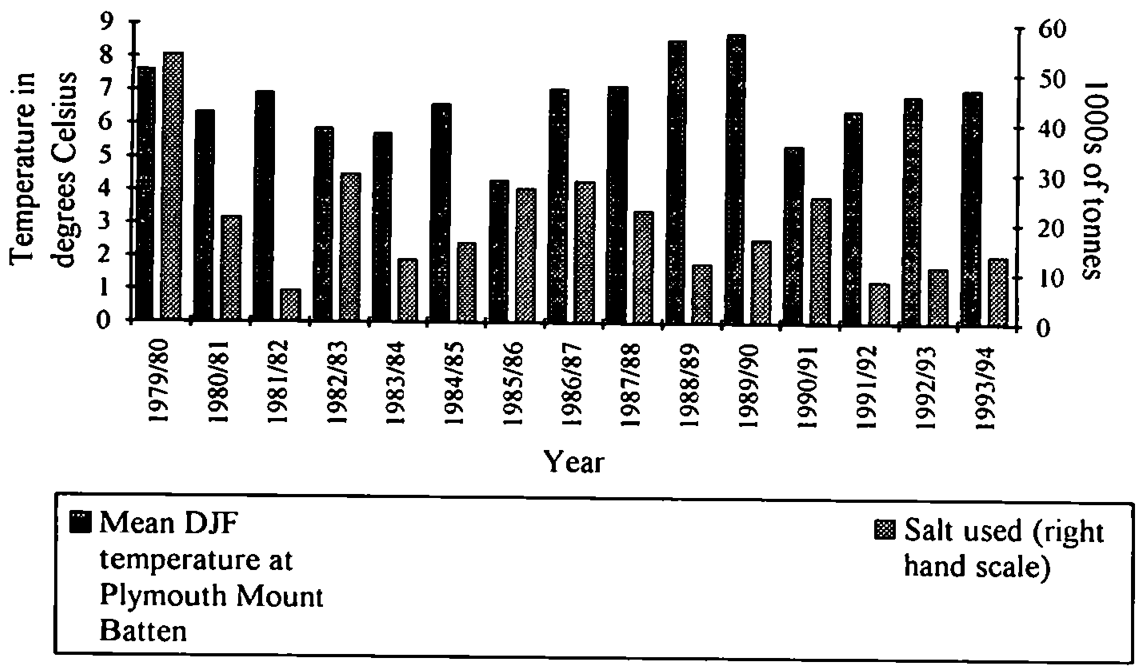

Figure 1.5 Salt used by Devon County Council between 1979 and 1994.

To improve winter road maintenance in Devon, an ice detection system has been installed with over 30 road weather stations. The first stations became operational in 1980, which partly explains the fall in salt used, between the 1979/80 and 1980/81 winters, shown by Figure 1.5. Appendices 2 and 3 show the station positions in use during the 1995/96 and 1996/97 winters respectively. Some stations are occasionally replaced, removed or relocated. Each station consists of 2 sets of sensors. The first, shown by Figure 1.6.1 is embedded in the road surface midway between the car tracks of the nearside lane and measure road surface temperature (± 0.5 deg. C) 1cm below the surface, surface wetness and surface salt cover using electrical resistance techniques. Selected road sensors record sub-surface temperatures at a depth of 40 cm as well. The second sensor set, shown by Figure 1.6.2 is located 3m above the surface, usually on the roadside verge, and records air temperature (± 0.1 deg. C), humidity and at three particular stations, wind velocity (± 1.0 ms^{-1}). The data are transmitted to Devon County Council's control room from where decisions on whether to salt and/or grit are taken. The data are also available to out-stations consisting of a computer and modem.

Figure 1.6.1 Ice Detection Station sensor embedded in road surface

Figure 1.6.2 Ice Detection Station sensors at 3m

It is more advantageous however to have a reliable forecast of road surface and meteorological conditions. Research carried out by McLean at the University of Plymouth (McLean, 1994) investigated the effects of micro-climate on road surface temperature due to altitude and exposure. Classification of all 32 road weather stations in Devon at that time, into categories of road freezing likelihood was achieved. A short study of the effects from cloud on road surface temperature was also undertaken which set the stage for this PhD project. The aims of this project as part of the PhD were to research the quantitative effects of varying cloud on surface temperature using a model and as a result, to improve real life forecasting of road surface temperatures for winter.

Influence of cloud on surface energy balance

Overnight cloud above Devon during winter impedes loss of thermal radiation to space. Conversely, clearing cloud greatly increases road surface cooling, consequently advancing the time of surface freezing. An accurately predicted time of this freezing, commonly called 'frost onset time' in this thesis, is invaluable for salting operations since it allows the control room to plan out an efficient timetable of road treatment. This is vital if a late shower were to occur which would dilute and wash away any salt. A wet surface would remain, possibly freezing after a cloud clearance. Rainfall radar images are useful for determining roads affected.

Chapter 5 reports on cloud sensitivity tests carried out using a one dimensional energy balance model called Roadsurf. Roadsurf itself, was an evolved version of a simpler model, Surftemp (developed from Outcalt, 1971). The modifications which transformed Surftemp into Roadsurf, using time differencing equations are detailed in Chapter 4.

Cloud parameterization and tracking

For Roadsurf to perform well in an operative environment, cloud has to be parameterized. The simplest method is to convert cloud cover (in oktas) to three parameters (Wood, 1977 and Thornes, 1983) which affects the incoming direct and diffuse solar radiation and outgoing thermal radiation components of the Earth's surface energy balance.

Past research, covered in the literature study of Chapter 2 confirmed that cloud can be tracked using sequential satellite images. Four case studies were undertaken from early 1994, two of which are covered in Chapter 3. Accuracy of cloud tracking is also dealt with in this chapter, since the sensitivity tests in Chapter 5 showed large effects on surface temperature resulting from inaccurate cloud observations.

1995 to 1997 case studies and algorithm development

The two main subject areas of cloud tracking and model research come together in Chapter 6 with extensive case studies from the 1995/96 winter in Devon. These studies presented the first opportunities of gauging Roadsurf's performance against real life situations under retrospective conditions.

For operational situations, algorithms to predict and parameterize boundary conditions need to be used to predict frost onset times and minimum surface temperature. The 1995/96 winter case studies were used to construct a set of algorithms for five different scenarios. Obviously, the algorithms have to be tested and sometimes modified using subsequent occurrences of the scenarios, though unfortunately this is restricted by the three year length of the PhD research. The 1996/97 winter was significantly different from the preceding one, so the algorithm from only one scenario could be tested and modified to improve its performance. Chapter 7 details this test.

There is scope for several other scenarios, which did not occur during the 1995/96 winter, likely to present road conditions requiring gritting or salting. One new scenario occurred in the 1996/97 winter, from which a 6th algorithm was constructed, which completes Chapter 7.

As a result of this research, parameterization of cloud effects on road surface temperatures will vastly improve the efficiency in terms of cost of winter road maintenance operations whilst retaining their effectiveness in keeping routes safe.

Discussions, conclusions and the need for future research on cloud cover and other factors which affect road conditions are covered in Chapters 8 and 9.

Chapter 2 Literature Survey

The literature study encompassed two areas of meteorology:- cloud detection and it's relationship with wind velocity, and road surface temperature. Sections 2.1 to 2.8 deal with aspects of cloud determination whilst 2.9 covers past research into road surface temperature modelling and prediction

Cloud tracking

Research during the early 1960s attempted to develop methods for determining atmospheric winds by studying cloud structures observed from ground level using radiosonde data. Erickson (1964) carried out research in this area of meteorology and concluded that a relationship between cloud type, wind direction and speed was strong. By examining radar echoes of cumuliform, he confirmed that cumulus clouds move with the wind at low levels, especially at 700 mb, though at a slower speed. Erickson also found that their structures tended to lean into the direction of vertical wind shear and noted that cirrus clouds tended to point into the direction of flow at 200 mb where the flow is normally more geostrophic than at lower levels where ageostrophic components of the wind are usually greater.

2.1 Cross-correlation method of cloud tracking.

Since the launch of remote sensing satellites during the 1970s, a new method of cloud tracking, called 'cross-correlations' has been widely used which gives reasonable estimates of cloud track speeds. The method developed by Leese et al (1970) involves identifying a particular cloud feature (for example, a cloud formation or clear window within a cloud sheet) on a satellite image and then attempting to track it through successive half-hourly Meteosat images. The feature must be large enough for the limited resolution of the satellite sensors to detect and show it clearly. Meteosat images usually have a resolution of 5 km in the infrared and 2.5 km in the visible (Hubert, 1979) so identifying small individual clouds is not possible. If the same feature can be identified accurately on a later image, the displacement of the cloud can be deduced and a cloud motion pattern constructed. Although both visible and infrared images can be used during daylight hours, the absence of suitable visible images during hours of darkness means that less data are available for overnight hours. Even when visible images are available, effects from the declination angle of the sun make them less suitable than infrared pictures. It is also much easier to use infrared pictures to distinguish cloud layers from one another (Hubert, 1979). Hubert cited two further reasons for using infrared rather than visible images:

(i) In the visible, many mid-level clouds appear as bright as low level stratocumulus whereas in infrared imagery, low level stratocumulus appears much darker than mid-level clouds.

(ii) Cirrus although poorly seen in the visible is very prominent in the infrared.

Schmetz et al (1993) used cross-correlation to track clouds using three successive infrared images by identifying a cloud clump of 32 by 32 IR pixels (160 km by 160 km) and using 30 minute time intervals between successive images.

The National Environmental Satellite Center conducted an experiment (Leese et al, 1970) using products from the ATS-1 satellite during 1969 with 24 minute intervals between each image. Obviously this was tedious, time consuming and unsuitable for real time analysis, so improved cross-correlation methods had to be developed to give results faster. Thus, Leese et al (1970) attempted to use a cross-correlation coefficient quantity, invented by Panofsky & Brier (1965) to represent a measure of the relationship between two successive images. When used with covariances and lag values between two images it can produce the speed and direction of cloud motions.

Leese et al (1970) considered a section of cloud shown on two successive images G_0 and G_1, at times t_0 and t_1 respectively. Cross-correlation coefficients for various lag values between two successive images were then calculated using

$$R(p,q)=\frac{Cov(p,q)}{\sigma_{t0}\sigma_{t1}} \qquad 2.1.1$$

where $R(p,q)$ = Cross-correlation coefficient at the two lag values p and q in the P and Q directions respectively (see Figure 2.1.1)

$Cov(p,q)$ = covariance at lags p and q

σ_{t0}, σ_{t1} = root mean square variations of the images G_0 and G_1 respectively

The cross-correlation coefficients were determined in the limits:-

$$-P \leq p \leq P \quad \text{and} \quad -Q \leq q \leq Q \qquad 2.1.2$$

where P and Q are as shown in Figure 2.1.1

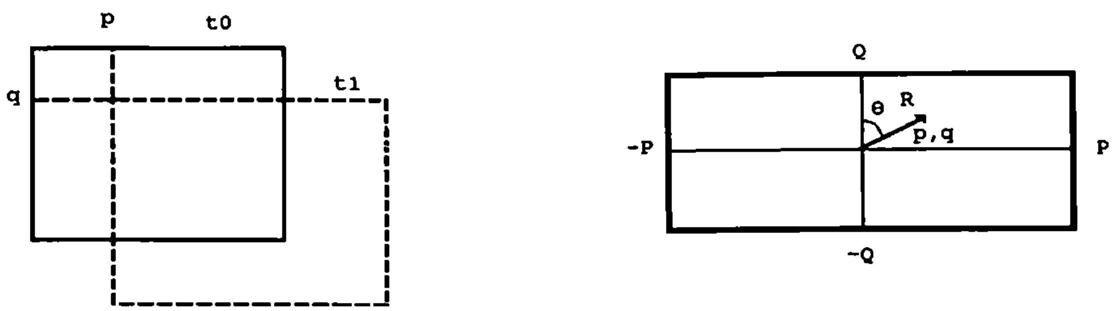

Cross correlation at lag p,q

Figure 2.1.1 Cross correlation matrix illustrating the bounds on P and Q.

The vector displacement of a cloud feature between the two successive images, with time interval Δt between them, is directly proportional to the region where the correlation coefficient is of largest magnitude. With p_{max} and q_{max} assigned the values of p and q that correspond to the maximum correlation coefficient,

$$R(p_{max},q_{max}) = \max\,[R(p,q)] \qquad 2.1.3$$

which gave the cloud track speed by:-

$$|C| = \frac{[(p_{max}\Delta x)^2 + (q_{max}\Delta y)^2]^{1/2}}{\Delta t} \qquad 2.1.4$$

where,

$|C|$ = cloud speed

Δx and Δy = sampling intervals of the image matrix in the i and j directions respectively

Δt = time interval between images

The method was fine for research, but a faster, automatic procedure for real time operational analysis would be advantageous. Calculating the cross-correlation coefficient was particularly time consuming for large spatial areas. It was thus realised that an alternative method, the fast Fourier Transform (fFT), could be used to calculate the cross-correlation coefficients more quickly. This method was researched extensively by Cooley and Tukey in 1965. Leese et al (1970) compared 300 cloud track speeds from the fFT method with conventional manual methods and found that only 18% of the speeds diverged by over 5 ms^{-1}. A step by step guide to the method for two-dimensional satellite images was produced. Unfortunately, fast Fourier transform techniques were cumbersome to use due to involvement of complex calculus and multiple summations.

Apart from improvements in accuracy, cross-correlation has essentially remained the same since the 1970s. Extensive moves have been made to automate the scheme using computers but the wide variety of cloud types and their unique motions caused several problems which became apparent during early studies of cloud motion. In particular, errors in cloud tracking arising from multi-layered clouds made attempts to automate the procedure rather complicated. Errors also resulted from the inconsistency of cloud images. Not all clouds lasted long enough to appear in more than 2 successive images. In particular, small cumuli frequently lasted no longer than thirty minutes (Hubert, 1979) since they formed from short-lived local convection. Low resolution of early meteorological satellites was a further source of error. Influences of this problem on the cross-correlation scheme's accuracy were variable and depended on the size of the feature to be tracked.

Turner and Warren (1989) used an automated cross-correlations technique to determine upper cloud motion vectors from images produced by polar orbiting satellites. They also used a completely manual technique to derive cloud motion vectors and found the manual system to be more accurate than cross-correlation but laborious and slow. Difficulties in identifying cloud cover above snow covered ground occurred frequently.

The relationship between cloud motion and actual flow is very close under most circumstances. Fast cloud motion normally indicates a fast motion of the surrounding air. The relationship is heavily influenced by the type, height and latitude of the cloud. Hubert (1979) noted that layered clouds at upper levels gave the most accurate cloud motion wind vectors. Comparisons of cirrus cloud movement with wind vectors measured using radiosondes showed that the relationship between the two was strongest at 300 mb over mid-latitudes and at 200 mb over tropical regions. There were areas though where this general rule failed due to orographic, mountain induced winds (Hubert, 1979). At these locations, low level moisture is often forced up by convection caused by the topography. However, the effects of this in Devon are small. Repetitive cloud features caused by lee waves on sheltered sides of mountains were also found to be unsuitable since they normally appear to be stationary in satellite imagery.

Wade et al (1992) tested a method of tracking cloud clusters in infrared Meteosat imagery to determine suitable cloud tracers. Cloud track speeds derived using these tracers were found to be more strongly related to wind speeds than speeds determined using tracers not selected from clustering processes.

Studies have been conducted to construct algorithms enabling calculation of wind vectors from cloud motion. These winds, called cloud motion winds (CMWs) have been produced using methods derived from studies comparing cloud motion vectors with wind data from radiosonde ascents. The accuracy of cloud motion winds compared to actual winds has been variable and highly dependent on the atmospheric level and type of cloud. At levels above 500mb, flow is more geostrophic than at lower levels and thus relationships between cloud movement and wind are usually stronger due to a Rossby number, Ro smaller in magnitude than 0.1. One circumstance of a lower accuracy occurred in or near jet streams. In these regions, cloud motion winds were consistently less than actual wind speeds (Schmetz, 1992). Schemtz also found that the wind derived from cloud motion may give a layer mean flow rather than a wind vector at a specific level.

2.2 Cloud height determination

Hubert and Whitney (1971) noted that since different level clouds normally moved in different directions and at different speeds, individual levels could be separated and studied uniquely. Cloud layers must be distinguished with particular layers being enhanced. More recently, Schmetz (1992) used a method called 'image filtering' to enhance the highest cloud layer. This used a 'spatial coherence' technique developed during the 1980s by Coakley and Bretherton which involved analysis of radiation deviation from a local mean. Cloud heights could then be estimated using infrared cloud brightness temperature data.

Steranka et al (1972) compared moisture patterns at 400 mb measured in the 6 to 7μm band from the Nimbus 4 Temperature Humidity Infrared Radiometer (THIR). A good agreement was found between wind direction and alignment of moisture patterns with deviations of less than 10 degrees in direction. However, caution was advised in regions of frontal cloud where moisture patterns were less reliable indicators of wind direction. No attempt appears to have been made in the study to compare wind speed with moisture patterns in satellite imagery.

2.3 Cloud tracking using water vapour data

A more detailed study using a similar concept to that used by Steranka et al was undertaken in 1979 by Kastner, Fischer and Bolle, followed by Eigenwillig and Fischer (1982). They attempted to analyse water vapour data from geostationary satellites. The

1979 study revealed that wind speeds derived from examining water vapour data agreed well with actual wind speeds. Deviations between the two were less than 7 ms^{-1} for a mean speed of 30 ms^{-1}.

A major difference between the 1982 study compared to Steranka et al's in 1972, was an attempt by Eigenwillig and Fischer to examine water vapour patterns present in regions of no cloud cover or at most, low level cloud cover. They found water vapour patterns to be strongly associated with 400 mb flow, measured using conventional radiosondes.

Eigenwillig and Fischer determined the height of derived water vapour (wv) wind vectors by analysing radiation emitted at various levels and comparing it with 'standard' results. For example, the lower troposphere emits more radiation than other levels in a dry, cloud free atmosphere, whilst the case for a moist atmosphere is the opposite. To determine wind vectors, various elements and features in wv imagery were identified and tracked using at least two successive images displayed on a television monitor. This method was generally successful, though problems were encountered in determining suitability of trackable markers due to fuzziness in wv images. These problems were greater during period of light wind. Parameters for choosing trackable markers were considered by Eigenwillig and Fischer. Suggested features included peaks in wv image brightness contours and edges of wv structures. Slow moving markers in wv images such as fronts could not be used to produce reliable wv wind speed observations. Fronts, however can be used to give an indication of low level wind direction since the angle between the flow and the plane of a front is usually large.

2.4 Cloud tracking using CO_2 channel data

A similar experiment to the previous but using CO_2 channel imagery from a visible infrared spin-scan radiometer atmospheric sounder (VAS) was carried out by Menzel, Smith and Stewart in 1982. They used CO_2 imagery with infrared and visible images to improve the accuracy of cloud tracking. Cloud height can be determined to a higher degree of accuracy using CO_2 data than with using infrared or visible images. A strong relationship between cloud track vectors and radiosonde wind data was found to be present. Menzel et al noted that errors were minimised because high level clouds overlaying low level cloud cover were not observed. Obviously, the use of CO_2 data would be flawed if used for studying high level cloud.

2.5 Cloud tracking using polar orbiting satellites

There has always been a tendency to use geostationary satellites for operational and research activities rather than polar orbiting satellites. Herman (1990) used polar orbiters in attempts to produce cloud motion vectors over high latitude regions of the Earth.

At latitudes higher than 65 ° north and south, coverage of the Earth's surface from geostationary satellites is of reduced resolution due to the Earth's curvature. It was obvious that using polar orbiting satellites above these regions would be the best way of gathering accurate data from satellite.

A significant problem with polar orbiters though, unlike geostationary satellites is due to their trajectory, limiting their use in cloud tracking due to long time intervals between successive images. Herman attempted to analyse data from two polar orbiting satellites whose orbits crossed several times each day thus producing successive images of high latitude regions where intervals between passes were shorter.

Herman showed that polar orbiters *can* be used to track cloud motions and produce cloud track wind derivations. The accuracy of wind speeds obtained though were sometimes poor.

Further work by Herman during the following three years significantly reduced errors that arose during his earlier research. Obliquity of sensors on polar orbiting satellites was a major error source, particularly at latitudes less than 65°. To allow for this, Herman suggested using images from polar orbiters in conjunction with geostationary satellite imagery for latitudes between 60 and 70°. Herman also increased the number of targets used in the cross-correlation algorithm from 104 to 233 which produced a much more accurate set of cloud motion and wind vectors.

Errors still occurred and were largest with very light flow. Surface features such as snow fields and mountains were difficult to distinguish from clouds. This was frequently exacerbated by inversions present above polar regions where the atmosphere was sometimes warmer than the surface. Care had to be taken to ensure that clouds were tracked rather than ground cover.

2.6 Wind vectors using the Tandem Satellite concept

An unusual method of determining wind vectors from satellite pictures used the 'Tandem Satellite' concept. This utilises two satellites producing images of the same cloud from two positions. A three dimensional picture of the cloud can be envisaged and the height/thickness characteristics calculated. Drescher (1988) produced a short paper on this but did not discuss or even detail any results.

2.7 Relationship between wind and cloud structure

Virtually all papers mentioned so far involved deriving winds by observing cloud movement rather than cloud structure. Barrett (1974) discussed the feasibility of determining wind speed and direction from cloud structures seen from satellites and noted that clouds elongate in the flow direction and lie along streamlines.

Analysis of cloud images by Merritt and Rogers (1965) led to them suggesting the cloud/wind relationships shown in Figure 2.7.1. These were most applicable to cumuliform and cumulonimbus clouds.

Merritt and Rogers noted that caution should be taken since cloud structures do not always form exclusively according to atmospheric flow. The method was crude and its reliability was not particularly consistent. Despite this, other researchers have developed similar methods. Anderson (1969) also drew conclusions about the low accuracy of the derived wind speeds. Bedient et al (1967) was more hopeful but strongly emphasised that a knowledge of local climatology was essential for the method to produce reliable results.

Polygonal cellular cumuliform and cumulonimbus clouds with mean winds of 5 to 10 ms^{-1}	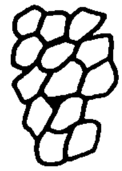 Open cells
Vermiculate cells with 10 to 15 ms^{-1} winds	 Scallops
Chaotic clouds with winds >15 ms^{-1}	 Chaotic clouds

Figure 2.7.1 Cloud/wind relationships from Merritt and Rogers (1965)

2.8 Administration of remote sensing research and current strategies

A problem with satellite research is the large number of individuals and groups of scientists researching similar ideas which have already been considered and it is certain that some 're-inventing of the wheel' has occurred. Common standards to which new methods should be compared also need to be set. In an attempt to avoid repetition, two large international groups of researchers were formed to co-ordinate satellite activities. These were the Co-ordination Group for Meteorological Satellites[*] (CGMS) founded in 1972 and the Committee on Earth Observation Satellites[♦] (CEOS) founded in 1984. Both groups agreed certain satellite data requirements which cloud motion winds are compared to in research.

Both groups acknowledge that there is still a vast amount of research to be carried out to fully understand cloud motion winds. Thus for this reason, no standard method of cloud track wind has been decided upon (Hinsman, 1993). New methods that could be useful in determining cloud track winds are still being developed. NASA has plans to develop a system of determining cloud motion winds using their 'Laser Atmospheric Wind Sounder'.

Baker (1993) reported their aim to install it onto a Japanese Earth observing station due for launch in 1998. If the instrument performs well in producing accurate wind vectors, it will form part of the NASA Earth Observing System.

* *http://www.wmo.ch/hinsman/cgmsp01.html*

♦ *http://gds.esrin.esa.it:80/ceos-about;sk=22E172A5*

2.9 Forecasting road surface temperature

Before computers became available, road surface temperature (RST) was usually predicted using regression and correlation with the air temperature. These were simple techniques which often gave unreliable forecasts, especially on occasions with changing cloud and wind conditions.

Computers during the late 1960s and early 1970s provided a platform for forecasting surface temperature using models which attempted to replicate real life changes of temperature using numerical methods.

Thornes (1972) developed a model in 1969 which used the following form of an equation produced by Reuter (1951):-

$$\Delta T = F\,(E + Bk + (\gamma - \gamma_d)\, c_a\, A)\, t^{1/2}$$

where,

ΔT = change in surface temperature between sunset and sunrise during a night of duration

t = length of night

$F = 2 / \pi^{1/2}\ [\, (\rho c k)^{1/2} + c_a(\rho_a A)^{1/2}\,]$

ρ = soil density

c = specific heat capacity of soil

k = heat conductivity of soil

c_a = specific heat capacity of air

ρ_a = air density

A = eddy conductivity of air

E = upward directed long-wave radiation from surface
B = lapse rate in soil at sunset
γ = lapse rate in air at sunset
γ_d = dry adibatic lapse rate
$\pi = 3.14$

Thornes tested his model using data from two Nottinghamshire sites from the 1968/69 winter as well as July 1969. It performed well, attaining almost 100 % accuracy in forecasting likelihood of surface freezing occurring but had a cold bias of 0.5 to 2.0 deg. C in minimum surface temperature prediction whenever surface freezing was predicted due to frost induced latent heat release which the model was unable to handle.

Outcalt (1971) developed a different model which consisted of an iterative scheme based on the following surface energy balance equation from the principle of conservation of energy:-

$$\begin{aligned}\text{Net radiation flux} = \; & \text{Sensible heat flux} \\ & + \text{Latent heat flux} \\ & + \text{Ground heat flux}\end{aligned}$$

A more detailed version of this equation for predicting surface temperature is discussed in Chapter 4 of this thesis.

Outcalt's model was modified by Wood (1977) to account for cloud effects of albedo and thermal emission. Thornes (1983) used similar cloud parameterisations for sensitivity tests on cloud cover for a site near Theale on the M4 motorway. Diurnal ranges of surface temperature varied from 9.4 deg. C under overcast low cloud to 25.1 deg. C under clear skies. Later tests undertaken by Thornes with Shao in 1991 confirmed the high influence of cloud on surface temperature. Air temperature was another major factor but model sensitivity to dew point temperature and thermal properties of the road such as heat capacity was small. Even a 20% range of conductivity and heat capacity had no significant effect on model surface temperature predictions.

A year later, Thornes and Shao published part of their research into applying selected UK

Meteorological Office (UKMO) mesoscale model output as inputs for the UKMO road ice prediction model (MORIPM). Root mean square errors of minimum surface temperature, averaged over 11 UK sites ranged from 1.37 to 2.4 deg. C depending on the number of grid points used for the mesoscale model. Unfortunately, these results were averaged from the period Jan. 2nd to 24th 1991 which concealed model performance on individual dates. Reasons for a cold bias of 1.0 deg. C which consistently occurred in the MORIPM were found to be due to the model failing to replicate real life processes accurately. A templet of mean hourly errors taken over seven day periods was applied to MORIPM 24 hour forecasts which improved accuracy of minimum surface temperature predictions by 10 to 20 % at 11 UK sites.

Investigations of cloud effects on RST prediction from the 1993 and 1994 winters were undertaken by McLean and Wood (1995). Their paper underlined problems with real time surface temperature prediction due to variable cloud. Forecasts from 65% of 12 forecast trials from the 1994 winter were accurate to ± 1 deg. C.

Bogren and Gustavsson (1994) tested a model which predicts RST for Sweden using a mixture of numerical calculations, statistical records and an empirical parameterisation of cloud amount and height. They found that effects of erroneous cloud forecasts were more of a problem during spring rather than mid-winter due to increases in solar radiation. However, their research appeared to be more concerned with predicting RST throughout the night rather than minimum RST.

Other factors influencing RST have also been studied including altitude (Thornes, 1991 and Shao et al, 1997), proximity to urban heat islands and exposure, for example caused by bridges above roads.

Jacobs and Raatz (1996) carried out tests on a model developed by the UK Meteorological Office for forecasting RST at a site 20 km outside of Frankfurt in Germany for Deutscher Wetterdienst (DWD). The model carried this out by predicting the energy fluxes which formed the basis of Outcalt's (1971) model, e.g. incoming solar radiation, heat loss from the surface during hours of darkness, sensible and latent heat fluxes and heat conduction within the ground. There was no process in the model to account for effects from exposure, topography and traffic. The model inputs included predictions of air and dew point temperature, wind speed, cloud cover and precipitation. Sensitivity tests using the model showed that the most important influences on surface temperature were due to low cloud, wind speed and air temperature. Changes in cloud cover from clear to overcast skies or vice versa resulted on average, in surface temperature changes of 5.0 deg. C. Increasing wind speed from calm to 10 ms^{-1} increased the RST by 3.0 deg. C due to mixing. Increase or decrease of air temperatures of 2.0 deg. C resulted in RST changes of 1.0 deg. C. Thus it was clear that inputs of cloud, wind speed and air temperature had to be accurately predicted for a reliable surface temperature prediction to be achieved.

The model generally predicted surface temperatures too low during hours of darkness, especially during cloudy conditions. Jacobs and Raatz noted that the volume of road traffic has an effect on RST by causing mixing close to the surface which could be accounted for in the model by using an increased wind speed input for busy traffic. A point raised by Lister (1991) was also discussed by Jacobs and Raatz about the accuracy of RST measurements due to sensor technology and possible poor installation of certain sensors.

Another RST prediction model based on the energy balance equation was developed by Sass and Voldborg (1994) in Denmark. They used predicted atmospheric data from the HIRLAM (High Resolution Limited Area Model) which was assimilated to provide accurate inputs for the RST model. Assimilation was needed for certain occasions when HIRLAM performance was likely to be insufficiently accurate and also for linearly interpolating predictions at HIRLAM grid points horizontally to road station sites. It was found that modifications to HIRLAM cloud predictions for the RST model were required throughout because HIRLAM predicted cloud based solely on atmospheric temperature and specific humidity which themselves were predicted to change.

Attempts were made to allow the RST model to account for effects of shading due to local topography during daylight hours. This was done by reducing the direct solar radiation parameter in the model by a factor related to the angle of the road surface to the top of the shading object. Thus the direct solar radiation was set to zero if a direct beam of sunlight failed to reach the road surface. For hours of darkness, effects due to shading were accounted for by reducing the net longwave radiation by a factor related to the solid angle covered by the shading object.

The wind speed was taken into account by the parameterization of sensible heat, H and Richardson number of stability, Ri:-

$$H = C_p \rho_1 C_s V_1 (\theta_1 - \theta_s)$$

where H = sensible heat flux (W m^{-2})

C_p = specific heat of moist air at constant pressure (J kg^{-1} K^{-1})

C_s = a dimensionless drag coefficient

$= [k / \ln (Z_1/z_0)]^2 \cdot f(Ri, Z_1 / z_0)$

ρ_1 = air density at height Z_1 (kg m^{-3})

V_1 = wind speed at height Z_1 (m s^{-1})

θ_1 = potential temperature at height Z_1 (K)

θ_s = potential temperature at surface (K)

z_0 = roughness length for heat and moisture (m)

$f(Ri, Z_1 / z_0)$ = dimensionless function of the Richardson number

The dependence of the Richardson number was assumed negligible by Sass and Voldborg during stable atmospheric conditions, i.e. when $\theta_1 > \theta_s$.

RST model performance for 163 sites in Denmark in December 1993 was good with mean differences between predicted and observed surface temperatures less than 0.8 deg. C for the first 5 hours of forecast period. Sass and Voldborg however found rapidly changing cloud conditions to be problematic. They concluded that a graphical manual correction procedure for automatic HIRLAM cloud cover predictions would lead to distinct progress in predicting RST.

Most models predict surface temperatures for single locations, but in real life, temperature variations along stretches of road can be significant as investigated by Bogren et al (1992). They used a mixture of surface temperature observations from fixed road stations and thermal mapping from moving vehicles equipped with infrared sensors pointed towards the road surface showing temperature change along roads in Sweden during three occasions in January 1986. Variations were found to be due to changes in exposure, altitude and screening. Screening effects were particularly noteworthy at road rock cuts where RSTs varied by 2.3 to 5.7 deg. C between exposed and screened road sections. As part of their research, Bogren et al developed a model to forecast RST variation along 14 km stretches of road. The main advantage of thermal mapping envisaged, was to enhance site specific model output so helping salting crews determine specific locations where treatment is required.

2.10 Summary

- Cross-correlation using satellite imagery can be used to determine cloud movement. It is most accurate when used to track frontal cloud than individual clouds, for example cumuli

- Manual methods of cross-correlation, although laborious to use, are more accurate than automatic methods for determining cloud velocity

- Cloud movement is related to air flow, especially at upper levels though this relationship was weaker in mountainous regions due to orographic clouds and within jet streams

- Imagery from polar, as well as geostationary satellites can be used to track cloud, though tracking using polar orbiters requires more targets to sustain equal accuracy to tracking from geostationary satellites due to viewer obliquity

- Energy balance models which have attempted to replicate real life situations have attained an accuracy to a level where differences of 1.0 deg. C between predicted and observed surface temperature have occurred when using templets to deal with model biases

- Effects of erroneous cloud forecasts on surface temperature prediction in Sweden have been a greater problem in spring than mid-winter. In Germany, surface temperature forecasts from models during cloudy conditions have been less accurate than with clear skies

- Surface temperature variations of between 2.5 and 5.7 deg. C due to exposure have been found to occur in Sweden

Chapter 3 Cloud tracking case studies

3.1 Introduction

Various series of satellite images were studied with an aim of detecting relationships between cloud track speeds and air flow, and satellite image brightness and cloud top height. Four case studies were carried out, two of which February 9th and 16th 1994, are detailed in this chapter. For each series, selected cloud pixels were tracked and compared with geostrophic winds calculated using synoptic analyses of geopotential height from the European Meteorological Bulletin, (EMB).

Radiosonde data were used to ascertain likely cloud top level which was compared to image brightness. Actual wind speeds recorded by radiosondes were compared to geostrophic wind speeds.

3.1.2 Cloud tracking

A manual version of cross-correlation, developed by Leese et al (1970) was used to carry out all cloud tracking exercises.

Distinctive cloud features were identified such as leading edges of cloud bands, individual cloud pixels and clear sky windows within major cloud formations. These were tracked using successive images of four hourly intervals. Effects due to lee waves were found to be negligible.

Errors which occurred in measurement of features present in the satellite imagery were largely due to limits in image resolution and precision of measurements.

Errors encountered with longitudinal cloud displacements were half those encountered with latitudinal movements due to the obliquity of the satellite's viewer caused by the Earth's curved surface. Since the latitude being considered was 55° North, east-west distances were observed with a greater resolution than north-south distances.

Errors expressed as percentages of cloud speed were dependent on actual cloud movements. Due to the precision of measuring instruments used, flow less than 5 ms^{-1}

could not be accurately ascertained to nearest whole numbers. Error percentages of speed decreased with increasing cloud speed though actual errors in ms^{-1} remained constant.

Errors related to cloud type and the nature of any fronts which may have been present varied considerably depending on the ease to which cloud features could be tracked. For example cloud formations within warm sectors were often more difficult to track than those within polar airstreams, due to a lack of sharp edges.

3.1.3 Geostrophic flow

Since mid latitude regions were being considered, it was assumed that flow was mostly geostrophic due to a significant Coriolis force, hence the geostrophic relationship (Equation 2.3.1) could be used to determine wind speed, though only in the direction parallel to geopotential height contours.

$$V_g = -\frac{g}{2\Omega\sin\phi}\frac{\partial z}{\partial n} \qquad 3.1.3.1$$

V_g= Geostrophic wind (ms^{-1})

$\partial z/\partial n$= Rate of change of height with horizontal distance perpendicular to geopotential height contours.

ϕ= latitude (51° North)

and Ω= angular velocity of the Earth (7.29×10^{-5} rad s^{-1}),

In Tables 3.1.3 and 3.1.3.2, $(\partial x)'$ is an error attributed to resolution limits of the printed charts and precision of ruler used to measure contour spacing.

Table 3.1.3.1 Effects of errors on measurement of geostrophic wind from analyses of geopotential height at 200 and 500 mb. $(\partial x)'=14.5$ km.

Wind Speed Band/ms^{-1}	V_g /ms^{-1}	∂x for V_g /km	$\partial x+(\partial x)'$ / km	V_g+V_g'/ ms^{-1}	V_g'/ ms^{-1}
0-5	2.5	2625.7	2640.2	2.486	0.014
5-10	7.5	875.3	889.8	7.377	0.122
10-15	12.5	525.2	539.7	12.164	0.336
15-20	17.5	375.1	389.6	16.849	0.651
20-25	22.5	291.8	306.3	21.435	1.065
25-30	27.5	238.7	253.2	25.925	1.575
30-35	32.5	202.0	216.5	30.323	2.177
35-40	37.5	175.1	189.6	34.631	2.869
40-45	42.5	154.5	170.0	38.853	3.647
45-50	47.5	138.2	152.7	42.989	4.511
50-55	52.5	125.0	139.5	47.044	5.455

Table 3.1.3.2 Effects of errors on measurement of geostrophic wind from analyses of geopotential height at 850 mb. $(\partial x)'=7.3$ km

Wind Speed Band /ms^{-1}	V_g /ms^{-1}	∂x for V_g /km	$\partial x+(\partial x)'$ / km	V_g+V_g'/ ms^{-1}	V_g'/ ms^{-1}
0-5	2.5	2625.7	2633.0	2.493	0.007
5-10	7.5	875.3	882.6	7.438	0.062
10-15	12.5	525.2	532.5	12.327	0.173
15-20	17.5	375.1	382.4	17.166	0.334
20-25	22.5	291.8	299.1	21.947	0.553
25-30	27.5	238.7	246.0	26.68	0.816
30-35	32.5	202.0	209.3	31.364	1.136
35-40	37.5	175.1	182.4	35.989	1.511

Tables 3.1.3.1 and 3.1.3.2 show that errors became larger with increased wind speeds because of closer contour spacing in geopotential height analyses. In an attempt to minimise this source of error, more contours were spanned in regions of strong winds in

order to decrease cumulative measuring errors. A limit in number of contours being spanned was set at two with a contour spacing of 80 metres for 200 and 500 mb level charts and one with contour spacing of 40 metres for 850 mb level charts. This upper limit was set otherwise any horizontal variation in geostrophic wind speed might have been suppressed.

3.2 February 9th 1994 cloud tracking exercise

3.2.1 General Discussion

Geostrophic wind speeds at 200, 500 and 850 millibars were calculated using Equation 3.1.3.1, from analyses of geopotential height (Figures 3.2.1.2a, b and c). These results, shown in Table 3.2.1.2 were compared with cloud track speeds from the satellite image series shown in Figures 3.2.1.1a to d. A tabular summary is shown in Table 3.2.1.3.

Table 3.2.1.1 Meteosat derived cloud track data from Feb. 9th 1994.

Location	Cloud feature	Time (UTC)	Displacement / km	Cloud speed/ $ms^{-1} \pm 4.0$	Dir.
Exmouth, Devon	i)Northern edge of a weak cold front.	1130-1230	80	22.2	N
		1130-1330	110	15.3	N
		1130-1430	180	16.7	N
			Mean:	18.1	
Straits of Dover	ii)Cloud clump of 50 km diameter.	1230-1430	189	26.3	NW
			Mean:	26.3	
Land's End, Cornwall	iii)Back edge of weak cold front.	1130-1230	85	23.6 19.6	N
		1130-1330	141		N
			Mean:	21.6	

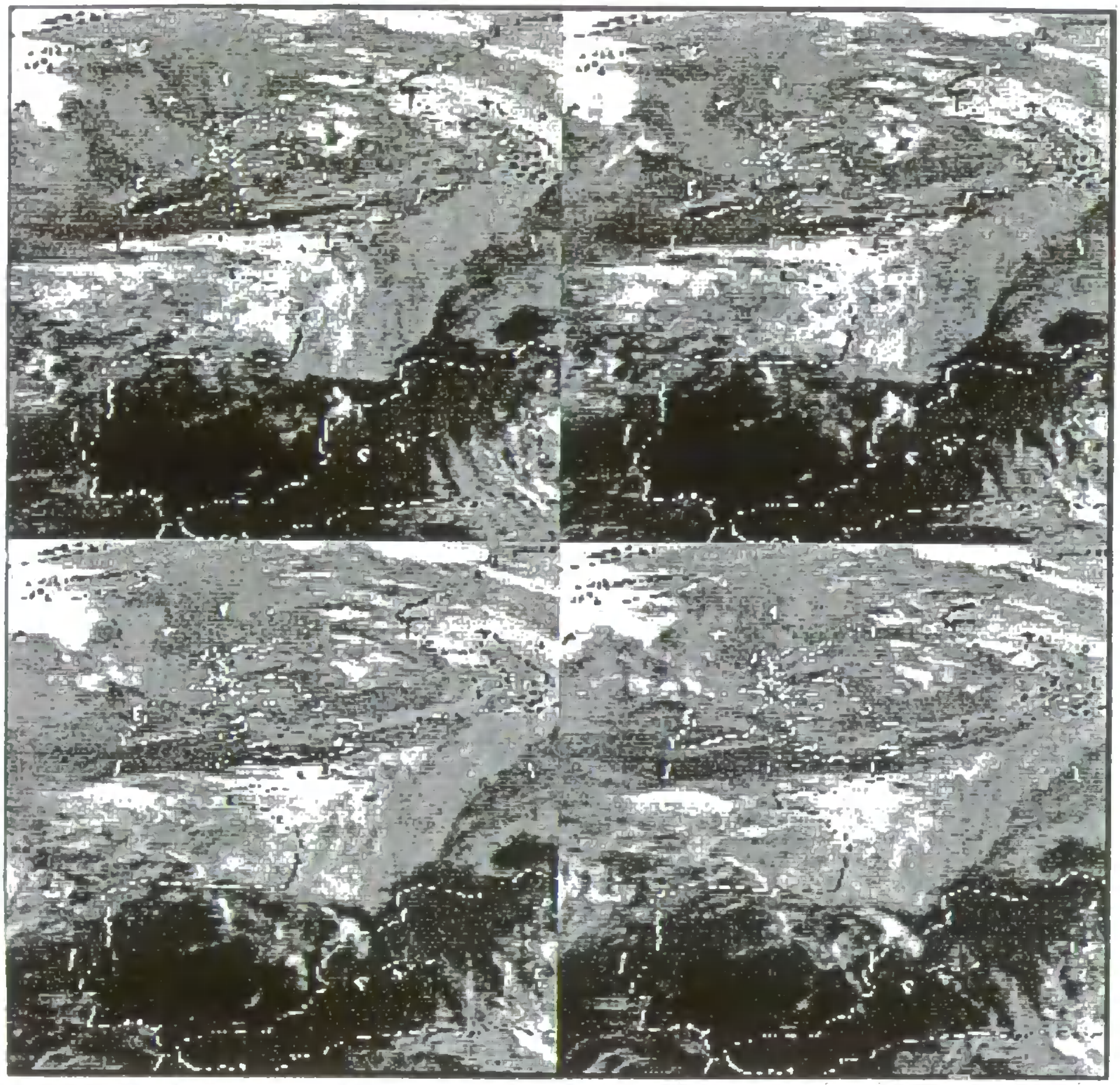

Figure 3.2.1.1 Infrared Meteosat imagery from
1130 UTC to 1430 UTC February 9th 1994

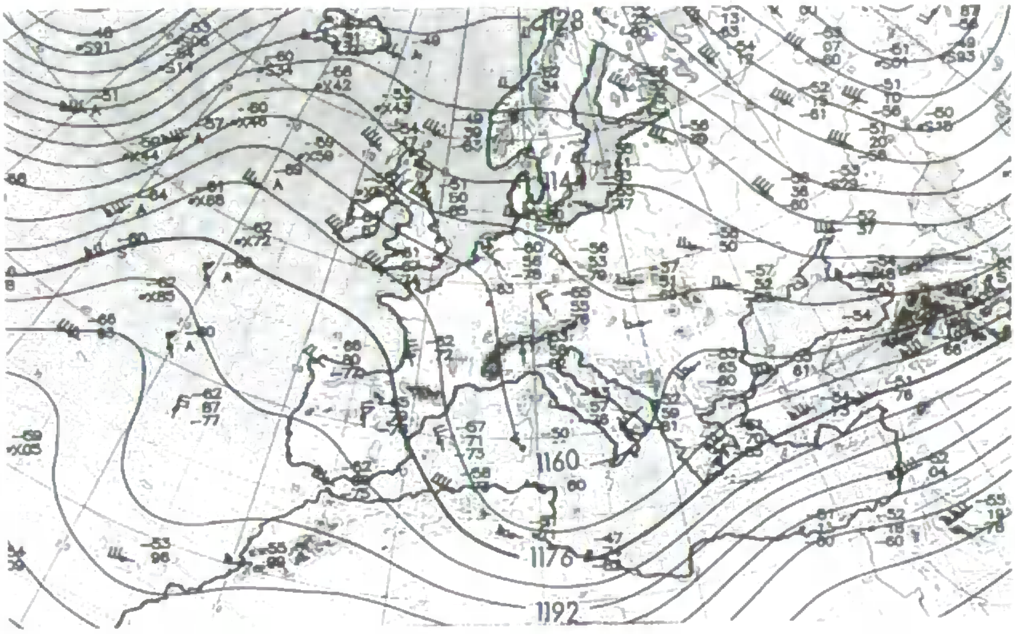

a. 200 mb

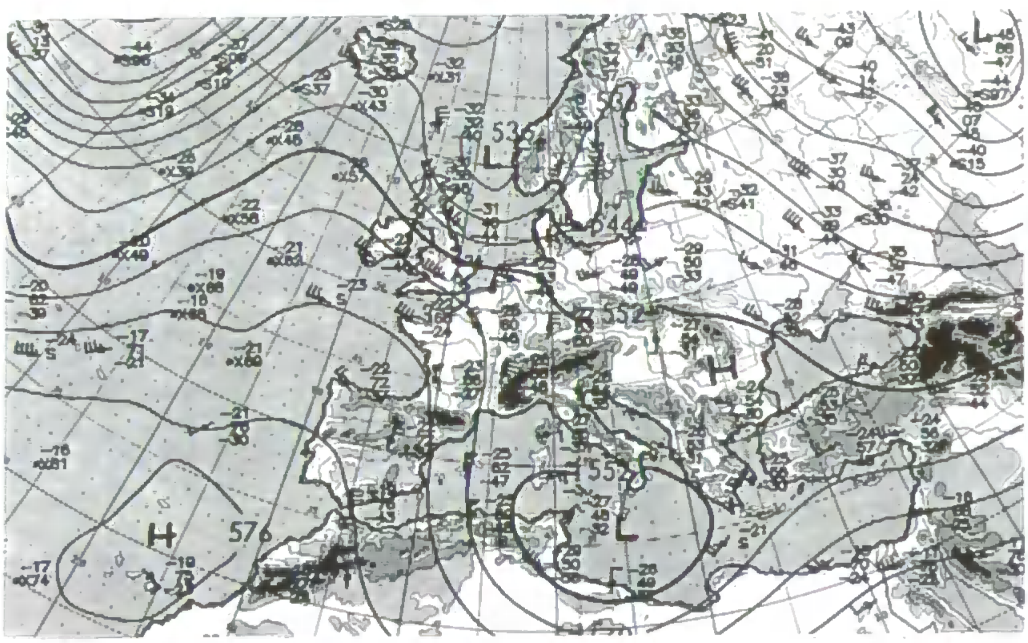

b. 500 mb

Figure 3.2.1.2 European Meteorological Bulletin geopotential height analyses from 1200 UTC Feb. 9th 1994

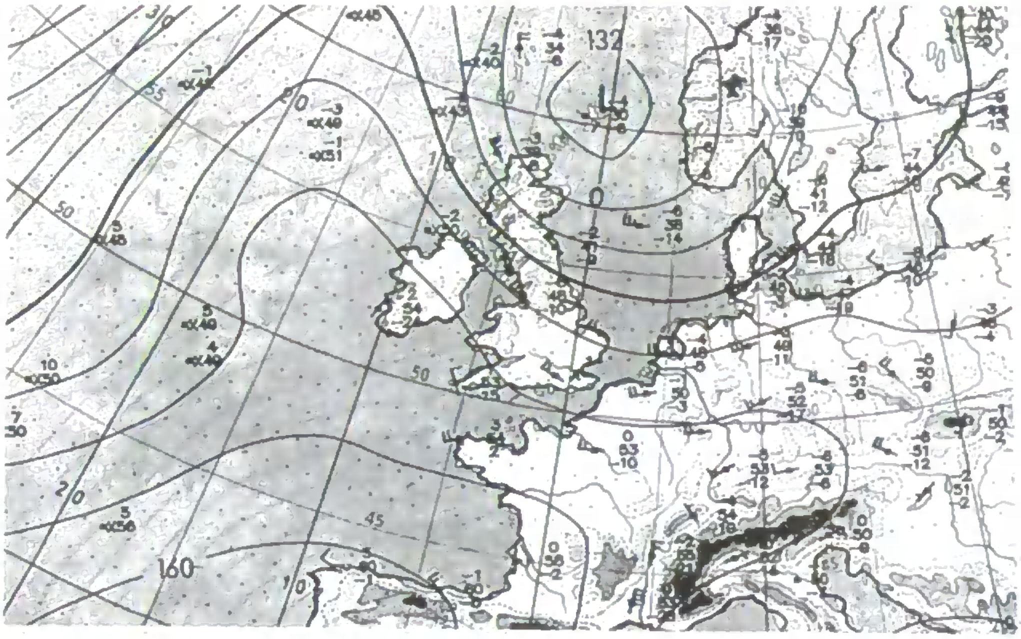

c. Geopotential height at 850 mb

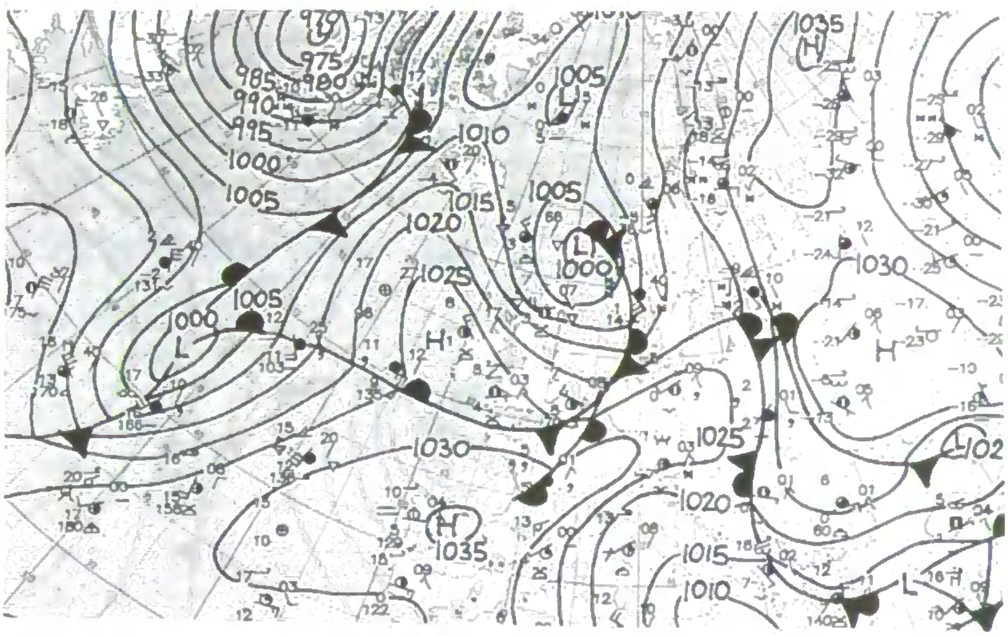

d. Surface pressure

Figure 3.2.1.2 European Meteorological Bulletin analyses
from 1200 UTC Feb. 9th 1994

Table 3.2.1.2 Geostrophic winds from EMB geopotential height analyses above selected regions at 1100 UTC Feb. 9th 1994.

Location	Pressure level/mb	Geostrophic wind, V_g/ms^{-1}	V/V_{g850}	Direction (from)
Southwest England	200	23.5±1.1	1.6	W
	500	18.9±0.7	2.0	NW
	850	11.7±0.2		W
Southern England	200	19.5±0.7	2.0	NW
	500	29.3±1.6	3.0	NW
	850	9.8±0.1		W
Southeast England	200	16.7±0.7	1.4	NW
	500	24.4±1.1	2.1	W
	850	11.7±0.2		W
Wales	200	22.7±1.1	1.7	NW
	500	34.1±2.1	2.5	NW
	850	13.7±0.2		NW
Northern England	200	28.4±1.6	1.2	NW
	500	40.1±3.6	1.8	NW
	850	22.8±0.6		NW
Ireland	200	23.4±1.1	1.2	NW
	500	28.4±1.6	1.5	NW
	850	19.5±0.3		NW
Scotland	200	25.3±1.6	0.9	NW
	500	35.1±2.9	1.2	NW
	850	29.3±0.8		NW
Sea area Sole	200	<5.0	<0.4	Var
	500	8.4±0.1	0.6	W/SW
	850	13.0±0.2		SW

Note: Var/W/NW:- Variable then Westerly veering north-westerly

W/NW:- Westerly veering north-westerly

W/SW:- Westerly backing south-westerly

Table 3.2.1.3 Comparison between selected cloud movements and geostrophic wind flow at 1200 UTC Feb. 9th 1994.

	Cloud i	Cloud ii	Cloud iii
Mean cloud speed /ms^{-1}	18.1±4.0	26.3±4.0	21.6±4.0
Geostrophic flow V_g /ms^{-1}:-			
200 mb	23.5±1.1	16.7±0.7	23.5±1.1
500 mb	18.9±0.7	24.4±1.1	18.9±0.7
850 mb	11.7±0.2	11.7±0.2	11.7±0.2

Table 3.2.1.4 Ground based cloud observations at the Plymouth Weather Centre from Feb. 9th 1994 from Feb. 9th 1994.

Time (UTC)	Total cloud cover in oktas	Cloud cover amount /oktas, type and level / mb	
		1000 to 700mb	Above 700mb
1200 Feb. 10th	7	1St(970) 1Sc(920)	1 As(650) 7 Ci(420)
1300	3	1 Cu(940)	2 Ci(420) 1 Ci(300)
1400	1	1 Cu(940)	1 Ci(420)
1500	1	1 Cu(930) 1 Sc(920)	1 Ci(420)
1600	1	1 Sc(920)	1 Ci(420)
1700	1	1 Sc(920)	1 Ci(420)
1800	1	-	1 Ci(420)

Tables 3.2.1.1 to 3.2.1.3 show that horizontal cloud movement speeds above Exmouth and Dover correlated best with the 500 mb geostrophic flow which indicated that 500 mb was most likely the cloud level, as opposed to 200 or 850 mb. Exceptions were track speeds above Land's End in Cornwall where cloud movement was slightly faster than the geostrophic flow at 500 mb. This cloud was more likely to have been higher than 500 mb

based on an assumption that cloud track speeds were solely dependent on wind speed. Land's End is roughly a hundred kilometres west of Plymouth , so surface based cloud observations taken at the Plymouth Weather Centre (Table 3.2.1.4) were compared with local cloud track speeds. These observations agreed very well with the earlier indication that cloud was present at upper levels. Upper level cirrus was present above 450 mb for much of the tracking period. Observations at the Weather Centre also showed a presence of various types of cloud at lower levels. It was not possible though to track this low level cloud using satellite imagery wherever high level cloud was located above it.

The cloud present above all three locations was part of a weak cold front passing from north to south over the English Channel. This was responsible for differences in altitude of the cloud being tracked, since fronts are sloped.

3.2.2 Ascent data

Radiosonde ascents from 1100 UTC and 1200 UTC Feb. 9th (Figures 3.2.2.1a,b,c...) showed much dryer air behind the cold front situated over the English Channel than within the warm sector. Ascents from Hemsby (3.2.2.1j.), Camborne (3.2.2.1i.) and Valentia (3.2.2.1c.) behind the cold front showed very well defined cloud top levels. Ascents taken at stations within the warm sector and also ahead of the warm front were significantly different with cloud top levels for Brest (3.2.2.1a.), Bordeaux (3.2.2.1d.) and Vienna difficult to detect. Within the warm sector, dew point depressions varied by less than 10 deg. C with height, hence to get a clear idea of cloud top height at stations within this sector, tephigrams were drawn for ascents at Trappes, Brest and Uccle, (Figures 3.2.2.2a,b and c.).

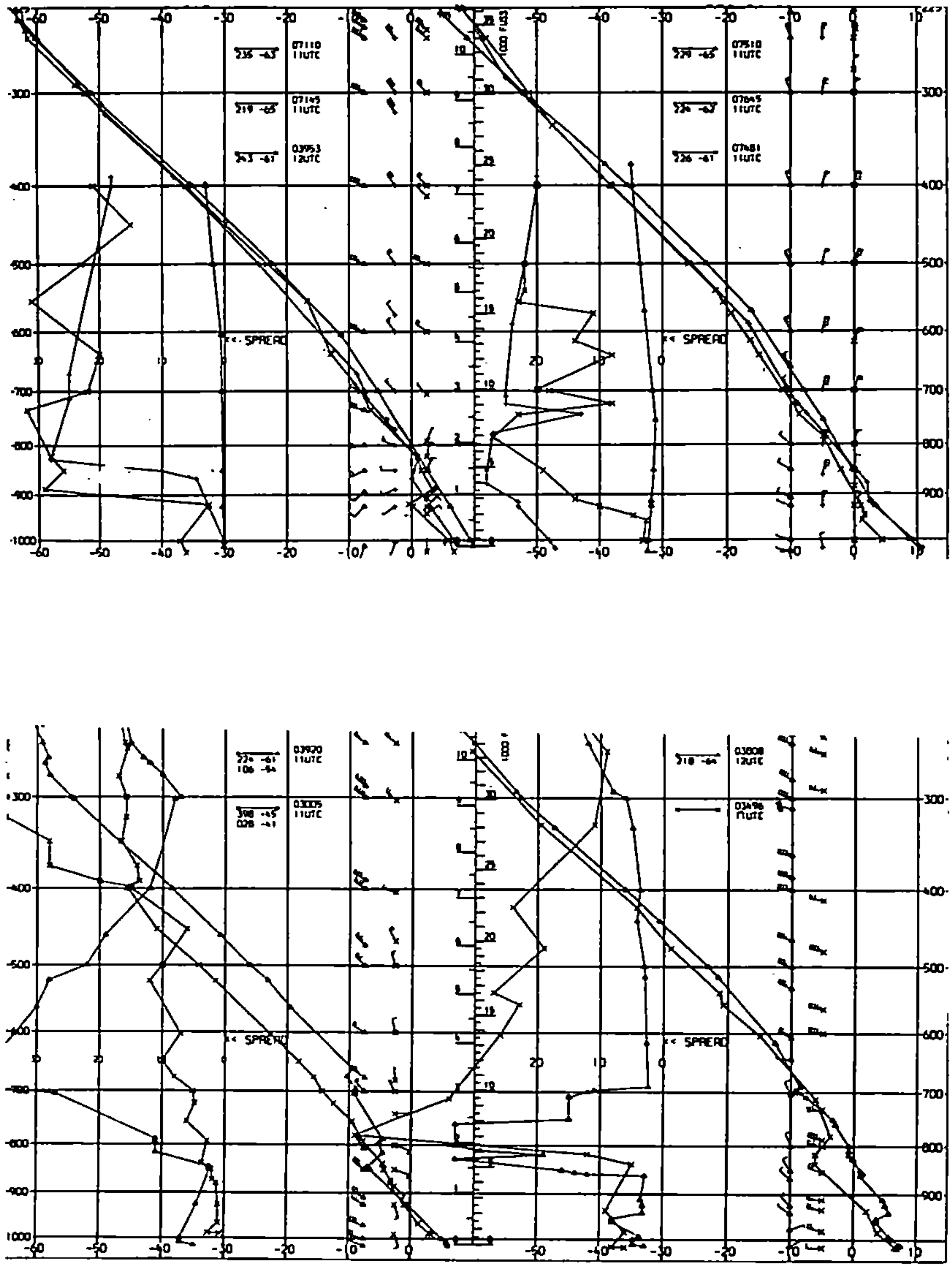

Figure 3.2.2.1 European Meteorological Bulletin radiosonde ascents from 1200 UTC Feb. 9th 1994

Station numbers:- (Locations shown in Appendix 1)

a. 07110	Brest	f. 07481	Lyon
b. 07145	Trappes	g.03920	Long Kesh
c. 03953	Valentia	h.03005	Lerwick
d. 07510	Bordeaux	i. 03808	Camborne
e. 07645	Nimes	j. 03496	Hemsby

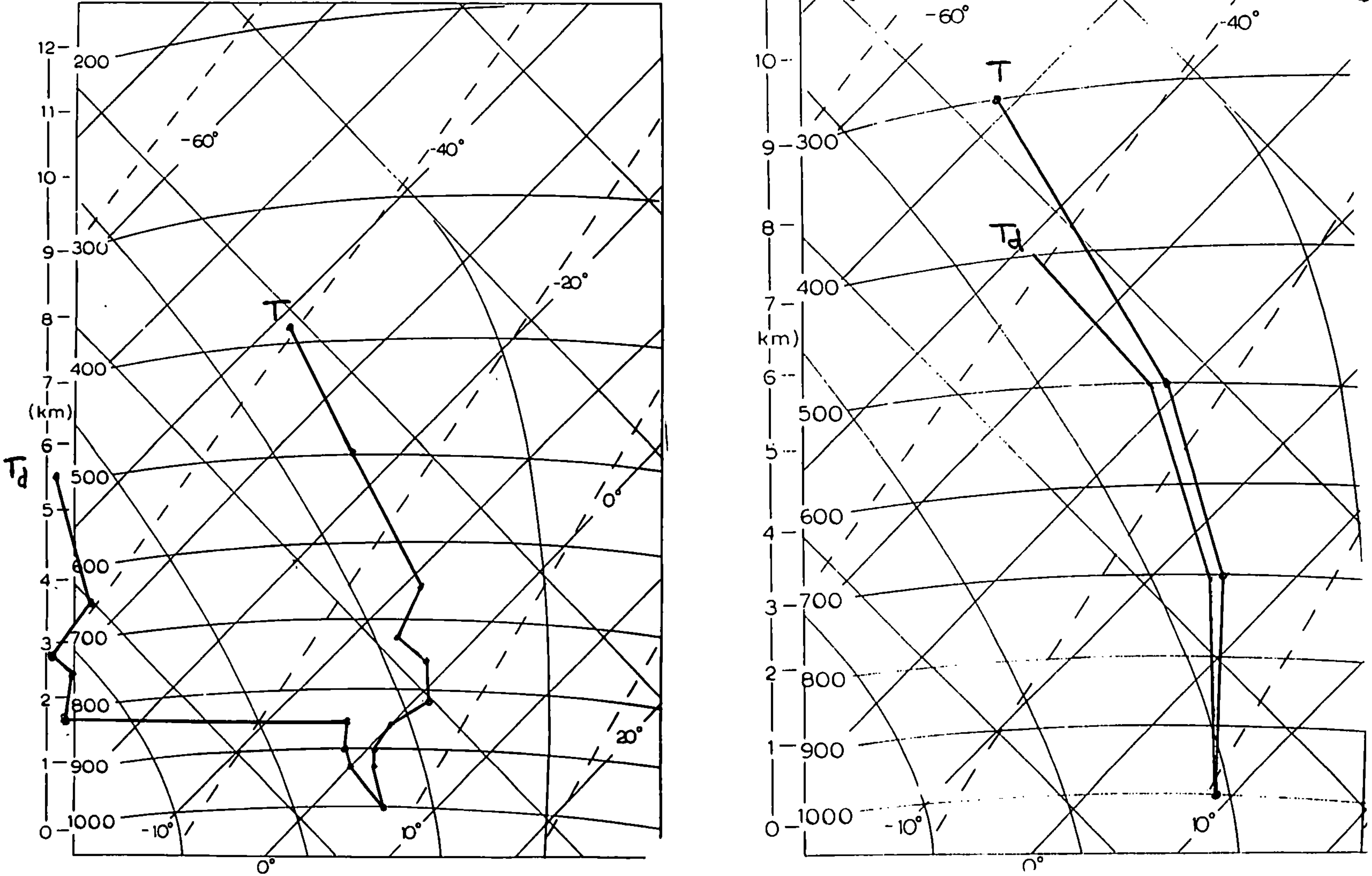

a. Trappes

b. Brest

Figure 3.2.2.2 Radiosonde ascents from 1100 UTC February 9th 1994

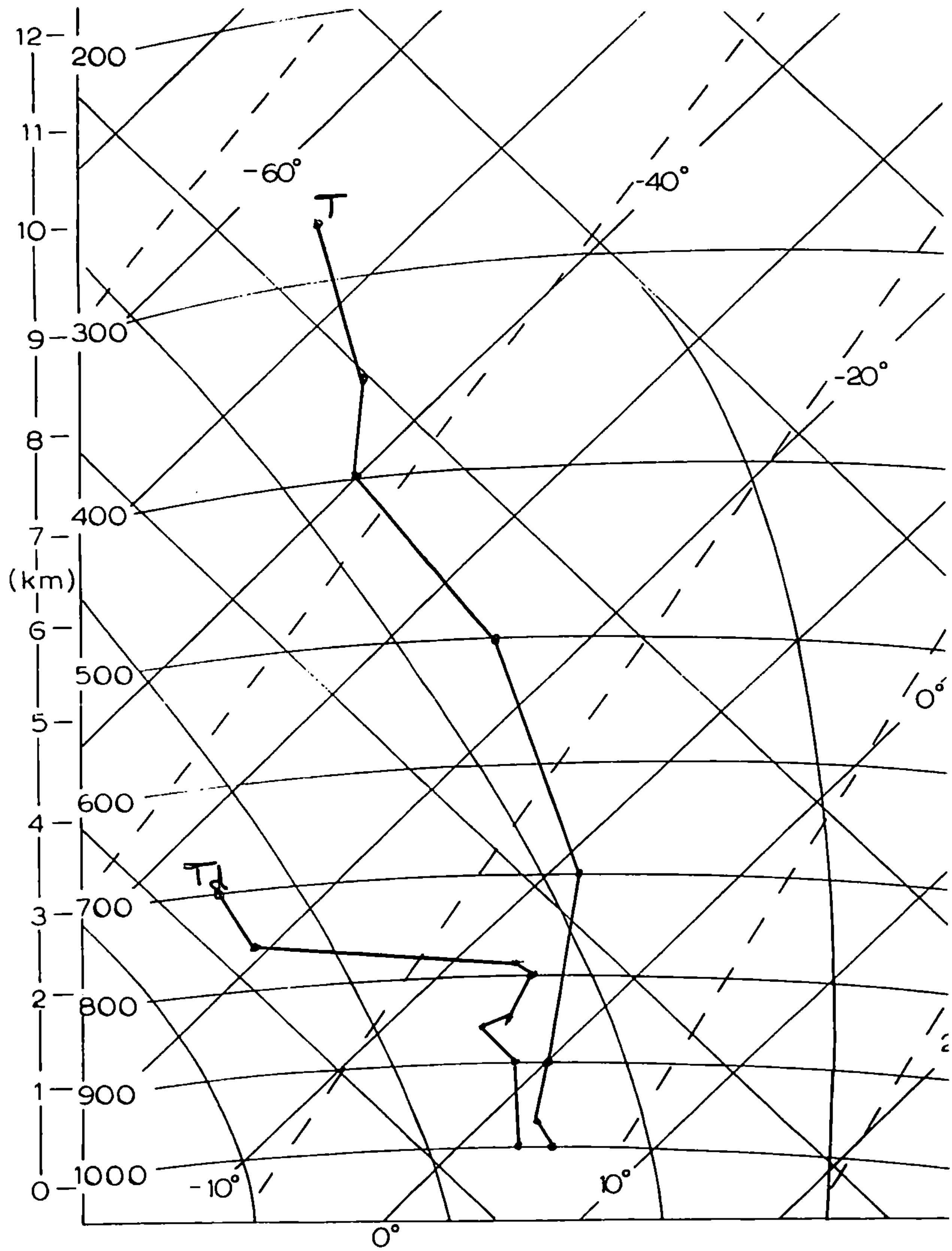

c. Uccle

Figure 3.2.2.2 Radiosonde ascents from 1100 UTC February 9th 1994

Trappes (near Paris)

From Figure 3.2.2.2a most cloud above Trappes occurred below 860 mb. Evidence of low level cloud between 1000 and 930 mb was supported by an environment lapse rate which occurred to the left of the saturated adiabatic lapse rate (ELR>SALR) which indicated conditionally unstable air (see Table 3.2.2.1). Absolutely stable air would have prevented any cloud from forming between 860 and 770 mb due to an inversion and dewpoint depressions of at least 20 deg. C. Although the atmosphere also appeared to be too dry between 760 and 720 mb for cloud to form due to dew point depressions larger than 15 deg.C, conditionally unstable air occurred in this region.

Low cloud showed up well in the infrared satellite imagery, despite it's shallowness. It is a known fact that not all low cloud can be remotely sensed by satellite, particularly when it's origin is early morning mist lifting which lifted.

Brest (Northwest France)

The ascent of air above Brest (Figure 3.2.2.2b) was significantly different from that above Trappes even though both sites were within the same air stream. Whereas parts of the atmosphere were rather dry above Trappes, above Brest it was very moist at almost all levels. Despite this, the lowest 500 mb of the atmosphere was generally stable, though above 700mb, conditionally unstable air occurred. The large moisture levels shown in Figure 3.2.2.2b were shown well by the corresponding satellite image of Brest

Uccle (near Brussels)

Figure 3.2.2.2c shows the ascent at Uccle, located within the warm sector with a very similar structure to that which occurred at Trappes. However low cloud at Uccle was 450 to 500 m deeper than at Trappes. The cloud top occurred between 780 and 800 mb at a height of 1.8 to 2.2 km despite high atmospheric stability from surface level to 3 km (Table 3.2.2.1), a kilometre above the assumed cloud top.

Table 3.2.2.1 Atmospheric stability above Trappes, Brest and Uccle at 1100 UTC Feb. 9th 1994, derived from Figures 3.2.2a, b and c.

Location and air pressure band / mb	Stability
Trappes: 1000-930	Conditionally unstable
930-900	Stable
900-860	Stable
860-770	Stable (Inversion)
770-720	Variable between stable and conditionally unstable
720-660	Stable
660-500	Variable between stable and conditionally unstable
Brest: 1000-700	Stable
700-300	Variable between stable and conditionally unstable.
Uccle: 1000-970	Conditionally unstable
970-700	Stable
700-400	Conditionally unstable.

Radiosonde ascents above other regions.

Radiosonde ascent data from Lerwick (Figure 3.2.2.1h.) clearly showed a showery airstream over Scotland as four individual cloud layers. Relationships between satellite imagery and radiosonde ascent data were strong in regions with little or no cloud shown by satellite. For example Nîmes in southern France was cloud free according to the satellite imagery, a fact strongly supported by a very dry radiosonde ascent (Figure 3.2.2.1e.), particularly at low levels. Relationships were weaker in other parts of the frontal system. One such region was Norfolk where radiosonde data from above Hemsby (Figure 3.2.2.1j.) showed very dry air situated above low level moist air. The satellite image tended to 'emphasise' the low level cloud, even though the thickness of air moist enough to form cloud was small.

3.2.3 Relationships between radiosonde derived flow data, geostrophic flow and cloud movement

Radiosonde ascents are a useful method of obtaining wind speeds with relatively little expense compared to using aircraft. Comparisons between radiosonde wind, geostrophic wind and cloud track speeds are shown in Table 3.2.3.1 which shows a wide variation in differences between geostrophic and radiosonde winds. For locations nearest the cold front, calculated geostrophic wind speeds were similar to radiosonde wind speeds with differences ranging from 0.2 ms^{-1} at 500 mb above Camborne to 9.7 ms^{-1} at 200 mb above Hemsby. Unfortunately, most geostrophic wind speeds were larger than actual radiosonde wind speeds. It is possible that errors occurred in measuring wind strength using radiosonde instruments, particularly in regions of wind speeds less than 5 ms^{-1} shown by the largest deviations in errors occurring at 850mb above Camborne, Valentia and Lerwick.

A cause of larger deviations which occurred above Valentia and Lerwick could have been due to the convective nature of a polar airstream behind the cold front. Individual cumulus or cumulonimbus cloud formations often have strong circulations within their structure whilst weak circulations may exist within clear sky windows less than 10 km away. Over smoothing of height contours or the use of too wide a spatial distance in calculating geopotential height gradients for the geostrophic wind also added a small error factor.

Table 3.2.3.1 Radiosonde and geostrophic wind speeds from 1100 UTC to 2000 UTC Feb. 9th 1994

Location	Radiosonde measured wind speed / ms^{-1}	Geostrophic wind speed / ms^{-1}
Camborne (SW England):		
200 mb	23.2	23.5±1.1
500 mb	18.0	18.9±0.7
850 mb	2.6	11.7±0.2
Hemsby (East Anglia):		
200 mb	25.7	16.7±0.7
500 mb	20.6	24.4±1.1
850 mb	10.3	11.7±0.2
Valentia (Ireland):		
200 mb	18.0	23.4±1.1
500 mb	15.4	28.4±1.6
850 mb	2.6	19.5±0.3
Lerwick (Scotland):		
200 mb	10.3	25.3±1.6
500 mb	7.7	35.1±2.9
850 mb	2.6	29.3±0.8

3.3 February 16th 1994 cloud tracking exercise

3.3.1 General Discussion

Geostrophic wind speeds at 200, 500 and 850 millibars were calculated using Equation 3.1.3.1, from analyses of geopotential height (Figures 3.3.1.2a, b and c). These results, shown in Table 3.3.1.2 were compared with cloud track speeds from the satellite image series shown in Figures 3.3.1.1a to d. A tabular summary is shown in Table 3.3.1.3.

Table 3.3.1.1 Meteosat derived cloud track data from Feb. 16th 1994

Location	Cloud feature	Time (UTC)	Displacement / km	Cloud speed / $ms^{-1} \pm 4.0$	Dir.
Northern Brittany, France	i)Southern edge of front.	1130-1430	125	11.6	N
			Mean:	11.6	
West of Eire	ii)First band of cloud of approaching system.	1130-1230	55	15.3	W
		1130-1330	85	11.8	W
		1130-1430	141	13.1	W
			Mean:	13.4	
100 km north of Norfolk coast	iii)Clear slot in thin cloud.	1130-1230	50	13.9	N
			Mean:	13.9	
The Midlands	iv)Thick cloud, 30-40 km width.	1130-1230	50	13.9	NW
			Mean:	13.9	
North coast of Spain	v)Coastal cloud band.	1130-1230	170	47.2	S
		1330-1430	100	27.8	S
			Mean:	37.5	
Southwest of Eire	vi)Approaching warm front.	1130-1230	70	19.4	W
		1230-1330	40	11.1	W
			Mean:	15.3	

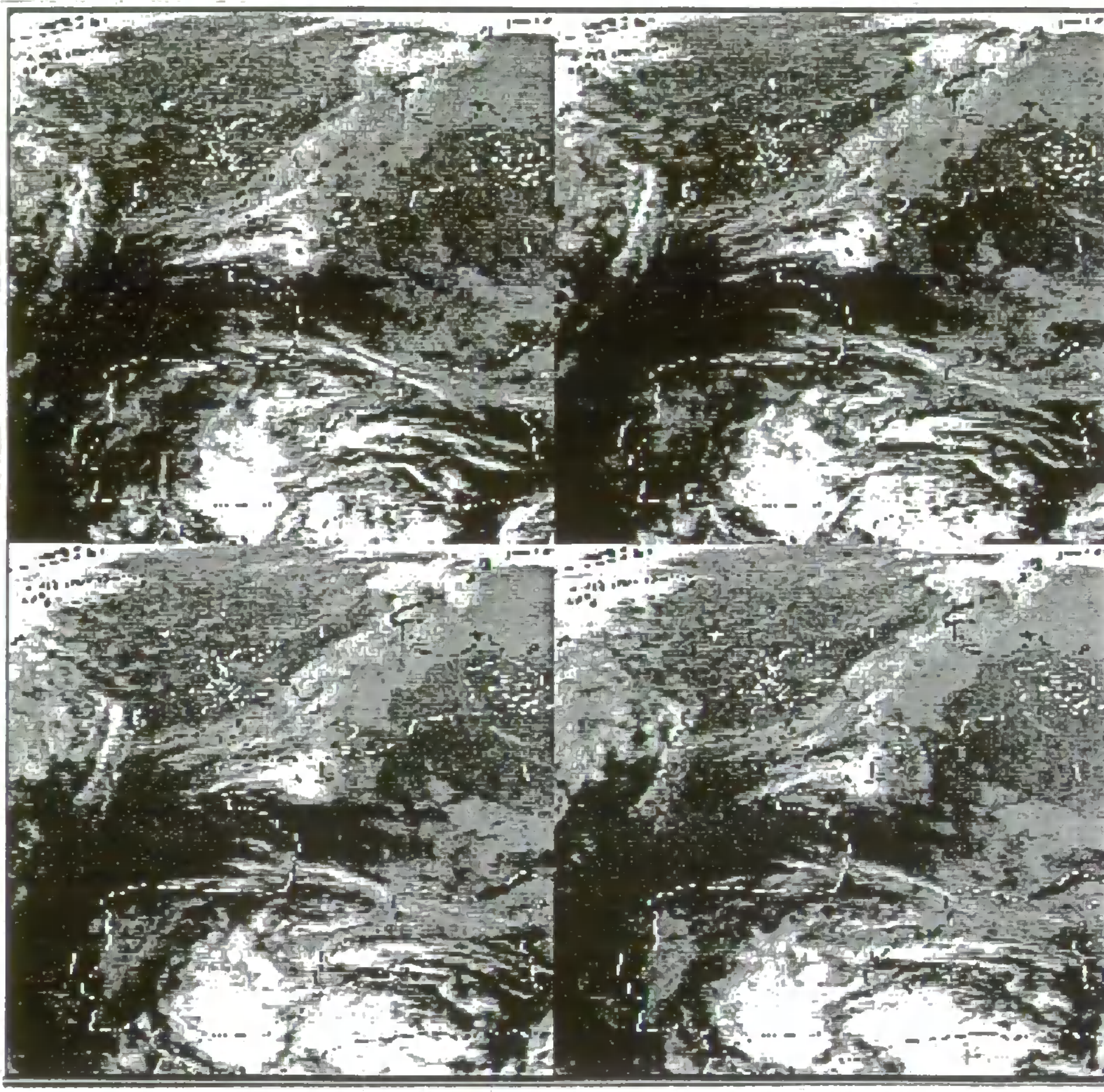

Figure 3.3.1.1 Infrared Meteosat imagery from
1130 UTC to 1430 UTC February 16th 1994

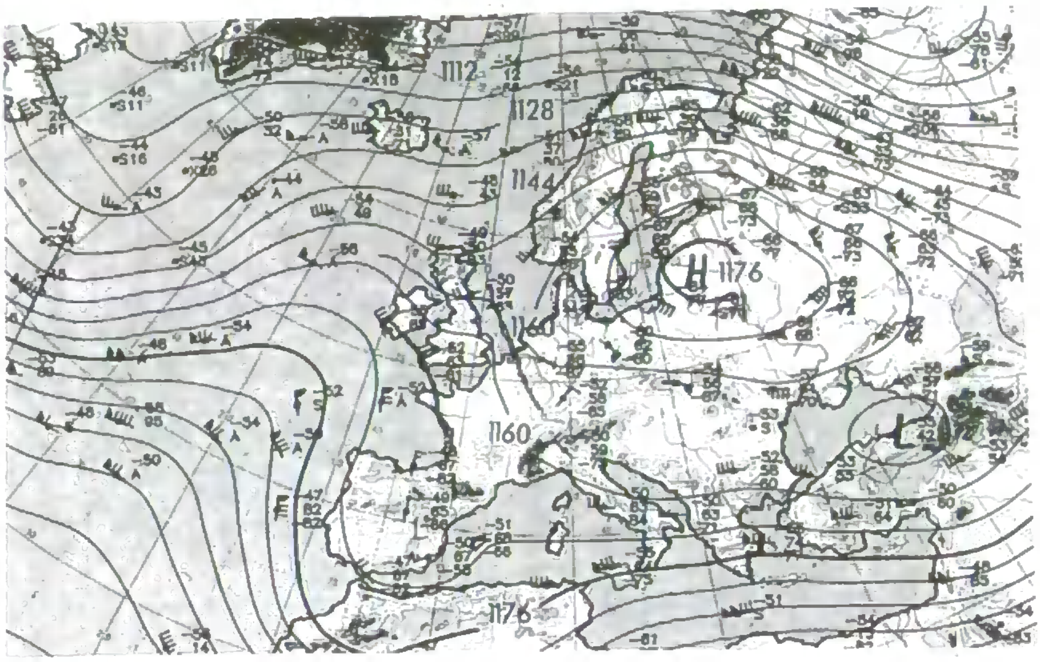

a. 200 mb

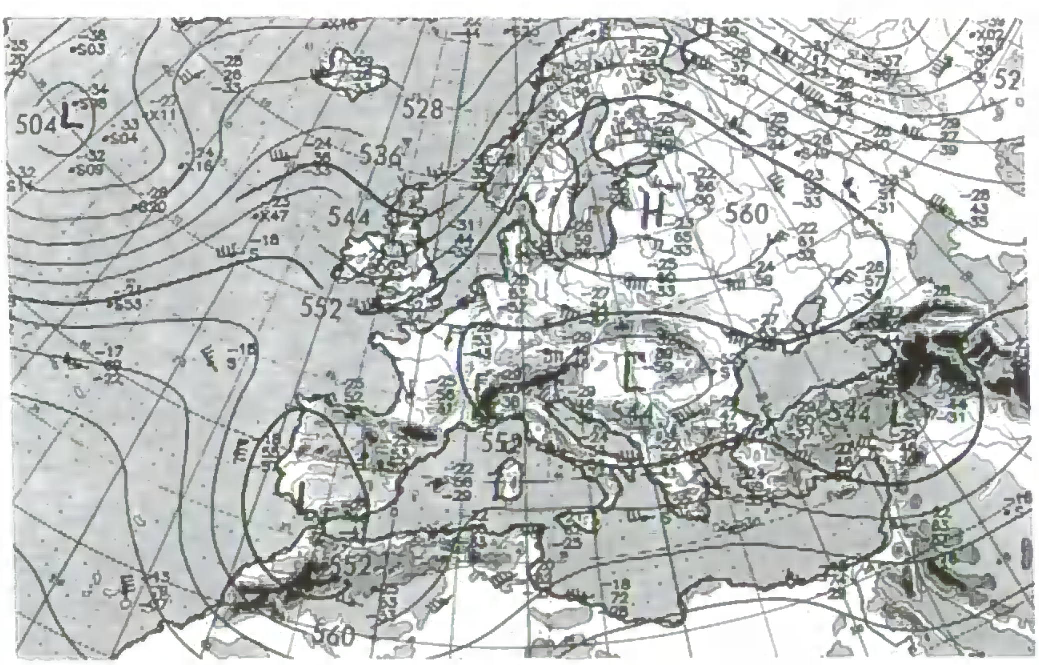

b. 500 mb

Figure 3.3.1.2 European Meteorological Bulletin geopotential height analyses from 1200 UTC Feb. 16th 1994

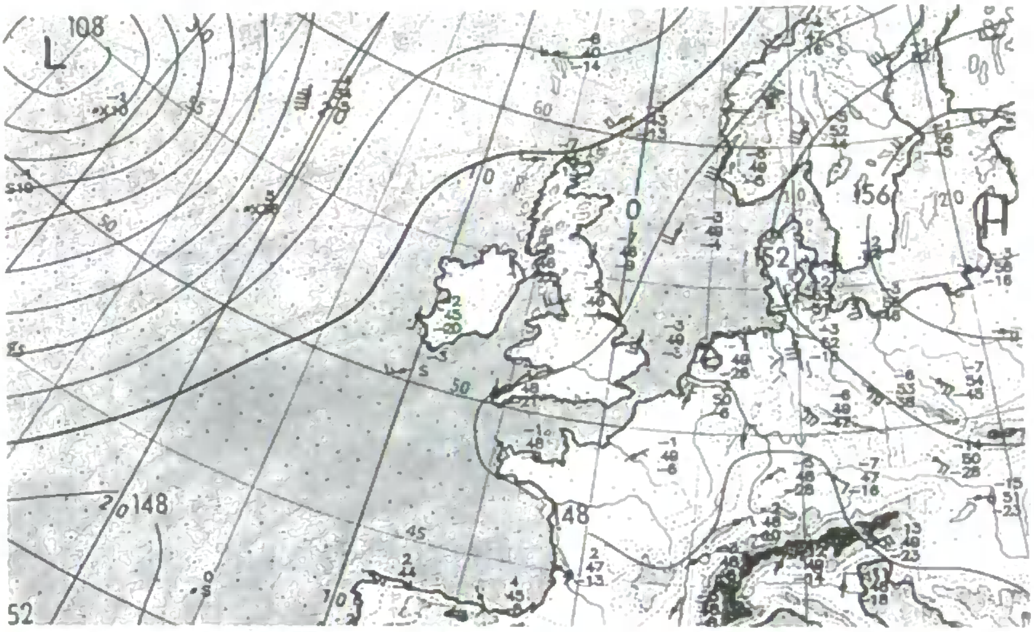

c. Geopotential height at 850 mb

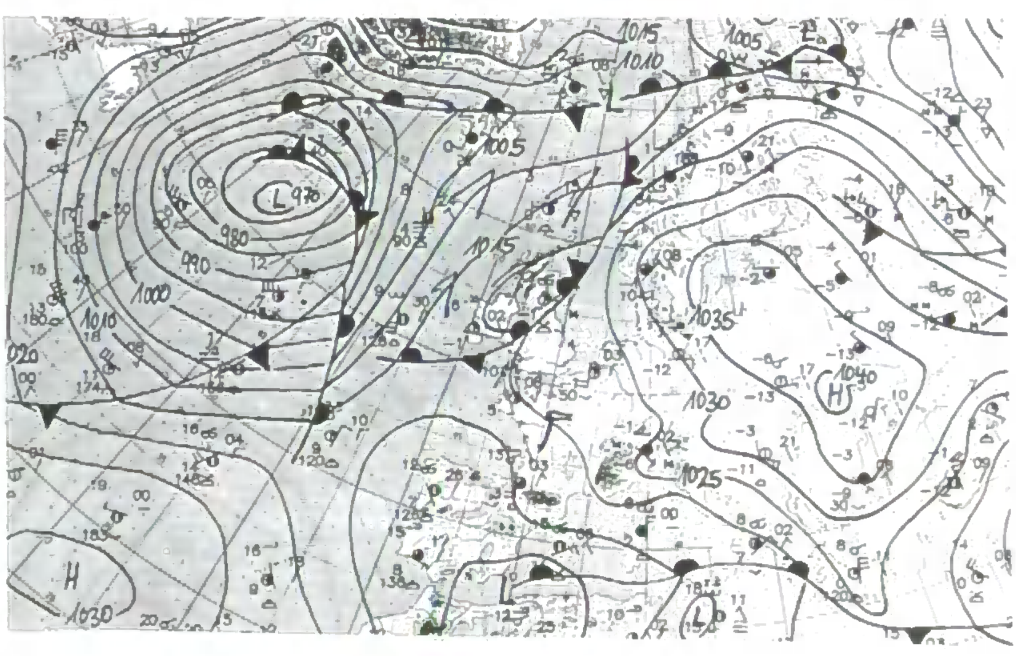

d. Surface pressure

Figure 3.3.1.2 European Meteorological Bulletin analyses
from 1200 UTC Feb. 16th 1994

Table 3.3.1.2 Geostrophic winds derived from EMB geopotential height analyses above selected regions at 1200 UTC Feb. 16th 1994

Location	Pressure level / mb	Geostrophic wind speed , V_g/ms^{-1}	V/V_{g850}	Wind direction (from)
Southwest England	200 500 850	7.6±0.1 11.4±0.3 5.9±0.1	1.3 1.9	N SW SW
Southern England	200 500 850	7.6±0.1 17.1±0.7 6.6±0.1	1.2 2.6	N SW SW
Southeast England	200 500 850	11.0±0.3 19.5±0.7 5.3±0.1	2.1 3.7	N SW S
Wales	200 500 850	11.8±0.3 15.2±0.7 <5.0	2.4 3.0	NW W SW
Northern England	200 500 850	11.4±0.3 14.5±0.3 4.9±0.1	2.3 3.0	W SW S
Ireland	200 500 850	14.6±0.3 14.5±0.3 5.0±0.1	2.9 2.9	NW NW S
Scotland	200 500 850	14.6±0.3 11.8±0.3 5.8±0.1	2.5 2.0	W W SW
Sea area Sole	200(E.Sole) 200(W.Sole) 500 850	17.5±0.7 46.8±4.5 11.4±0.3 5.3±0.1	3.3 8.8 2.2	N/W SW N/W/SW Var
Bergen, Norway	850	14.6±0.3	-	SW

Notes: N/W:- Northerly backing westerly

N/W/S:- Northerly backing westerly backing southerly.

Var:- Variable in direction

Table 3.3.1.3 Selected cloud displacements and geostrophic wind speeds at 1200 UTC Feb. 16th 1994

	Cloud ii	Cloud iii	Cloud iv	Cloud vi
Mean cloud speed / ms^{-1}	13.4±4.0	13.9±4.0	13.9±4.0	15.3±4.0
Geostrophic wind:-				
V_g at 200 mb / ms^{-1}	17.5±0.7* 47.0±4.5**	11.0±0.3	11.5±0.3	17.5±0.7* 47.0±4.5**
V_g at 500 mb / ms^{-1}	11.4±0.3	19.5±0.7	14.5±0.3	11.4±0.3
V_g at 850 mb / ms^{-1}	5.5±0.1	5.5±0.1	5.0±0.1	5.5±0.1

Note: *:- East Sole

**:- West Sole.

The 1200 UTC Feb. 16th EMB surface pressure analysis (Figure 3.3.1.2d) shows a weak, inactive, occluded front situated over Northern England and Wales which moved into England from the southeast but became stationary by 1200 UTC before it appeared to move back as a more vigorous Atlantic depression approached Ireland. Tracking cloud associated with this occluded front in the available infrared imagery was difficult. Cloud formations were shallow and scattered which made detection of suitable markers time consuming. At some locations, it was easier to track clear sky windows in cloud masses rather than actual cloud features.

Results in Table 3.3.1.1 showed frontal cloud movement to be less than 15 ms^{-1}. The geostrophic wind (Table 3.3.1.2) was also slow, especially at 850 and 200 mb, south of the occluded front where flows of less than 12 ms^{-1} occurred compared to 15 to 20 ms^{-1} at 500 mb. Table 3.3.1.3 showed cloud movement above southern England, south of the surface occluded front which correlated very well with the fastest atmospheric flow, especially at 500 mb where differences between geostrophic and cloud track wind speeds at some locations, were less than 5 ms^{-1}.

Cloud top brightness shown by Dartcom image analysis software produced further evidence that cloud most likely occurred at 500 mb. No cloud formations appeared dark enough to exist at 850mb.

As mentioned, a vigorous Atlantic system approached Ireland. The leading edge of a warm front associated with the system was easy to detect and track due to a lack of any major cloud formations ahead of it. Because of the forward sloped nature of warm fronts, its leading cloud edge was represented best by flow at 200 mb rather than at 850 or 500 mb. South-westerly winds at 200 mb above sea area Sole became very strong whilst low level winds remained light. However, the speed of cloud approaching Ireland was no different to that of cloud *not* associated with the approaching depression and was similar to the 200 mb flow.

At first, rapid cloud motion appeared to occur above northern Spain. However the local topography and unsettled weather indicated that cloud above this region may have ceased to exist whilst new cloud formed out at sea. This produced an illusion of translation in an offshore direction. Cloud track speeds in this region were consequently prone to errors. Furthermore, northerly flow at upper levels above this area would have prevented cloud at 200 mb from moving out to sea in this region.

3.3.2 Radiosonde ascent data

Comparisons between EMB radiosonde derived cloud top heights were compared with infrared Meteosat image brightness determined by the Dartcom software. Six stations, Stavanger, Lerwick, Valentia, Uccle, Trappes and Lyon, required conventional tephigrams (Figures 3.3.2.2a to e) due to inconclusive EMB ascent charts (Figures 3.3.2.1j, m, s, h, q, u.) in order to ascertain cloud top levels:

Results from this exercise are shown in Table 3.3.2.1.

Results of this exercise (Figure 3.3.2.3) showed up a problem:- most cloud tops were at low levels despite moderate values of cloud image brightness. Unfortunately, this range of cloud top levels was too small to form any firm conclusions. Despite this, cloud top levels appeared to be related very strongly to image brightness *within* the small range of brightness levels recorded.

The exercise was repeated with a few alterations so as to deliberately provide results with a wider range of brightness levels. Locations were chosen depending on their local cloud brightness level and attempting to determine the cloud top level using nearest ascent site data.

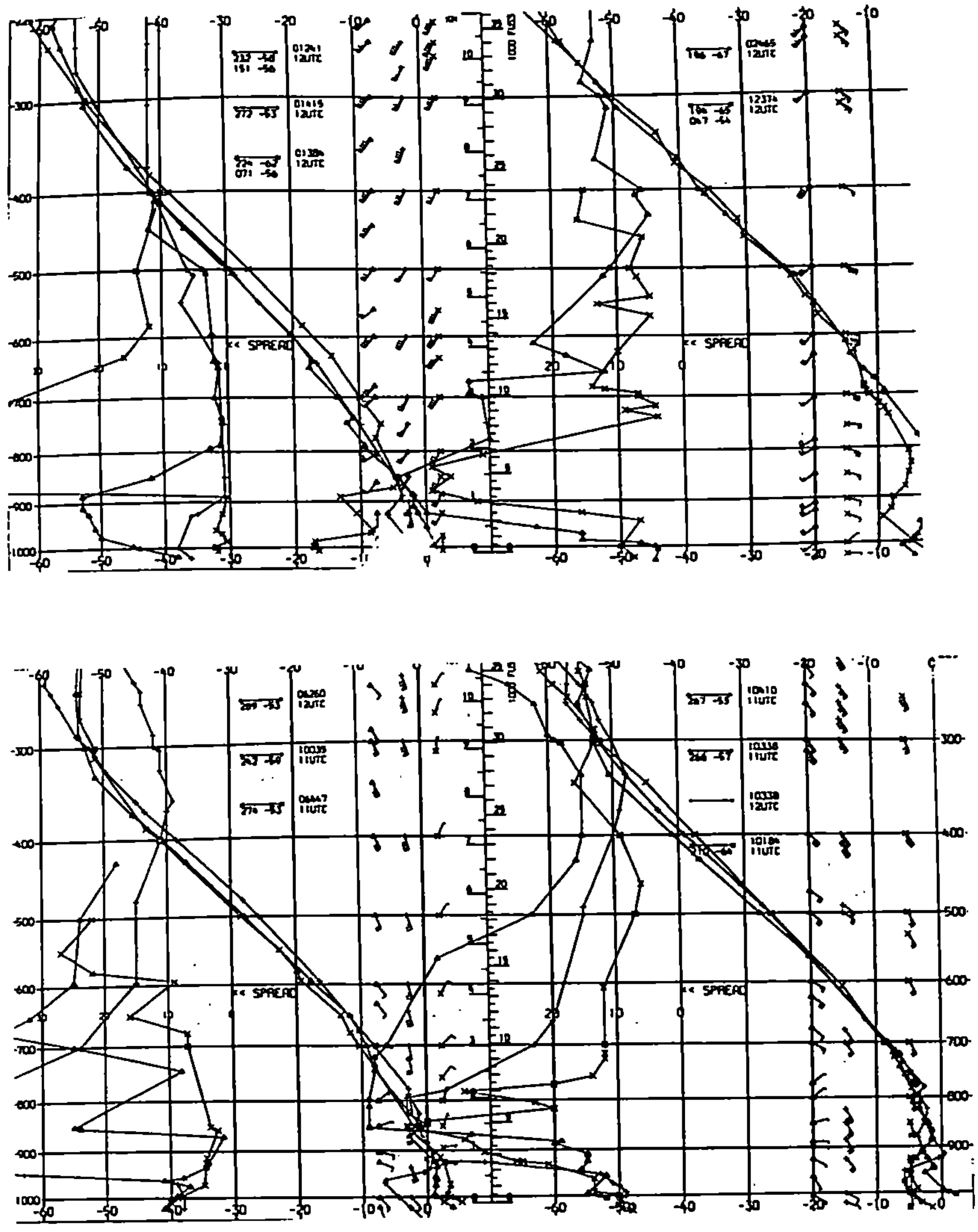

Figure 3.3.2.1 European Meteorological Bulletin radiosonde ascents from 1200 UTC February 16th 1994

Station numbers:- (Locations shown in Appendix 1)

a. 01241	Orland	g. 10035	Schleswig
b. 01415	Stavanger	h. 06447	Uccle
c. 01384	Oslo	i. 10410	Essen
d. 02465	Stockholm	j. 10338	Hannover
e. 12374	Legionowo	k. 10184	Greifswald
f. 06260	De Bilt		

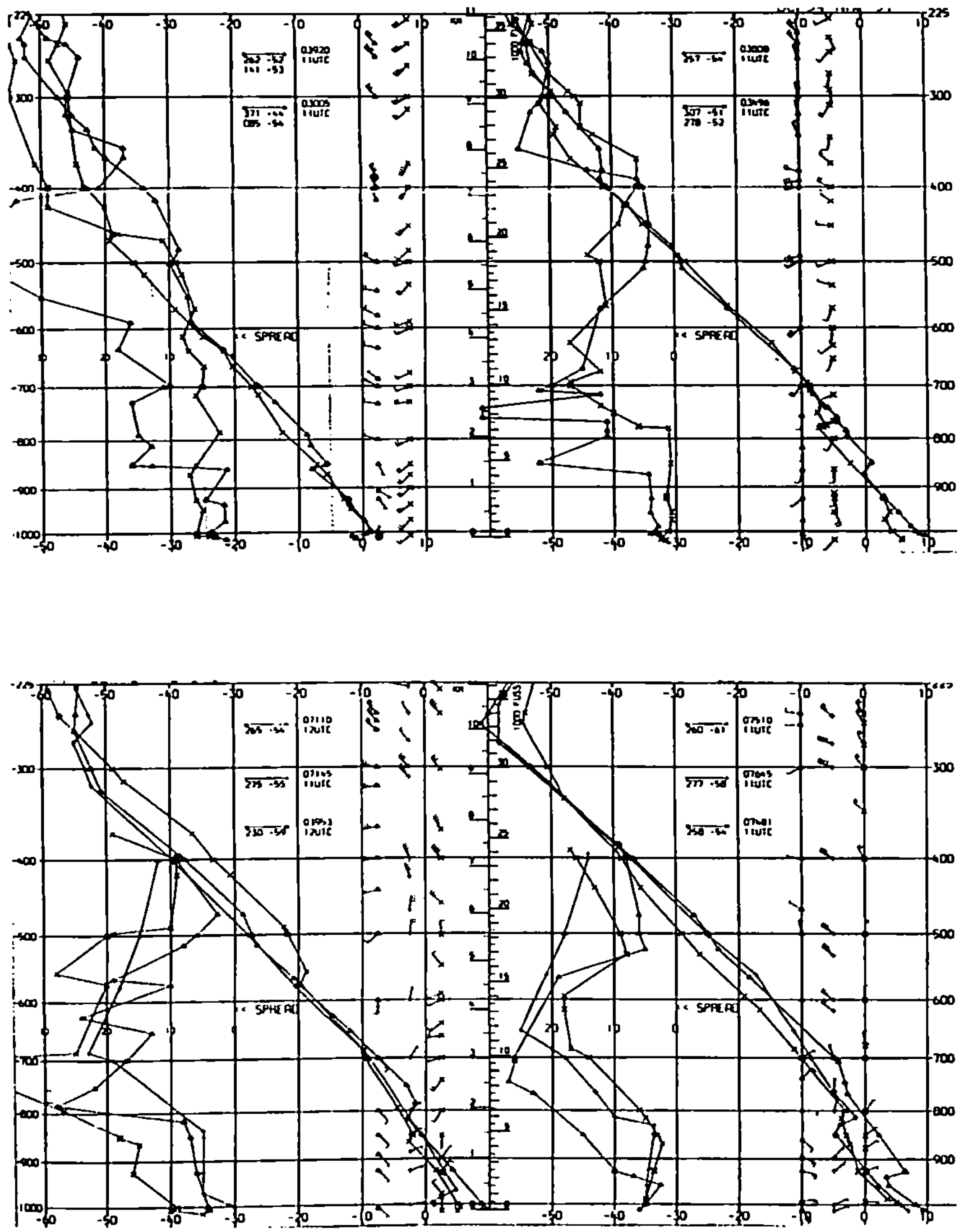

Figure 3.3.2.1 European Meteorological Bulletin radiosonde ascents from 1200 UTC February 16th 1994

Station numbers:- (Locations shown in Appendix 1)

l. 03920	Long Kesh	q. 07145	Trappes
m.03005	Lerwick	r. 07510	Bordeaux
n. 03808	Camborne	s. 03953	Valentia
o. 03496	Hemsby	t. 07645	Nimes
p. 07110	Brest	u. 07481	Lyon

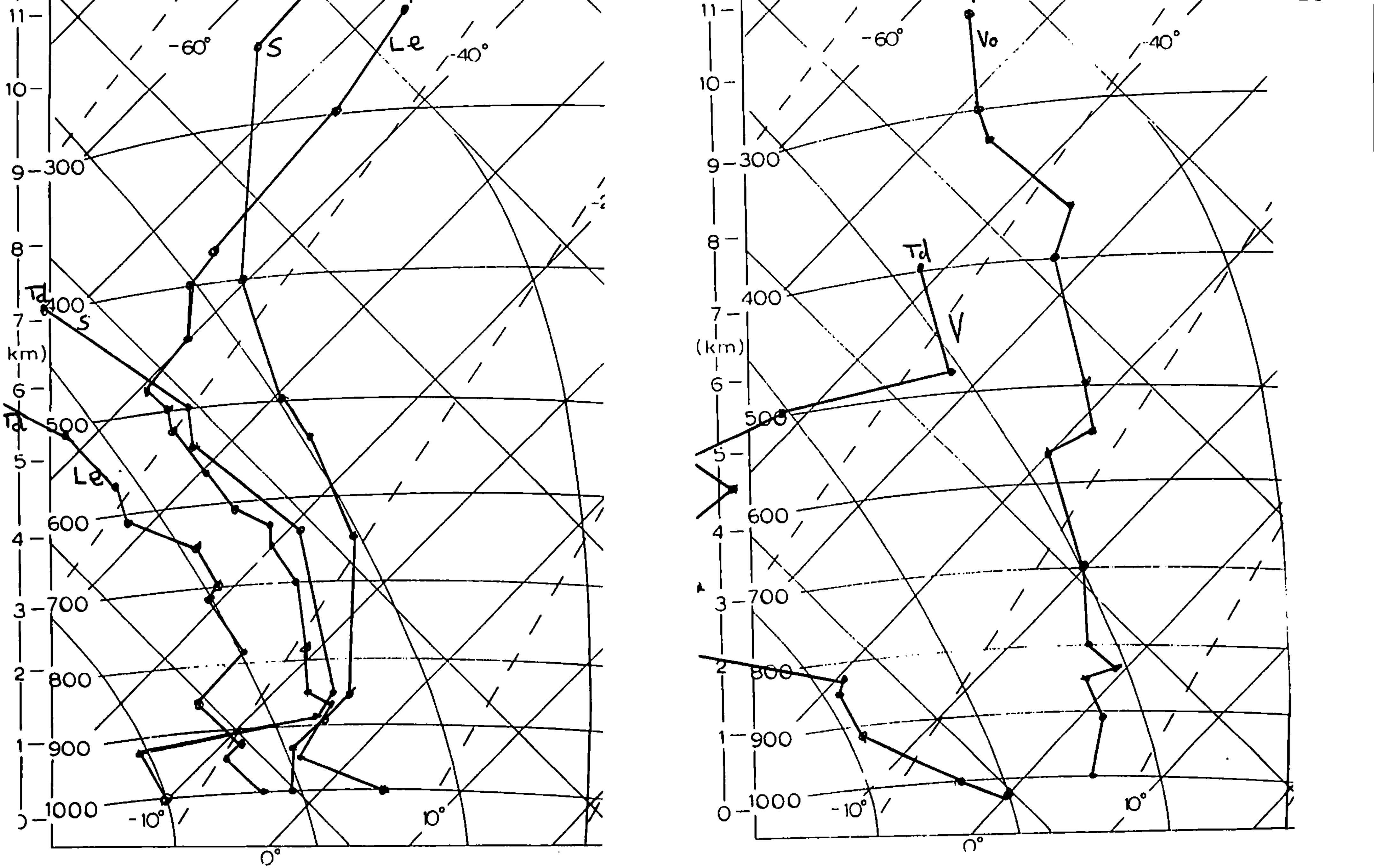

Figure 3.3.2.2 Radiosonde ascents from 1100 UTC February 16th 1994

a. Stavanger (S) **b. Lerwick (Le)** **c. Valentia (V)**

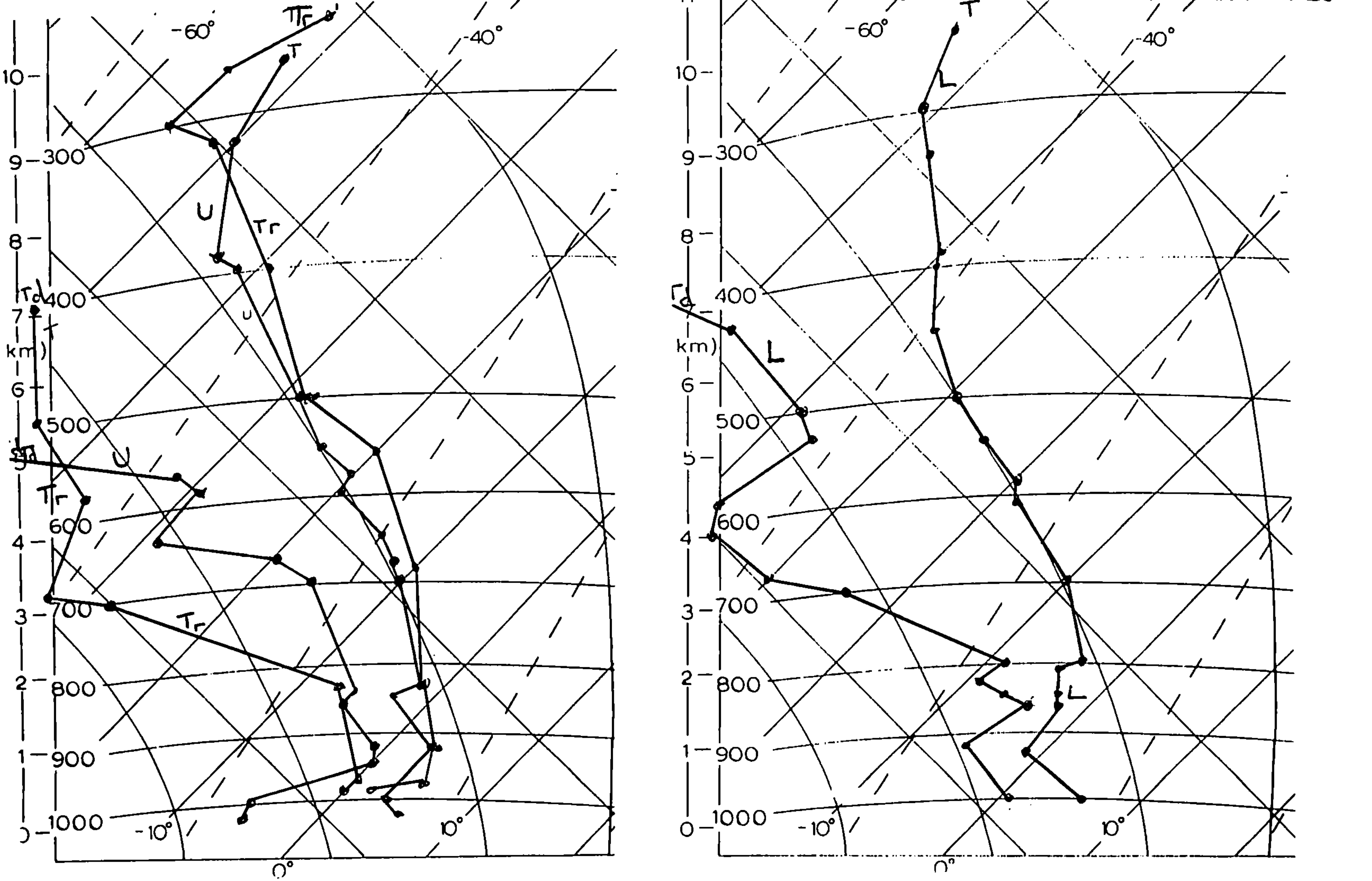

Figure 3.3.2.2 Radiosonde ascents from 1100 UTC February 16th 1994

d. Uccle (U) **e. Trappes (Tr)** **f. Lyon (L)**

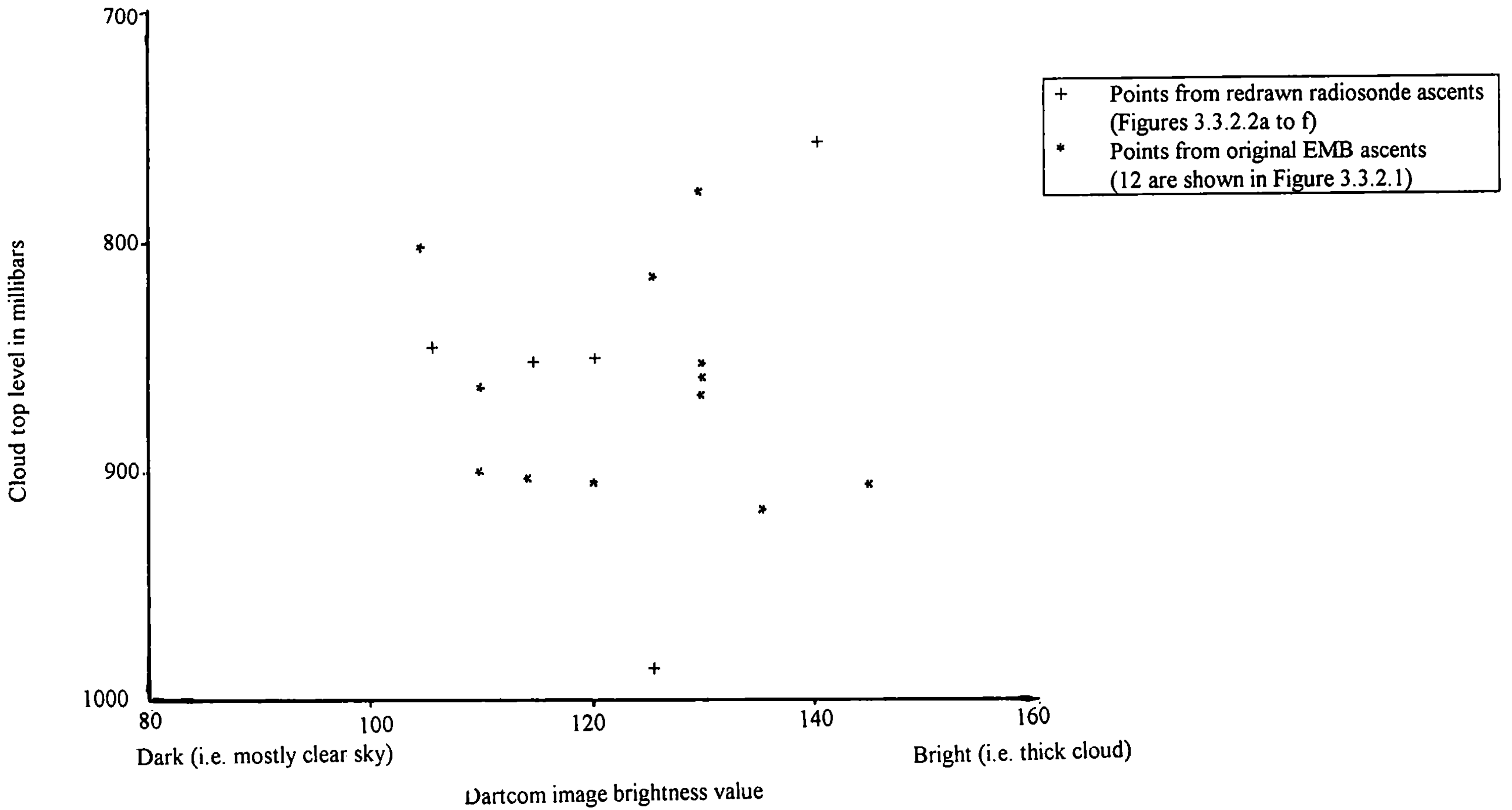

Figure 3.3.2.3 Cloud brightness versus probable cloud top level at 1200 UTC February 16th 1994

Table 3.3.2.1 Radiosonde derived cloud tops and infrared satellite image brightness between 1100 and 1200 UTC Feb. 16th 1994.

Site	Figure showing ascent	Cloud top level / mb	Image brightness
1)Stavanger	3.3.2.2a	600±50	150±5
2)Stockholm	not shown	905±5	145±5
3)Gothenburg	not shown		
4)Lerwick	3.3.2.2b	760±10	140±10
5)Hemsby	3.3.2.1o	780±10	130±10
6)Camborne	3.3.2.1n	860±10	130±5
7)Longkesh	3.3.2.1l	855±5	130±5
8)Valentia	3.3.2.2c	850±5	115±5
9)Copenhagen	not shown	905±5	120±10
10)De Bilt	3.3.2.1f	860±10	110±5
11)Uccle	3.3.2.2d	845±5	105±10
12)Payerne	not shown	865±5	130±15
13)Brest	3.3.2.1p	800±10	105±10
14)Trappes	3.3.2.2e	985±5	125±10
15)Lyon	3.3.2.2f	850±10	120±10
16)Bordeaux	3.3.2.1r	920±10	135±10
17)Nîmes	3.3.2.1t	815±5	125±10
18)Greifswald	3.3.2.1k	900±10	110±10
19)Dresden	not shown	900±10	115±10

Although, this would weaken any relationships due to varying spatial distances between station and cloud pixel location, it is worth noting that radiosonde balloons usually drift horizontally as well as vertically and therefore *may* actually move towards some cloud pixel locations. Most radiosondes take at least 20 minutes to reach upper atmospheric levels. Results of this latest exercise are shown in Table 3.3.2.2 and by Figure 3.3.2.4

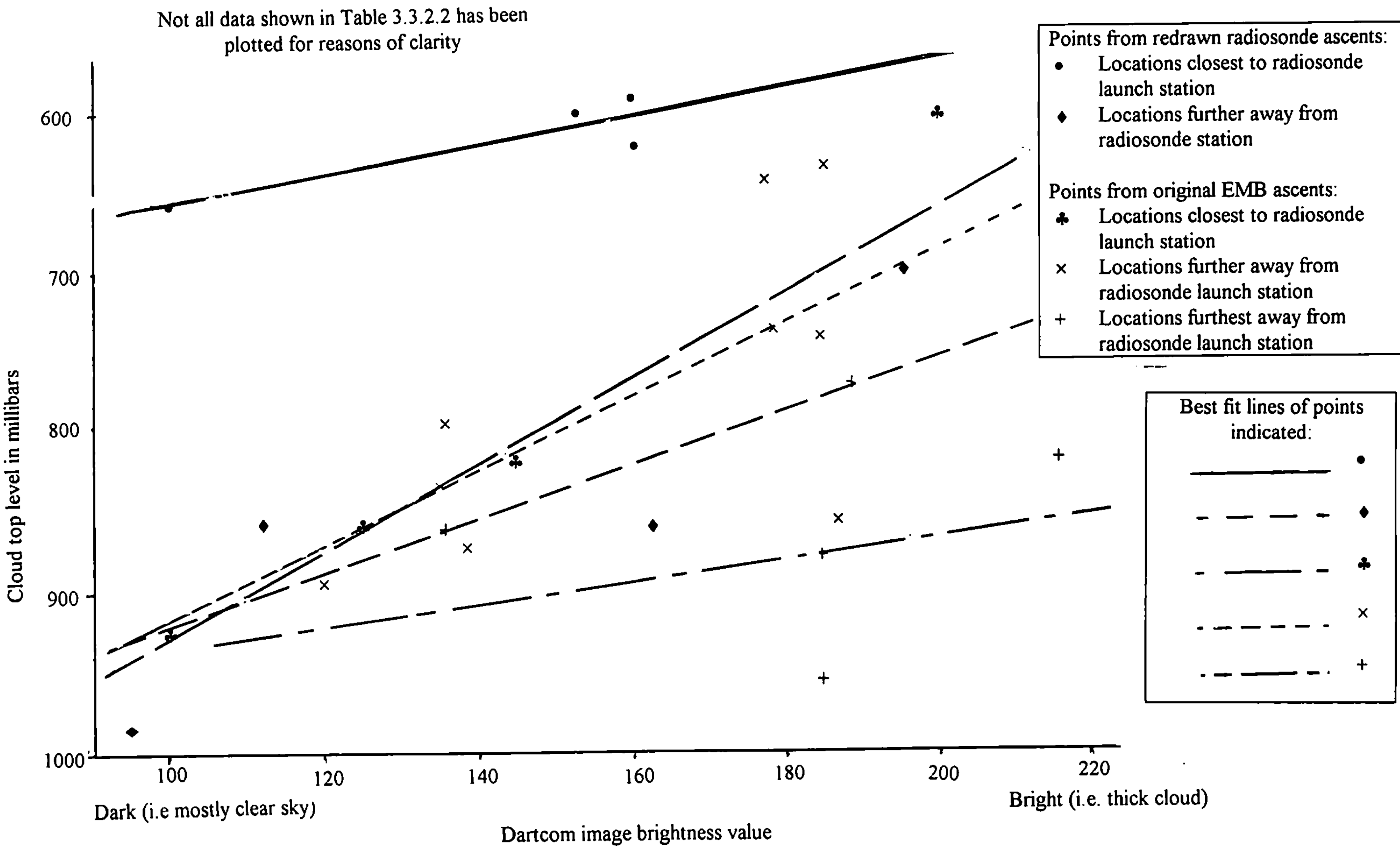

Figure 3.3.2.4 Cloud brightness versus probable cloud top level at 1200 UTC February 16th 1994 (version 2)

Table 3.3.2.2 Cloud brightness and likely cloud top levels between 1100 and 1200 UTC Feb. 16th 1994.

Location of cloud pixel	Cloud brightness	Nearest radiosonde ascent	Distance d/km (see below)	Likely cloud top level / mb
1. Corsica	91	Rome	400	N/A
2. Biscay	95	Bordeaux	200	925±5
3. NW France	95	Trappes	240	985±5*
4. SE France	98	Lyon	140	800±10*
5. Belgium	100	Uccle	30	660±10*
6. SW France	100	Bordeaux	0	925±5
7. S France	103	Nîmes	180	820±10
8. W Eire	112	Valentia	250	860±10*
9. Denmark	120	Copenhagen	210	920±10
10. Germany	120	Dresden	120	900±10
11. Scotland	125	Shanwell	210	N/A
12. N Ireland	125	Longkesh	60	860±5
13. Brittany	135	Brest	100	800±10
14. N Wales	136	Longkesh	450	860±5
15. Austria	138	Munich	110	870±10▽
16. S France	145	Nîmes	20	820±10
17. Norway	153	Stavanger	60	600±50*
18. Shetland	160	Lerwick	40	590±5* 620±5*
19. Southern Irish Sea	162	Valentia	250	860±10*
20. Cardigan Bay	170	Camborne	210	860±10
21. North Sea	170	Lerwick	210	590±5 620±5
22. NE England	171	Shanwell	500	N/A
23. Mid Norway (65° North)	178	Orland	140	640±5▽ 740±5†
24. Mid Norway (62° North)	185	Orland	140	640±5▽ 740±5†
		Oslo	300	875±10▽ 960±10†
25. Norwegian Sea	185	Orland	800	640±5▽ 740±5†
26. S Wales	187	Camborne	170	860±10
27. Cornwall	188	Camborne	100	860±10
28. The Midlands	188	Hemsby	480	775±5
29. English Channel	190	Camborne	220	860±10
30. N France	195	Trappes	220	700±5*
31. Sussex	195	Hemsby	210	775±5
32. Iceland	199	Keflavik	20	600±10
33. S Spain	215	Lisbon	600	N/A
34. Majorca	216	Nîmes	450	820±10
35. N Norway	222	Orland	850	640±5▽ 740±5†

Notes:

$^{\nabla}$ Cloud top height based on dewpoint and instability profile, † : cloud top based on instability only,

* : cloud top levels derived using the fully redrawn tephigrams of Figures 3.3.2.2a to f.

d : horizontal distance between the studied cloud pixel and the nearest radiosonde launching station.

The legend of the graph in Figure 3.3.2.4 shows the accuracy of results based on horizontal distance between cloud pixels and radiosonde launch site and whether likely cloud top levels were derived from EMB ascents (Figure 3.3.2.1) or redrawn tephigrams (Figures 3.3.2.2a to f)..

Figure 3.3.2.4 shows a weak relationship between cloud top height and cloud brightness. Four out of six best fit lines produced using least squares regression showed a general increase in image brightness with increasing cloud top height above the surface. Thus:-

Cloud brightness $\propto$ cloud top height $\propto$ (1000-cloud top level in millibars)

3.3.3 Comparison between cloud brightness above Plymouth and ground based observations

The Dartcom software registered the following cloud brightnesses above Plymouth:- (all times UTC)

156±1 at 11:30

168±2 at 12:30

178±4 at 13:30

172±2 at 14:30

(based on a scale of 0-255 where increasing number indicates brighter pixels.)

Table 3.3.3.1 shows corresponding cloud observations taken from the ground by the Plymouth Weather Centre which showed that during the period in which the satellite pictures were taken, the cloud cover changed little. This lack of change correlated well in very small variations in these four cloud brightness values quoted above.

It must be pointed out that ground based observations are taken from *below* cloud and obviously report features more prominent at cloud base rather than cloud top, where as satellites view cloud formations from *above*.

Divergence between the two sets of observations would have varied depending on cloud thickness and type. For instance, thick cumulonimbus would produce the largest deviations whilst thin alto-stratus would produce more similar sets of results.

Table 3.3.3.1 Surface based cloud observations from the Plymouth Weather Centre from Feb. 16th and 17th 1994

Time (UTC)	Total cloud cover in oktas	Cloud amount /oktas, type and level / mb	
		1000 to 700 mb	Above 700 mb
1200 Feb. 16th	7	2 St(900)	7 Ci(470)
1300	7	1 St(970)	7 Ci(470)
1400	7	1 Sc(940)	7 Ci(470)
1500	6	1 Sc(940)	6 Ci(470)
1600	6	-	6 Ci(470)
1700	5	1 Sc(940)	1 Ac(570) 5 Ci(470)
1800	6	2 St(980)	2 Ac(570) 5 Ci(470)
1900	6	1 St(980)	6 Ci(470)
2000	2	-	2 Ci(480)
2100	?	?	?
2200	7	7 Sc(940)	-
2300	8	8 Sc(950)	-
0000 Feb. 17th	7	7 Sc(980)	-
0100	7	2 St(960) 7 Sc(980)	-

3.4 Case study summary and conclusions

3.4.1 February 9th 1994

- Difficult to select suitable cloud tracers:- only three were deemed trackable. Cloud formations in Southern England moved at speeds most similar to geostrophic flows at 500 and 200 mb. Variations in cloud movement were small. Table 3.2.1.3 showed a range of 18 ms^{-1} to 26 ms^{-1}, probably due to all three locations being part of the same cold front. Small differences were due to the sloped nature of the cold front.

- A clearing cold front over Southern England gave an excellent example of rapid cloud clearance after the front had passed, shown by cloud observations taken from surface level by a met observer at the Plymouth Weather Centre. These results showed that despite advanced technology, ground based observations by humans are still an invaluable part of cloud observation.

Conclusions from ascent data

- Ascent data showed large ranges in humidity either side of the cold front (Figures 3.2.2.1 and 3.2.2.2). Cloud tops behind the front were much easier to determine compared to within the warm sector ahead of the front.

- Large variations in cloud top height within the same air mass, shown by cloud only forming at low levels above Trappes, (see Figure 3.2.2.2a), whilst above Brest (Figure 3.2.2.2b), cloud had formed at upper levels as well.

- Thick cloud can exist in stable air, shown by the ascent above Uccle in Figure 3.2.2.2c and Table 3.2.2.1.

- Infrared satellite imagery over-emphasised the thickness of low level cloud.

• Comparisons between radiosonde measured flow and calculated geostrophic winds gave mixed results, though producing firm evidence of relationships between the two. However, differences between measured and calculated geostrophic winds were smaller at locations closer to the front. The lack of further relationships being detected was attributed to large spatial distances between sonde launch sites and the fact that wind speeds from only one occasion (1100 or 1200 UTC) were available.

3.4.2 February 16th 1994

• Cloud movement was most like the geostrophic flow at 500 and 200 mb (Table 3.3.1.3).

• Cloud formations near the northern coast of Spain showed a potential problem in cloud tracking due to an ability of cloud to form quickly at one location whilst evaporating nearby giving illusions of cloud movement. The occurrence of this problem was realised quickly using wind direction data. Since cloud north of Spain appeared to move against the wind, the track results were deemed meaningless at this location.

• Cloud brightness/cloud top level comparisons derived from radiosonde data showed a need for a wide spread of brightness 'input' values for any relationships to be detected. Cloud brightness was related to cloud top height, giving a straight line graph (Figure 3.3.2.4) of the form:-

$$y=mx+c$$

where,

x = cloud brightness,

y = cloud top height,

c = constant (intercept of 'y' axis),

and m = slope of straight line.

Chapter 4 Surftemp and Roadsurf

Surftemp, a one dimensional balance model was developed during the early 1970s (Outcalt, 1971). It was originally written to represent energy fluxes which would normally occur in a surface-atmosphere system shown in Figure 4.1.1 and to predict surface temperatures. The fundamental structure behind the model's mechanism has generally remained unchanged since 1970, though modifications have been made and additional features added to take account of cloud cover for example.

The principles of the model are based on solving an equation form of the energy balance equation (4.1), visualised in figure 4.1.1:-

$$\text{Net radiation flux} = H + LE + GHF \qquad 4.1$$

where H = sensible heat flux,

LE = latent heat flux,

GHF = ground heat flux.

Net radiation flux

This is the combination of net solar radiation and net thermal radiation emitted by the Earth's surface out to space and is represented by:-

$$\text{Net radiation} = (1 - \text{albedo})\, S - \sigma\, KCLOUD\, \varepsilon\, Ts^4 \qquad 4.2$$

where σ = Stefan Boltzmann constant (5.67×10^{-8} W m^{-2} K^{-4})

ε = combined emissivity of surface and sky

$= 0.18 + 0.25 \times 10^{-0.126v}$

and Ts = surface temperature

S is the downward solar radiation incident on the surface and consists of three components:-

'Direct' beam:- The energy from a direct beam from the sun which reaches the surface

'Diffuse' radiation:- Solar radiation which reaches the surface after passing through clouds

'Back-scattered' radiation:- Radiation which is scattered back to the surface by clouds and the atmosphere.

All three terms are dependent on cloud cover, especially the direct beam which reduces with increasing cloud, so that it is zero during overcast conditions.

The term denoted by ε in equation 4.2 represents the combined emissivity of the surface and sky. A further term, KCLOUD is dependent on cloud cover amount and height and humidity of the atmosphere at 3m. During cloud increase, less energy emitted by the Earth's surface is able to escape to space and hence the magnitude of σ KCLOUD εTs is reduced.

Sensible heat flux, H

This is the heat transported as a result of a vertical temperature gradient between the atmosphere and surface and is parameterised in Surftemp by:-

$$H = D_h \, UA \, (TA + DRYADB \, Za - Ts) \qquad 4.3$$

where UA = 2m wind speed (ms^{-1}),

DRYADB = dry adiabatic lapse rate ($K \, m^{-1}$)

Za = damping depth (m).

D_h = bulk transfer coefficient for convective heat transfer ($kJ \, m^{-3} \, K^{-1}$)

= EXXO κ

EXXO is a dimensionless parameter related to atmospheric stability and κ is the latent heat capacity of the atmosphere (kJ m^{-3} K^{-1}).

Latent Heat Flux, LE

This term arises due to condensation of water vapour present in the atmosphere and evaporation of water at the surface and is parameterised in Surftemp by:-

$$LE = D_e\, UA\, (e_a - e_s) \qquad 4.4$$

where D_e = bulk transfer coefficient for latent heat transfer (kJ m^{-3} mb^{-1}),

UA = wind speed at 3m (ms^{-1}),

e_a = vapour pressure of the air (mb)

and e_s = vapour pressure at the surface temperature Ts (mb)

Ground heat flux, GHF

The ground heat flux is the energy which passes between the ground of temperature TH and the surface by conduction and is parameterised in Surftemp by the following series of iteration terms:-

ZT=ZG/2

ZZ=ZT/2

ZX=ZZ/2

ZU=ZX/2

*TT(i)=TT(i-1)+RD((T(i-1)-2TT(i-1)+TH)/(ZT*ZT))*1.2E3*

*TZ(i)=TZ(i-1)+RD((T(i-1)-2TZ(i-1)+TT(i-1))/(ZZ*ZZ))*1.2E3*

*TX(i)=TX(i-1)+RD((T(i-1)-2TX(i-1)+TZ(i-1))/(ZX*ZX))*1.2E3*

*TU(i)=TU(i-1)+RD((T(i-1)-2TU(i-1)+TX(i-1))/(ZU*ZU))*1.2E3*

S(i)=(RK/ZU)(TU(i)-T(i))*

(where i = a dummy variable, TT, TZ, TX and TU are temperatures and ZT, ZG, ZX and ZU are depths.)

These forced a time delay between energy transfer between the ground and surface and changes in temperature at the surface. Obviously, heat will flow from the ground layer to the surface if the ground is warmest.

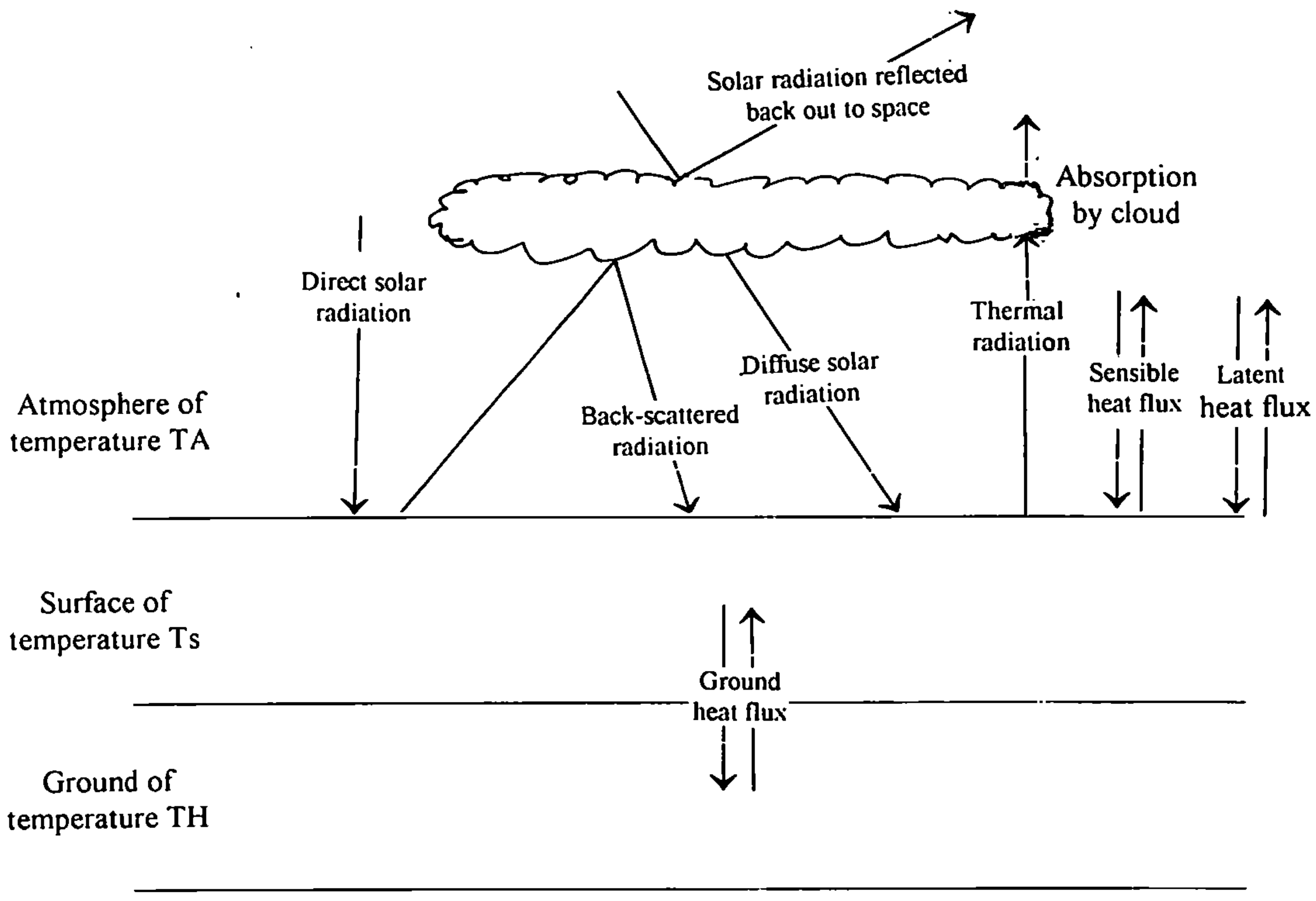

Figure 4.1.1 Ground-atmosphere set-up on which Surftemp was based.

Sensitivity tests carried out on Surftemp (Chapter 5) revealed a spurious prediction which was considered to be a result of the iterations in the ground heat flux equations. Surftemp was thus modified, to become 'Roadsurf', by removing these iterations and using finite differencing methods to predict surface temperature.

It was decided to create two new layers of ground material situated di ectly below the surface to form an atmosphere-ground system with two sub-surface layers. The resulting two layers of ground material were assigned fixed depths based on individual thicknesses of an average road surface and are denoted by D2 and D3 in any equations and diagrams. The surface was attributed a finitely small thickness in order so that heat transfer equations (to be derived later) were able to correctly compute temperatures without problems of runaway results. Horizontal areas of all three layers of 'ground' were considered to be unity.

Atmosphere of temperature Ta (fixed)

///////////////////////////**Surface** of temperature Ts (varying)/////////////////D1//////

↑

'd' layer of temperature Td (varying) D2

↓

↑

'cl' layer of temperature, Tcl (varying) D3

↓

Positive direction of all fluxes is downward. Hence negative fluxes are directed upwards.

Figure 4.1.2 New atmosphere-ground set-up.

Finite differencing equations.

If there is a temperature difference between two materials which are in physical contact, heat will try to flow from warmer material into cooler material in order to create a balance. This heat flow is due to conduction and therefore, the rate of heat transfer is highly dependent on the conductivity of material of the ground. This heat flow may be represented by an equation of the form:-

$$\text{Flux of heat} = \kappa\frac{\partial T}{\partial z} = Mc\frac{\partial T}{\partial t} \qquad 4.5$$

where, κ = thermal conductivity,

$\partial T/\partial z$ = subsurface lapse rate, M = mass of ground layer,

c = specific heat,

and $\partial T/\partial t$ = change in temperature with time.

($\partial T/\partial t$) can be approximated by a number of 'finite difference' expressions having varying degrees of accuracy with errors dependent largely on time interval, ∂t. Finite difference equations are sometimes known as 'time difference' equations.

Derivation of surface temperature finite difference equations.

The surface receives and emits radiation from and to the atmosphere and beyond so a term specifically representing incoming solar radiation will be represented by ΣF in any finite difference equations.

As well as energy fluxes interacting with the surface from above, there are also heat fluxes interacting between the surface and 'd' layer below. If we let *Ts* and *Td* be surface and 'd' layer temperatures, then the vertical temperature gradient across the two layers will be:

$$\frac{\partial T}{\partial z} = \frac{Ts-Td}{0.5(D1+D2)} \qquad 4.6$$

where D1 and D2 are depths shown in Figure 4.1.2

If F1 is the flux of heat that leaves the surface by conduction, then:-

$$F1 = \kappa \frac{\partial T}{\partial z} \qquad 4.7$$

where κ is the thermal conductivity of material which makes up the surface and 'd' layer.

The total heat energy therefore absorbed at surface level is given be ΣF-$F1$.

Now using equation 4.5, we have:-

$$H = M_S\, c\frac{\partial Ts}{\partial t} = \Sigma F - F1 \qquad 4.8$$

where H = heat absorbed by surface,

M_S= mass of surface, (infinitesimally small in real life but required for model to run)

c = specific heat of material at surface.

So combining this equation with equations 4.7 and 4.8 and replacing mass by density ρ gives:-

$$\Sigma F - F1 = \Sigma F - \frac{(Ts-Td)\kappa}{0.5(D1+D2)} = \rho D1c\frac{\partial Ts}{\partial t} \qquad 4.9$$

therefore,

$$\frac{\partial Ts}{\partial t} = \frac{\Sigma F}{\rho D1c} - \frac{(Ts-Td)}{\rho c0.5D1(D1+D2)} \qquad 4.10$$

Introducing thermal diffusivity, $K=\kappa/\rho c$ and rearranging gives:-

$$\frac{\partial Ts}{\partial t} = \frac{\Sigma F}{\rho D1c} + \frac{(Td-Ts)K}{0.5D1(D1+D2)} \qquad 4.11$$

To convert equation (4.11) into a finite difference form, $\partial Ts/\partial t$ was approximated by $\{Ts(1)-Ts(0)\}/dt$ where Ts(0) and Ts(1) denotes surface temperature initially and after one time interval, dt, respectively.

The left hand side of equation 4.7 is substituted for this approximation which gives:-

$$\frac{Ts(1)-Ts(0)}{dt} = \frac{\Sigma F}{\rho c D1} + \frac{(Td(0)-Ts(0))K}{0.5D1(D1+D2)} \qquad 4.12$$

which is rearranged to give an expression for Ts(1). This is a 'forward' time differencing scheme, so called because of the usage of a set of data from one time step only (time zero) to predict in a 'forward' i.e. future direction.

After the first time step, there is a data set of temperatures at time 0 and time 1 i.e. Ts(0), Ts(1) etc. And so, a slightly different time differencing scheme can be used called 'centred' time differencing for subsequent steps. 'Centred' time differencing can only be used as long as there are two sets of 'input' data. 'Centred' time differencing is also sometimes referred to as a 'leapfrog' scheme. An equation for surface heat exchanges using 'centred' time differencing is:-

$$\frac{Ts(i+1)-Ts(i-1)}{2dt} = \frac{\Sigma F}{\rho c D1} + \frac{(Td(i) - Ts(i))K}{0.5D1(D1+D2)} \qquad 4.13$$

where i (a dummy variable) is an increasing whole number with minimum value of unity. Equation 4.13 is rearranged to give an expression for Ts(i+1) in terms of Ts(i), Ts(i-1) and Td(i).

Advantages of 'centred' differencing over 'forward' differencing.

'Forward' time differencing technique *can* actually be used for all time steps (as well as the first). However, because finite differencing methods are approximations of partial differential expressions, they have an error term which arises out of the approximation. With 'forward' time differencing, this error is of order O(dt), whilst with 'centred' time differencing, the order is $O(dt)^2$. It follows that when dt is less than unity (which it normally is), errors produced using 'centred' time differencing are smaller in magnitude than with 'forward' differencing.

Using 'centred' time schemes does not lead to completely error free results, indeed they can cause problems with repetitive errors due to a phenomena called 'computational mode'. To suppress these effects, a simple 'time filter equation' is used after each time step:-

$$Ts(i) = Ts(i) + t_{ff}(Ts(i+1) - 2Ts(i) + Ts(i-1)) \qquad 4.14$$

where t_{ff} is a 'time filter factor' and is a number (<0.1). This equation smoothes out any sudden large errors hence preventing Roadsurf from running away as a result of 'recycling' any errors. t_{ff} must be assigned to a number sufficiently small to make a 'strong enough' filter.

Derivation of 'deep' (d) layer temperature finite difference equation.

Similar equations as to those used for surface heat exchanges are used for this level except that equations representing heat exchanges through the 'd' layer are used instead. There is no ΣF term but there is a new term to take account of heat fluxes between the 'd' and 'cl' layer. An analytical equation for 'd' layer temperature exchanges is thus:-

$$\frac{\partial Td}{dt} = \frac{-(Td-Ts)K}{0.5D2(D1+D2)} + \frac{(Tcl-Td)K}{0.5D2(D2+D3)} \qquad 4.15$$

As with the surface, 'forward' time differencing is used for the initial time step and 'centre' time differencing used for all following steps. Equations 4.16 and 4.17 respectively show 'forward' and 'centre' differencing schemes of equation 4.15. Rearranging gives two expressions for Td(1) and Td(i+1) respectively:-

$$\frac{Td(1)-Td(0)}{dt} = \frac{-(Td(0)-Ts(0))K}{0.5D2(D1+D2)} + \frac{(Tcl(0)-Td(0))K}{0.5D2(D2+D3)} \qquad 4.16$$

$$\frac{Td(i+1)-Td(i-1)}{2dt} = \frac{-(Td(i)-Ts(i))K}{0.5D2(D1+D2)} + \frac{(Tcl(i)-Td(i))K}{0.5D2(D2+D3)} \qquad 4.17$$

The filter for preventing computational mode occurring was also used, though with 'd' layer temperatures in the 'filter' equation (4.18) instead of surface 's' temperatures:-

$$Td(i) = Td(i) + t_{ff}(Td(i+1) - 2Td(i) + Td(i-1)) \qquad 4.18$$

Derivation of 'climate' (cl) layer temperature finite difference equation.

A further similar equation is used to predict 'cl' layer temperatures. There is no flux of heat passing from the surface directly into the 'cl' layer (or vice versa) because of no physical contact between the two, hence no contribution to the 'cl' equation from surface temperature. The analytical form of the 'cl' equation is:-

$$\frac{\partial Tcl}{\partial t} = \frac{-(Tcl-Td)K}{0.5D3(D2+D3)} \qquad 4.19$$

whilst corresponding 'forward' and 'centre' time differencing equations used are respectively:-

$$\frac{Tcl(1) - Tcl(0)}{dt} = \frac{-(Tcl(0) - Td(0))K}{0.5D3(D2+D3)} \qquad 4.20$$

$$\frac{Tcl(i+1)-Tcl(i-1)}{2dt} = \frac{-(Tcl(i)-Td(i))K}{0.5D3(D2+D3)} \qquad 4.21$$

Which are rearranged to give expressions for Tcl(1) and Tcl(i+1).

The filter equation for the 'cl' layer, not surprisingly, has a similar structure to earlier forms:-

$$Tcl(i)=Tcl(i) + t_{ff}(Tcl(i+1)-2Tcl(i)+Tcl(i-1)) \qquad 4.22$$

It was hoped that using finite difference equations would not require 'forced' time lag algorithms.

Other modifications to Surftemp.

Alterations had to be made to components of ΣF due to alterations in ground to atmosphere heat fluxes.

Damping depth algorithms, present in Surftemp were no longer required.

The ground temperature notation present in Surftemp, TH was no longer required since it was replaced by the surface, 'd' and 'cl' layer temperatures.

All units throughout the model were converted to SI units for ease for use in carrying out any modifications.

4.2 Summary of this chapter

- Ground heat flux representation in Surftemp was modified to use finite differencing techniques to predict surface temperature. The modified model was given the name 'Roadsurf'.

- The three layer ground-atmosphere set-up in Surftemp was changed to become a four layer system in Roadsurf comprising of an atmospheric layer, the surface and two sub-surface layers. The aim of this was to resemble a standard road structure.

Chapter 5 Sensitivity tests on Roadsurf

Table 5.1.1 shows input values of cloud parameters which depend upon extent and altitude of any cloud cover compiled from Wood (1977 and 1978) and Thornes (1983). DPLUS is a factor of the diffuse component of the solar radiation whilst KCLOUD controls the reduction of thermal radiation lost as a result of cloud. The main trends with increasing cloud amount are increases in ALBEDO and DPLUS with simultaneous decreases in KCLOUD, though the rate of change in individual parameters also vary.

It is useful to run Surftemp or Roadsurf with differing cloud cover amounts to model effects on temperature due to a passing front. To do this, both models contained an algorithm to select different values of ALBEDO, DPLUS AND KCLOUD, depending on how many time steps had passed. Hence tables of cloud input factors used for actual model runs (e.g. Table 5.1.2.1) will have several values of cloud adjustment factors though of course, they would only be different if changes in cloud cover were to occur. A revised set of ALBEDO, DPLUS AND KCLOUD come into 'play' after every three hours of time steps. Later values of these factors are denoted by as ALBEDO2, ALBEDO3 and so on...

Table 5.1.1 Cloud adjustment input factors for Surftemp and Roadsurf.

	ALBEDO	DPLUS	KCLOUD
Clear	0.0	0.5	1.0
1-2 oktas:			
Low	0.2	0.6	0.87
Medium	0.1	0.6	0.91
High	0.05	0.5	0.96
3-5 oktas:			
Low	0.5	0.8	0.58
Medium	0.3	0.8	0.72
High	0.1	0.5	0.86
6-7 oktas:			
Low	0.9	1.0	0.32
Medium	0.9	1.0	0.54
High	0.3	0.6	0.78
Overcast	1.0	1.0	Values of 6-7 oktas

The words:- 'time lag' appear several times in this chapter. To avoid confusion, 'time lag' has been taken to mean the time it takes for changes in atmospheric energy fluxes, for example a rise in solar energy, to have an effect on the particular ground layer being discussed.

5.1 Sensitivity tests and results carried out on Surftemp.

A run was carried out on Surftemp with the boundary conditions and constants shown in Table 5.1.3 to compare the affects of a clear sky with an overcast sky. Table 5.1.2 shows the cloud input values used in the two model runs. Two graphs of results and predictions obtained (Figures 5.1.1.1 and 5.1.1.2) not surprisingly showed large differences in some, but **not** all fluxes dependent on cloud cover.

Throughout the runs, the atmospheric temperature, windspeed, surface wetness and humidity were held constant.

Table 5.1.2 Cloud input factors for Surftemp runs whose predictions are shown in Figures 5.1.1.1 and 5.1.1.2

	Clear sky	Overcast sky
ALBEDO	0.00	1.00
DPLUS	0.50	1.00
KCLOUD	1.00	0.54

Table 5.1.3 Boundary conditions during Surftemp runs.

Declination of sun, DEC	-22.345° (winter solstice)
R (fraction of sun-earth distance)	0.983
Atmospheric temperature, TA	6.0 °C
Wet bulb temperature, TW	4.0 °C
Ground temperature, TH	7.0 °C
Windspeed, U_3	0.5 ms^{-1}
Density of ground layers and surface, ρ	2100 kg m^{-3}
Dry adiabatic lapse rate,	0.01 K m^{-1}
Latitude, XLAT	50.35°N
Surface wetness, SRHF	1 (wet)

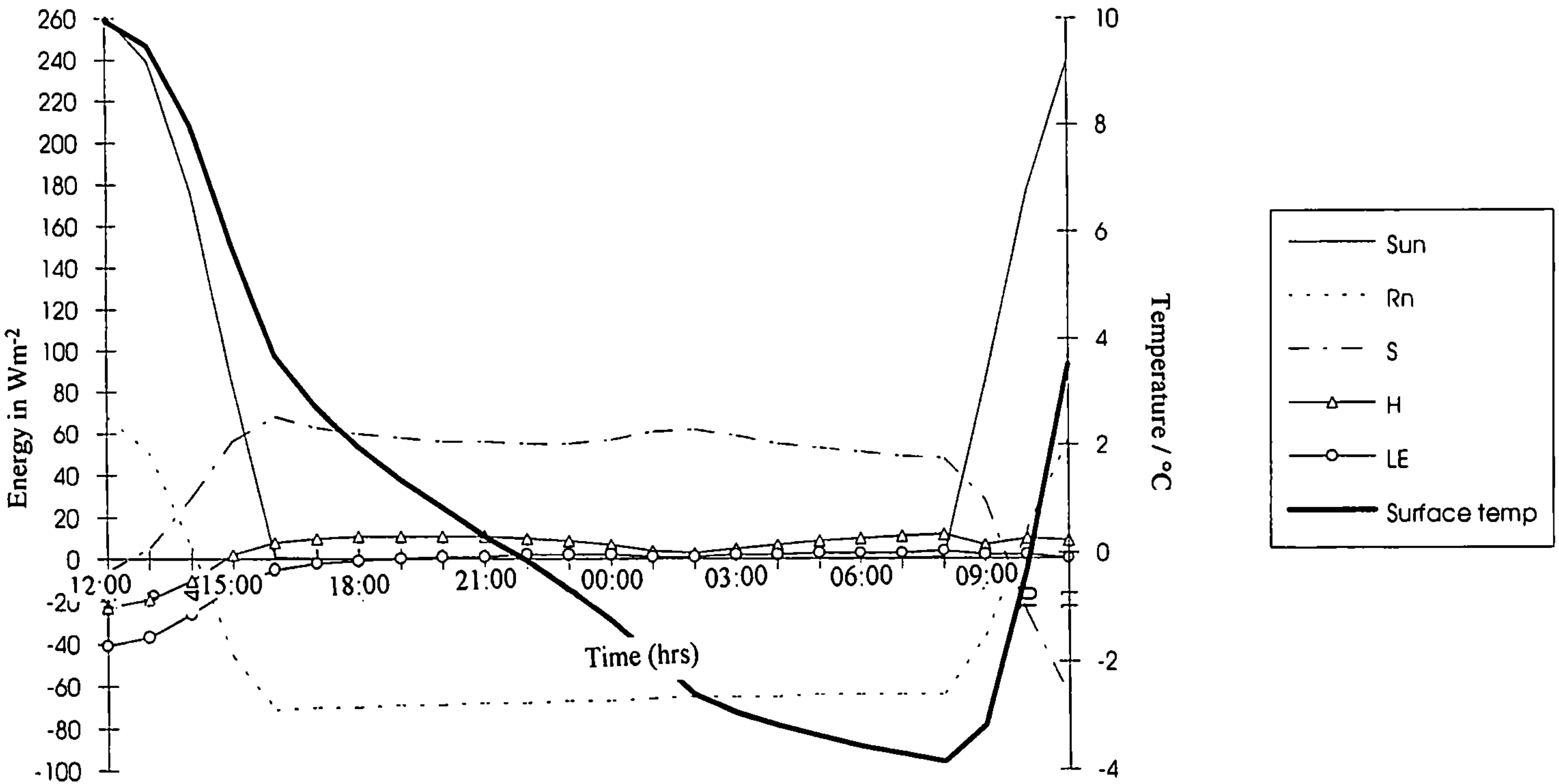

Figure 5.1.1.1 Surftemp predictions of energy fluxes and surface temperature under a clear sky

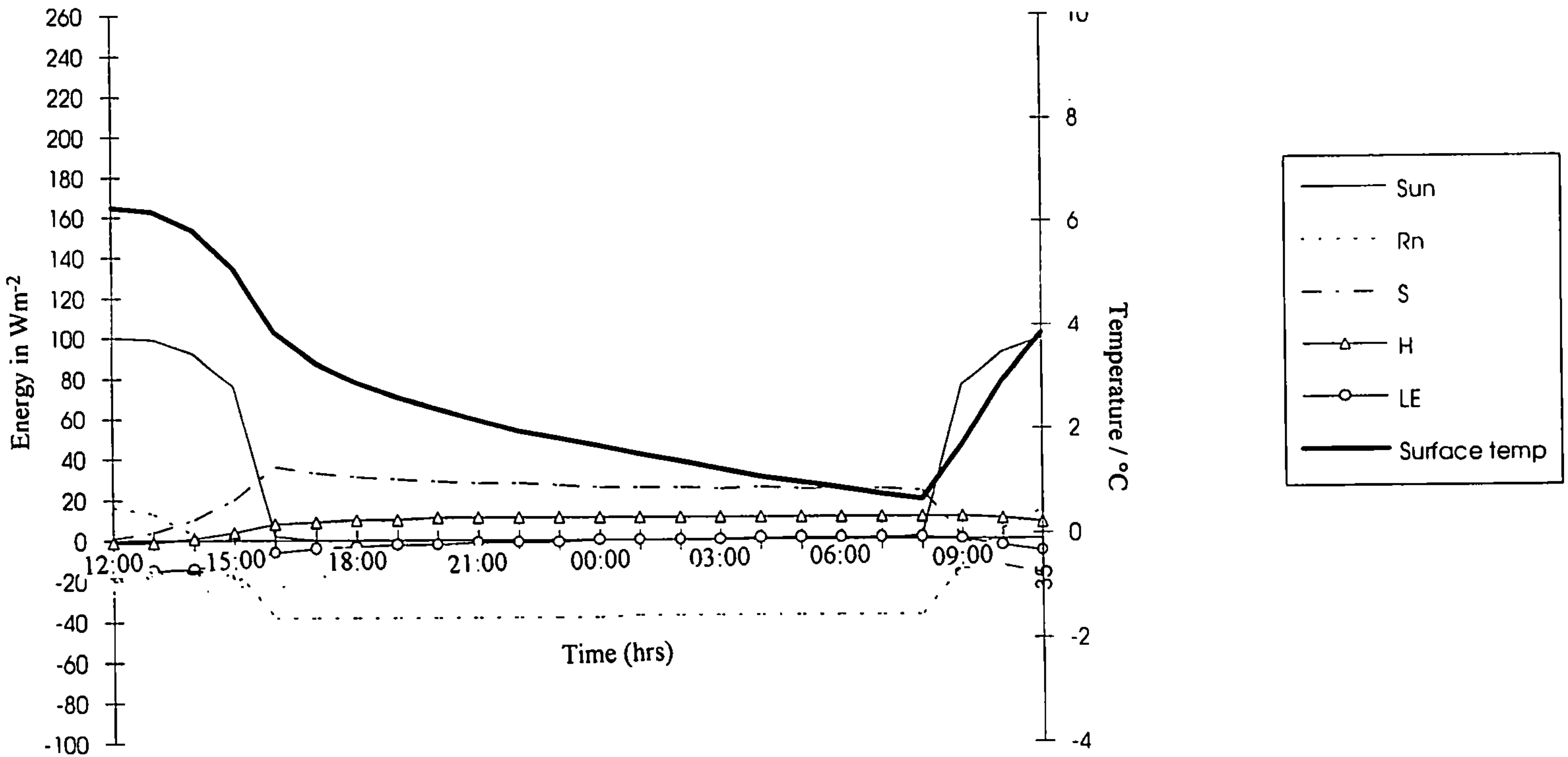

Figure 5.1.1.2 Surftemp predictions of energy fluxes and surface temperature under an overcast sky

General results from both Surftemp runs.

i) A four hour timelag occurred in four out of the five energy balance fluxes, particularly well shown by the net radiation curves in Figures 5.1.1.1 and 5.1.1.2. A timelag occurred in the surface temperature predictions, but was not clearly visible because Surftemp was run from midday rather than dawn. If Surftemp was run for more than 24 hours, results would have shown a timelag in surface temperature.

ii) Dependence upon increasing solar radiation is shown very well by the net radiation (Rn) and ground to atmosphere energy (S) fluxes in Figure 5.1.1.2, though this was not surprising. Solar influence on the sensible and latent heat fluxes was more subtle since they were indirectly dependent on solar energy by way of surface temperature and its effect on other atmospheric parameters such as the Richardson stability number.

Comparisons between overcast and clear sky Surftemp predictions.

Effects on Surftemp predictions from overcast skies compared to clear skies included the following:-

1) The peak in solar radiation under overcast skies was 38% of the corresponding peak which occurred under clear skies.

ii) Net radiation predicted under overcast conditions was less than 54% in magnitude of the clear sky run. This difference was even greater when net radiation was positive (directed downwards) with 'overcast' net radiation less than 25% of 'clear sky' values between 1200 and 1400 hrs.

iii) Differences caused by cloud cover on calculated sensible and latent heat fluxes were small (<$3Wm^{-2}$) whenever the fluxes were positive, but were considerably more dependent on cloud when negative.

Apart from the effects of cloud on the energy fluxes discussed above, an unexpected phenomenon occurred in Surftemp predictions of sensible and latent heat under clear sky conditions. A sharp decrease in both energy fluxes occurred between 0100 and 0200 hrs though after 0200 hrs, they resumed values similar to those before the decrease. This temporary minimum, shown in Figure 5.1.1.1 *did not* occur under overcast conditions (Figure 5.1.1.2).

It was this minimum which prompted the initial moves to consider modifying Surftemp (previous Chapter). Surftemp was modified and became '**Roadsurf**'.

Because of the scale of modifications carried out, a complete new tuning of the modified Surftemp model (Roadsurf) had to be carried out to obtain suitable predictions and eradicate bugs. Details of the tuning runs on Roadsurf are not discussed here. Table 5.1.4 however shows most physical constants required by Roadsurf. A standard virtual road (Wood, 1977) was seen as the most appropriate ground/atmosphere systems for which Roadsurf would be useful, hence the reason for the thermal properties mentioned in Table 5.1.4.

Table 5.1.4 Physical constants required by Roadsurf.

Parameter	Value
Ground layer constants:-	
Thermal diffusivity of surface (rolled asphalt), κs	0.003×10^{-4} $m^2 s^{-1}$
Thermal diffusivity of d layer (lean concrete), κd	0.007×10^{-4} $m^2 s^{-1}$
Thermal diffusivity of cl layer (hoggin), κcl	$0.007 \times 10^{-4} m^2 s^{-1}$
Density of surface (rolled asphalt), ρs	2100 kgm^{-3}
Specific heat of surface (rolled asphalt), Cs	920 $Jkg^{-1}K^{-1}$
surface thickness (required for model to run), D1	0.1m
d layer, D2	0.25m
cl layer, D3	0.25m
Atmospheric constants:-	
Karman constant, KARMAN	0.4
Atmospheric heat capacity, c	1.2×10^{-3} $Jkg^{-1}K^{-1}$
Atmospheric density, ρa	1.25 kgm^{-3}
Dry adiabatic lapse rate, DALR	0.01 K m^{-1}
Dry bulk transfer coefficient for dry air, Dh	1.66×10^{-3} $kJm^{-3}K^{-1}$
Surface wetness factor, SRHF	1.0 (wet)
Parameters affecting extraterrestrial influences:-	
Latitude, XLAT	50.35°N
Declination of sun, DEC	-22.345°
Fraction of sun-earth distance	0.983

5.2 Roadsurf sensitivity tests, results and discussions.

5.2.1 Base run.

A base run was carried out on Roadsurf with initial parameters as follows:-

Surface temperature, Ts(0)= 10°C

'd' layer temperature, Td(0)= 6°C

'cl' layer temperature, Tcl(0)= 6°C

Throughout this run, the air temperature was held constant at 6°C and wind speed at 0.5 ms^{-1} and all cloud input factors were set to clear sky values. Results are displayed as graphs in Figures 5.2.1.1, 5.2.1.2 and 5.2.1.3.

Similar predictions to those produced by Surftemp occurred. However the sensible heat flux was negative in the Roadsurf run for longer than during the Surftemp runs. This was due to a higher initial surface temperature used in Roadsurf than the one used in Surftemp.

The removal of forced timelag algorithms and addition of finite differencing algorithms had to enable a suitable timelag to still occur in Roadsurf. It was pleasing then, to note that such a timelag had occurred in the Roadsurf base run predictions, though interestingly in different parameters than with Surftemp. Figures 5.1.1.1 and 5.1.1.2 of the Surftemp run results showed a timelag in net radiation, but the graph of the Roadsurf base run (Figures 5.2.1.1 and 5.2.1.2) did not. Indications of a three hour timelag occurred in the 'd' layer temperatures between 1200 and 1700 hrs instead. No timelag appeared to have been present in surface temperature during this time due to run's start time (1200 hrs). An hour long timelag did occur in surface temperature at sunrise, 18 hours later.

Figure 5.2.1.3 shows a ground temperature profile produced by Roadsurf which illustrates very clearly, ranges in ground temperature with depth. In this particular run, the surface was the warmest layer of the ground from 1200 hrs (midday) until shortly after 1500 hrs. After 1600 hrs, ground temperature increased with depth. Insulative properties of the surface and 'd' layer were responsible for the small change in 'cl' layer temperature shown Figure 5.2.1.3. The 'cl' layer only cooled by 1.2 deg. C during the twenty four hours of model run compared to a 5 deg. C cooling in the 'd' layer and a cooling three times as large at the surface. This large surface cooling was partly due to the high initial temperature to which the surface was assigned.

After 1800 hrs, a cooling in the 'd' layer occurred, associated with an upward heat flow towards the surface. Due to the lag, no upward heat flow occurred between the 'd' and 'cl' layers until 2100 hrs.

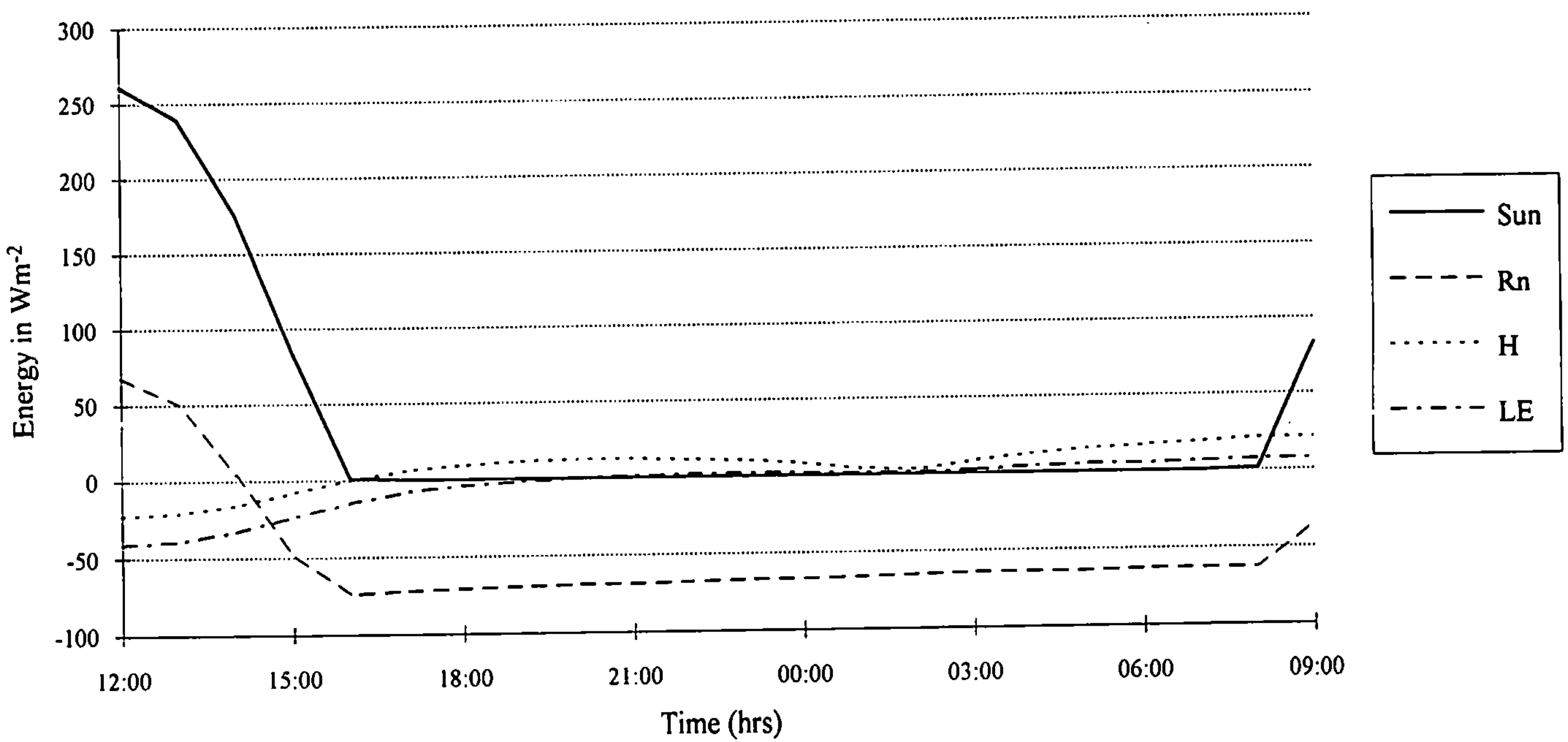

Figure 5.2.1.1 Predicted energy fluxes from Roadsurf base run (5.2.1)

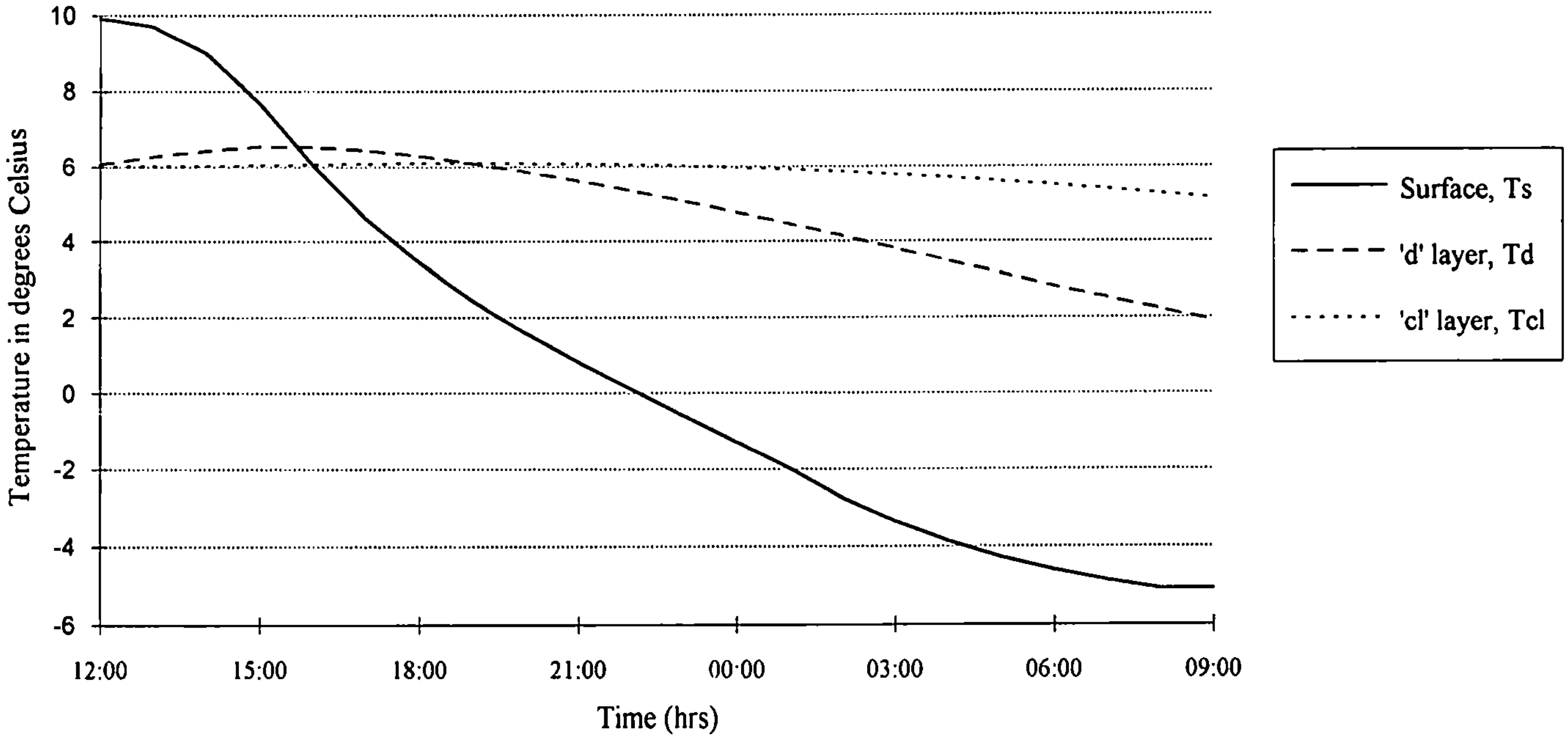

Figure 5.2.1.2 Predicted temperatures from Roadsurf base run (5.2.1)

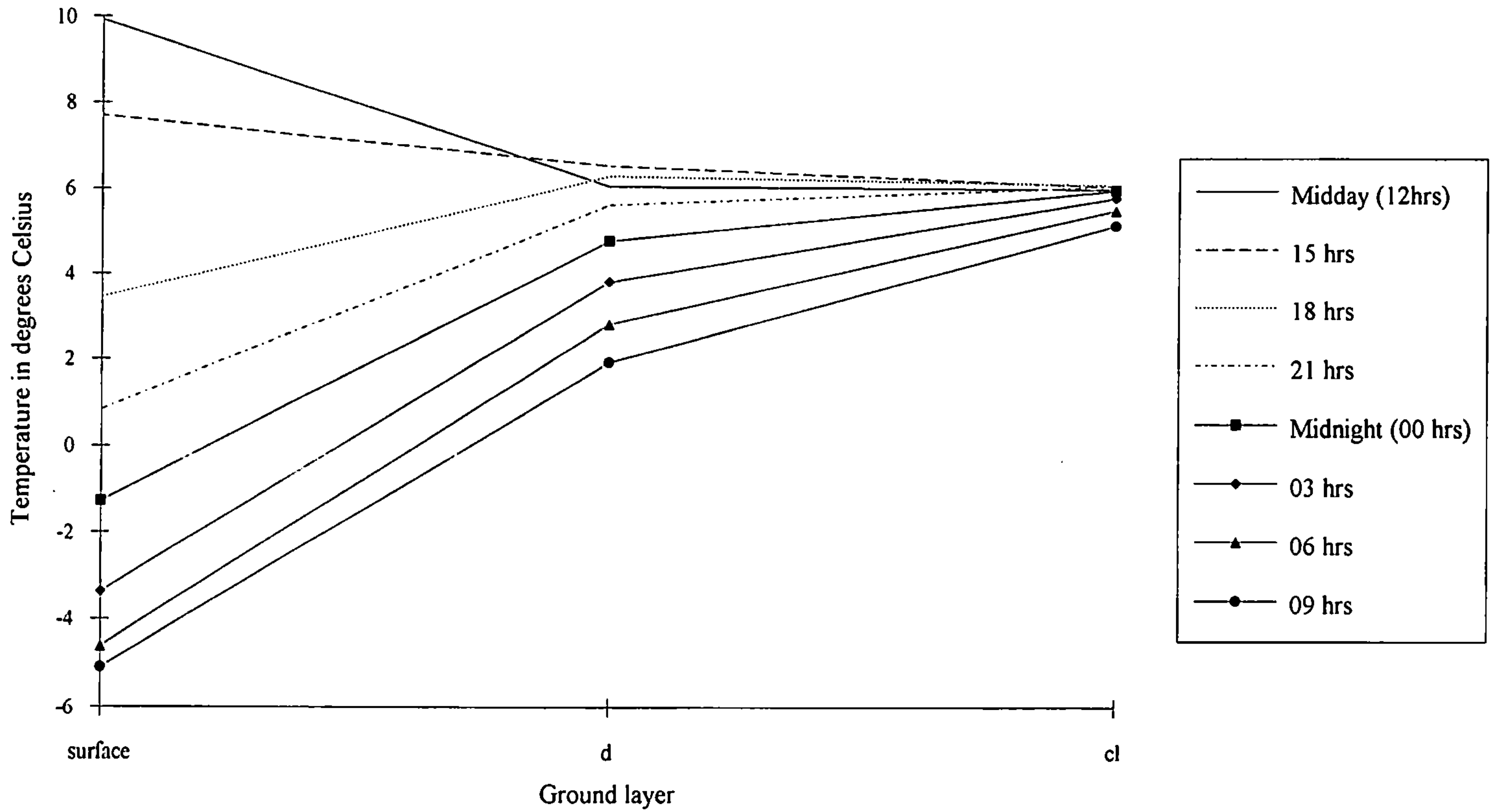

Figure 5.2.1.3 Predicted ground temperature profile from Roadsurf base run (5.2.1)

5.2.2 **Roadsurf run with different initial surface temperature.**

Roadsurf was re-run with initial surface temperature, Ts(0)=0.0°C which produced results and predictions shown by Figures 5.2.2.1 and 5.2.2.2. All other initial conditions and constants were unchanged. Clear skies were present throughout.

This time, the surface temperature curve looked more dramatic which inspired an initial thought that a surface warming between 1200 and 1500 hrs, (see Figures 5.2.2.1 and 5.2.2.2), was due to a delayed reaction from the solar energy because of a timelag. However, this warming was due to the initial surface temperature being set too low. Since Ts(0) was six degrees less than the initial 'd' layer temperature, there was an initial flow of heat to the surface from below. This was in addition to solar radiation heating the surface from above. Evidence of any possible timelag in surface temperature was obscured.

The temporary minimum of the latent heat flux which occurred in the Roadsurf base run reoccurred in run 5.2.2, though four hours earlier.

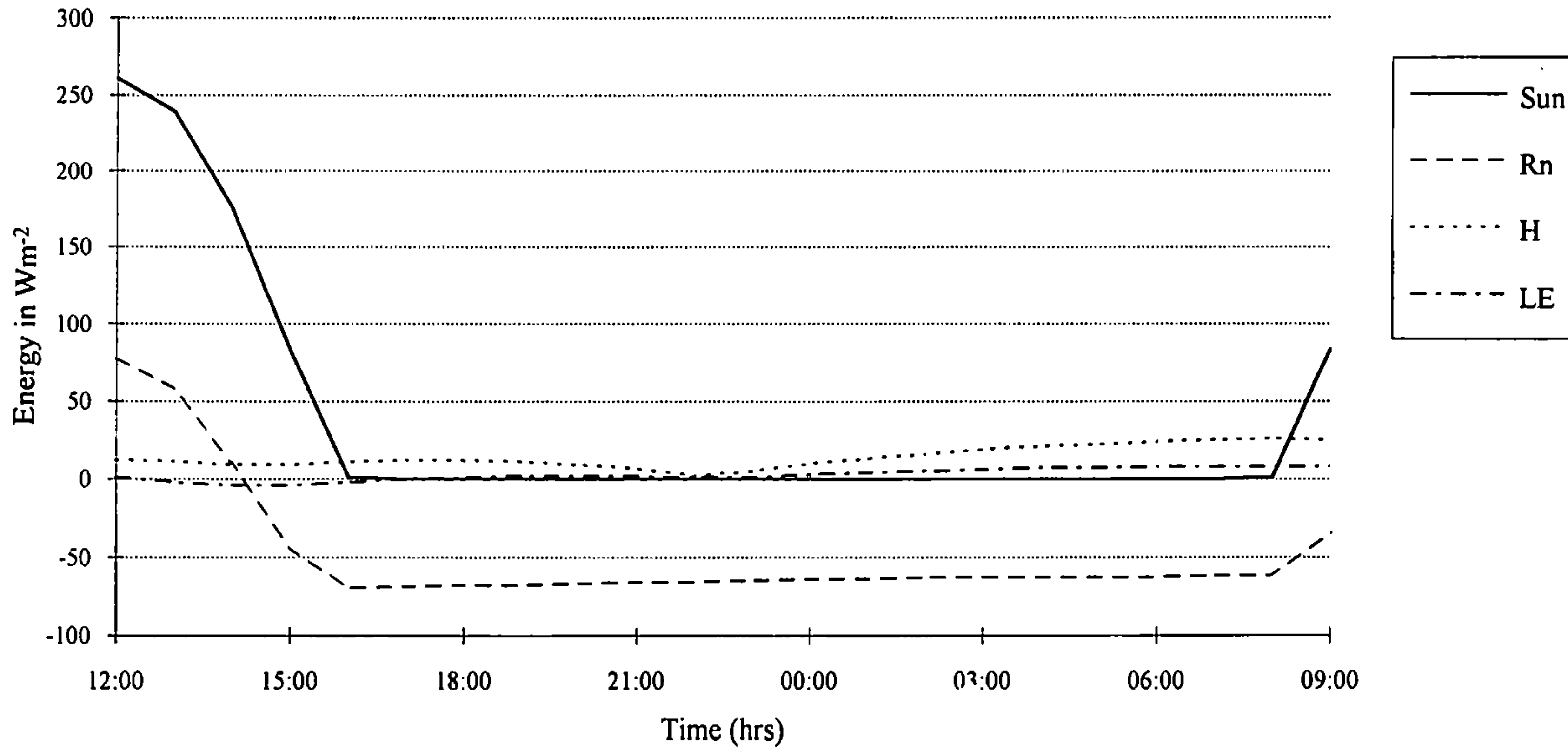

Figure 5.2.2.1 Predicted energy fluxes from Roadsurf run 5.2.2

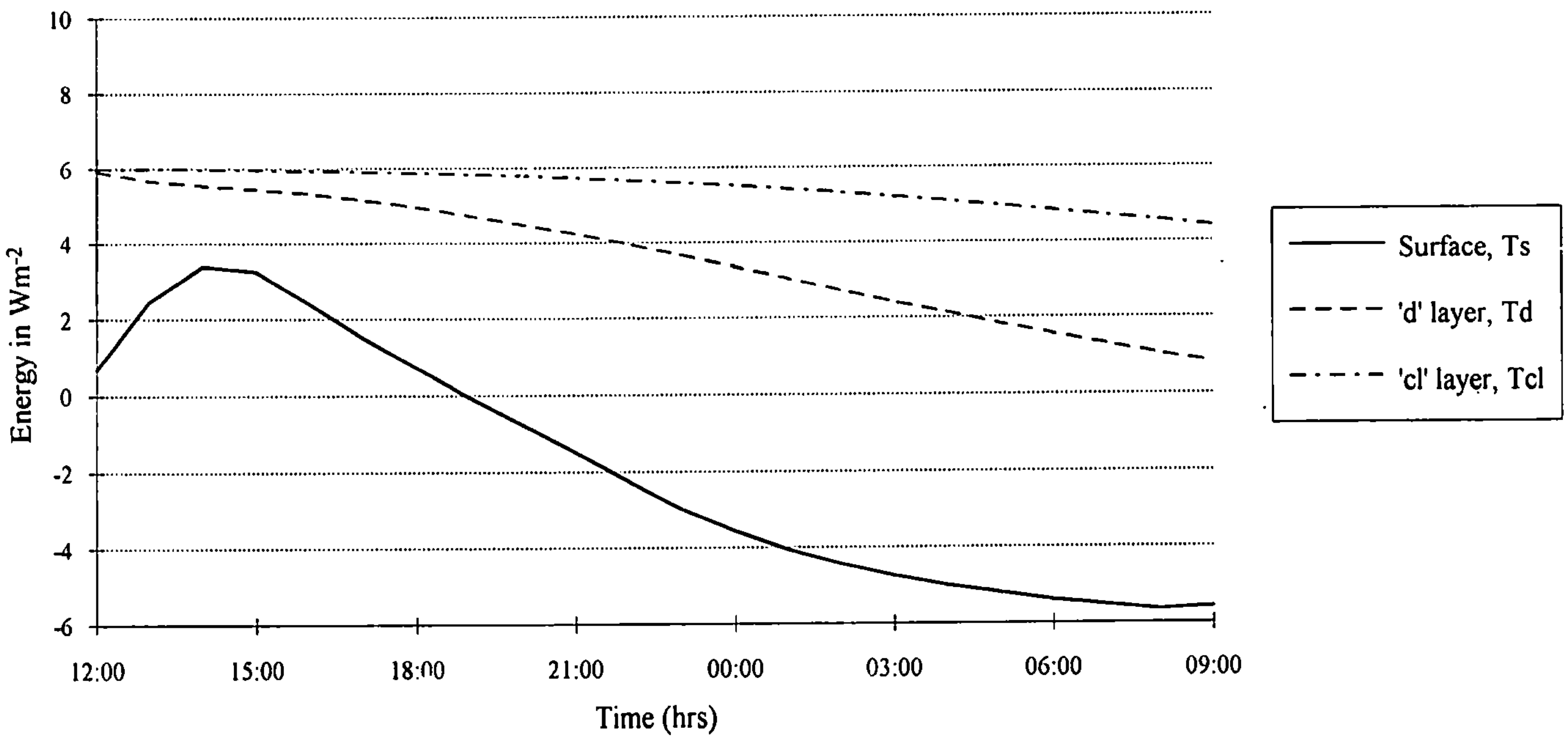

Figure 5.2.2.2 Predicted temperatures from Roadsurf run 5.2.2

5.2.3 Roadsurf run with initial surface and subsurface temperatures set to 0 °C.

Setting initial temperatures of the surface and the 2 sub-surface ground layers to 0 °C, and re-running Roadsurf with clear skies gave predictions (Figures 5.2.3.1, 5.2.3.2 and 5.2.3.3) which showed the best indications of a timelag so far.

Since Ts(0)=Td(0)=Tcl(0), there was no flow of heat between the ground layers at the model start. Hence the surface, heated only as a result of incoming solar radiation between 1200 and 1400 hrs and sensible heat, since the atmosphere was initially warmer than the surface, would show a timelag more clearly than before.

Given that solar radiation peaks at 1200 hrs, the surface temperature peaking at 1400 hrs (Figure 5.2.3.2) indicated a maximum timelag of 2 hours at the surface.

A timelag also occurred in the 'd' layer temperature of 4.0±0.5 hours and there was even evidence of a timelag of 7.0±0.5 hours in the 'cl' layer (Figure 5.2.3.1).

A ground temperature profile (Figure 5.2.3.3) shows the surface initially to be warmer than the sub-surface layers. Variations of 'cl' layer temperature with time, as in the ground temperature profile from the previous Roadsurf run, were small compared to at other depths. At all depths, the range in temperature was smaller in this latest run than previously due to the equal initial temperatures, closer in magnitude to minimum predicted temperature.

The surface was shown by Figure 5.2.3.3 to cool most rapidly between 1500 and 2100 hrs. The fastest fall in the adjacent 'd' layer occurred between 2100 hrs and midnight instead. These two results were further evidence of a timelag effect on temperature; the effect of a large surface cooling on the 'd' layer was delayed.

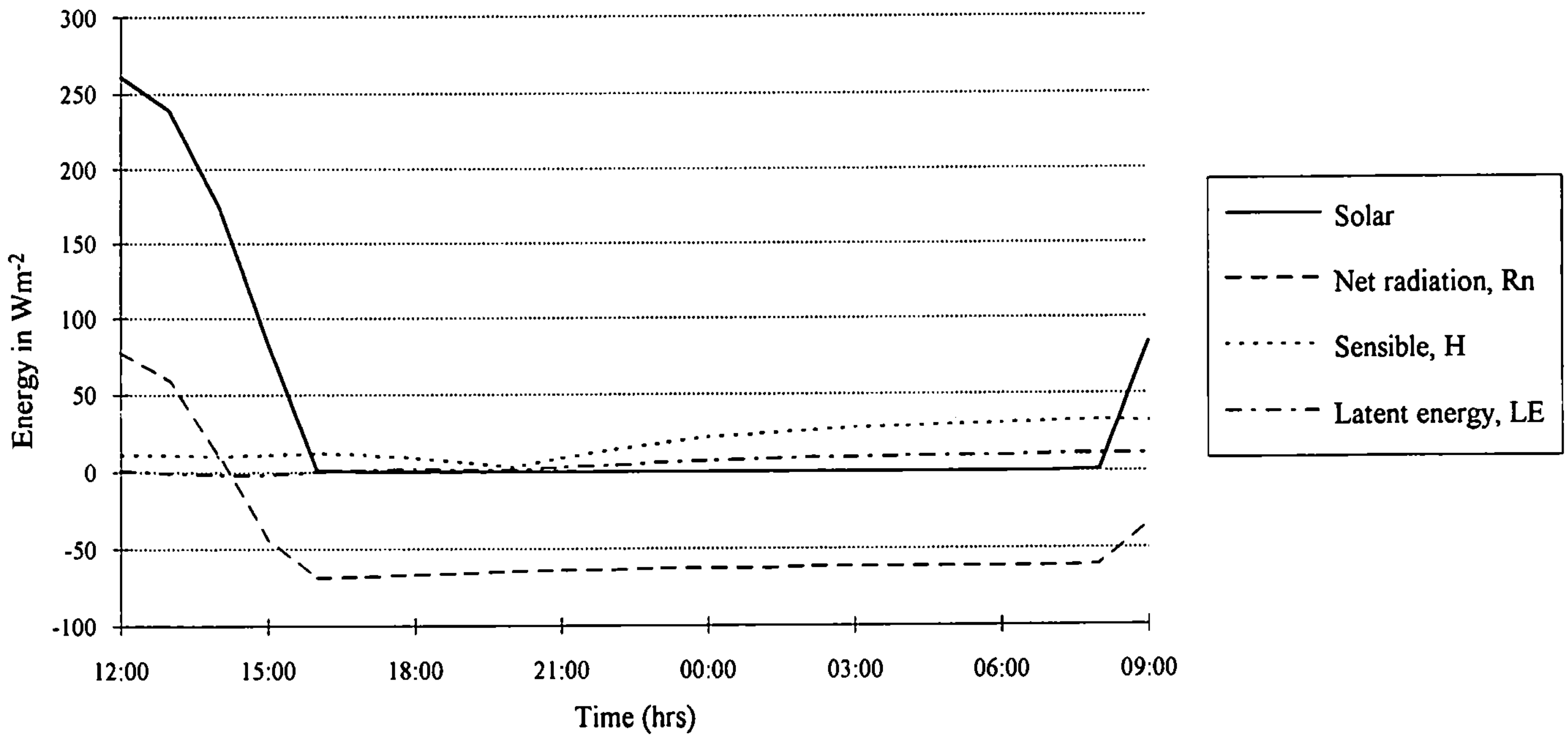

Figure 5.2.3.1 Predicted energy fluxes from Roadsurf run 5.2.3

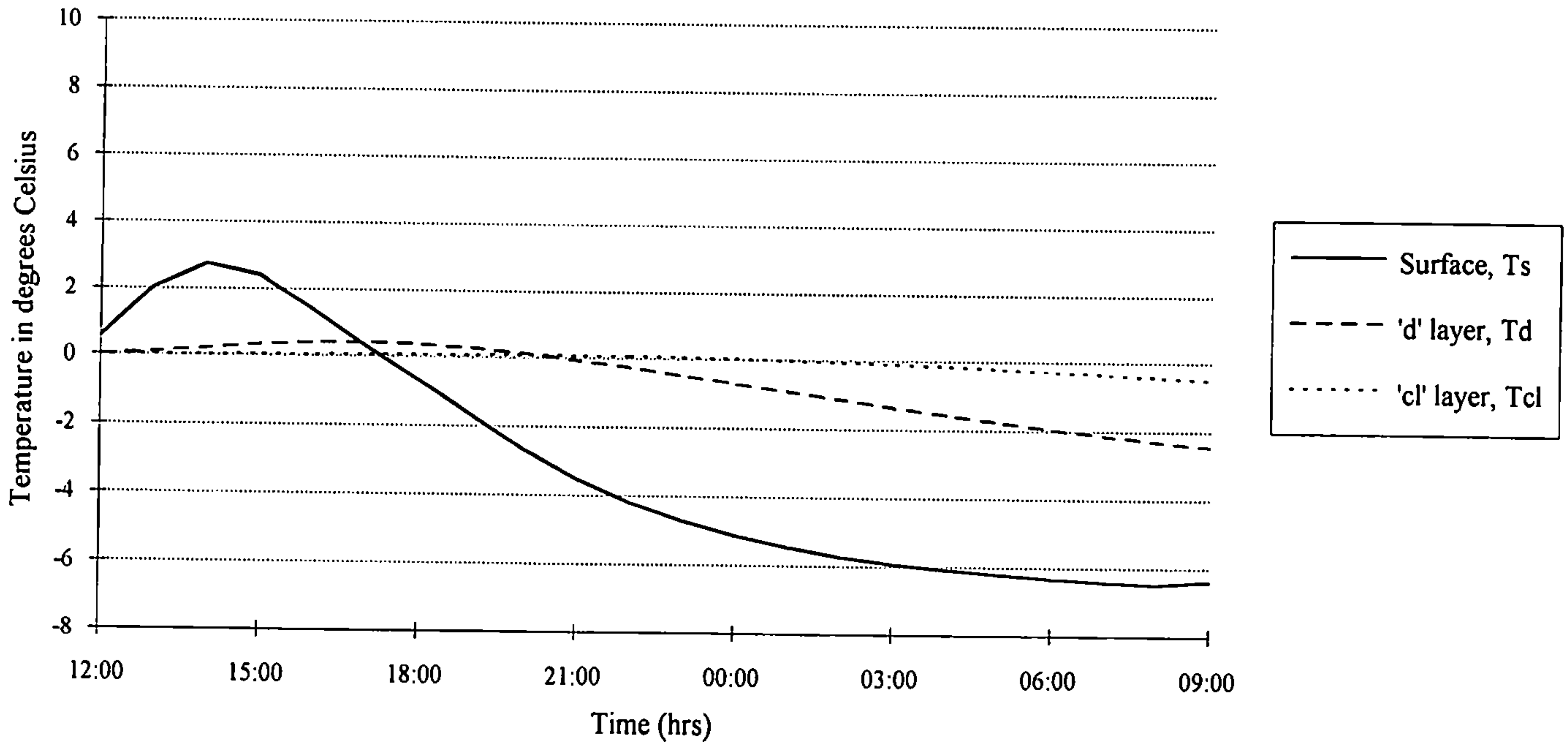

Figure 5.2.3.2 Predicted temperatures from Roadsurf run 5.2.3

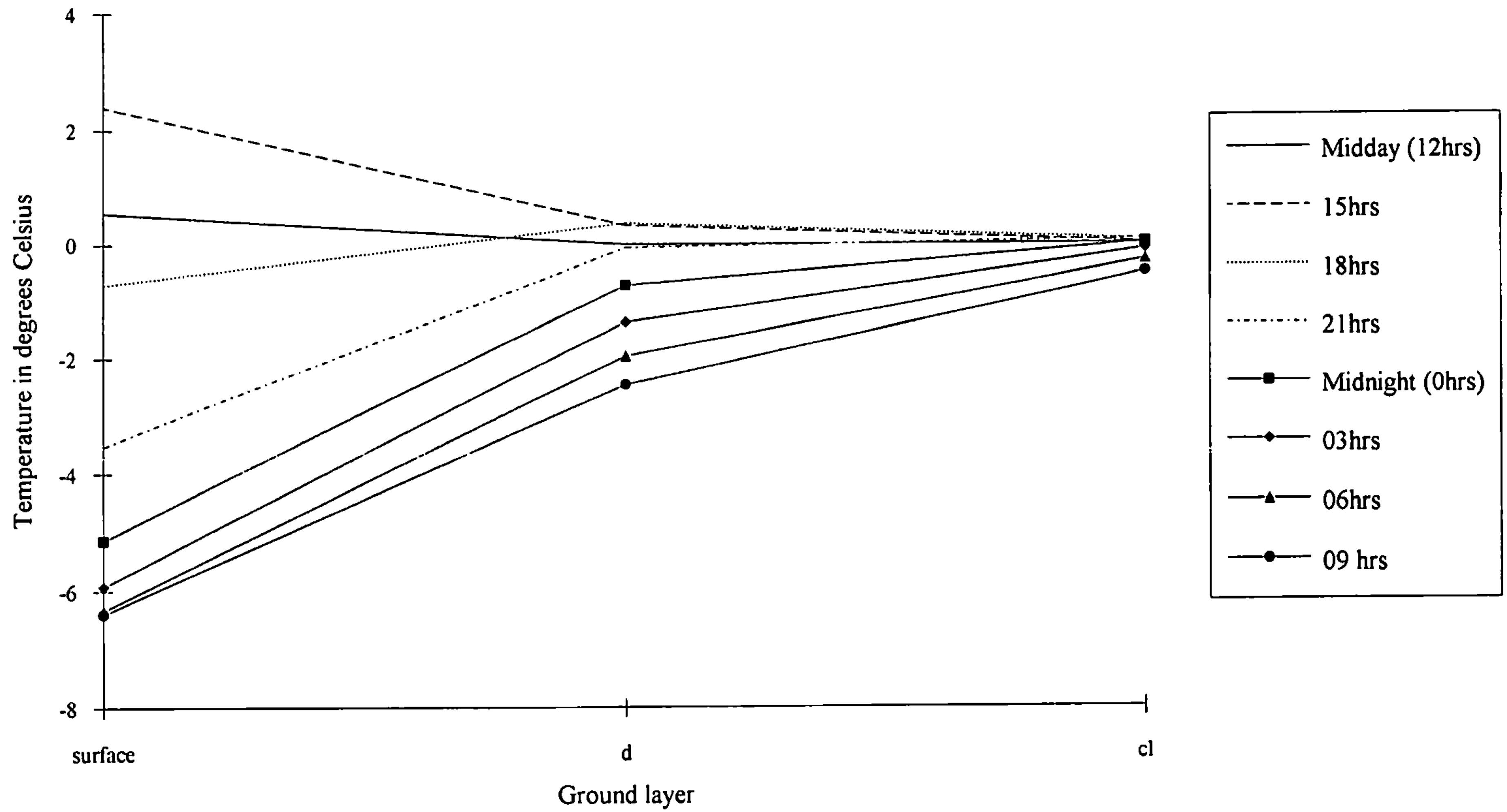

Figure 5.2.3.3 Predicted ground temperature profile from Roadsurf run 5.2.3

Discussion regarding appropriate initial temperatures.

As can be seen from runs 5.2.2 and 5.2.3, initial temperatures have high influences on Roadsurf predictions, particularly during the early hours of a model run. It was therefore necessary to decide a suitable set of initial temperatures considered most likely in a real life scenario on a Devon road in midwinter.

An initial (1200 hrs) surface temperature of 0 °C for a model run could be thought of as being a worst possible scenario in terms of causing road problems due to ice formation in Devon. This is because of a small margin between precipitation falling as either rain, sleet or snow and freezing (or not) when it comes into contact with the ground. Although lower initial temperatures at first glance could cause greater problems, this is unlikely. Rain falling onto frozen ground producing black ice is more troublesome than snow falling onto frozen ground. However, if Roadsurf is to be used for an 'average' winter night in Devon, then this worse case scenario of **initial** freezing temperatures is very unlikely to happen. It was decided, also that an initial temperature of 10°C and above would be too high. 6°C was decided upon as being a reasonably realistic initial (1200 hrs) temperature for all three layers of ground under 'normal' conditions for a winter run for Devon based on observations.

Investigating the effects of cloud on Roadsurf predictions of temperature

5.2.4 **A set of Roadsurf runs with different cloud cover fractions.**

As seen from the two runs of the original Surftemp involving a clear and then overcast sky (see 5.1), surface temperature is highly dependent upon cloud cover.

In an attempt to determine further the affects of cloud on Roadsurf, six runs of the model were carried out, each with a different set of cloud cover parameters from Table 5.1.1. Initial (1100 hrs) surface and subsurface temperatures were set to 6°C. All other boundary conditions and constants remained unchanged from previous runs. Figure 5.2.4.1 shows the predictions obtained.

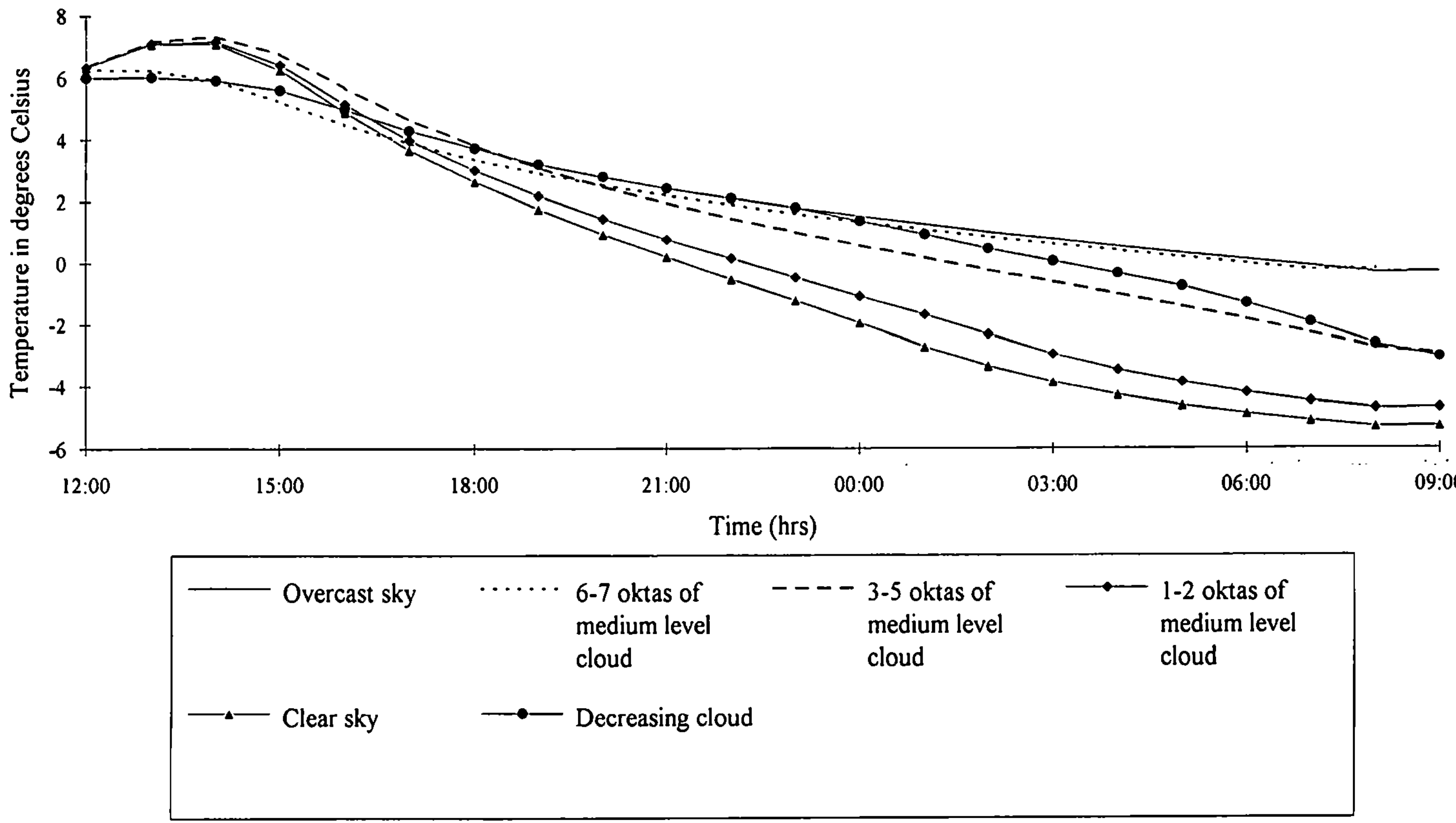

Figure 5.2.4.1 Predicted surface temperature from Roadsurf runs in 5.2.4 showing effects of cloud on surface temperature

The following points were noted:-

i) Surface temperatures were mostly unaffected by cloud at 1600 hrs (4pm 'local time') but were approximately 1.5 deg. C lower than initially, shown in Figure 5.2.4.1 by an intersection of five of the six temperature curves at 1600 hrs.

ii) The largest dependence in surface temperature on cloud occurred shortly before sunrise. The difference between surface temperature predictions under 3-5 oktas of cloud to those under 6-7 oktas at 0900 hrs was 3.1 deg. C at this time.

iii) Totally overcast conditions had much the same effect on surface temperature as 6-7 oktas of cloud.

iv) The timing of minimum temperature was mostly independent of cloud cover amount. There *were* small variations in the timing depending on cloud cover but these were so small, they were deemed negligible.

v) An interval of over 3 hours occurred between the freezing onset time under 1-2 oktas and 3-5 oktas, which clearly emphasised the importance of accurately forecasting partly cloudy conditions. The freezing onset time of the 'decreasing cloud' run was later than under constant cloud scenarios of less than 6 oktas which indicated a timelag caused by earlier, more extensive cloud.

Figure 5.2.4.2 shows a corresponding graph of solar energy absorbed by the surface layer during each of the six runs.

By comparing Figures 5.2.4.1 and 5.2.4.2, it can be deduced that a timelag of two hours occurred in the surface temperature predictions by 0700 hrs. This is shown by the solar insolation which increased immediately after sunrise at 0700 hrs whereas the surface temperature did not rise until at least two hours later.

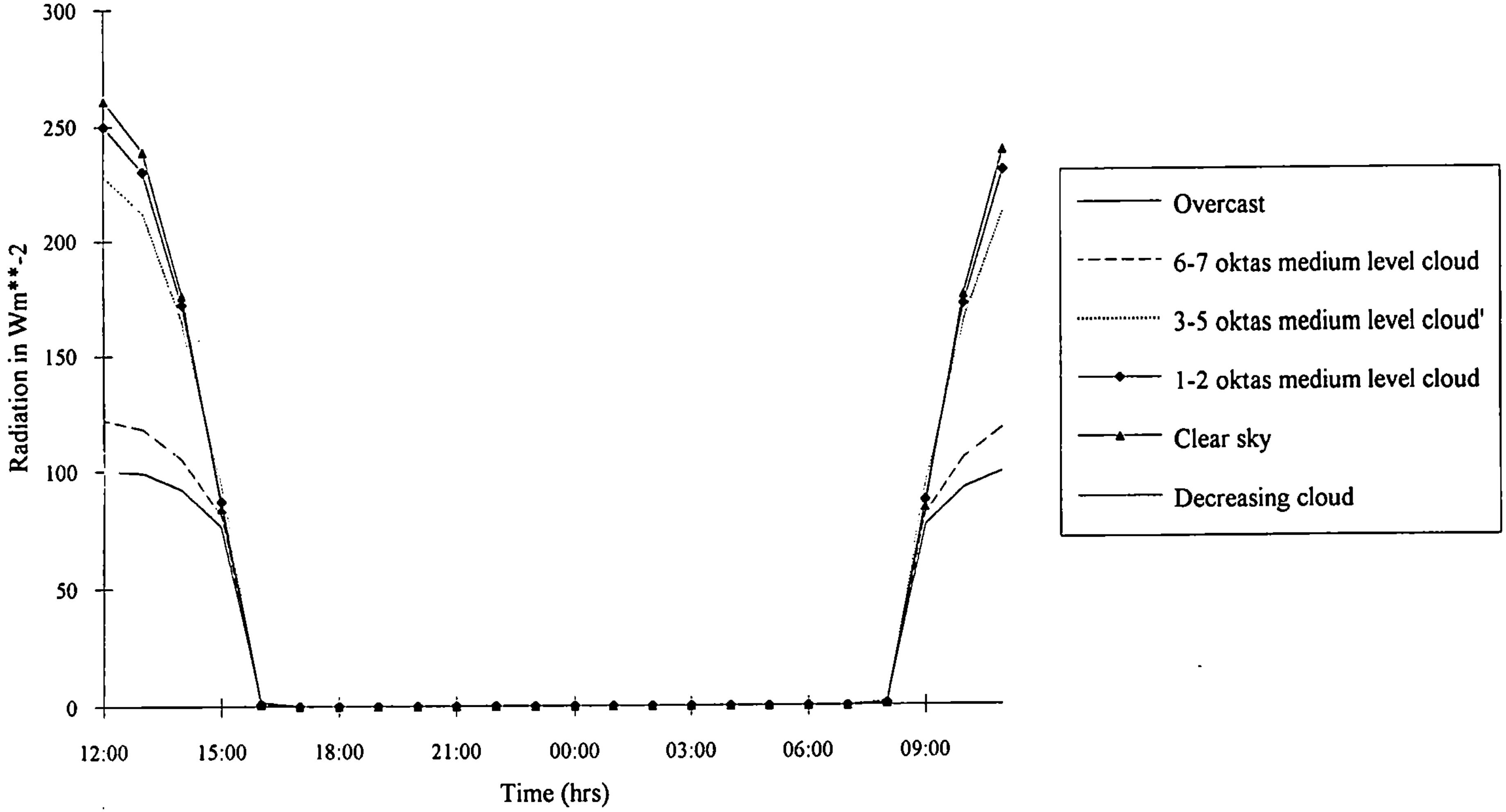

Figure 5.2.4.2 Predicted incoming solar radiation from Roadsurf runs in 5.2.4 showing effects of cloud on solar radiation

The curves in Figures 5.2.4.1 and 5.2.4.2 of most importance are the 'decreasing cloud' curves. These would hopefully have given good representations of surface temperatures underneath the backward edge of a cold front passing over Devon. Initial cloud with possible precipitation from a cold front would clear as the front passes away. Decreasing cloud runs would therefore hopefully have given a realistic guide to surface temperature trends under these conditions. The most important aspect of a 'decreasing cloud' run is the predicted time of surface freezing. Figure 5.2.4.1 shows this to be 0300 hrs. This frost onset time was later than that which occurred with all constant cloud curves of five oktas or less (see Table 5.2.4.2).

The rate of cloud clearance in the 'decreasing cloud' curve (Table 5.2.4.1) was suitable for a 'base' run of a decreasing cloud situation. However cloud clearances behind real life cold fronts are usually more erratic. Cloud clearances from seven to one okta within two hours is not rare. Furthermore, cold fronts not always begin to clear during early morning hours; they can clear just as quickly before midnight!

Table 5.2.4.1 Rate of cloud clearance which produced the 'decreasing cloud' results in Roadsurf run 5.2.4.

Time	'Decreasing cloud' scheme
1200-1800	Overcast
1800-0000	6-7 oktas medium level cloud
0000-0600	3-5 oktas medium level cloud
0600-1200	1-2 oktas medium level cloud

Further complications arise frequently even after a cold front has completely cleared. Real life polar airstreams behind cold fronts are often showery and that of course means some degree of cloud amount is present.

Table 5.2.4.2 Minimum temperatures and frost onset times of Roadsurf runs involving various cloud cover scenarios

Cloud cover / oktas and height level.	Minimum RST / °C	Minimum RST in base run / °C	Freezing onset time / hrs	Freezing onset time in base run / hrs
Overcast	-0.3	-5.1	06:30	22:15
6-7 medium	-0.2	-5.1	07:00	22:15
3-5 medium	-2.9	-5.1	01:30	22:15
1-2 medium	-4.7	-5.1	22:30	22:15
clear	-5.3	-5.1	18:45	22:15
decreasing	-3.5	-5.1	03:00	22:15

5.2.5 Effects of varying cloud.

As a consequence of the above discussion, extra runs of Roadsurf were carried out, each with different cloud cover variations to represent more realistically, the effects of cloud clearance on surface temperature. Table 5.2.5.1 shows the inputted cloud adjustment factors and Figure 5.2.5.1 shows temperature predictions obtained.

Table 5.2.5.1 Cloud schemes for Roadsurf runs in section 5.2.5

Time (hrs)	Portion of sky covered by cloud (in oktas)					
	i	ii	iii	iv	v	vi
1200-1500	8	8	8	8	8	Clear
1500-1800	8	8	8	8	8	Clear
1800-2100	6-7	8	8	8	8	Clear
2100-0000	6-7	8	8	8	Clear	1-2
0000-0300	3-5	6-7	3-5	8	Clear	3-5
0300-0600	3-5	3-5	1-2	Clear	1-2	6-7
0600-0900	1-2	1-2	Clear	Clear	3-5	8
0900-1200	1-2	Clear	Clear	Clear	1-2	8
Min Temp/°C	-3.04	-2.64	-3.81	-3.66	-4.13	-3.36
Time of 0°C ±0.15	03:10	04:30	02:45	03:40	23:40	21:25

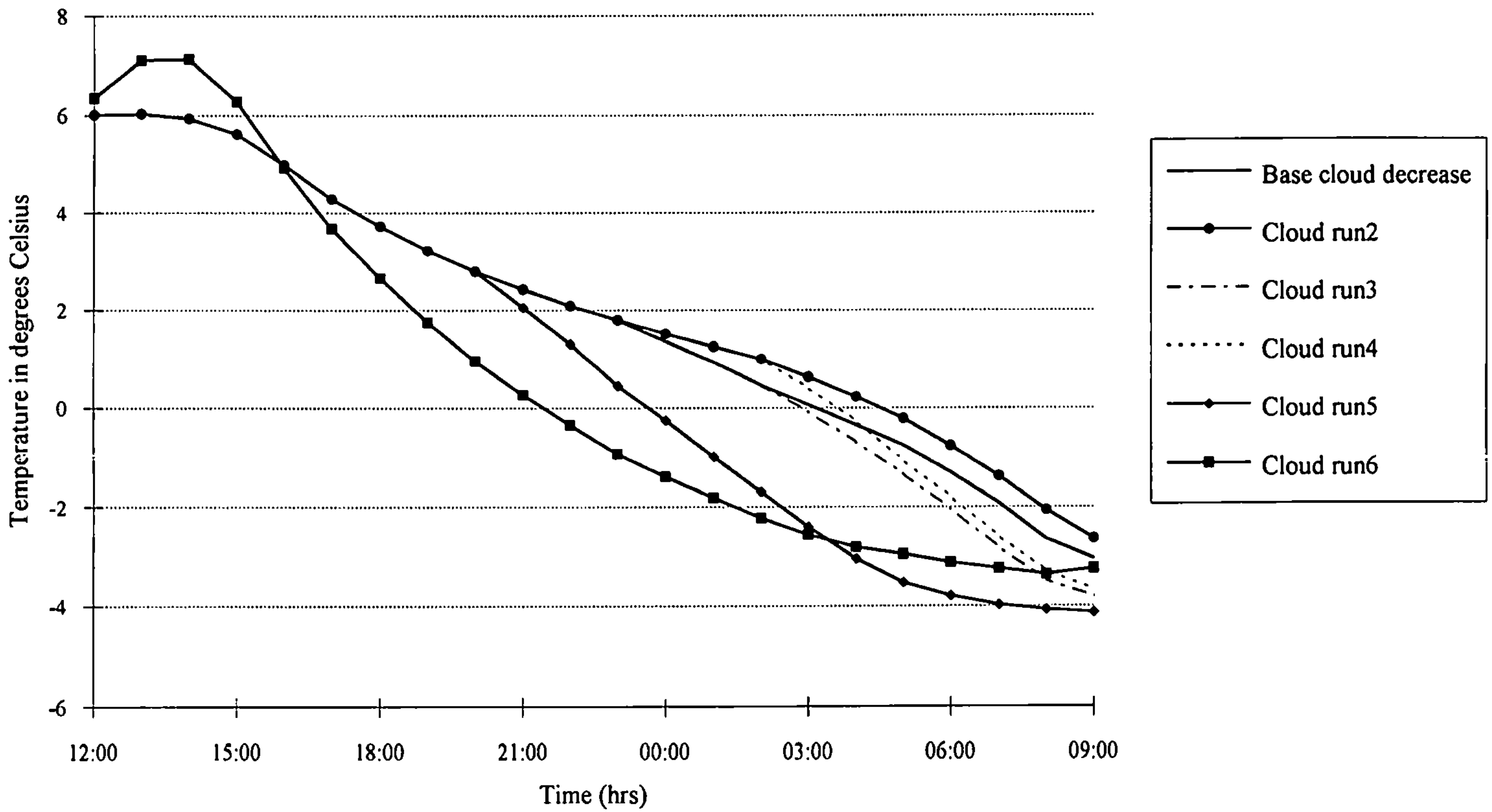

Figure 5.2.5.1 Predicted surface temperature from Roadsurf runs in 5.2.5 showing dependence of surface temperature on rate of cloud change

For the purpose of ALBEDO, DPLUS AND KCLOUD (Table 5.1.1), cloud cover was assumed to be at medium levels.

The run involving a clearance followed by a cloud increase (v) predicted the lowest surface temperatures. The same cloud scheme (v) generally produced lower temperatures, with a six hour clear sky period than schemes (iv) and (vi) with nine hours of clear sky. The timing of clear sky periods in this set of tests was therefore very influential on the minimum temperature overnight and was also more important than their duration.

A wide variation in surface freezing onset times (see bottom row of Table 5.2.5.1) occurred with the earliest at 2130 hrs under initially clear sky (vi), and the latest at 0430 hrs under an overcast sky which later cleared. This variation was expected because of wide ranges of cloud clearance used. The latest frost onset time occurred with cloud scheme (ii) due to overcast conditions which dominated for twelve hours before a cloud clearance commenced. The clear sky in this run, which occurred after 0900 hrs was too late to have any affect on freezing onset time, which had already occurred four and a half hours earlier!

Runs which started under cloudy conditions gave interesting predictions once cloud clearance had commenced. Comparisons between cloud clearance rates and predictions of temperature showed evidence of heat transfer timelags occurring in the subsurface layers, shown remarkably well by comparing predictions using cloud scheme (i) with those using scheme (ii) (Figure 5.2.5.1). The cloud cover in these two runs differed after 1800 hrs, but corresponding surface temperature predictions took 5 hours to differ. This timelag was due to the 'd' and 'cl' layers supplying enough heat to the surface to temporarily reduce rates of surface cooling.

5.3 Sensitivity test conclusions

- The new model, Roadsurf performs very well

- Roadsurf clearly shows strong influences from changes of cloud cover amount and height on predicted surface temperature. Large consequences in predictions of surface temperature arise from erroneous cloud forecasts

- The peak of solar radiation which reaches the surface under overcast skies is a third of that under clear skies

- Latent and sensible heat fluxes are much more dependent on cloud cover when negative (directed upwards) than when positive

- Roadsurf reproduces timelags between variance of extraterrestrial influences and surface temperature change which were very similar to those which occur in real life due to heat capacity

- Initial surface temperature in Roadsurf strongly influences frost onset time; Roadsurf with initial surface temperature input of 6 °C as opposed to 10 °C gives frost onset time 3 hours earlier

- Totally overcast skies have a similar effect on surface temperature as 6 or 7 oktas of medium level cloud

Chapter 6 Retrospective case studies from 1995/96 winter

Case studies in this chapter are sub-divided into two parts. The first is really an analysis of what happened, as well as comparisons between observations and predictions obtained using Roadsurf. The second part of each case study is concerned with developing a suitable algorithm for that particular scenario in order to better predict road surface temperature evolution for a period of 24 hours. Firstly though, a short text to ascertain the best method of surface temperature prediction:-

There are three methods of producing a surface temperature forecast:-

1. Manual, which does not use Roadsurf, instead relying on human knowledge and expertise.

Advantages:-

- Accurate on most occasions, especially if expertise and knowledge of the influences of meteorology on local climate is available
- Many different cloud and synoptic scenarios can be catered for based on predetermined local knowledge.

Disadvantages:-

- Laborious and time consuming
- Requires a trained meteorologist with local knowledge, - can be expensive and difficult to come by. Needs to know how to calculate energy flux changes, and to possibly track cloud cover if no cloud forecast is available.
- Human error in temperature prediction algorithms.

2) Automatic, where temperature predictions are produced by Roadsurf, with no human intervention.

Advantages:-

- Quick and easy:- insert input data and press a button
- No need for trained meteorologist, though there is of course still a need for accurate cloud predictions though these would be supplied from elsewhere.

Disadvantages:-

- Effects of different scenarios are **not** accounted for, which affect ground-atmosphere heat transfer, for example, advection of continental as opposed to maritime air causes significantly differing effects on road surface temperature
- Only basic heat transfer processes are realised
- A poor quality input data set will produce wrong predictions, which unfortunately could be overlooked.

3) Melange of automatic and manual methods, similar to the second method, except that adjustments to model predictions are made to account for different scenarios and site parameters.

Advantages:-

- Different scenarios are accounted for
- Only a limited amount of meteorological knowledge is needed, mostly to ascertain scenario type.
- Faster and easier than manual methods and, though slower than purely automatic methods, increased accuracy is gained improving effectiveness of salting operations.

A mixture of automatic and manual methods would be the most beneficial. It was decided to use the standard Roadsurf model to produce prediction sets which would have scenario and site attribute dependent adjustments applied to them. This method can be implemented by anyone with a limited meteorological knowledge.

It is assumed, that in an operational environment, satellite imagery would be available. This would permit cloud tracking to be carried out, thus producing cloud cover parameters for the Roadsurf model inputs. However, cloud forecasts may be also available from elsewhere, such as the Internet (see Appendix 4).

An alternative method of accounting for different scenarios by using modified versions of Roadsurf *is* however attempted in a case study from February 4th and 5th 1996.

Updating Predictions

Since, the following case studies were carried out retrospectively, accurate sets of data obtained directly from observations were used for Roadsurf inputs required by the model at specific occasions **during** model runs. These included air temperature, wind velocity and humidity observations. Observations of surface temperature however, were only used at the start of model runs i.e. Roadsurf was not updated with observed surface temperatures at any point in time, even if predictions of surface temperature were poor.

In a real life situation however, updated inputs of surface temperature could be useful in improving a bad Roadsurf prediction, using later observations as updated surface and ground temperature inputs in place of preceding predictions when they become available, e.g. from 1800 UTC. Usually this would help to achieve an adequate Roadsurf performance from then onwards. Occasionally, this practice would have detrimental effects on Roadsurf performance by upsetting equilibriums achieved, potentially causing computational instability.

Acceptability of errors

Models are always prone to errors and consequently it is often easy to be pessimistic about their performance, even if errors are small. Some margin of error is acceptable when predicting road surface temperatures (RSTs). It was therefore necessary to determine the maximum size an error can be for a model prediction to be acceptable.

There are two important types of error when using Roadsurf:-

i. Time difference between forecast and observed surface freezing,

ii. Difference between forecast and observed surface temperature.

Determination of acceptable error margin

Under the Devon County Council (D.C.C.) 1991/92 winter maintenance and emergency plan, decisions on salting operations were influenced by several factors in addition to predicted surface temperature. Their overnight procedure has usually been to initiate preparations for salting whenever the RST falls to +0.5°C, with final decisions dependent on surface wetness, *pre*salting operations and likelihood of precipitation. Thus an error in a Roadsurf prediction would have been unacceptably large if the RST fell to +0.5°C or less but was predicted to stay higher than +0.5°C. Hence, the size of error which renders a prediction unacceptable is not fixed.

A degree of acceptability of predictions at all temperatures was also required since Roadsurf uses its own surface temperature predictions to forward step the model. Using an unacceptable prediction to produce following predictions is not advantageous. Determining the extent of permissible error for this aspect of acceptability was difficult and depended on time. For example, Roadsurf occasionally had a tendency to poorly handle solar radiation peaks, producing large errors in surface temperature prediction between 1400 UTC and 1600 UTC, especially with cloud free conditions. Although errors during these occasions appeared unacceptably large, they did not necessarily render later predictions unacceptable.

The following table attempts to summarise acceptability of predictions resulting from points discussed above. D.C.C. are most interested in the surface freezing onset time predictand.

Table 6.i Acceptability of Roadsurf predictions

Predictand	Acceptability
Surface freezing onset time	Unacceptable if error is > 2 hours late/early when $\partial Ts/\partial t \geq 1.0$ deg. C/hr Unacceptable if error is > 4 hours late/early when $\partial Ts/\partial t < 1.0$ deg. C/hr
Surface temperature between 0.0 °C and 3.0°C	Unacceptable if error > 1.0 deg. C*
Surface temperature higher than 3.0 °C	Unacceptable if error >3.0 deg. C when between sunrise and sunset (daytime)
	Unacceptable if error >2.0 deg. C when between sunset and sunrise (night time)

* deliberately fixed value to avoid complication

The Case Studies:-

1. November 18th/19th 1995
2. January 23rd/24th 1996
3. February 4th/5th 1996
4. December 5th/6th 1995
5. February 6th/7th 1996

Since Roadsurf does not actually predict cloud formation and its runs were retrospective, satellite imagery was used to derive cloud cover input parameters, at three hourly intervals.

6.1 November 18th/19th 1995

Scenario:- Cloud forming in situ under settled anticyclonic conditions.

6.1.1 General synoptic conditions, cloud movement and effects on temperature

An anticyclone of 1030 millibars dominated Southwest England with a strong inversion at 0000 UTC Nov. 18th and 19th (Figures 6.1.1.1a and b). The nearest fronts to Devon during Nov. 18th and 19th were further than 400 km away.

Table 6.1.1.1 shows details of any substantial medium level cloud which occurred between 0000 UTC and 0600 UTC Nov.19th ascertained from NOAA infrared imagery in Figures 6.1.1.2a to d and its effects on temperature increase rates which occurred. It became clear that both 2m air and road surface temperatures (RSTs) rose considerably whenever cloud was present. Rates of increase between the two temperature parameters were very close with differences between them being within 1 deg. C for 13 of the 14 cloud 'events' studied. The only exception occurred at Cross Farm between 2330 UTC and 2345 UTC Nov. 18th, where an anomalous 4.7 deg. C/hr rise in air temperature occurred. Initially, it was thought that satellite imagery analysis may have failed to detect possible cloud which could have caused a warming at Cross Farm. However, even if cloud *did* suddenly form, it would have been unlikely to have warmed the air by more than 2 deg. C/hr. The air temperature sensor at Cross Farm was unfortunately rather sheltered by foliage producing a warm bias in air temperature reports, so in view of this rapid rise in air temperature, it was thus interesting to note that a warming caused by cloud between 0115 UTC and 0800 UTC Nov. 19th was less than 1 deg. C/hr. The road temperature sensor at Cross Farm during this time behaved very similarly to those at other stations, recording temperature increases of no more than 0.7 deg. C/hr whenever cloud was present.

Cloud cover changes during the period studied could have been classified as 'ideal' for a retrospective study of this type due to a wide range of cloud durations occurring within the same airstream and period of time. This gave an excellent opportunity to compare

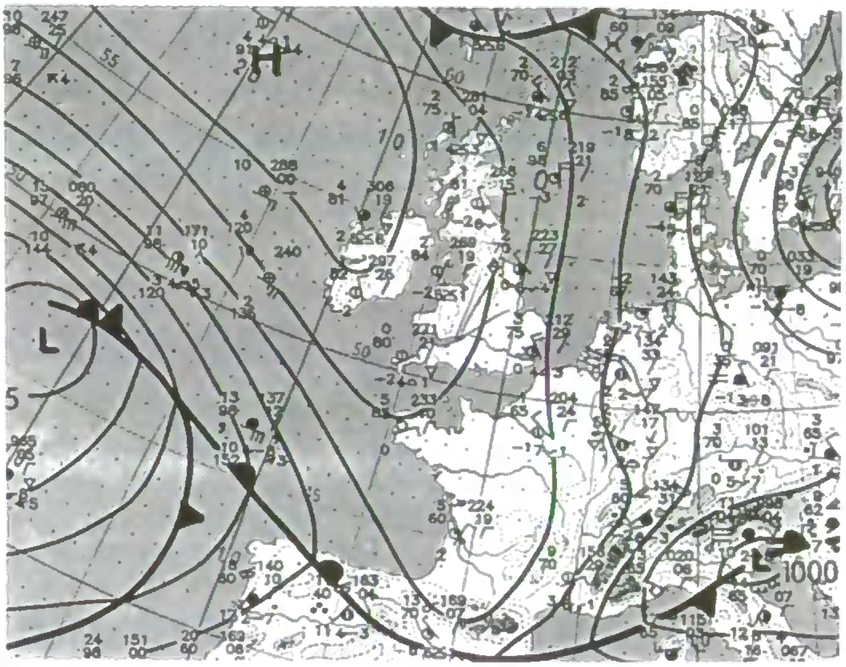

a. 0000 UTC Nov. 18th 1995

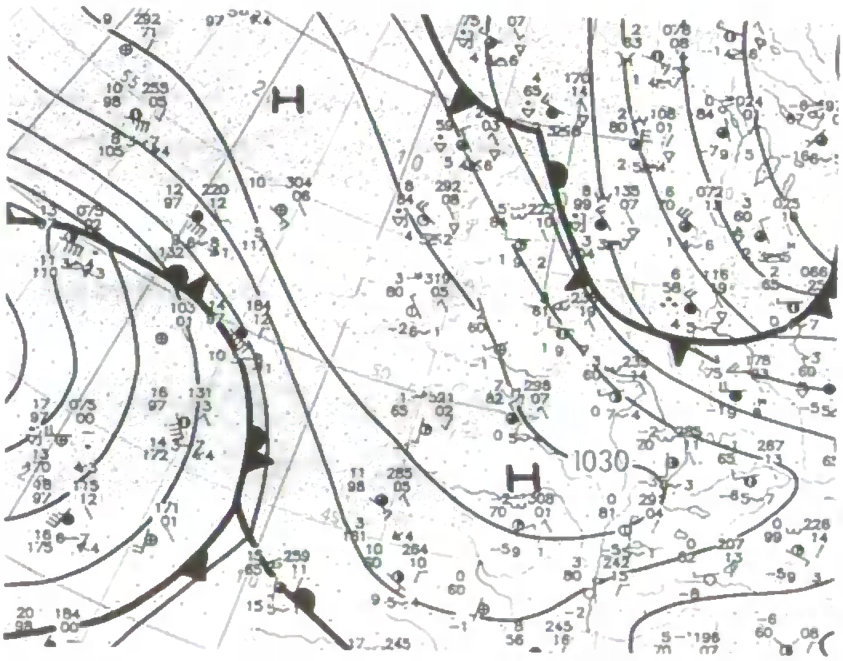

b. 0000 UTC Nov. 19th 1995

Figure 6.1.1.1 European Meteorological Bulletin surface analyses

a. 1918 UTC Nov. 18th

c. 0335 UTC Nov. 19th

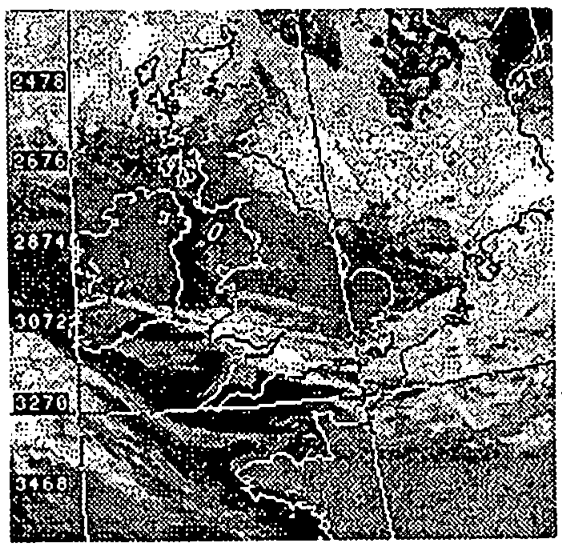

b. 0154 UTC Nov. 19th

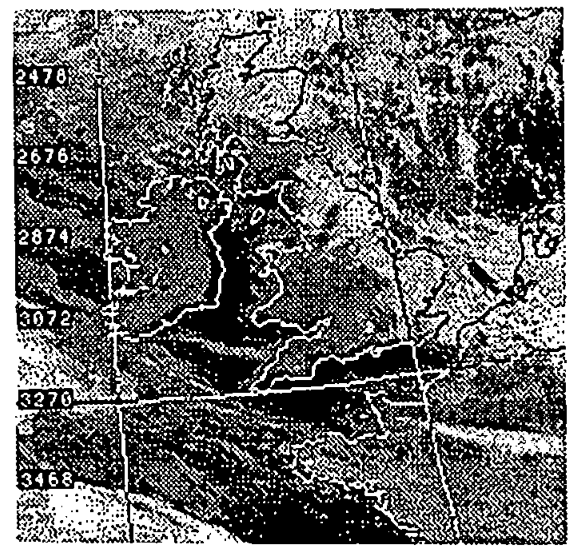

d. 0715 UTC Nov. 19th

Figure 6.1.1.2 NOAA infrared satellite images
from Nov. 18th and 19th 1995

warming effects due to differing cloud durations. Cloud associated surface warming occurred at Pridhamsleigh, where air and road surface warmings of 4.5 deg. C and 2.5 deg. C occurred respectively between 0545 UTC and 0900 UTC Nov. 19th. Similar warmings under cloud occurred at Whiddon Down, Slade Cross and Sourton Cross. Results at Kingsteignton though, were somewhat different: cloud persisted for longer than five hours but neither the air or road surface temperature rose by any more than 2 deg. C throughout. This was due to the station's location on a bridge.

Movement of cloud during Nov. 18th and 19th was rather complicated . Cloud displacement from NOAA satellite images from 1918 UTC Nov. 18th to 0154 UTC Nov. 19th gave an illusion of low level cloud movement towards the Northeast, yet from 0300 UTC to 0715 UTC, cloud appeared to move in the reverse direction. This variation in displacement was due to local variability in air flow no stronger than 5 knots, as well as the synoptic conditions present at the time.

Table 6.1.1.1 Cloud cover, air and road surface temperature fluctuations between 0000 and 0900 UTC Nov. 19th 1995.

Station	Hours of cloud cover /UTC	Cloud cover duration /hrs	Rise in air temperature under cloud /deg. C	Rise in surface temperature under cloud /deg. C	Rate of rise in:-	
					Air temp under cloud /deg.C hr^{-1}	Road temp under cloud /deg.C hr^{-1}
Pridhamsleigh	0545-0900	3.25	4.5	2.5	1.38	0.76
Whiddon Down	0130-0630	5	3.0	3.5	0.6	0.7
Kingsteignton	0130-0700	6.5	0.5	1.5	0.08	0.23
Slade Cross	0145-0700	5.25	3.5	2.0	0.67	0.38
Gallows Gate	0445-0900	4.25	3.0	3.5	0.71	0.82
Sourton Cross	2300-0545♰	6.75	3.5	2.0	0.51	0.30
	0200-0545	3.75	2.5	3.0	0.67	0.80
Friars Hele	0115-0700⌖	5.75	3.0	2.5	0.52	0.43
	0030-0130	1.0	0.0	0.5	0.0	0.50
	0245-0400	1.25	2.0	1.0	1.6	0.80
	0530-0630	1.0	0.5	0.5	0.5	0.50
Halwill Junction	0330-0700	3.5	3.0	2.0	0.86	0.57
Cross Farm	2330-2345✠	0.75	3.5	0.5	4.67	0.67
	0115-0800	6.75	4.0	2.5	0.59	0.37

See subscript notes

Subscripts to Table 6.1.1.1

♰ Scattered cloud was present above Sourton Cross from 2300 but was less than 4 oktas. After 0200, cloud was generally more widespread of 6-7 oktas.

♦ Available NOAA satellite images showed cloud above Friars Hele from 0115 to 0700. However, a sharp fall in air temperature between 0130 and 0200 raised suspicion of human error in satellite imagery analysis; the infrared image showed most cloud to be of equal brightness as the land mass.

✲ Cloud was not shown to be present in NOAA imagery above Cross Farm between 2330 and 2345 but the road weather station reported a sharp 3.5 deg. C warming of the air in this fifteen minute interval indicating that low cloud *may* have been present which the satellite failed to detect.

6.1.2 **Initial Roadsurf predictions.**

Roadsurf was used to predict road surface temperature evolution for 5 stations: Haldon Hill, Roborough, Sourton Cross, Cross Farm and Bratton Down using major input parameters from Tables 6.1.2.1 and 6.1.2.2 from 1100 UTC Nov. 18th to 0900 UTC Nov. 19th.

Table 6.1.2.1 Cloud parameter inputs for Roadsurf runs of 1100 UTC Nov. 18th to 1200 UTC Nov. 19th 1995.

Time /UTC	Haldon Hill	Roborough	Sourton Cross	Cross Farm	Bratton Down
1200 Nov.18	3-5	6-7	1-2	1-2	1-2
1500	3-5	6-7	1-2	1-2	1-2
1800	6-7	8	8	8	4
2100	8	6-7	6-7	6-7	6-7
0000 Nov.19	6-7	1-2	2-3	2-3	8
0300	6-7	2-3	8	8	8
0600	8	8	8	8	6-7
0900	6-7	6-7	6-7	6-7	6-7

Table 6.1.2.2 Major parameter inputs for Roadsurf for runs of 1100 UTC Nov. 18th to 1200 UTC Nov. 19th 1995.

Parameter (Times in UTC)	Haldon Hill	Roborough	Sourton Cross	Cross Farm	Bratton Down
TA at 1200 Nov.18 /°C	3.8	5.0	4.5	6.5	4.1
Ts at 1200 Nov.18 /°C	7.9	9.5	2.5	1.0	7.9
Td at 1200 Nov.18 /°C	6.7	8.0	5.0	4.0	7.0
Tcl at 1200 Nov.18 /°C	6.7	7.0	7.0	7.0	6.0
UA(throughout)/ms^{-1}	0.4	0.4 (using Sourton ob)	0.4	0.4 (using Sourton ob)	0.4 (Using Haldon ob)
DWB (throughout) / deg. C	0.1	2.5	4.1	2.9	1.7
Surface state at 1200 Nov. 18th	Dry	Dry	Dry	Dry	Dry

Notes:

TA: air temperature,

Ts: road surface temperature,

Td: 'd' layer temperature (immediately below surface),

Tcl: 'cl' layer temperature (immediately below 'd' layer),

UA: wind speed,

DWB: depression of wet bulb temperature,

ob: observation

Surface freezing occurred at all 5 stations (see Tables 6.1.2.3 and Figures 6.1.2.1a to e), though it was only predicted at 2, which indicated that either cloud input parameters sourced from the NOAA imagery had over emphasised cloud cover or Roadsurf had exhibited a warm bias. On this occasion, Roadsurf poorly predicted freezing onset times with errors of 5 and 4 hours at Sourton Cross and Cross Farm respectively (Tables 6.1.2.3c and d). Frost was not predicted to occur at Haldon Hill, Roborough and Bratton Down even though it *did* occur. Thus a quick glance at this aspect of Roadsurf's performance would leave the reader somewhat disappointed with the model, at least on this occasion.

Timelags between cloud cover variance and road surface temperature (RST) minima occurred at all 5 stations (Figures 6.1.2.1a to e). Timelags in Roadsurf predictions however, were 1 to 2 hours longer than of those in observations. Nevertheless, a 3 hour timelag between cloud and RST minimum at Sourton Cross (Figure 6.1.2.1c) *was* predicted to within 10 minutes of the observed lag duration. Furthermore, it appeared from observations at all stations, that increasing cloud cover corresponded more with increasing air than with surface temperature.

Observed and predicted surface temperatures fell rapidly between 1800 and 2100 UTC Nov. 18th due to a lack of solar radiation and an initially sharp fall in air temperature, which promoted heat transfer from surface to atmosphere.

Observed warming at 2m, which occurred after 2100 UTC at Haldon Hill, Sourton Cross, Cross Farm and Bratton Down (Figures 6.1.2.1a, c, d and e) was partly due to warm

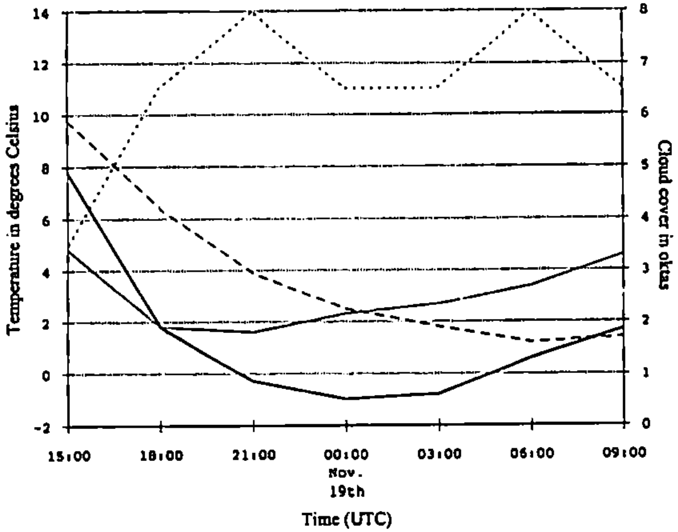

a.Haldon Hill

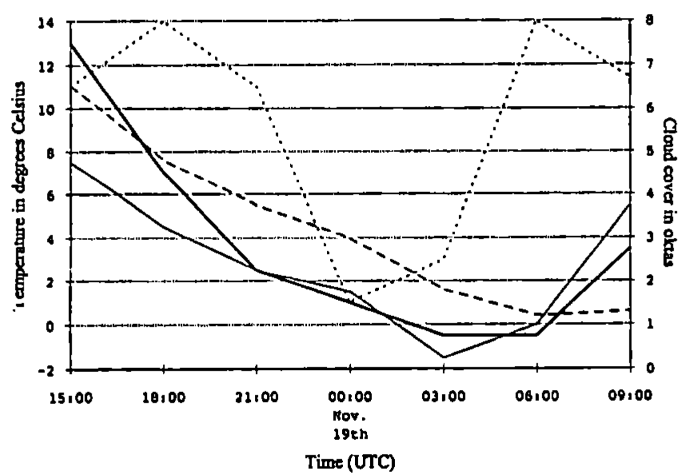

b.Roborough

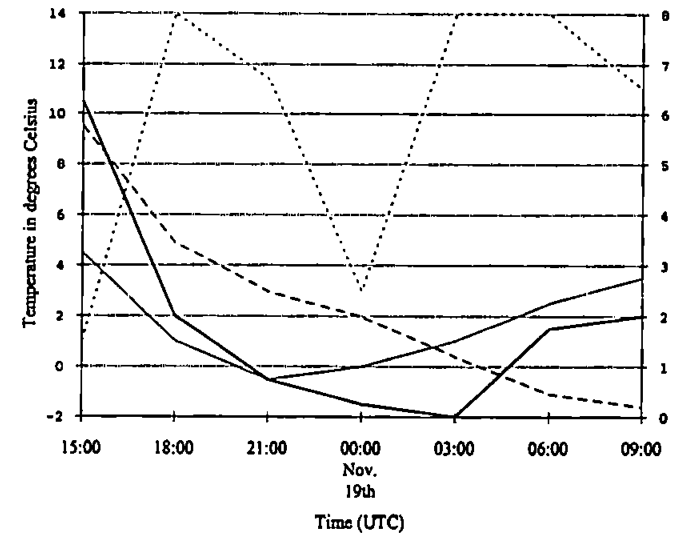

c.Sourton Cross

- - - - Predicted surface temperature
—— Observed surface temperature
—— Observed air temperature
······ Observed cloud cover (right hand scale)

Figure 6.1.2.1 Roadsurf predictions and observations from 1500 UTC Nov. 18th to 0900 UTC Nov. 19th 1995.

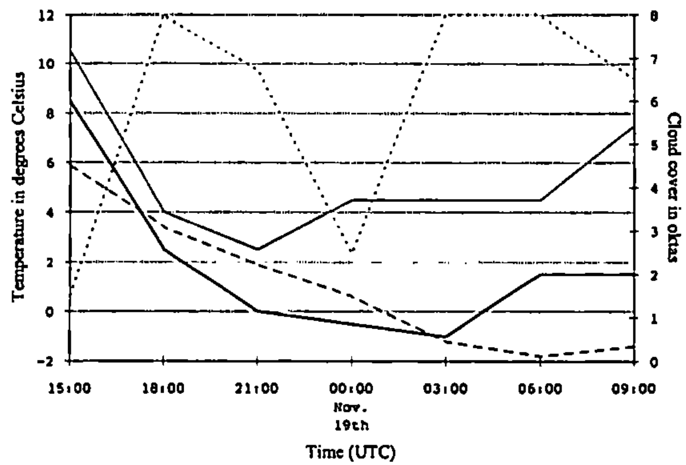

d.Cross Farm

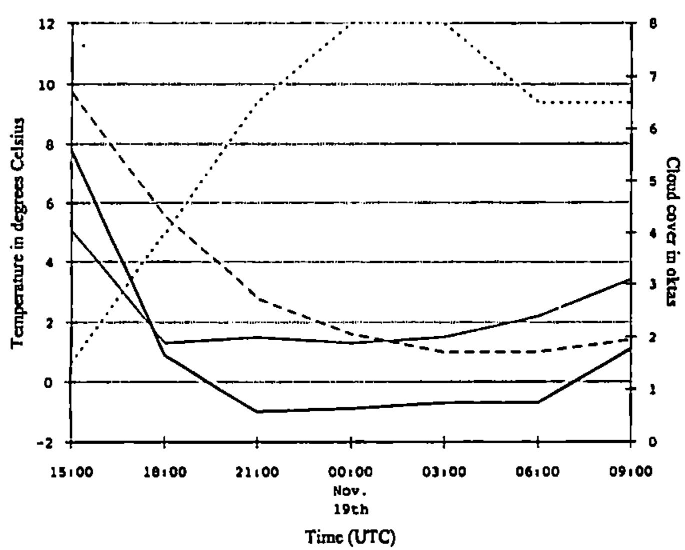

e.Bratton Down

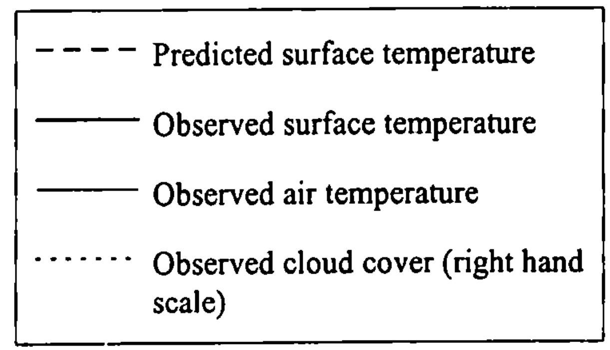

Figure 6.1.2.1 Roadsurf predictions and observations from 1500 UTC Nov. 18th to 0900 UTC Nov. 19th 1995.

air advection associated with approaching cloud from Cornwall. A relatively warm 11°C sea surface temperature west of Cornwall provided much of this increased heat.

Throughout the Roadsurf runs, the 2m air temperature was held constant at 1200 UTC Nov. 18th values (i.e. the initial temperature) which produced a warm bias in the model especially after more than 3 hours of clear sky during darkness. Roadsurf is not capable of predicting horizontal heat transport, assuming it to be zero. Therefore, updated air temperatures at 3 hourly intervals are required by Roadsurf.

Roadsurf performed best at Cross Farm, where RST predictions were within a degree of observations for 37% of the period 1500 UTC Nov. 18th to 0600 UTC Nov. 19th. Furthermore, the predicted minimum RST was only 0.8 deg. C lower than observed, though its timing was 3 hours late. Despite the relative success achieved at Cross Farm, frost onset prediction was 4 hours wrong, an unacceptable error for salting operations. Unfortunately this occurred during a 2 hour period when errors were greatest. From 1730 to 2100 UTC Nov. 18th, differences between observed and predicted RSTs increased from 0 to 2 deg. C coinciding with supposed gradually clearing cloud. During this period, parameterising cloud cover into oktas was difficult since it existed as multiple bands.

Table 6.1.2.3 Important Roadsurf predictions and observations from run of 1200 UTC Nov. 18th to 0900 UTC Nov. 19th 1995.

a) Haldon Hill.

	Predicted	Actual	Error
Time of 0°C Minimum RST	none 1.2°C	2030 UTC 1.6°C	na 0.4 deg. C too low
Average error in predictions: +2.0 deg. C			

b) Roborough.

	Predicted	Actual	Error
Time of 0°C Minimum RST	none 0.5°C	0205 UTC -0.5°C	na 1.0 deg. C too high
Average error in predictions: +0.6 deg. C			

c) Sourton Cross.

	Predicted	Actual	Error
Time of 0°C Minimum RST	0400 UTC -1.9°C	1924 UTC -2.0°C	8hrs 36 mins late negligible
Average error in predictions: +0.7 deg. C			

d) Cross Farm.

	Predicted	Actual	Error
Time of 0°C Minimum RST	0115 UTC -2.0°C	2100 UTC -1.0°C	4hrs 15mins late 1.0 deg. C too low
Average error in predictions: -0.5 deg. C			

e) Bratton Down.

	Predicted	Actual	Error
Time of 0°C Minimum RST	none 1.2°C	1922 UTC -1.0°C	na 2.2 deg. C too high
Average error in predictions: +2.0 deg. C			

Table 6.1.2.4 Error analysis of Roadsurf surface temperature predictions compared to observations. Percentage of run durations with errors as shown.

	Percentage of duration of accuracy between predicted and observed RST					
	Period 1500 to 2359 UTC, Nov. 18th 1995		Period 0000 to 0900 UTC, Nov.19th 1995		Error at min. temp / deg.C	Largest error / deg. C
	<1deg. C	<2 deg. C	<1 deg. C	<2 deg. C		
Haldon Hill	0	0	35	57	0.5	4.6
Roborough	28	54	19	57	0.5	3.0
Sourton Cross						
Cross Farm	23	96	39	54	0.3	3.5
Bratton Down	0	1	18	78	3.0	4.6

6.1.3 Algorithm formation.

An algorithm was constructed from this case study for a scenario of cloud forming in situ. The simple chosen method was to form an algorithm using average differences between predicted and observed surface temperatures, for example, the simplest algorithm for Haldon Hill, would be to subtract 2 deg. C from all surface temperature predictions (see Table 6.1.2.3a). This would obviously have been inappropriate for periods when the actual surface temperature was higher than predicted or when predictions were 'close' to actual observations. 'Close' to in this case would be temperatures within a degree, though this is debatable. Predictions of surface temperature to enable forecasting of ice need to be within a degree of actual values, since there are slight horizontal and vertical variations across the road surface. Pathways of vehicle tyres tend to be slightly less cold than the rest of the road due to friction.

A periodic change in algorithm was more suitable, for example using six hour periods dependent on time of night and perhaps cloud duration. This would obviously be more realistic since differences between Roadsurf output and actual temperature vary from 0.3 deg. C to 4.6 deg. C. Such an algorithm for Haldon Hill is shown by Table 6.1.3.1a, though this algorithm is not yet cloud dependent. Table 6.1.3.1 b to e also has '6 hour period' derived algorithms for other stations.

Table 6.1.3.1 Proposed algorithms for Haldon Hill, Roborough, Sourton Cross, Cross Farm and Bratton Down during a 'Cloud formation in situ under settled anticyclonic conditions' scenario derived from Nov. 18th and 19th 1995 results.

a) Haldon Hill

Time (UTC)	Operation*
1200-1800 Nov. 18th	subtract 0.5 deg. C
1800-2359	subtract 4.5 deg. C
0000-0600 Nov. 19th	subtract 3.5 deg. C
0600-1200	none needed

b) Roborough

Time (UTC)	Operation*
1200-1800 Nov. 18th	add 0.5 deg. C
1800-2359	subtract 2.0 deg. C
0000-0600 Nov. 19th	subtract 2.5 deg. C
0600-1200	add 1.5 deg. C

c) Sourton Cross

Time (UTC)	Operation*
1200-1800 Nov. 18th	add 0.4 deg. C
1800-2359	subtract 3.2 deg. C
0000-0600 Nov. 19th	subtract 3.0 deg. C
0600-1200	add 3.1 deg. C

d) Cross Farm

Time (UTC)	Operation*
1200-1800 Nov. 18th	add 1.0 deg. C
1800-2359	subtract 1.5 deg. C
0000-0600 Nov. 19th	subtract 0.5 deg. C
0600-1200	add 3.0 deg. C

e) Bratton Down

Time (UTC)	Operation*
1200-1800 Nov. 18th	add 1.0 deg. C
1800-2359	subtract 5.0 deg. C
0000-0600 Nov. 19th	subtract 2.2 deg. C
0600-1200	subtract 0.5 deg. C

* 'operation' is the modification which would be applied to Roadsurf predicted surface temperatures to produce scenario dependent prediction.

Figures 6.1.3.1a to e show a clear advantage of using a time dependent algorithm. Of course, not all occasions have exactly the same temperature fluctuations, even within a similar scenario, during the same month at the same station. However, it makes sense to keep algorithms simple, developing them cautiously. It is less useful to have a complicated set of processes that takes time to implement.

Cloud cover has been plotted in Figures 6.1.3.1a to e in an attempt to detect any relationships between cloud and flaws in the algorithm of Table 6.1.3.1a.

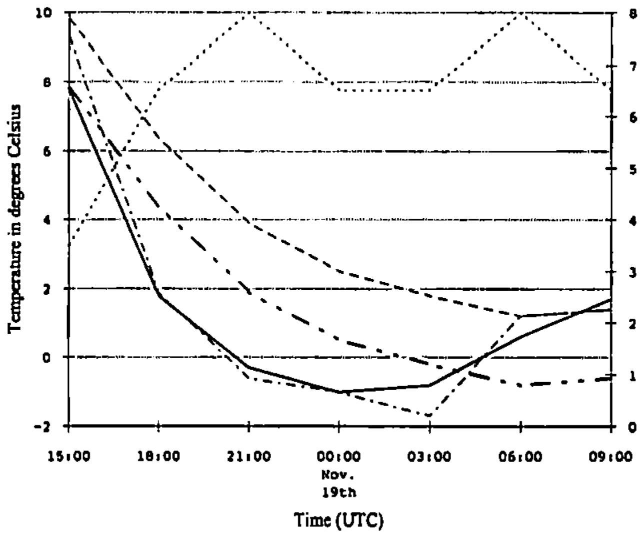

a. Haldon Hill

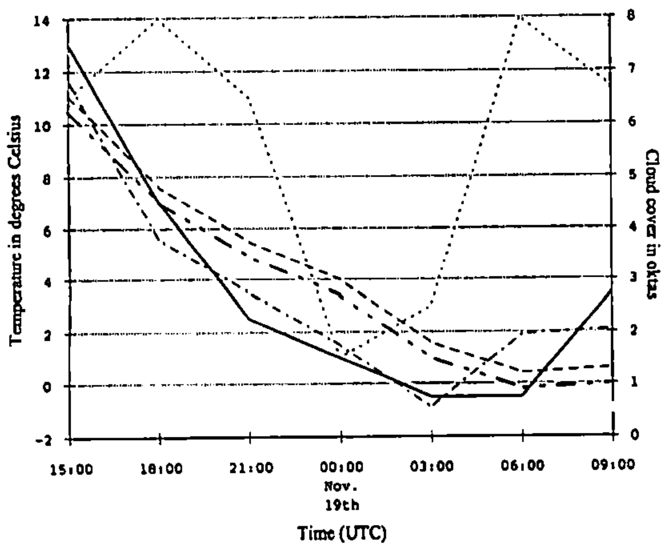

b.Roborough

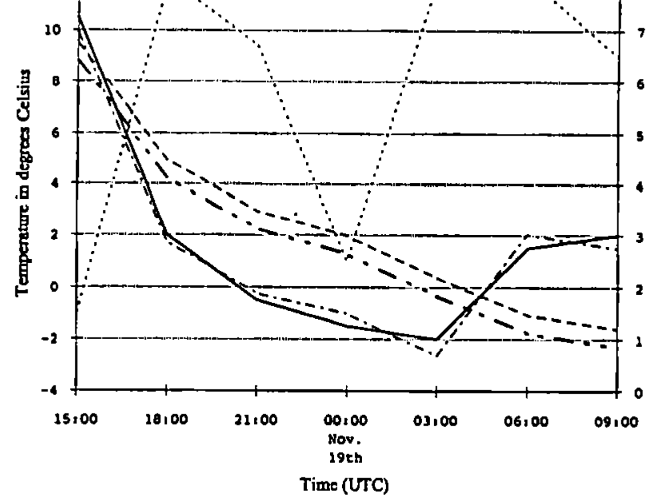

c.Sourton Cross

Observed surface temperature

Unmodified Roadsurf surface temperature predictions

Predicted surface temperature using simple 'subtract 2 deg. C from Roadsurf predictions' algorithm

Predicted surface temperature using algorithms based on '6 hour average corrections' algorithm.

Observed cloud cover (right hand scale)

Figure 6.1.3.1 Predicted surface temperature and observations from 1500 UTC Nov. 18th to 0900 UTC Nov. 19th 1995 (Algorithm tests)

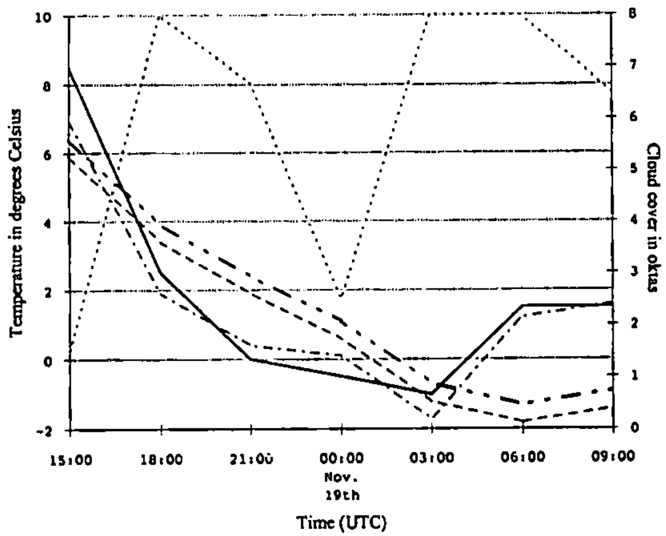

d.Cross Farm

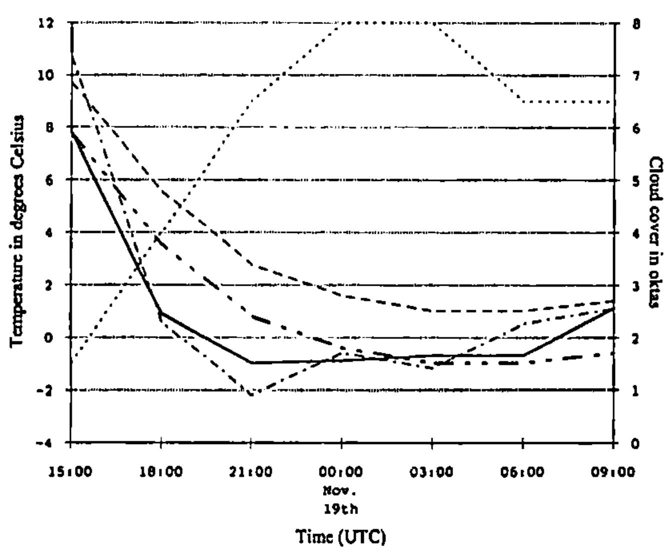

e.Bratton Down

Observed surface temperature

Unmodified Roadsurf surface temperature predictions

Predicted surface temperature using simple 'subtract 2 deg. C from Roadsurf predictions' algorithm

Predicted surface temperature using algorithms based on '6 hour average corrections' algorithm.

Observed cloud cover (right hand scale)

Figure 6.1.3.1 Predicted surface temperature and observations from 1500 UTC Nov. 18th to 0900 UTC Nov. 19th 1995 (Algorithm tests)

6.1.4 Relationships between error in Roadsurf surface temperature prediction and cloud cover ascertained from Figures 6.1.4.1a to e.

(The word 'difference' is used to mean the difference between Roadsurf predictions and observations, and is positive whenever predicted temperature is higher than observed)

Haldon Hill:-

Cloud increase$\propto$difference increase and vice versa until 0300 UTC.

Roborough:-

Cloud increase$\propto$difference increase and vice versa until 0000 UTC then totally opposite.

Sourton Cross:-

Cloud increase$\propto$difference increase from 1500 to 2100 UTC. Confused relationship between 2100 UTC Nov.18th and 0300 UTC Nov. 19th. Cloud increase$\propto$difference **decrease** thereafter.

Cross Farm:-

Cloud increase$\propto$difference increase from 1500 to 1800 UTC and vice versa from 2100 to 0000 UTC. After 0300 UTC Nov. 19th, a large **negative** increase in difference occurred during 8 oktas of cloud.

Bratton Down:-

Cloud increase$\propto$difference increase from 1400 to 1800 UTC. After 1800, difference decreased despite continued cloud cover of over 5 oktas.

From Figures 6.1.4.1a to e, the algorithms detailed in Table 6.1.3.1 must be cloud dependent, especially for 1500 to 2100 UTC Nov. 18th. The five graphs show that if the algorithms remain unchanged, they will be inaccurate for clear sky occasions and times outside of the period 1500 UTC to 2100 UTC.

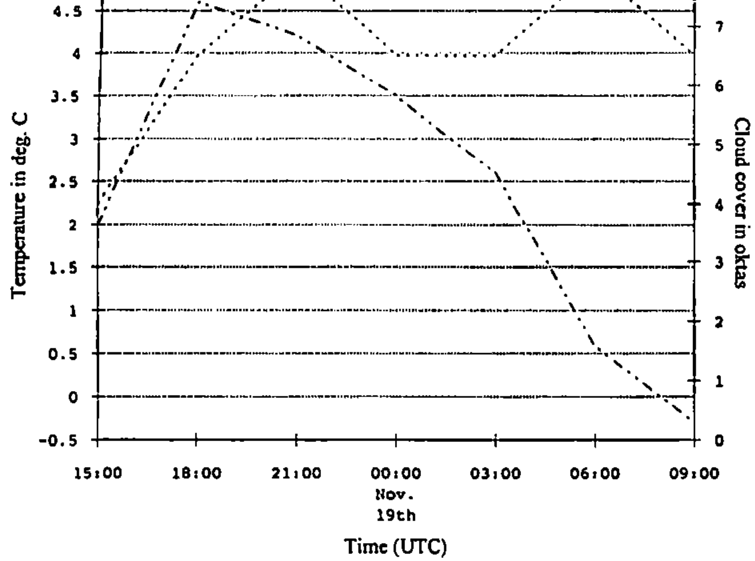

a.Haldon Hill

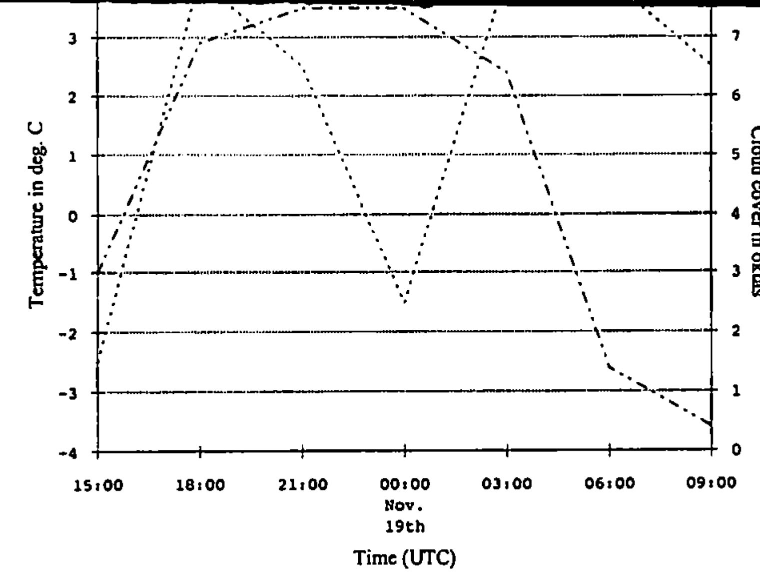

c.Sourton Cross

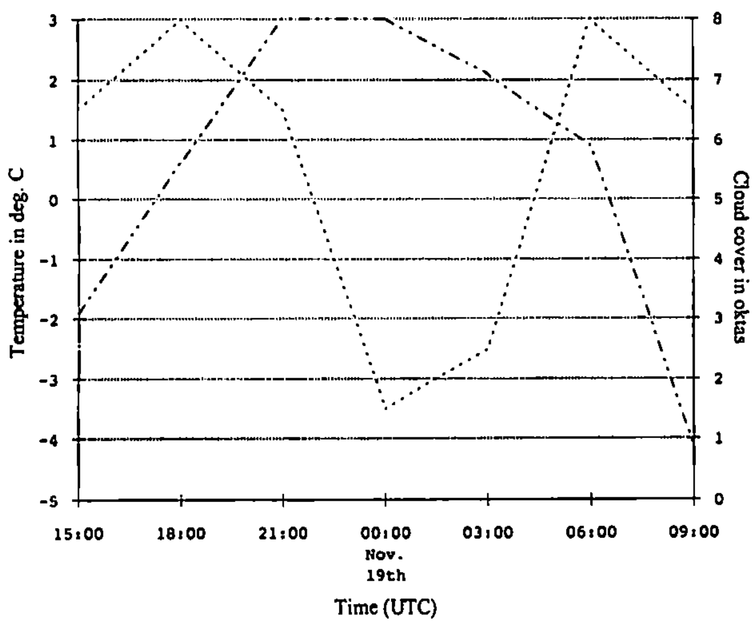

b.Roborough

-·-·- Difference between observed and Roadsurf predicted surface temperature (positive values indicate temperatures predicted higher than observed)

······ Observed cloud (right hand scale)

Figure 6.1.4.1 Relationships between cloud cover and errors in Roadsurf predictions from 1500 UTC Nov. 18th to 0900 UTC Nov. 19th 1995.

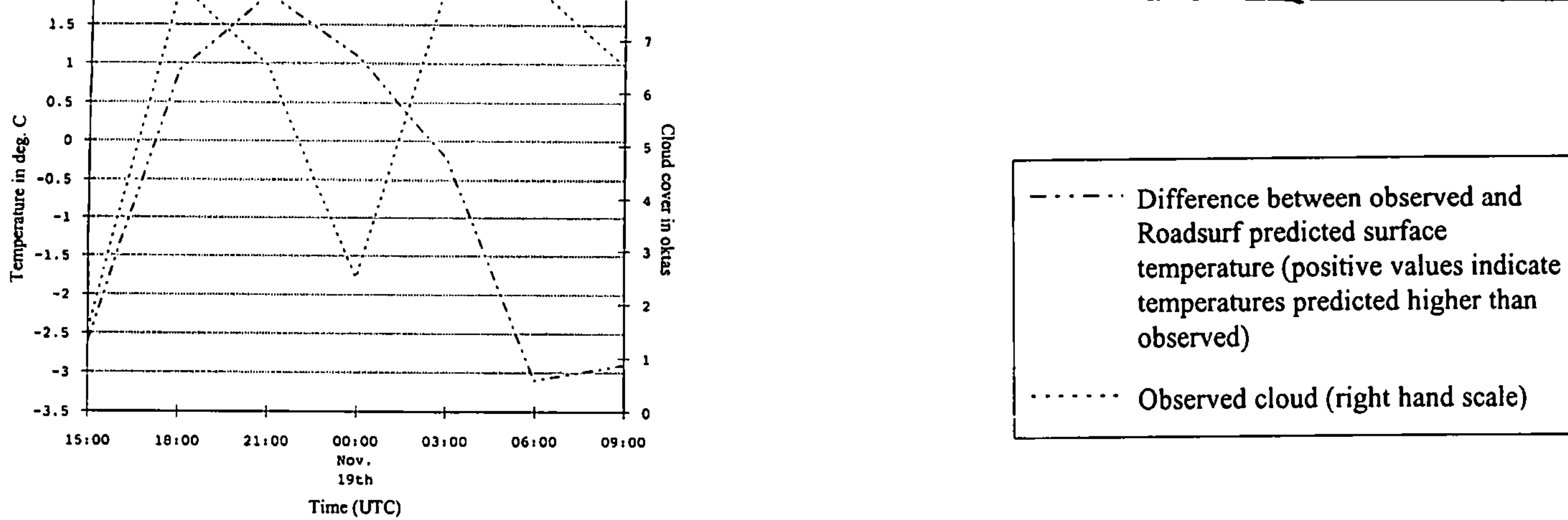

d.Cross Farm

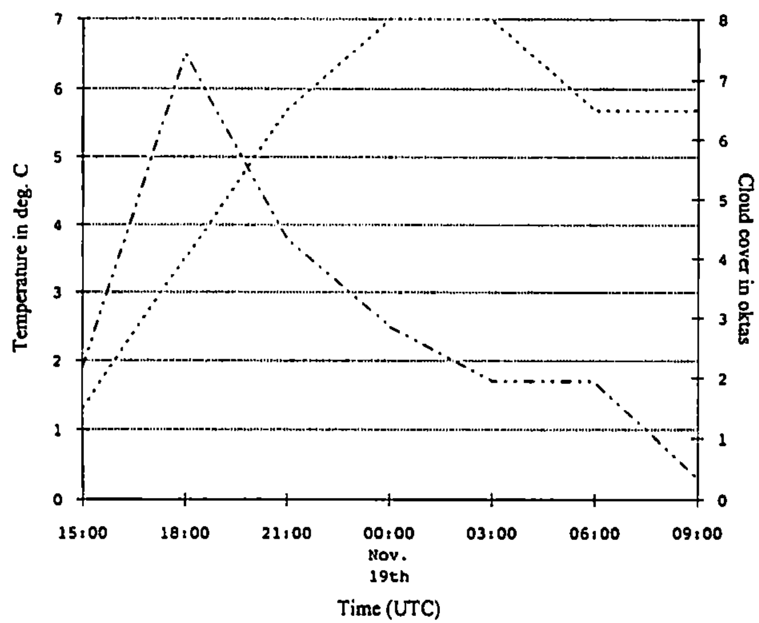

e.Bratton Down

Figure 6.1.4.1 Relationships between cloud cover and errors in Roadsurf predictions from 1500 UTC Nov. 18th to 0900 UTC Nov. 19th 1995.

If cloud forms, the algorithms must be designed to produce a larger modification to predicted surface temperature than under clear skies. This was certain for all five stations, but only between 1800 UTC and 2200 UTC. A confused algorithm dependency on cloud existed from 0000 to 0600 UTC which resulted from differing effects on surface temperature due to cloud. Differences between observed and Roadsurf predicted surface temperature decreased and even became negative, i.e. surface temperature predicted to be lower than observed, at Roborough, Sourton Cross and Cross Farm despite continued cloudy skies.

Therefore, the algorithms of Table 6.1.3.1a to e have been modified to those shown in Table 6.1.4.1. Cloud cover, N in the algorithm has been divided into two separate categories:- 0 to 4 oktas, and more 4 oktas. These new algorithms are expected to produce the most accurate surface temperature predictions for cloudy conditions which occur before midnight. The algorithms have been left unchanged for after midnight, since Roadsurf performed increasingly well as the period 0000 to 0600 UTC progressed.

The choice of algorithm for cc<4 oktas has been derived by rerunning Roadsurf using the same inputs as earlier in this case study, but with a sky of 1 to 2 oktas of medium level cloud. Figures 6.1.4.2a to e show the subsequent Roadsurf predictions.

Table 6.1.4.1 Cloud dependent algorithms for Haldon Hill, Roborough, Sourton Cross, Cross Farm and Bratton Down during a 'Cloud formation in situ under settled anti-cyclonic conditions' scenario derived from Nov. 18th and 19th 1995 results.

a) Haldon Hill

Time (UTC)	Operation*
1200-1800 Nov. 18th	none if cc<4 oktas
	subtract 0.5 deg. C if cc≥4 oktas
1800-2359	subtract 2.2 deg. C if cc<4 oktas
	subtract 4.5 deg. C if cc≥4 oktas
0000-0600 Nov. 19th	subtract 3.5 deg. C
0600-1200	none

b) Roborough

Time (UTC)	Operation*
1200-1800 Nov. 18th	add 1.0 deg. C if cc<4 oktas
	add 0.5 deg. C if cc≥4 oktas
1800-2359	add 1.2 deg. C if cc<4 oktas
	subtract 2.0 deg. C if cc≥4 oktas
0000-0600 Nov. 19th	subtract 2.5 deg. C
0600-1200	add 1.5 deg. C

c) Sourton Cross

Time (UTC)	Operation*
1200-1800 Nov. 18th	add 5.0 deg. C if cc<4 oktas
	add 0.4 deg. C if cc≥4 oktas
1800-2359	add 1.0 deg. C if cc<4 oktas
	subtract 3.2 deg. C if cc≥4 oktas
0000-0600 Nov. 19th	subtract 3.0 deg. C
0600-1200	add 3.1 deg. C

d) Cross Farm

Time (UTC)	Operation*
1200-1800 Nov. 18th	add 0.4 deg. C if cc<4 oktas
	add 1.0 deg. C if cc≥4 oktas
1800-2359	add 0.7 deg. C if cc<4 oktas
	subtract 1.5 deg. C if cc≥4 oktas
0000-0600 Nov. 19th	subtract 0.5 deg. C
0600-1200	add 3.0 deg. C

e) Bratton Down

Time (UTC)	Operation*
1200-1800 Nov. 18th	add 0.7 deg. C if cc<4 oktas
	add 1.0 deg. C if cc≥4 oktas
1800-2359	subtract 2.7 deg. C if cc<4 oktas
	subtract 5.0 deg. C if cc≥4 oktas
0000-0600 Nov. 19th	subtract 2.2 deg. C
0600-1200	subtract 0.5 deg. C

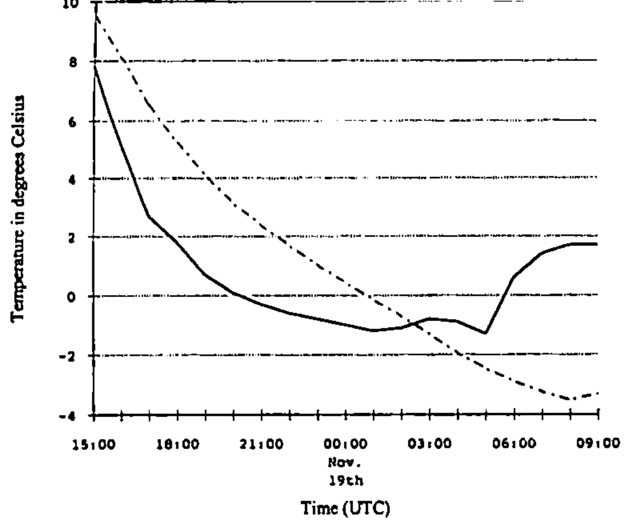

a. Haldon Hill

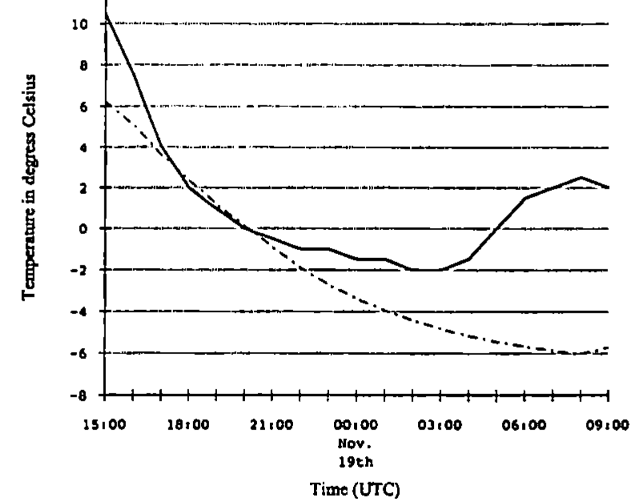

c. Sourton Cross

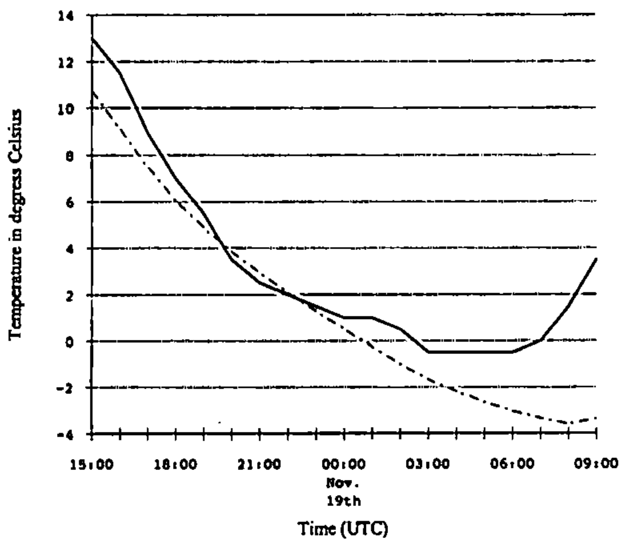

b. Roborough

Observed surface temperature

Roadsurf predicted surface temperature under a false cloud cover scenario of 1 to 2 oktas.

Figure 6.1.4.2 Observations and special Roadsurf (see Legend) predictions of surface temperature from 1500 UTC Nov. 18th to 0900 UTC Nov. 19th 1995.

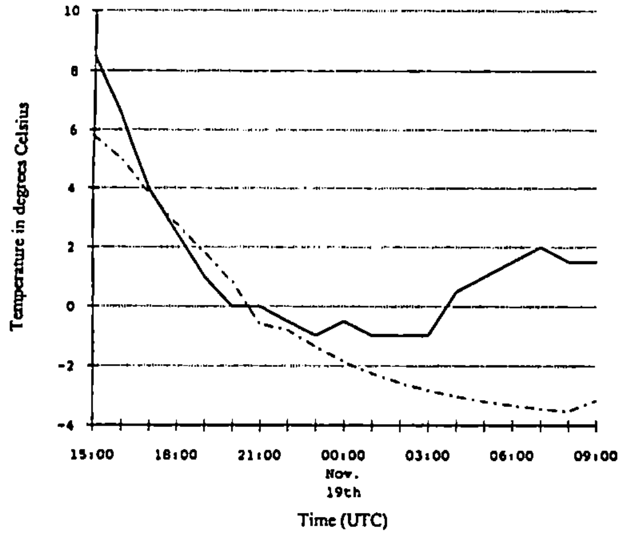

d.Cross Farm

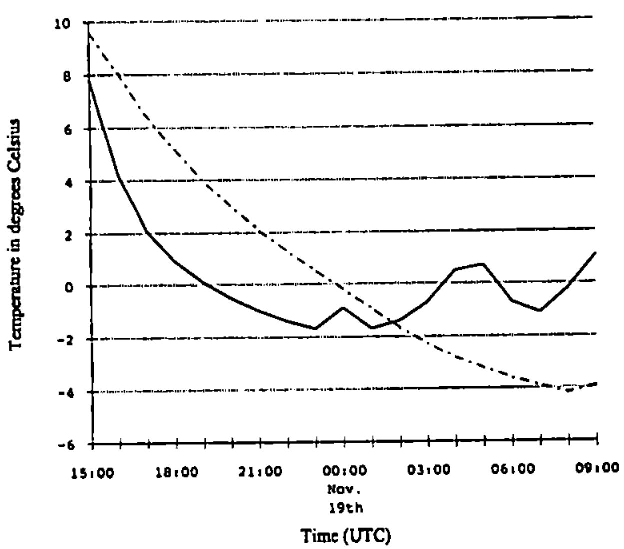

e.Bratton Down

——— Observed surface temperature

— · — · Roadsurf predicted surface temperature under a false cloud cover scenario of 1 to 2 oktas.

Figure 6.1.4.2 Observations and special Roadsurf (see Legend) predictions of surface temperature from 1500 UTC Nov. 18th to 0900 UTC Nov. 19th 1995.

* 'operation' in Table 6.1.4.1 is the modification which would be applied to Roadsurf predicted surface temperatures to produce scenario dependent prediction.

Cloud prediction for Roadsurf

Since the algorithms and Roadsurf itself are dependent on cloud, it is obvious that a good cloud forecast is a basic requirement. A 24 hour (for 1200 UTC next day) forecast from Météo France is available on the Internet* which gives an indication of the likely cloud pattern, but for this scenario with the possibility of cloud formation and dissipation in situ, a midday image is not always a reliable indication of overnight cloud.

Convective cloud present during daylight hours tends to disperse after sunset due to mid-level descent caused by cooling air. However, low level cloud can form in situ during hours of darkness if boundary layer humidity is high.

Frontal cloud is unlikely to exist for more than twelve hours under anticyclonic conditions so it could be unwise to produce a twenty-four hour cloud forecast by tracking observed bands in satellite imagery under the assumption that their size, trajectory and speed will be constant throughout the forecast.

**http://www.meteo.fr/tpsreel/images/isp.gif*

2m wind prediction for Roadsurf

Under this scenario, changes in surface flow are negligible so a suitable value for this parameter could easily be taken from the most recent observation before 1200 UTC.

6.1.5 Evaluation of the UK Meteorological Office Mesoscale Model on November 18 and 19th 1995.

Air temperature predictions for the period 1200 UTC Nov. 18th to 0900 UTC Nov. 19th from the UK Meteorological Office Mesoscale Model are shown in Figures 6.1.5.1a to e whilst Table 6.1.5.1 shows the model's performance for this particular occasion using error analysis. The observed air temperatures in Figures 6.1.5.1a to e were obtained from road weather station air sensors.

Observed 2m air temperatures were predominantly higher than predicted with consistently large errors. This was especially so at Cross Farm where predictions were never within a degree of observed values and within 2 deg. C for only 2 % of the period 1200 to 2359 UTC Nov. 18th. Foliage sheltering the air sensor would have been responsible for only a small warm bias in recorded data. At 0300 UTC Nov. 19th, an 8 deg. C error occurred clearing showing that the mesoscale model was of little use in forecasting a likelihood of frosty conditions at this station on this particular night.

Better performances occurred at 5 other stations, with most accurate predictions for Haldon Hill between 1200 UTC and 2359 UTC Nov. 18th. However, even at Haldon Hill, the model still failed to predict air temperatures to within a degree of observations for more than half of the period studied.

As expected, errors in prediction were largest during the second half of the night, i.e. from 0000 UTC to 0900 UTC Nov. 19th. Table 6.1.5.1 shows also that 4 of the 6 locations, air temperature predictions were never within 2 deg. C of observations during this period. It was interesting to note that of the whole 1200 UTC to 0900 UTC forecast period, prediction errors were greatest for two thirds of the locations at the time of minimum air temperature, between 0000 UTC and 0300 UTC and not at the end of the run. Air frosts, predicted for all 6 locations, occurred only at Roborough and Sourton Cross. Furthermore, at these two, the predicted onset time of the frosts were 7 and 2.5 hours too early. However, it is more advantageous to have a model which predicts a frost early rather than late.

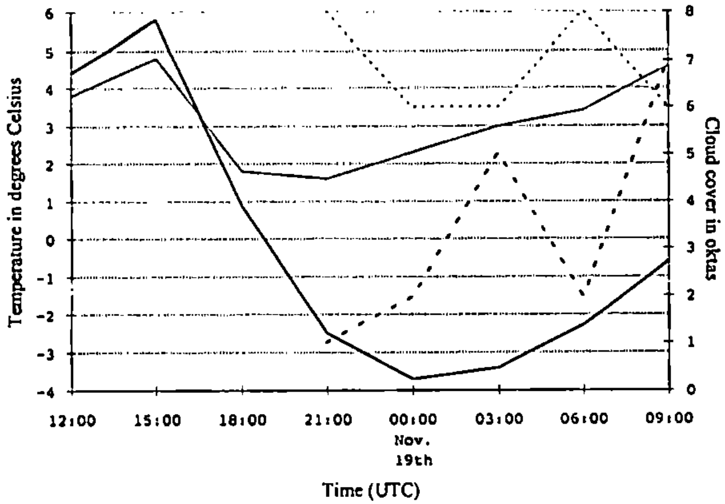

a.Haldon Hill

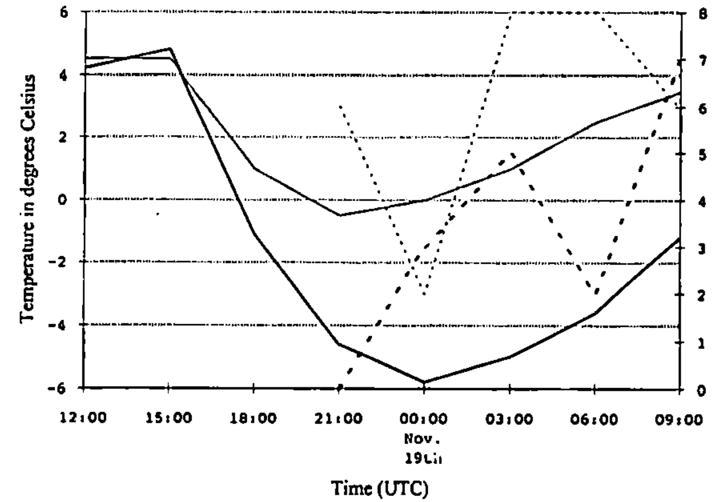

c.Sourton Cross

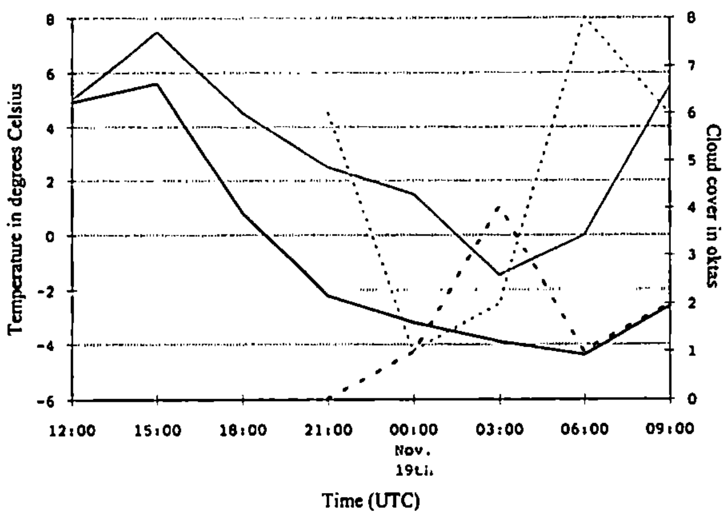

b.Roborough

Predicted air temperature from Mesoscale model

Observed air temperature

Predicted cloud in oktas (right hand scale)

Observed cloud in oktas (right hand scale)

Figure 6.1.5.1 UK Meteorological office mesoscale model predictions and observations from 1200 UTC Nov. 18th to 0900 UTC Nov. 19th 1995.

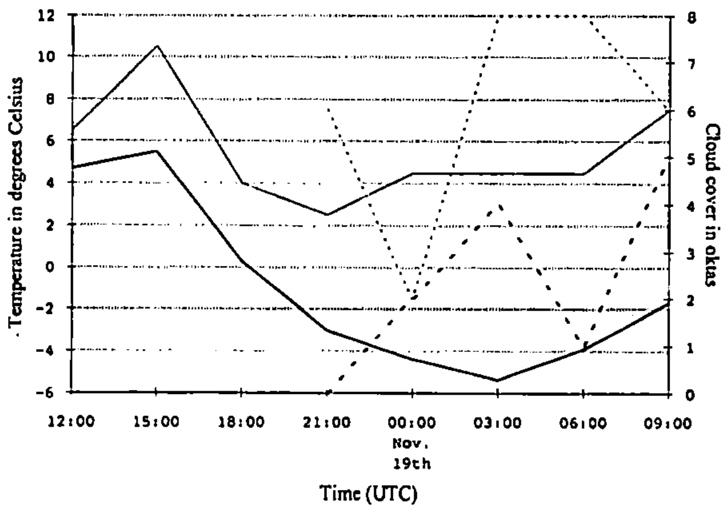

d.Cross Farm

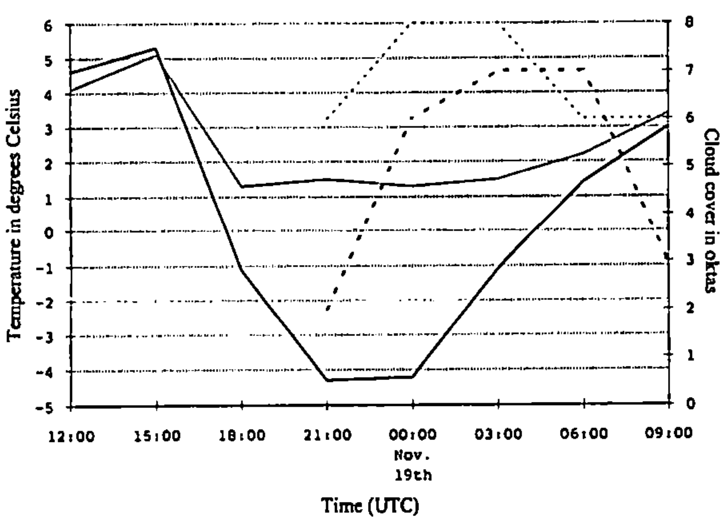

e.Bratton Down

Predicted air temperature from Mesoscale model

Observed air temperature

Predicted cloud in oktas (right hand scale)

Observed cloud in oktas (right hand scale)

Figure 6.1.5.1 UK Meteorological office mesoscale model predictions and observations from 1200 UTC Nov. 18th to 0900 UTC Nov. 19th 1995.

Table 6.1.5.1 Error analysis of mesoscale air temperature predictions compared to observations. Percentage of run durations with errors as shown.

	Percentage of duration of accuracy between predicted and observed air temperature.					
	Period 1200 UTC to 2359 UTC Nov. 18th 1995		Period 0000 UTC to 0900 UTC Nov.19th 1995		Error at minimum temp. / deg.C	Largest error / deg. C
Accuracy⇒	<1deg. C	<2 deg. C	<1 deg. C	<2 deg. C		
Haldon Hill	50	58	0	0	6.0	6.4
Stopgate Cross	30	55	17	48	3.2	3.7
Roborough	13	28	0	0	4.5	8.0
Sourton Cross	40	49	0	0	5.9	5.9
Cross Farm	0	2	0	0	10.0	10.0
Bratton Down	38	47	37	54	1.8	5.8

Cloud cover prediction by the mesoscale model.

Comparisons of cloud forecasts with observations using infrared satellite imagery presented many problems, since determining cloud cover in oktas and it's level from satellite imagery can be difficult. Unfortunately, routine ground based cloud observations are no longer carried out since the closure of the Plymouth Weather Centre, so satellite images were the only data available. Despite this, a few comparisons of results in Figures 6.1.5.1a to e could be made, though these showed mostly where model output of cloud cover contained large errors. Cloud cover at Stopgate Cross and Cross Farm was poorly predicted with errors of at least 4 oktas, whilst cloud predictions at Haldon Hill were good.

It is obvious that in enabling a mesoscale model to accurately predict air temperatures and hence frost onset times from Roadsurf, it must first be able to accurately forecast cloud cover. The poor cloud forecasts which the mesoscale model produced explain why the model was not especially successful in the air temperature predictions in Table 6.1.5.1.

Another reason is due to the mesoscale model not taking variations in micro-climate into account, for example topography and exposure.

6.1.6 Algorithm summary

For the following scenario, the process below should be used to produce reliable forecasts of the likelihood of icy conditions for a road surface in Devon.

Scenario:-

Cloud forming in situ under settled anticyclonic conditions with wind speed not more than 1 ms^{-1}.

Algorithm:-

1. At a chosen station, determine surface flow for start of forecast period using latest possible observation. Under this scenario, changes in wind velocity are likely to be negligible for the 24 hours from start of forecast.

2. Estimate cloud cover for forecast period using satellite imagery from the same period, but 24 hours earlier to ascertain likelihood of formation and dissipation in situ. See text in earlier section of this case study.

3. Estimate air temperature for forecast period split into three hour intervals. A little knowledge of average air temperature fluctuation for this type of scenario is valuable. Observations from the previous night can be reliable *only* if the scenario and cloud pattern is expected to remain unchanged.

Three hourly approximate air temperature predictions can be calculated as well from forecasts of minimum temperature.

4. Run Roadsurf for the chosen station and apply to the surface temperature predictions, the operations specified in Table 6.1.4.1 for the station nearest to chosen station.

6.2 January 23rd/24th 1996

Scenario: Surface depression slowly moving into Devon from the Southeast with associated occluded front, whilst blocking high pressure system existed over Eastern Europe and Scandinavia.

6.2.1 Cloud cover and synoptic conditions for January 23rd/24th 1996.

For several hours preceding 2200 UTC Jan. 23rd, Devon was entirely enveloped with thick altostratus cloud (see Figure 6.2.1.1) due to a weak occluded front with a clearly defined south-eastern edge. This edge moved at 30 km hr^{-1} towards the north-west introducing thinner cloud, but not necessarily clearer skies into Southeast Devon from 2200 UTC Jan. 23rd. By 0100 UTC Jan. 24th, only thin low level cloud remained over Southwest England. Medium level cloud, 200 km wide moved over Devon from 0200 UTC Jan. 24th (see Figure 6.2.1.2).

The European Meteorological Bulletin E.M.B. surface analysis (Figure 6.2.1.3) shows that synoptic conditions at 0000 Jan. 24th were unsettled with a shallow surface depression in the English Channel, moving towards Devon from the Channel Islands. Surface pressure at its centre was 995 mb. Although shallow, signatures of this disturbance at 1200 UTC Jan. 24th were detectable above the English Channel at 850 and 500 mb (see Figure 6.2.1.4). Despite the feature having a hurricane shaped appearance shown by Meteosat imagery, 2m flow was less than 10 ms^{-1}, north-easterly in direction at 0000 UTC Jan. 24th. Radiosonde data from Camborne at 1200 UTC Jan. 24th and geopotential height charts from 0000 UTC Jan. 24th showed flow also no stronger than 10 ms^{-1} at most atmospheric levels as far up as 10 km.

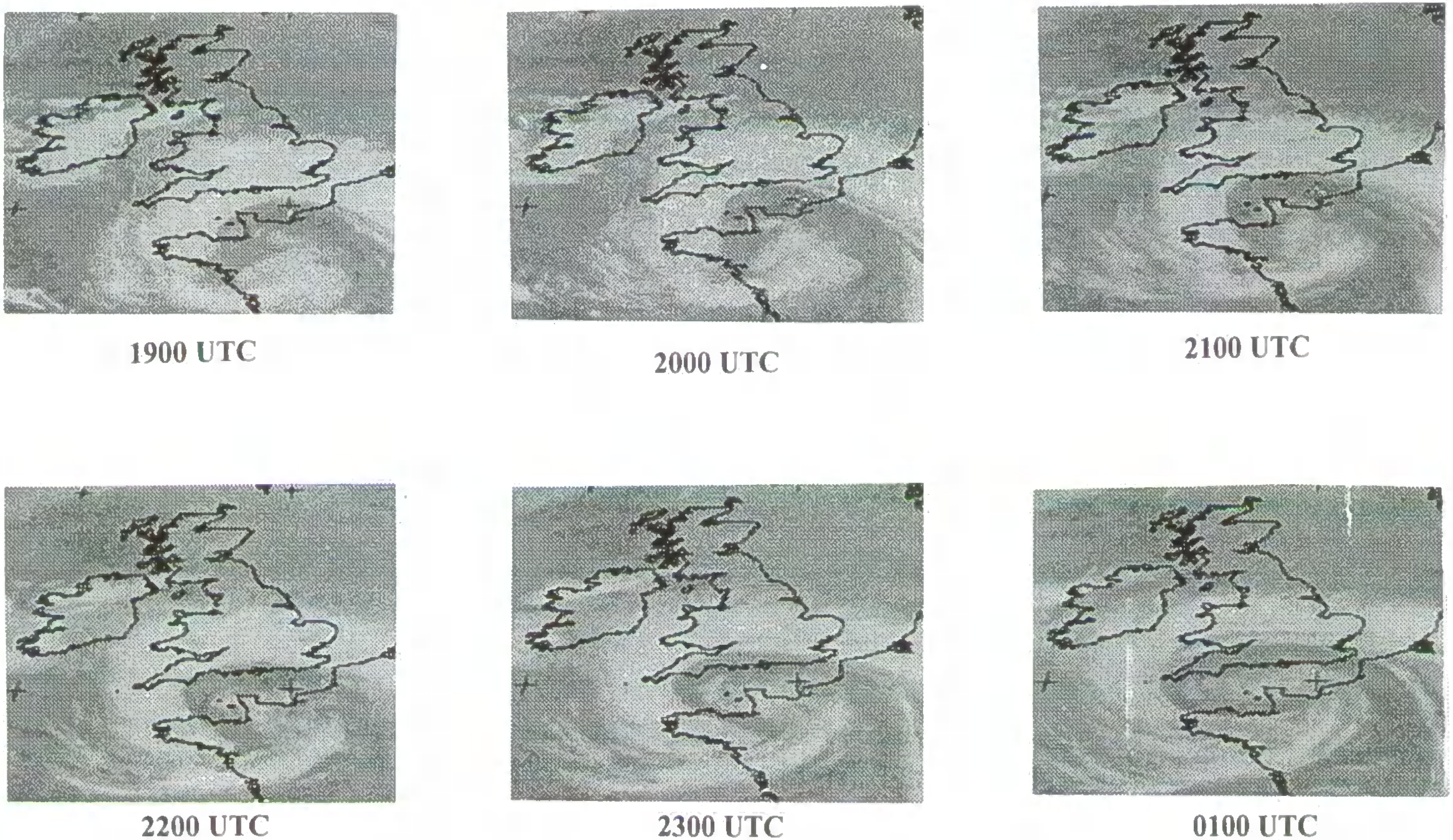

Figure 6.2.1.1 Meteosat infrared imagery from 1900 UTC Jan. 23rd to 0100 UTC Jan. 24th 1996.

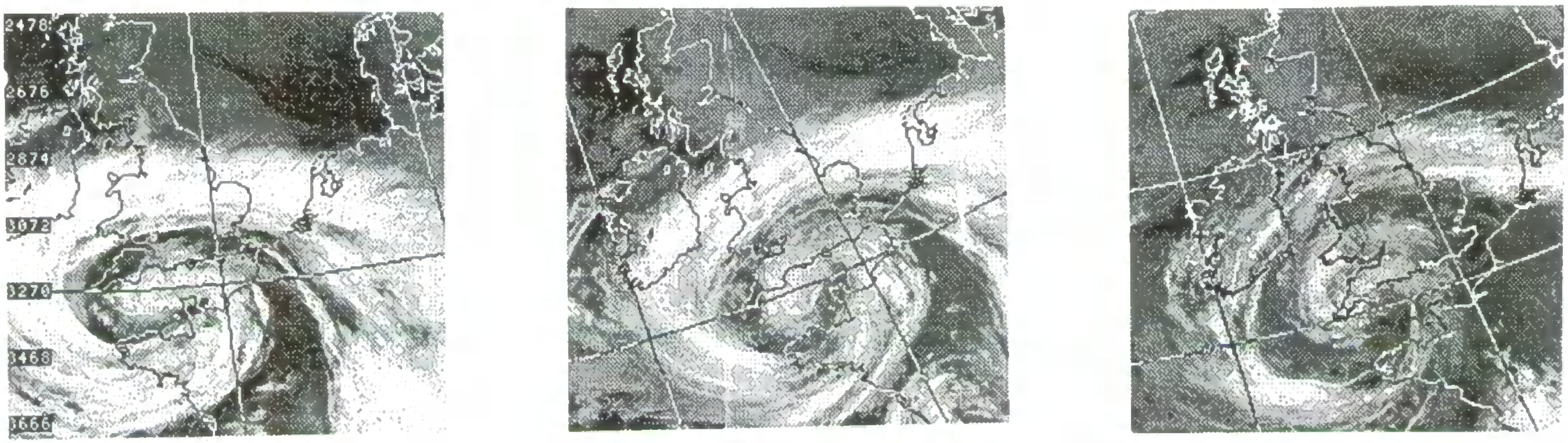

0143 UTC　　0324 UTC　　0819 UTC

Figure 6.2.1.2 NOAA infrared imagery from Jan. 24th 1996.

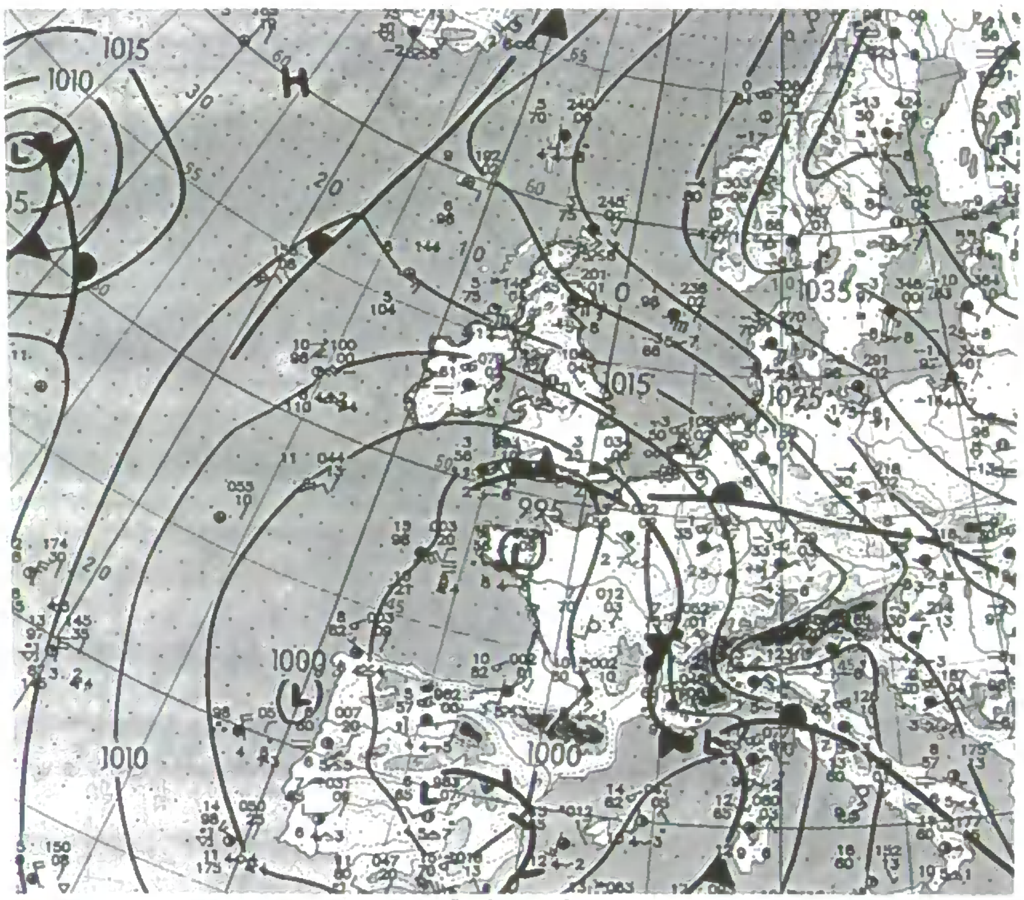

Figure 6.2.1.3 European Meteorological Bulletin surface analysis from 0000 UTC Jan. 24th 1996

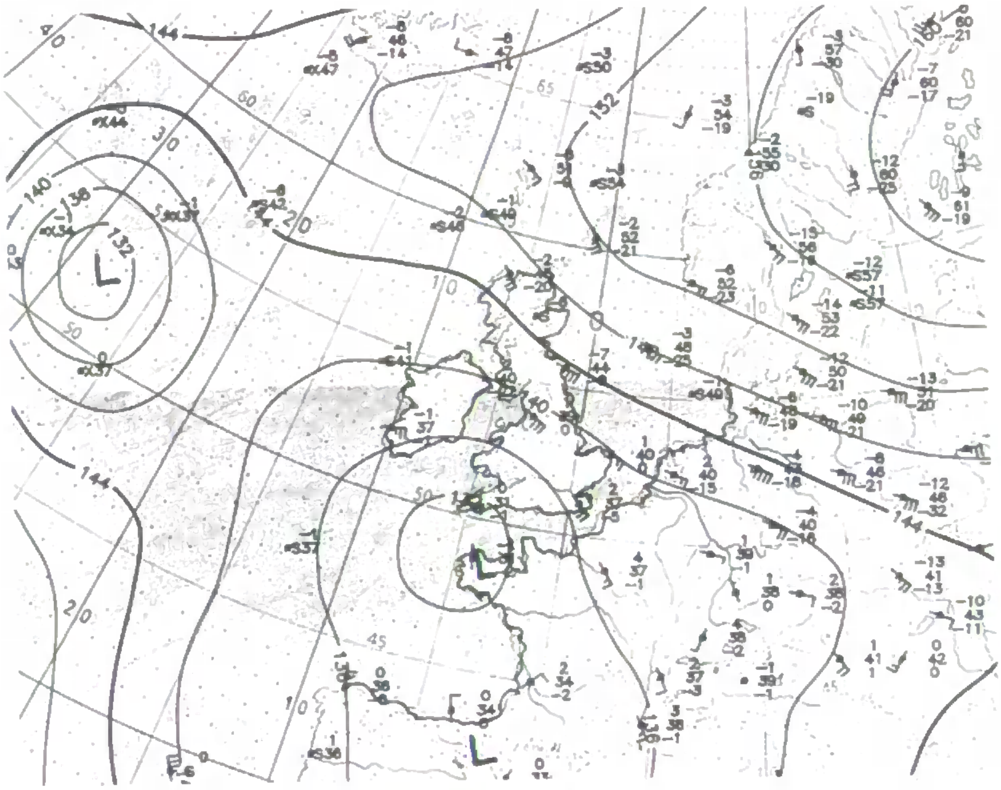

850 mb level

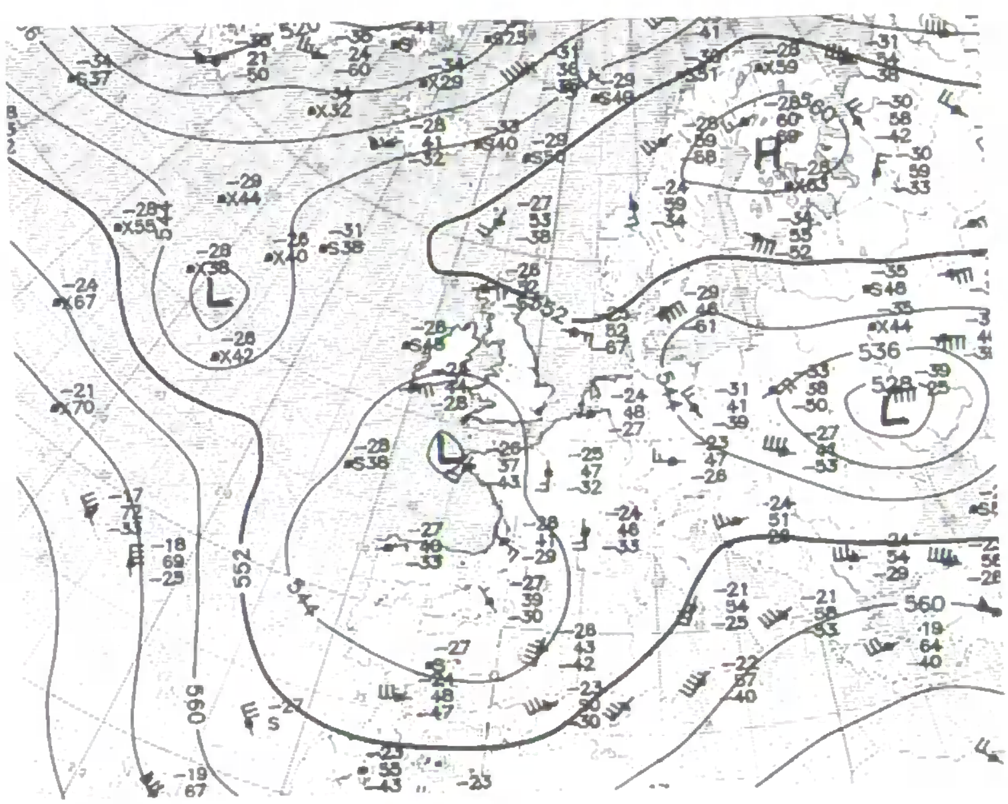

500 mb level

Figure 6.2.1.4 European Meteorological Bulletin geopotential height analyses from 1200 UTC Jan. **24th** 1996
(Charts from 0000 UTC Jan. 24th were not available)

6.2.2 Effects of cloud on surface and air temperatures in Devon during and after passage of occluded front from 2200 UTC Jan. 23rd.

Table 6.2.2.1 shows significant timelags between medium level cloud clearance at 2200 UTC Jan. 22nd and decrease in air and road surface temperature. Road surface temperature response to clearing skies at Roborough took 2 hours to occur, though at many stations, lags were unexpectedly longer than 5 hours due to misleading Meteosat and NOAA infrared images of the clearance.

Throughout Jan. 23rd and 24th, a completely clear sky never existed over Devon, even after the supposed clearance. This was due to the sheet of low cloud which persisted even after the medium level cloud had moved away from Devon. Its presence can be seen clearly in the 0324 UTC Jan. 24th NOAA image by comparing grey scales over the Bristol Channel with those close to the Norwegian coastline. Rapid surface cooling was consequently suppressed so that surface freezing occurred late; post 0530 UTC Jan. 24th or not at all.

Small depth variations of the low cloud and altitude were responsible for variations in surface temperature decrease rate between various road weather stations (Table 6.2.2.1)

A depression over the English Channel can cause significant snowfall during mid-winter if its northern edge is likely to produce precipitation. Cold air advection from the east or north-east further increases the possibility of frozen precipitation. Surface and air temperature during this type of scenario are not unusually cold, indeed air temperatures were above freezing point at most locations at 0000 UTC Jan. 24th.

Table 6.2.2.1 Timelags between cloud clearance and temperature fluctuations after 2200 UTC Jan. 23rd 1996.

Station	Time of cloud clearance /UTC (±10 min)	Time taken after clearance for effect on temperature to occur: in hours (±10 min)		Temperature decrease rate: in deg.C/hr		Surface freezing onset time
		Air temperature	Road surface temp	Air temp:	Surface temp:	
Kingsteignton	2200	3hr 20min	4hr	0.8	1.0	0544
Gallows Gate	2200	2hr 15min	5hr 10min	0.5	1.0	0615
3 Horse Shoes	2210	3hr 50min	5hr 20min	0.2	0.6	none
Totnes Cross	2210	no data	5hr 30min	-	1.0	0650
Marley Head	2210	5hr 15min	5hr 45min	0.8	1.0	not known
Stopgate Cross	2215	3hr	3hr 45min	0.2	0.5	0459
Pridhamsleigh	2220	4hr 40min	5hr 25min	0.7	1.0	none
Culver Bottom	2230	4hr 40min	5hr 30min	0.5	1.7	none
Sampford Peverell	2230	5hr 30min	5hr 15min	0.5	0.5	0744
Roborough	2250	1hr 15min	2hr 10min	0.3	0.5	none
Whiddon Down	2300	5hr 15min	5hr 15min	0.2	0.8	0530
Wellparks	2300	4hr 45min	5hr 30min	0.3	0.5	none
Beaford Moor	2310	2hr 50min	3hr 50min	0.2	0.4	0531
Bratton Down	2340	1hr 50min	2hr 20min	0.1	0.2	already <0°C
West Country Inn	2340	4hr 20min	5hr 40min	0.5	1.2	0631

Notes: i. Cloud clearance time is the time when cloud cover estimated from satellite imagery became less than 3 oktas.

ii. No known frost onset time at Marley Head due to road surface sensor failure at 0644 UTC.

Sleet was reported at Camborne, which could have easily fallen as snow over high ground such as Dartmoor and Exmoor. A marginal situation had occurred which rendered snow prediction difficult at some locations in Devon.

6.2.3 Initial Roadsurf predictions

Roadsurf was ran for 24 hours from 1200 UTC Jan. 23rd for Haldon Hill and Roborough using input data from Table 6.2.3.1. This exercise was carried out for only two stations since cloud cover across Devon was mostly independent of location during run duration. Its aim was to investigate how changes of cloud height affect surface temperature. Plausible flaws in satellite imagery evaluation relating to low level cloud clearly became apparent when the occluded front cleared Devon. An untrained observer of the 0143 UTC Jan. 24th image for example would have assumed the presence of a clear sky obscured by less than 3 to 4 oktas when viewed from ground level sites in Northwest Devon. This case study demonstrates the need for users of satellite imagery to consider a wide area in order to correctly ascertain differences in image brightness between low cloud and clear sky regions.

Errors in prediction, i.e. the difference between predicted and measured surface temperature were time dependent and varied from less than 0.1 deg. C to larger than 2.0 deg. C. Roadsurf performed best between 0000 UTC and 0600 UTC Jan. 24th.

Sharp surface cooling shown in Figures 6.2.3.1 and 6.2.3.2 occurred between 1800 UTC and 2000 UTC Jan. 23rd at Haldon Hill and Roborough. Roadsurf failed to replicate this event due to cloud cover inputs of 8 oktas until 2100 UTC Jan. 23rd and 0000 UTC Jan. 24th at Haldon Hill and Roborough respectively. The cooling at Haldon Hill (see Figure 6.2.3.1) of 3.0 deg. C within 2 hours indicated that a brief cloud clearance at all atmospheric levels must have occurred between 1800 UTC and 2000 UTC Jan. 23rd.

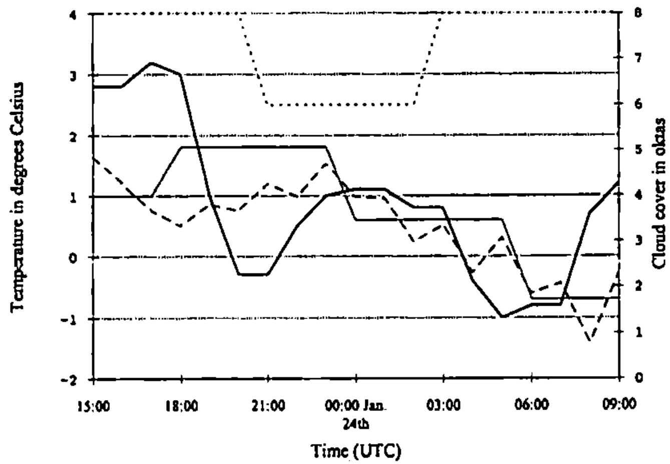

Haldon Hill

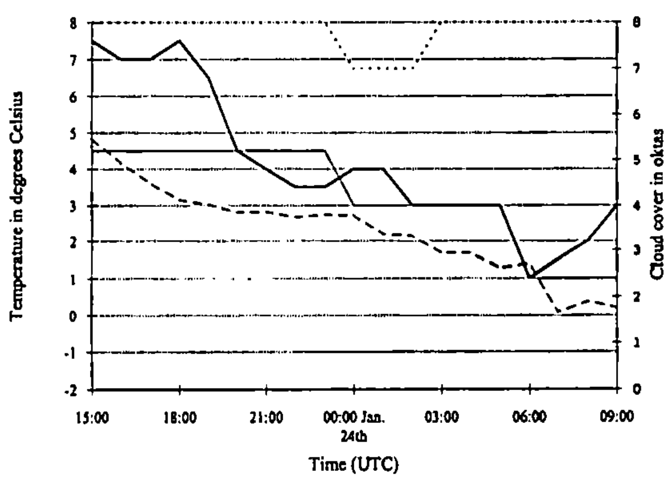

Roborough

- - - - Roadsurf surface temperature prediction

——— Observed road surface temperature

——— Air temperature used by Roadsurf

· · · · · · · Cloud cover (right hand scale)

Figure 6.2.3.1 Evolution of conditions between 1500 UTC Jan. 23rd and 0900 UTC Jan. 24th 1996

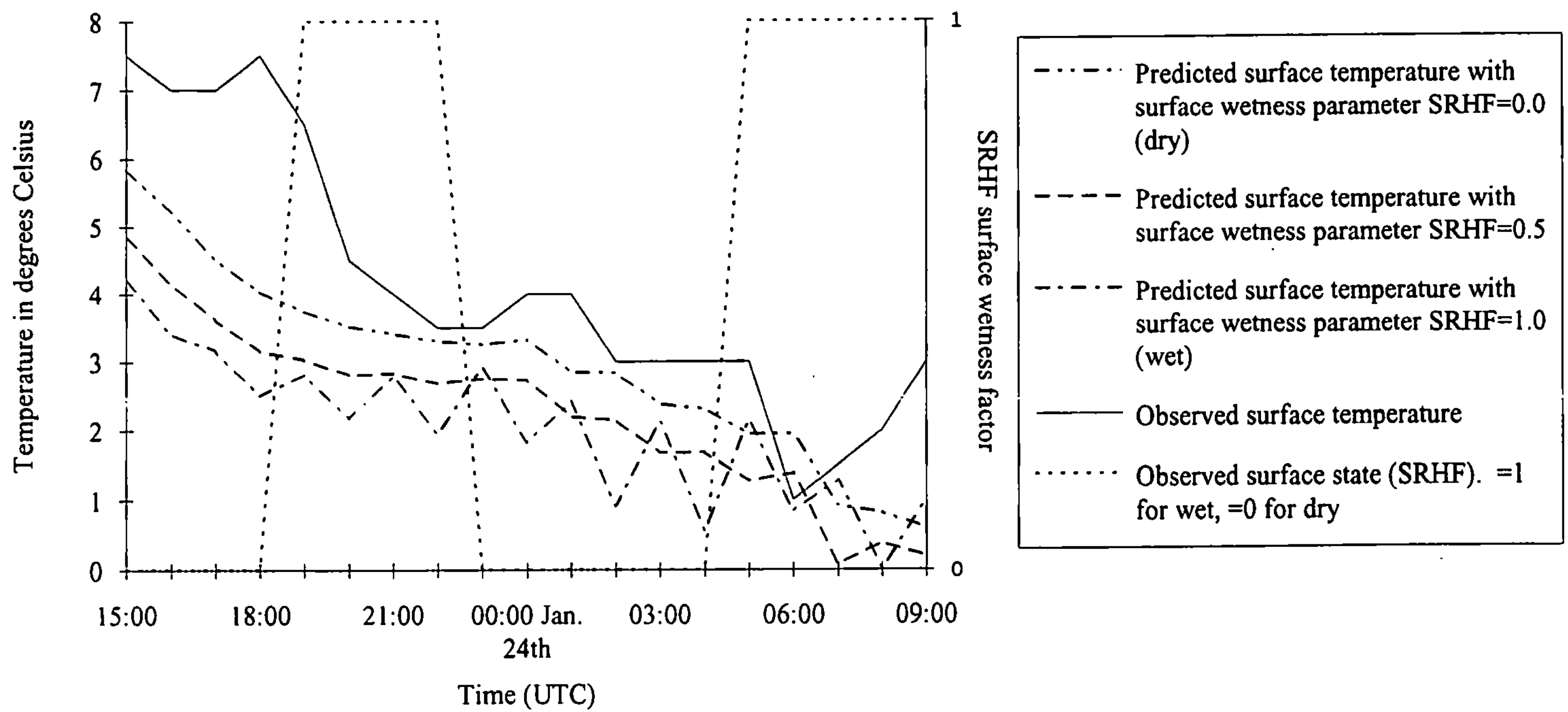

Figure 6.2.3.2 Effects of surface wetness on Roadsurf surface temperature prediction for Roborough from 1500 UTC Jan. 23rd to 0900 UTC Jan. 24th 1996

If there was such a clearance, it would have been of a shorter duration than 2 hours. Such a clearance was *not* detected by satellite. Reasons would have been due to a melange of factors including inadequate evaluation of infrared Meteosat imagery from 1800 to 2000 UTC Jan. 23rd due to grey scale deficiencies. *NOAA* images were not available from 1800 UTC to 2000 UTC Jan. 23rd due to the NOAA satellites passing too far east of Devon during this time. It was interesting to note an absence of simultaneous 2m air cooling mostly due to horizontal air advection.

Table 6.2.3.1 Most important inputs required by Roadsurf for 1200 UTC Jan. 23rd to 0900 UTC Jan. 24th 1996 runs.

Parameter (Times in UTC)	Haldon Hill	Roborough
Cloud:- (in oktas)		
1200 to 1459 Jan. 23rd	8 at medium level	8 at medium level
1500 to 1759 Jan. 23rd	8 at medium level	8 at medium level
1800 to 2059 Jan. 23rd	6 at medium level	8 at medium level
2100 to 2359 Jan. 23rd	6 at **low** level	8 at medium level
0000 to 0259 Jan. 24th	8 at low level	7 at **low** level
0300 to 0559 Jan. 24th	8 at **medium** level	8 at medium level
0600 to 0859 Jan. 24th	8 at medium level	8 at medium level
Air temperature:- (in °C)		
1200 Jan. 23rd	1.0	4.5
1800 Jan. 23rd	1.8	4.5
0000 Jan. 24th	0.6	3.0
Ts at 1200 Jan. 23rd /°C	2.1	7.5
Td at1200 Jan. 23rd /°C	2.4	6.0
Tcl at1200 Jan. 23rd /°C	4.4	4.4
UA(throughout)/ms^{-1}	3.1 (from obs at Haldon)	3.1 (using Haldon obs)
DWB(throughout)/deg. C	0.0	1.5
Surface state at 1200 Jan. 23rd	wet, SRHF=1.0	dry then wet, SRHF=0.5

Notes:

Ts: road surface temperature,

Td: 'd' layer temperature (immediately below surface),

Tcl: 'cl' layer temperature (immediately below 'd' layer),

UA: wind speed,

DWB: wet bulb temperature depression,

obs: observations

SRHF: parameter used in model to depict surface wetness, observed by road surface sensor at station (1 for wet surfaces, 0 for dry)

Roadsurf gave different responses to the change from 8 oktas of medium level to 7 oktas of low level cloud at Haldon Hill and Roborough. At Haldon Hill, clearance of the medium level component allowed surface cooling for only an hour before a 0.5 deg. C rise. This rise could have been due to 'computational mode' resulting from finite difference equations used in the Roadsurf computer code. Roadsurf has a tendency to attempt to reverse any perturbations which may briefly occur during settled conditions during which the air temperature is close (within a degree) to the surface temperature.

At Roborough, the change from medium to low level cloud occurred later than at Haldon Hill and resulted in a clearly identifiable surface cooling at 0000 UTC Jan. 24th. This cooling was gradual and was also contributed to by an air temperature input at 0000 UTC Jan. 24th, 1.5 deg. C cooler than before 0000. No visible signatures of 'computational mode' occurred at this time at Roborough.

Surface wetness parameterization

At Roborough, the surface sensor reported a fluctuating road wetness as shown in Figure 6.2.3.2 by the 'observed surface state' curve. Roadsurf uses a fixed parameter to represent wetness, SRHF which attains zero for a dry surface or unity for wet. It was thus necessary to decide a suitable SRHF for the conditions at Roborough. During Roadsurf's first run for Roborough, an SRHF of 0.5 was used since durations of dry and wet surfaces within the forecast window were very similar. However, as Figure 1.2.3.2 shows, a fixed SRHF of 0.0 produced more accurate predictions (i.e. closer to observations) than with using an SRHF of 0.5. The affect of SRHF on surface freezing onset at Roborough on this occasion was negligible since risk of frost was small. Figure 6.2.3.2 also showed that the 'computational mode' discussed above ,which occurred in predictions for Haldon Hill, would have occurred at Roborough if surface conditions were wet.

It *is* possible to modify Roadsurf to use variable states of surface wetness but this would not necessarily be beneficial. It is often helpful to prevent a model from becoming too complex. Furthermore, using fluctuating SRHF inputs may introduce errors resulting from misleading observations since the accuracy of surface wetness sensors is poor. The sensor detects moisture by recording electrical conductivity across a small area of road surface, often giving invalid observations if salt or dirt are present.
As an aside, Figure 6.2.3.2 shows that Roadsurf exhibits an extenuated cold bias if wet surface conditions prevail, due to evaporative cooling.

6.2.4 Consequences of poor evaluation of satellite imagery

This case study showed the perils of not thoroughly evaluating satellite imagery. At first glance, it was thought cloud had cleared at all atmospheric levels behind the occluded front which passed over Devon between 1900 and 2200 UTC Jan. 23rd. Figures 6.2.4.1 and 6.2.4.2 show that if this first evaluation of cloud had been accepted (see Table 6.2.4.1) and used for forecasting, Roadsurf would have produced unacceptable predictions for the forecast period after 2300 UTC Jan. 23rd. Forecasts of surface frost onset would have been predicted 5 hours late at Haldon Hill.

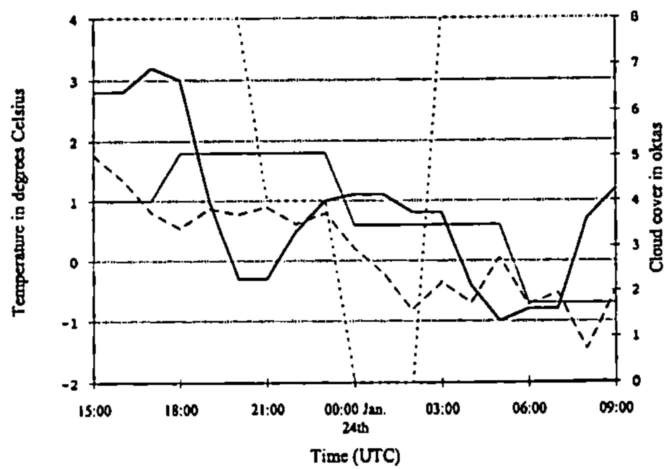

Haldon Hill

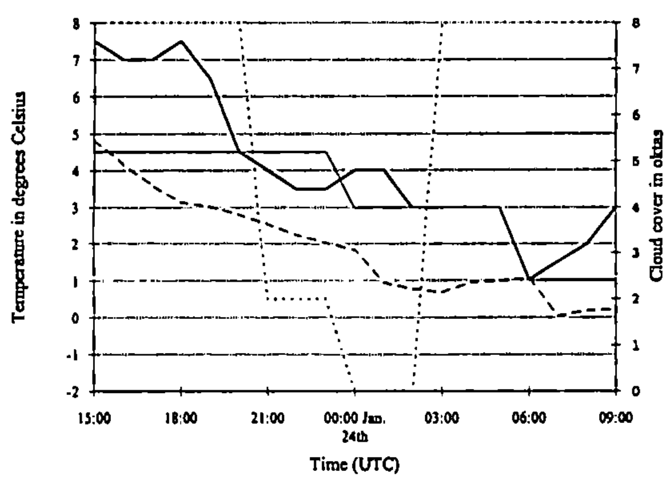

Roborough

- - - - Roadsurf surface temperature prediction

——— Observed road surface temperature

——— Air temperature used by Roadsurf

······ Poorly evaluated cloud cover (right hand scale)

Figure 6.2.4.1 Evolution of conditions between 1500 UTC Jan. 23rd and 0900 UTC Jan. 24th 1996 using poorly evaluated cloud

Table 6.2.4.1 Poorly evaluated cloud cover at Haldon Hill and Roborough from 1200 UTC Jan. 23rd to 0859 UTC Jan. 24th 1996.

Time (UTC)	Cloud cover (oktas)	
	Haldon Hill	Roborough
1200-1459 Jan. 23rd	8	8
1500-1759 Jan. 23rd	8	8
1800-2059 Jan. 23rd	8	8
2100-2359 Jan. 23rd	4 (medium level)	2 (medium level)
0000-0259 Jan. 24th	0	0
0300-0559 Jan. 24th	8 (medium level)	8 (medium level)
0600-0859 Jan. 24th	8 (medium level)	8 (medium level)

Inaccuracy was greater at Roborough than at Haldon Hill, especially between 2200 UTC Jan. 23rd and 0700 UTC Jan. 24th.

6.2.5 Algorithm construction.

Despite the appearance of the surface depression looking like that of a hurricane in Meteosat imagery of late Jan. 23rd, an algorithm for this situation was simple to construct since cloud was always present. Roadsurf handled the situation adequately without requiring any modifications whenever cloud inputs were accurate.

Hence a suitable algorithm merely consists of predicting a cloud track ahead of, within, and behind an occluded front moving north-west towards Devon and Cornwall. This can be done by identifying the height of observed cloud at 1200 UTC Jan. 23rd and analysing contours of geopotential height to determine likely geostrophic wind at cloud level using the **geostrophic wind equation** (6.2.5.1). Cloud displacement is related to flow at cloud level as discussed in the literature survey (Chapter 2).

Geostrophic wind equation

$$V_g = -\frac{g}{2\Omega\sin\phi}\frac{\partial z}{\partial n} \qquad 6.2.5.1$$

where,

V_g= geostrophic wind in vector form (ms^{-1})

$\partial z/\partial n$= rate of change of height with horizontal distance perpendicular to geopotential height contours

ϕ= latitude (51° North)

g= acceleration due to gravity (9.8 ms^{-2})

and Ω= angular velocity of the Earth (7.29×10^{-5} rad s^{-1}),

Analyses in Figures 6.2.5.1a and b showed signatures of the surface disturbance at 1200 UTC Jan. 23rd at 850 and 500mb, the horizontal locations of which depended on height. Unfortunately track predictions of surface features can not accurately be produced using these signatures due to:-

i) Differences between surface feature and signature movement velocity,

and ii) Large intervals of at least 6 hours between successive geopotential height analyses.

Table 6.2.5.1 shows that cloud above the English Channel, south of Devon moved at a similar velocity to geostrophic flow above nearby areas at 850 and 500 mb at certain times during Jan. 23rd and 24th. The cloud displacement rates in Table 6.2.5.1 were determined by analysing the sequential Meteosat images of Figure 6.2.1.1 from 1900 UTC to 2300 UTC Jan. 23rd using the 'plane sailing' method of estimating distance (Mclean and Wood, 1995). This period was most suitable since cloud was passing over Devon in a well defined band at the time. Tracking the edges of a cloud band produces more accurately measured observations than those obtained tracking scattered cloud clumps since a cloud band usually exists for longer. The cloud band in this particular case study was also easier to track compared to individual cloud formations.

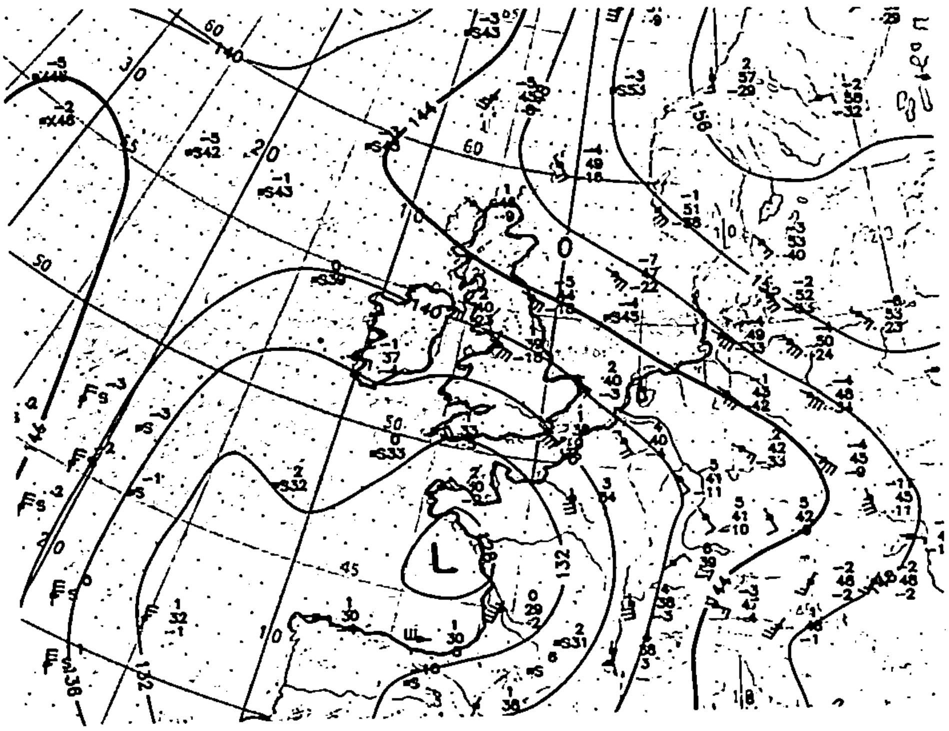

a. 850 mb level

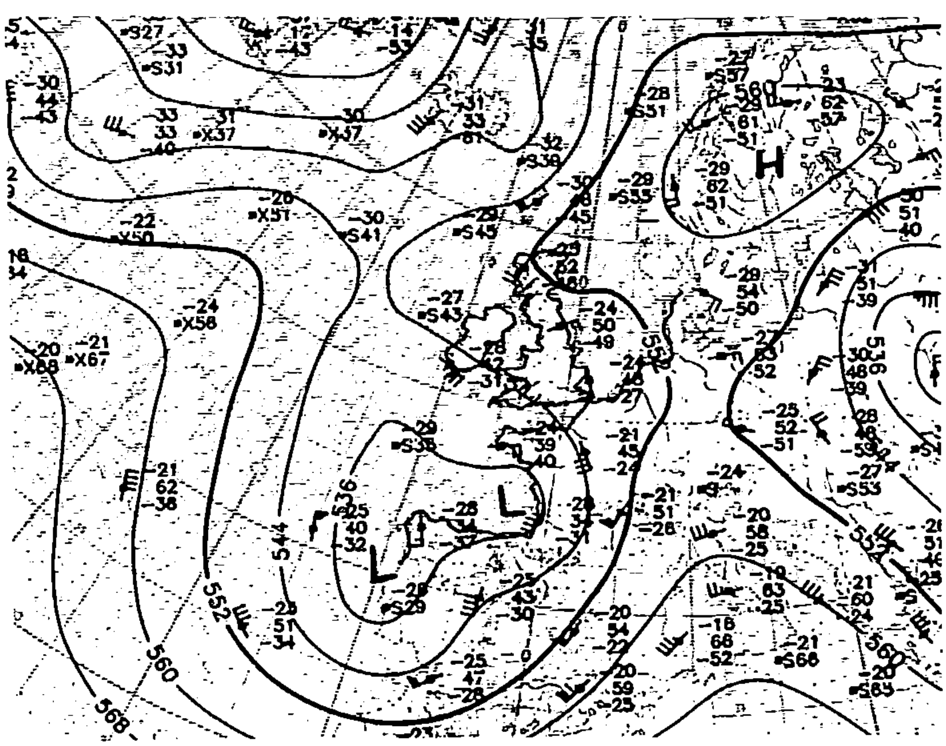

b. 500 mb level

Figure 6.2.5.1 European Meteorological Bulletin geopotential height analyses from 1200 UTC Jan. **23rd** 1996.

Velocity fluctuations at 850 and 500 millibars can be assumed small over durations of less than 6 hours permitting predictions of flow and thus cloud velocity at levels where cloud is known to have occurred at the start of a model run. In this scenario, cloud height can be predicted by examining height difference between cloud bands at the start of a forecast period. Convective air flow is small in this type of scenario, shown by the lack of precipitation during Jan. 23rd and 24th, so changes in cloud band height can be assumed negligible over periods of less than 12 hours. Radiosonde ascents can be used to gain accurate cloud heights for cloud bands covering Camborne, Brest and Valentia.

Table 6.2.5.1 Cloud movement and air flow at 850 and 500 millibars during Jan. 23rd and 24th 1996.

Cloud movement (between 1900 and 2300 UTC Jan. 23rd)

Feature	Cloud speed / ms^{-1}
Forward edge of cloud over sea area between Cornwall and Eire	13
Back edge of cloud between Devon and Finnistere	14
Back edge of cloud over Finnistere	5

Air flow (1200 UTC Jan. 23rd)

	850 millibars level	500 millibars level
Geostrophic flow calculated using geopotential height analysis (Figure 6.2.5.1)	17 ms^{-1} E	18 ms^{-1} SE
Radiosonde observation at Camborne	10 ms^{-1} NE	5 ms^{-1} SE
Radiosonde observation at Brest	10 ms^{-1} ENE	10 ms^{-1} E
Radiosonde observation at Valentia	8 ms^{-1} E	15 ms^{-1} SE

Air flow (1200 UTC Jan. **24th**)

	850 millibars level	500 millibars level
Geostrophic flow calculated using geopotential height analysis (analysis not included)	25 ms^{-1} SE	17 ms^{-1} E
Radiosonde observation at Camborne	8 ms^{-1} E	8 ms^{-1} E
Radiosonde observation at Brest	<5 ms^{-1} Variable	10 ms^{-1} Variable
Radiosonde observation at Valentia	13 ms^{-1} E	13 ms^{-1} ENE

Based on the results from Jan. 23rd/24th 1996, Roadsurf and its output need no special modifications to adequately perform under the scenario type being considered. Roadsurf should be ran using initial observations and predicted cloud cover derived from the cloud movement forecasts.

The weather situation of Jan. 23rd/24th 1996 was only representative of continuous cloudy conditions with a shallow depression between Devon and the Channel Islands. A different algorithm *might* be needed if a **complete** cloud clearance occurred. such a situation with the same surface pressure field was unfortunately not available.

Surface flow and 2m air temperature

Under this scenario, a fixed parameterization of the average surface flow is suitable for Roadsurf, estimated from the most recent observations and predicted surface pressure charts. A modified version of Equation 6.2.5.1 can be used (Equation 6.2.5.2).

$$V_g = -\frac{1}{\rho 2\Omega \sin\phi}\frac{\partial p}{\partial n} \qquad 6.2.5.2$$

where,

$\partial p/\partial n$= pressure gradient (Pa m^{-1})

ρ= air density at surface (1.25 kg m^{-3}).

During the case study, less than a 2 deg. C cooling of the 2m air temperature occurred due to cloud and an absence of cold air advection. Thus for an operational case, a similar range would be a suitable for Roadsurf.

6.2.6 Algorithm summary

For the following scenario, the process below should be used to produce reliable forecasts of the likelihood of icy conditions for a road surface in Devon.

Scenario:-

Shallow, non-developing low pressure system situated close to or over Devon during January or February. Blocking high pressure system over Scandinavia. Non precipitating cloud band passing directly above Devon. Surface flow less than $20ms^{-1}$, without feed of air from high pressure region.

Algorithm:-

1. Determine geostrophic wind at 850 and 500 millibars using 1200 UTC geopotential height analyses and Equation 6.2.5.1

2. Estimate likely cloud track for the following 18 hours

3. Ascertain the height of cloud being tracked

4. From the track prediction, estimate cloud cover prediction in oktas for a chosen site for the duration of forecast window (usually up to 0900 UTC following day) at 3 hourly intervals

5. Estimate 2m air temperature and wind flow for forecast period.

6. Run Roadsurf using initial observations, cloud height and cover prediction as input variables

7. Plot graph of surface temperature for forecast period and note the expected frost onset time and minimum surface temperature for the chosen site.

6.3. February 4th/5th 1996

Scenario:- Frontal cloud moving eastward from the Atlantic into very cold anticyclonic air over Eastern England.

6.3.1 Summary of cloud and synoptic conditions.

The infrared satellite images in Figures 6.3.1.1 and 6.3.1.2 show that an Atlantic sourced cloud band moved into Devon from the west during the evening of Feb. 4th and morning of Feb. 5th. After several hours of mostly clear skies, overcast conditions became dominant above the whole of Devon by 0000 UTC Feb. 5th halting ubiquitous rapid cooling of road surfaces at four locations in Devon:- Stopgate Cross, Haldon Hill, Ashmill and Tuelldown. Synoptic conditions at this time were of high pressure associated with a very cold boundary layer east of Devon, and milder but unsettled air west of Devon over the Atlantic ocean (see Figures 6.3.1.3 and 6.3.1.4)

This scenario was interesting for three reasons:-

i) For investigating impact of increasing cloud on surface temperature
ii) Prediction of snow/rain probability and
iii) Investigation of the movement of approaching mild air, for example, its ease in rising over the cool air near the surface and penetration of the front into an anticyclone.

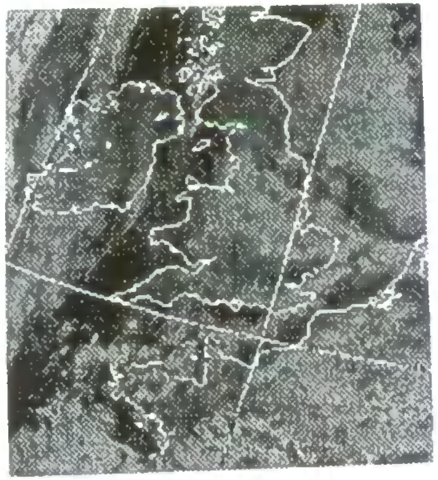

a. 1259 UTC Feb. 4th 1996

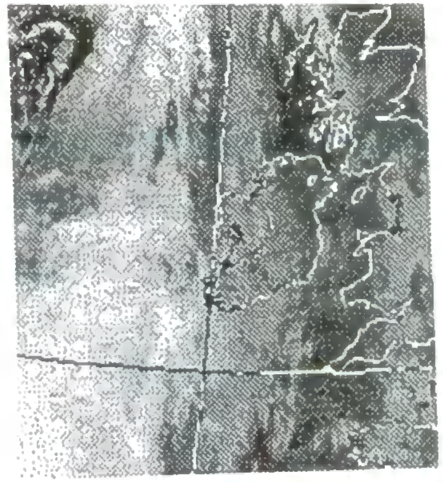

b. 1441 UTC Feb. 4th 1996

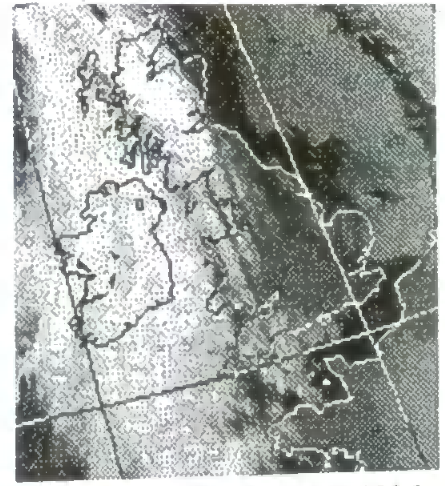

c. 0254 UTC Feb. 5th 1996

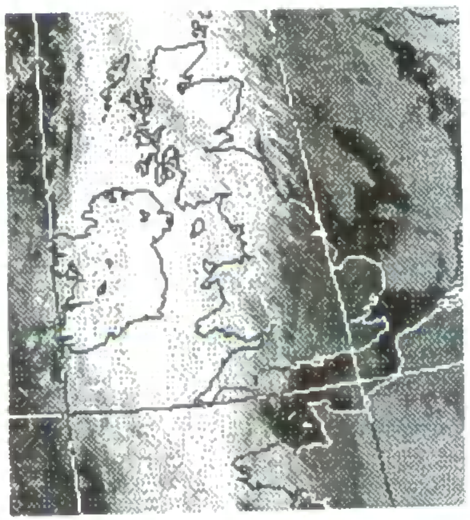

d. 0717 UTC Feb. 5th 1996

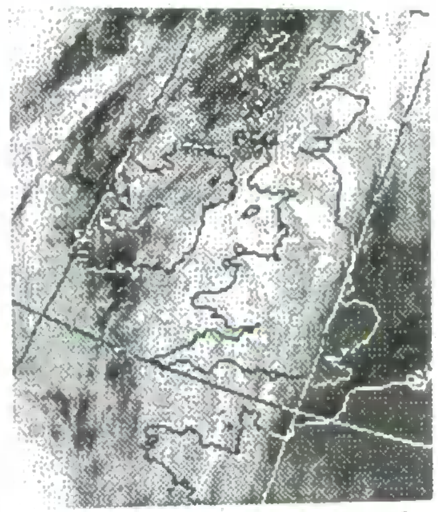

e. 1259 UTC Feb. 5th 1996

Figure 6.3.1.1 NOAA infrared satellite images from Feb. 4th and 5th 1996

a. 1800 UTC Feb. 4th 1996

b. 2000 UTC Feb. 4th 1996

c. 2200 UTC Feb. 4th 1996

d. 0000 UTC Feb. 5th 1996

Figure 6.3.1.2 Meteosat infrared satellite images from evening of Feb. 4th 1996

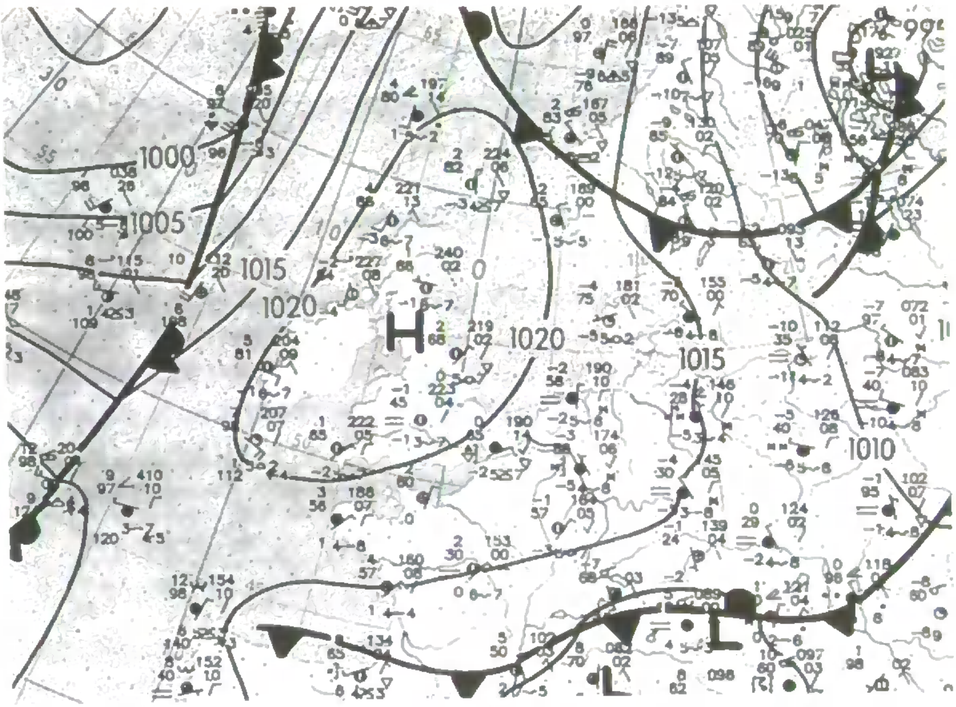

a. 0000 UTC Feb. 4th

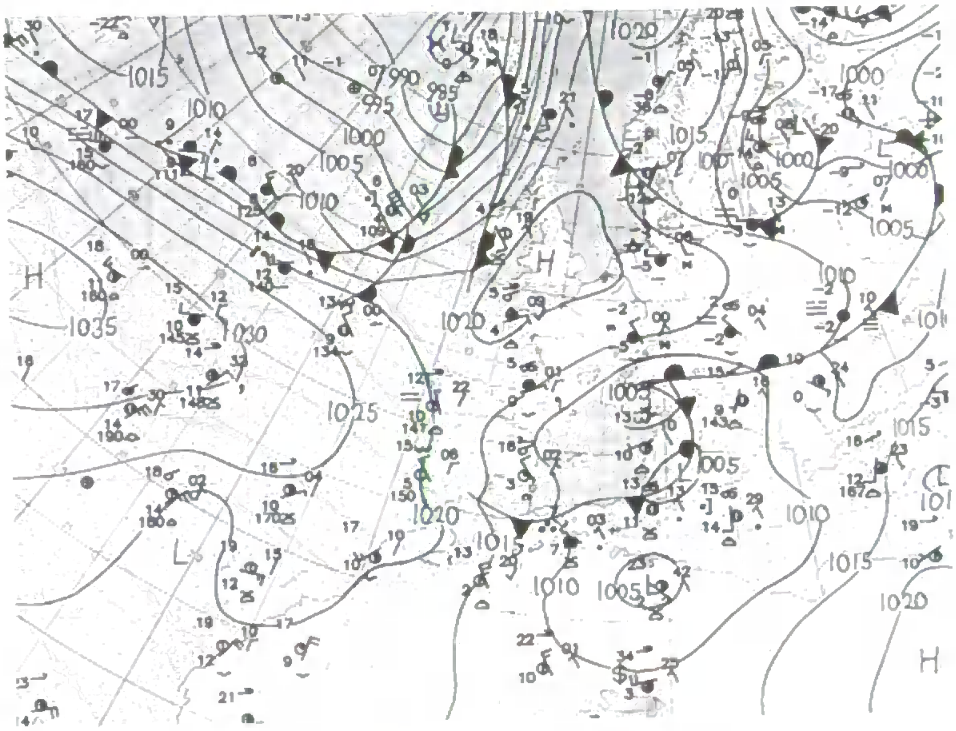

b. 1200 UTC Feb. 4th

Figure 6.3.1.3 European Meteorological Bulletin surface analyses from Feb. 4th 1996

a. 0000 UTC Feb. 5th

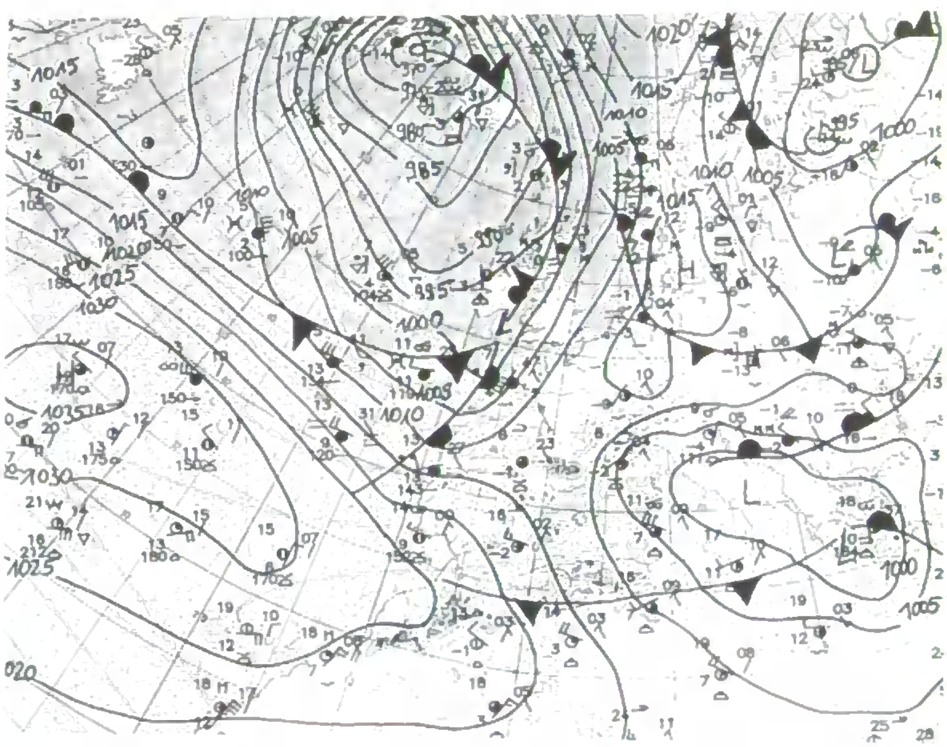

b. 1200 UTC Feb. 5th

Figure 6.3.1.4 European Meteorological Bulletin surface analyses from Feb. 5th 1996

6.3.2 Initial Roadsurf predictions.

Initial Roadsurf predictions (graphs in Figure 6.3.2.1) using inputs specified in Table 6.3.2.1 for Stopgate Cross, Haldon Hill and Tuelldown showed an inability of the model to react fast enough to changes in cloud cover of more than 2 to 3 oktas per hour. This sensitivity resulted in poorly predicted cooling curves of surface temperature. The reason for this seemingly slow ability to react to cloud build-up was partly due to a fixed wind speed used by Roadsurf, as opposed to a variable wind speed throughout the run durations. After 1800 UTC Feb. 4th, 2m air flow strengthened as Atlantic cloud moved in. At 1800 UTC Feb. 4th, the 2m flow speed was $1ms^{-1}$, but had increased to $6ms^{-1}$ by 0600 Feb. 5th. The 'fixed' 2m wind speed input for Roadsurf, taken from a 1200 UTC Feb. 4th observation at Haldon Hill ($0.5\ ms^{-1}$) was thus rather inappropriate. Due to the increasing 2m flow, mixing occurred which helped warm the surface; warming which Roadsurf obviously was unable to sufficiently replicate.

Table 6.3.2.1 Major Roadsurf inputs for initial runs of 1200 UTC Feb. 4th to 1200 UTC Feb. 5th 1996. (Hereby referred to as scheme i of Table 6.3.2.3)

Parameter (Times in UTC)	Stopgate Cross	Haldon Hill	Tuelldown
2m Air temperature /°C			
1200 Feb. 4th	0.7	1.5	3.0
1800 Feb. 4th	-0.9	-1.0	-1.0
0000 Feb. 5th	-0.5	0.0	1.0
0600 Feb. 5th	1.8	2.0	2.0
Ts at 1200 Feb. 4th /°C	3.6	3.5	1.0
Td at 1200 Feb. 4th /°C	2.8	3.0	3.2
Tcl at 1200 Feb. 4th /°C	2.0	2.6	2.8
UA(throughout)/ms^{-1}	0.5	0.5	0.5
DWB/ deg. C	2.0	2.2	2.4
Surface state	Wet (SRHF=1.0)	Wet (SHRF=1.0)	Wet (SHRF=1.0)

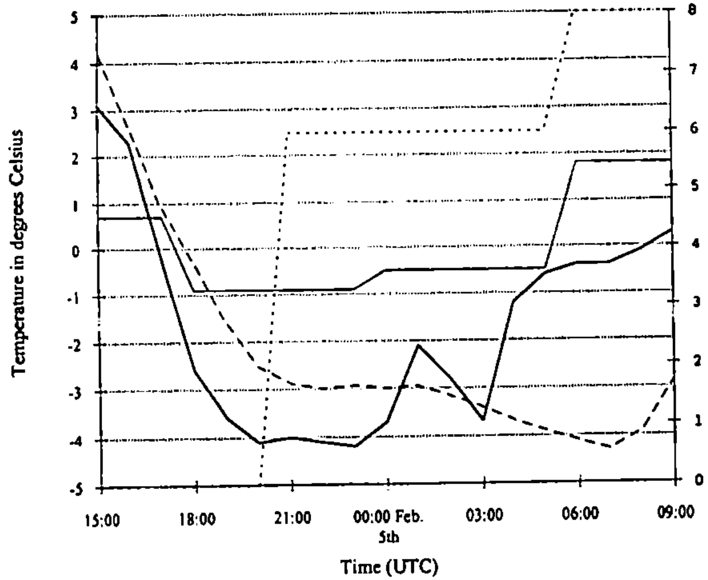

a. Stopgate Cross

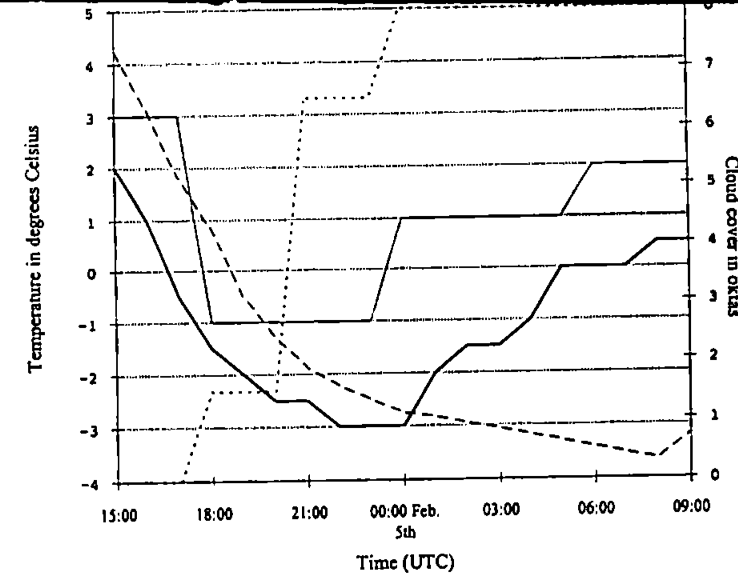

c. Tuelldown

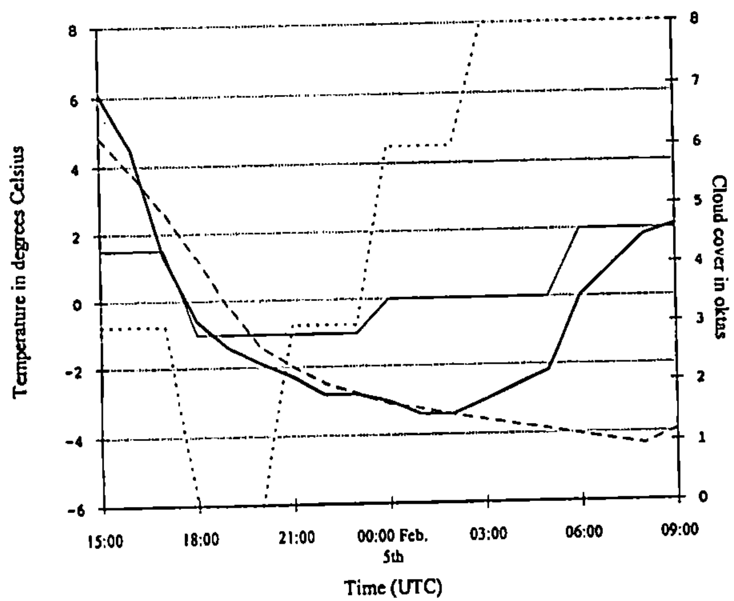

b. Haldon Hill

——— Observed air temperature

——— Observed road surface temperature

– – – Roadsurf surface temperature prediction

· · · · · Observed cloud cover (right hand scale)

Figure 6.3.2.1 Observations and Roadsurf predictions from 1500 UTC Feb. 4th to 0900 UTC Feb. 5th 1996.

Notes for Table 6.3.2.1

Ts: road surface temperature,

Td: 'd' layer temperature (immediately below surface),

Tcl: 'cl' layer temperature (immediately below 'd' layer),

UA: 2m wind speed,

DWB: depression of wet bulb temperature,

SRHF: parameter used in model to depict surface wetness, observed by road surface sensor at station (1 for wet surfaces, 0 for dry)

Roadsurf exhibited a warm bias before 0000 UTC Feb. 5th, but cold afterwards. Roadsurf adequately predicted frost onset times as shown in Table 6.3.2.2 at Stopgate Cross and Haldon Hill to within 70 minutes of its observed occurrence.

Table 6.3.2.2 Roadsurf performance using fixed wind speed of 0.5 ms^{-1} and input parameters from Table 6.3.2.1 (scheme i of Table 6.3.2.2)

Frost onset prediction

Location	Frost onset time prediction		
	Actual / UTC	Predicted / UTC	Error in prediction
Stopgate Cross	1700	1745	5 min
Haldon Hill	1745	1850	1 hr 5 min
Tuelldown	1645	1840	1 hr 55 min

Table 6.3.2.2 Cont'd.

Minimum surface temperature prediction

Location	Minimum surface temperature				
	Actual / °C	Pred / °C	Error / deg.C	Actual time of minimum RST /UTC	Predicted time of minimum Ts /UTC
Stopgate C.	-4.2	-4.2	none	2300	0700
Haldon Hill	-3.4	-4.4	-1.0	0100	0800
Tuelldown	-3.0	-3.6	-0.6	0000	0800

Table 6.3.2.3 Schemes used in Roadsurf runs of Feb. 4th into Feb. 5th 1996

Scheme
i Original values of KCLOUD, spot air temperatures (from 6 hourly intervals) and fixed wind speed. ii. KCLOUD at **95%** of its original values, spot air temperatures (from 6 hourly intervals) and variable wind speed iii. **Original** KCLOUD values, spot air temperatures (from 6 hourly intervals) and variable wind speed iv. KCLOUD at **95%** of its original values, air temperatures **averaged** over time (6 hour periods) and variable wind speed v. **Original** KCLOUD values, air temperatures **averaged** over time (6 hour periods) and variable wind speed

Modifications to Roadsurf

To improve Roadsurf performance, the model code was modified to enable **variable**, as opposed to **fixed** wind speeds to be used and to increase suppression of surface cooling during periods of increasing cloud. The suppression of surface cooling was achieved by reducing KCLOUD to 95% of the original values quoted by McClean and Wood, (1995). This would have increased suppression of surface cooling during *large* amounts of cloud cover. Because of the multiplication factor, changes in KCLOUD of *small* cloud amounts would be negligible.

Roadsurf with these two modifications, hereby known as scheme ii in Table 6.3.2.3, using the 2m flow speeds in Table 6.3.2.4 produced more accurate surface temperature predictions for Stopgate Cross (see results in Table 6.3.2.5 and relevant graph in Figure 6.3.2.2). The new version also performed well at Haldon Hill and Tuelldown (Figure 6.3.2.2.b and c), especially in predicting frost onset times (Table 6.3.2.5).

Table 6.3.2.4 Modified 2m wind speed inputs into Roadsurf (Scheme ii of Table 6.3.2.2)

(Times in UTC, Winds in ms^{-1})	Stopgate Cross	Haldon Hill	Tuelldown	Ashmill
1200-1759 Feb. 4th	1.0	1.0	1.0	2.0
1800-2359 Feb. 4th	1.0	1.0	1.0	1.0
0000-0559 Feb. 5th	4.0	3.0	1.0	2.0
0600-1159 Feb. 5th	6.0	6.0	3.0	5.0

However, Table 6.3.2.5 showed a warm bias in minimum predicted surface temperature at Haldon Hill, Tuelldown and Ashmill which indicated that weaker suppression of surface cooling would have been more beneficial, i.e. KCLOUD between 95% and 100% of its original values.

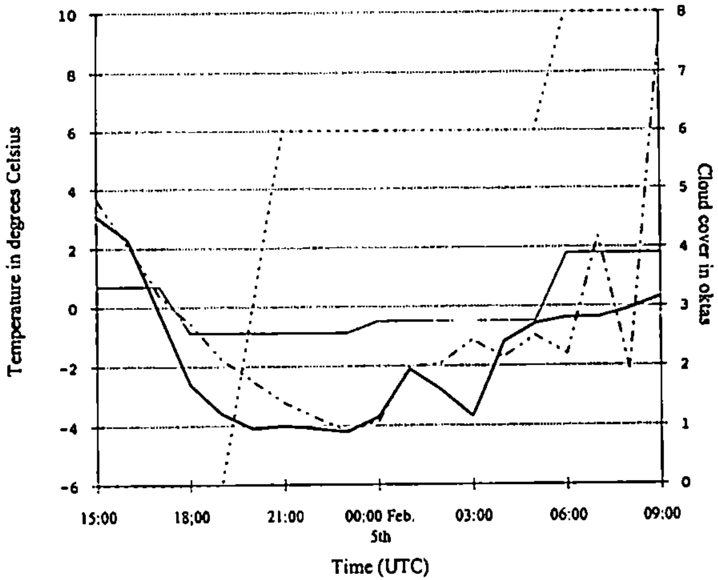

a.Stopgate Cross

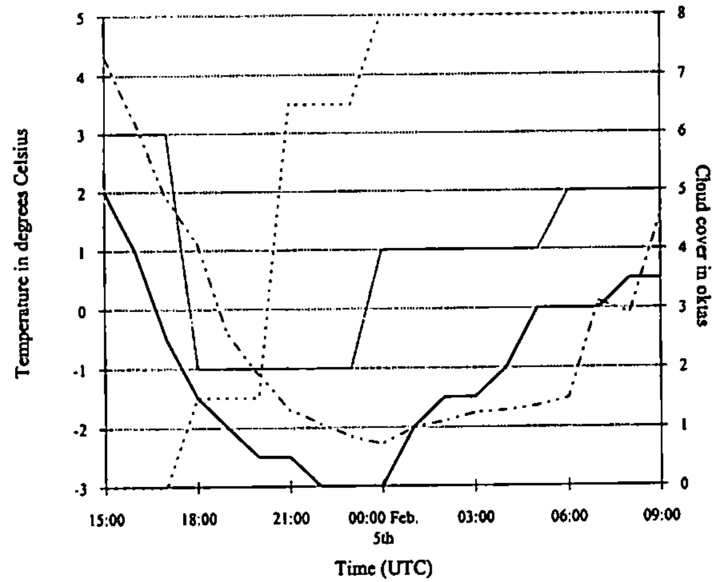

c. Tuelldown

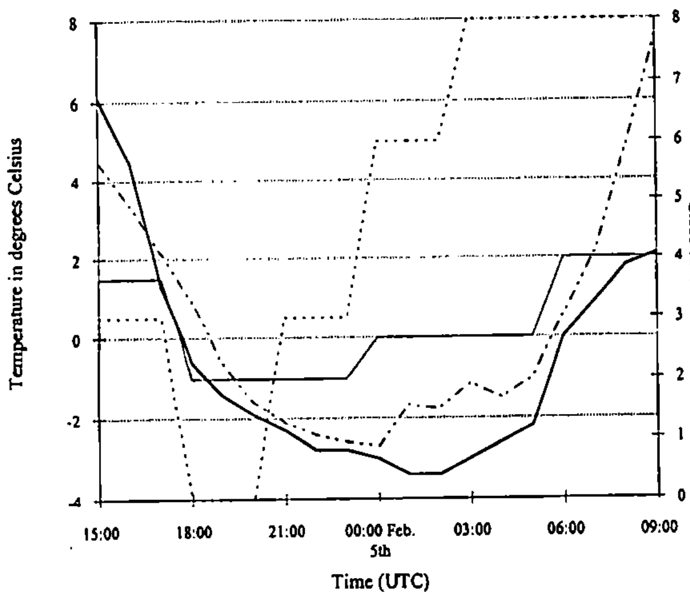

b. Haldon Hill

Observed air temperature

Observed road surface temperature

Roadsurf surface temperature prediction using reduced KCLOUD, a variable wind and spot air temperatures

Observed cloud cover (right hand scale)

Figure 6.3.2.2 Observations and predictions using modified Roadsurf from 1500 UTC Feb. 4th to 0900 UTC Feb. 5th 1996.

Table 6.3.2.5 Results using modified Roadsurf with variable wind speed and reduced KCLOUD (scheme ii of Table 6.3.2.3).

	Frost onset time			Surface minimum temperature		
	Actual /UTC	Pred. /UTC	Error	Actual / °C	Pred. / °C	Error/deg.C
Stopgate Cross	1700	1725	25 min	-4.2	-4.2	+0.0
Haldon Hill	1745	1835	50 min	-3.4	-2.6	+0.8
Tuelldown	1645	1845	2 hr	-3.0	-2.3	+0.7
Ashmill	1730	0245	9hr 15min	-5.0	-0.1	+4.9

Note: pred. :- predicted

Modified Roadsurf performed abysmally at Ashmill (see Table 6.3.2.5). It predicted frost 9 hours late and a minimum surface temperature 5 deg. C too high.

A rerun of Roadsurf using a variable wind but **original** KCLOUD parameters (scheme iii of Table 6.3.2.3) performed better (see scheme iii results in Tables 6.3.3.2a and b and Figure 6.3.2.2e).

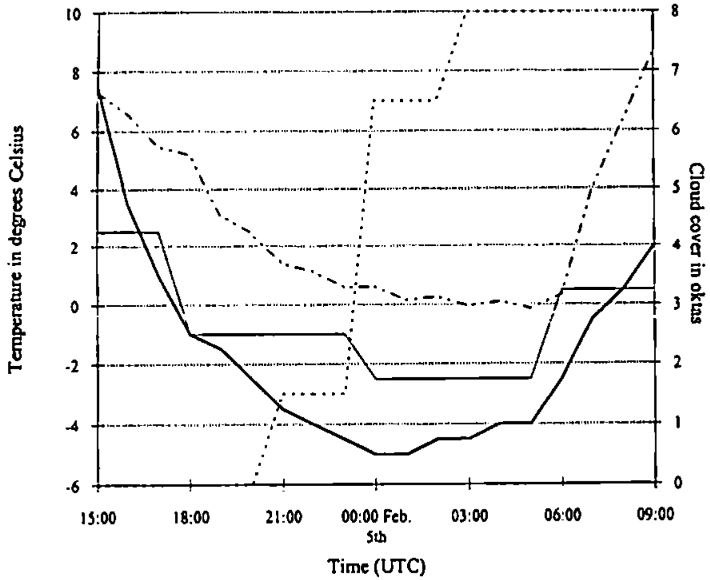

Observed air temperature

Observed road surface temperature

Roadsurf surface temperature prediction with reduced KCLOUD, a variable wind and spot air temperatures

Observed cloud cover (right hand scale)

Figure 6.3.2.2d Observations and predictions using modified Roadsurf at Ashmill from 1500 UTC Feb. 4th to 0900 UTC Feb. 5th 1996.

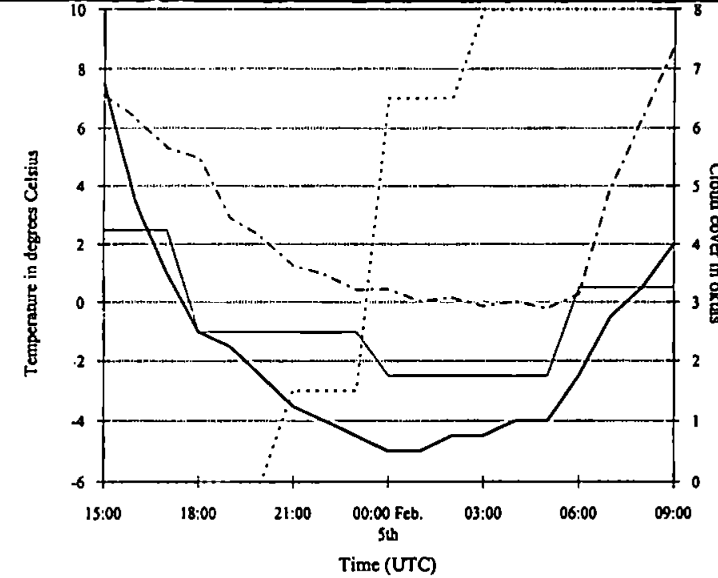

Observed air temperature

Observed road surface temperature

Roadsurf surface temperature prediction with original KCLOUD values, a variable wind and spot air temperatures

Observed cloud cover (right hand scale)

Figure 6.3.2.2e Observations and predictions using unmodified Roadsurf with variable wind at Ashmill from 1500 UTC Feb. 4th to 0900 UTC Feb. 5th 1996.

6.3.3 Experiment using mean air temperatures for model inputs

So far in this particular case study, spot observations taken at 6 hourly intervals formed the sole air temperature inputs used by Roadsurf. An attempt at producing improved surface temperature predictions used air temperatures averaged over 6 hour periods instead (scheme v of Table 6.3.2.3). Inputs from Table 6.3.3.1 were used, and Figures 6.3.3.1a to d show model output.

Table 6.3.3.1 Mean air temperatures used as Roadsurf inputs for schemes iv and v shown in Table 6.3.2.3.

(Times in UTC, temperatures in °C)	Stopgate Cross	Haldon Hill	Tuelldown	Ashmill
1100-1759 Feb. 4th	0.2	1.1	2.6	2.6
1800-2359 Feb. 4th	-1.0	-1.0	-1.3	-3.2
0000-0559 Feb. 5th	0.6	0.3	0.5	-0.7
0600-1159 Feb. 5th	1.5	2.0	2.2	2.1

The graphs in Figures 6.3.3.1a to d show that Roadsurf's predictions using mean air temperatures (Scheme v results in Tables 6.3.3.2a and b) were much improved with an error of 2 hours in frost onset prediction time, and less than 3 deg. C in predicted minimum surface temperature.

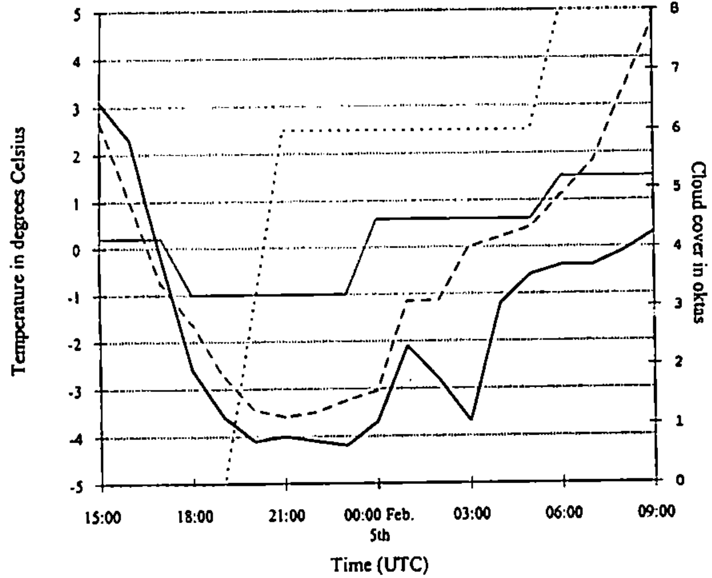

a. Stopgate Cross

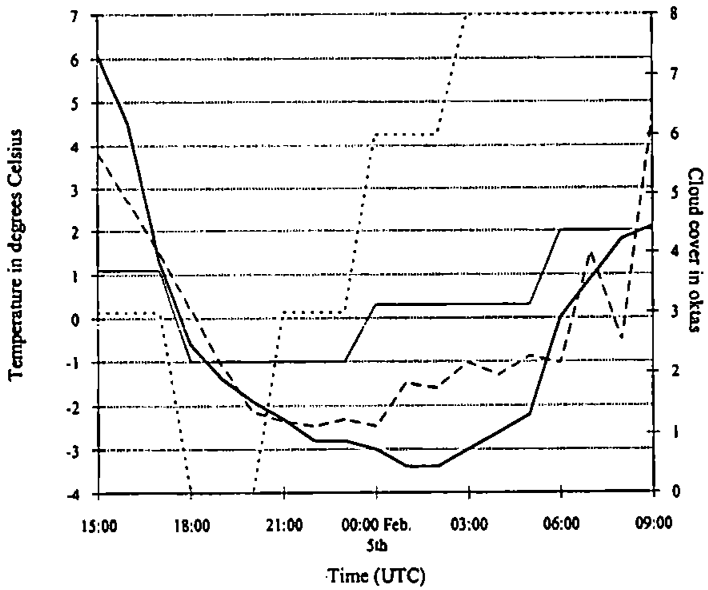

b. Haldon Hill

Observed mean air temperature averaged over 6 hour periods used by Roadsurf

Observed road surface temperature

Roadsurf surface temperature prediction with orginal KCLOUD values, a variable wind AND mean air temperature inputs

Observed cloud cover (right hand scale)

Figure 6.3.3.1 Observations and predictions using Roadsurf under specified conditions from 1500 UTC Feb. 4th to 0900 UTC Feb. 5th 1996

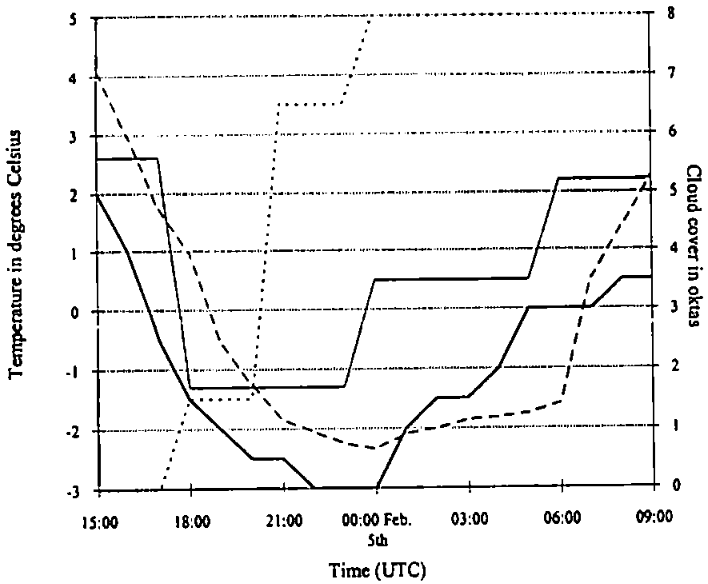

c. Tuelldown

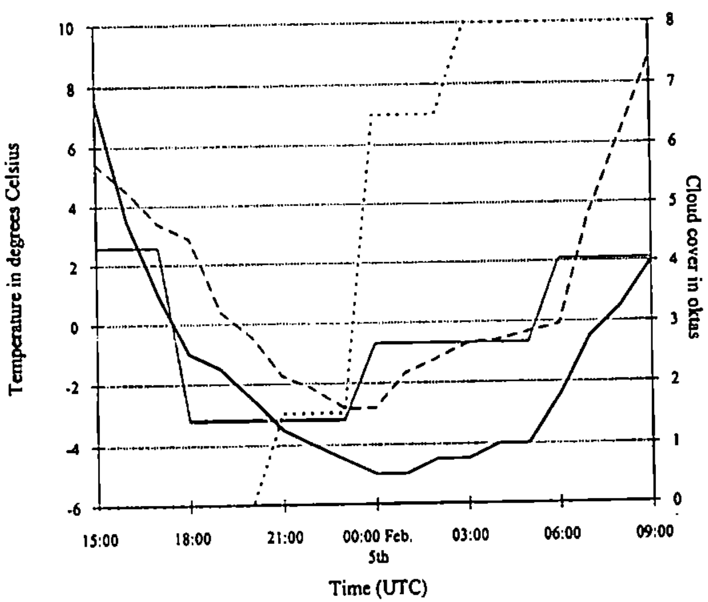

d. Ashmill

Observed mean air temperature averaged over 6 hour periods used by Roadsurf

Observed road surface temperature

Roadsurf surface temperature predictions with orginal KCLOUD values, a variable wind AND averaged air temperature inputs

Observed cloud cover (right hand scale)

Figure 6.3.3.1 Observations and predictions using Roadsurf under specified conditions from 1500 UTC Feb. 4th to 0900 UTC Feb. 5th 1996

Table 6.3.3.2a Frost onset times and minimum surface temperature predictions and observations at **Ashmill** between 1200 UTC Feb. 4th and 1200 UTC Feb. 5th 1996.

Scheme (see Table 6.3.2.3)	Frost onset time			Surface minimum temperature		
	Actual (UTC)	Predicted (UTC)	Error	Actual /°C	Predicted /°C	Error/deg.C
i	1730	0300	9hr 15min	-5.0	-0.1	+4.9
iii	1730	0100	7hr 30min	-5.0	-0.3	+4.7
v	1730	1945	2hr 15min	-5.0	-2.8	+2.2

Table 6.3.3.2b Errors in accuracy of Roadsurf predictions of surface temperature at **Ashmill** averaged from 1200 UTC Feb. 4th to 0700 UTC Feb.5th 1996.

Scheme	Duration of model run when differences between predicted and observed surface temperatures were:-			
	< 1 deg. C	<2 deg .C	<3 deg. C	<4 deg. C
i	7 %	9 %	11 %	21%
iii	9 %	10 %	13 %	24 %
v	4%	15 %	53%	92%

Large differences in surface heating rates between locations within 100 km of each other occurred in this case study which complicated attempts to produce a uniform algorithm for the scenario. At the 4 stations studied, air temperatures increased after 2200 UTC Feb. 4th but at significantly different rates due to elevation, exposure and location relative to the front.

Reducing net heat loss by modifying KCLOUD was a successful method of forcing Roadsurf to produce improved freezing predictions at Ashmill. Results in Table 6.3.3.3 show the errors in Roadsurf predictions from runs under scheme v (see Table 6.3.2.3). At 3 of the 4 locations studied, predicted surface freezing time and minimum temperature were excellent, and compared very well with results under scheme i (Table 6.3.2.3), i.e. **with** reduced KCLOUD and spot air temperatures (see results in Table 6.3.2.5).

Thus to improve prediction of freezing conditions for this particular evening, mean air temperature inputs **were** necessary whereas modifications to KCLOUD were **not**.

The occurrence of anomalous errors at Ashmill compared to other stations was unique on this particular occasion but even here, mean rather than spot air temperatures produced the most accurate surface temperature forecasts (see Table 6.3.3.2a).

Table 6.3.3.3 Roadsurf performance using variable wind speeds, **mean** air temperatures, and **original** KCLOUD values (scheme v of Table 6.3.2.3).

	Frost onset time			Surface minimum temperature		
	Actual /UTC	Predicted /UTC	Error	Actual /°C	Predicted /°C	Error /deg.C
Stopgate Cross	1700	1615	45 min	-4.2	-3.8	+0.4
Haldon Hill	1745	1750	5 min	-3.4	-3.2	+0.2
Ashmill	1730	1945	2hr 15min	-5.0	-2.4	+2.6
Tuelldown	1645	1830	1hr 45min	-3.0	-2.3	+0.7

Algorithms for the scenario of cloud build-up from the west would thus be most successful if they first attempted to predict the likely air temperature evolution.

6.3.4 Algorithm construction

For an algorithm to be successful in the scenario of Feb. 4th/5th 1996, surface wind velocity and air temperature have to be predicted as well as cloud.

a.) Surface wind prediction

Surface flow can be predicted using the geostrophic equation (6.2.5.2) using charts of surface pressure.

Table 6.3.4.1 shows the geostrophic wind V_g for Feb. 3rd, 4th and 5th using the following analyses:-

Figure 6.3.4.1 (1200 UTC Feb. 3rd)
Figure 6.3.1.3a (0000 UTC Feb. 4th)
Figure 6.3.1.3b (1200 UTC Feb. 4th)
Figure 6.3.1.4c (0000 UTC Feb. 5th)
Figure 6.3.1.4d (1200 UTC Feb. 5th).

In the scenarios like this one, which occurred on Feb.4th/5th 1996, it is important that the timing of the approaching depression is accurate or prediction times of the strengthening surface winds will lead to errors in temperature prediction.

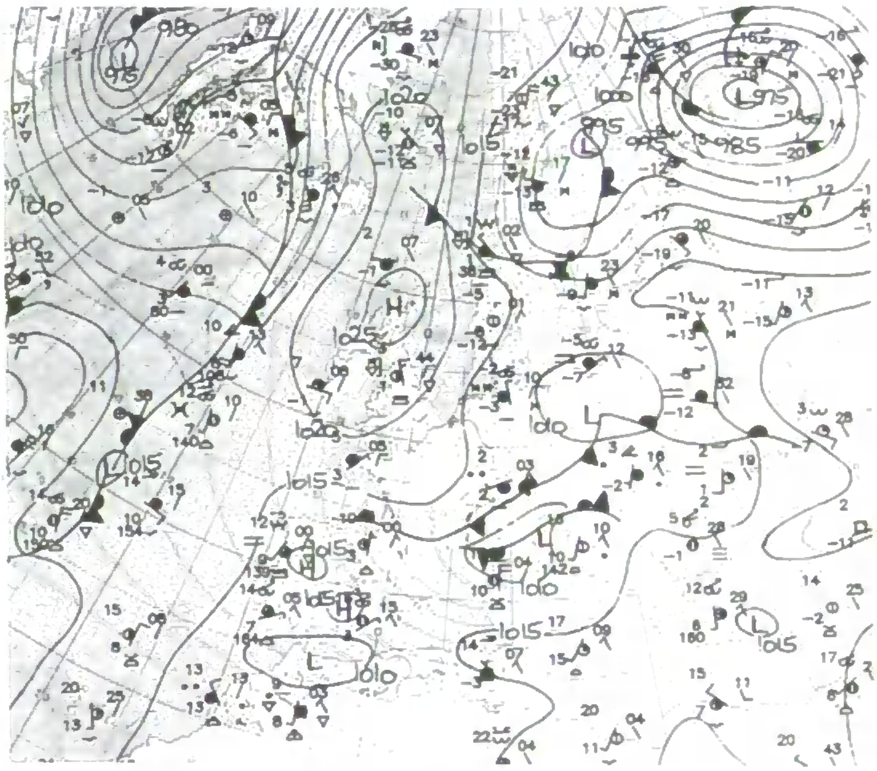

Figure 6.3.4.1 European Meteorological Bulletin surface analysis from 1200 UTC Feb. 3rd 1996

Table 6.3.4.1 Geostrophic flow at times shown, derived from surface pressure analyses from Feb. 3rd, 4th and 5th 1996.

(Times in UTC)	Location	Geostrophic wind / ms^{-1}
1200 Feb. 3rd	Brittany	6.5 ←
0000 Feb. 4th	English Channel	8.5 ←
1200 Feb. 4th	English Channel	<5.0 variable direction
0000 Feb. 5th	Sea area between Cornwall and Eire	27.0 ↗
0000 Feb. 5th	Devon	9.0 ↗
1200 Feb. 5th	Devon	21.0 ↗

b.) Air temperature prediction

Roadsurf does not predict air temperature, so predictions must be obtained from other sources. It is affected by synoptic conditions, i.e. the presence of a warm sector and distance from **surface** fronts, intensity of any precipitation and relief. Construction of a simple algorithm involved studying air temperatures recorded from surface locations already beneath cloudy skies. This data set gave a maximum limit to which air temperature could rise during hours of darkness if the cloud was to move over Devon. The data also gave an accurate horizontal air temperature gradient which enabled determination of the rate of temperature increase when the cloud moved into Devon. Air temperature data recorded from buoys or boats at sea must be modified, because:-

i. Air temperatures at sea are highly influenced by sea surface temperature,

ii. Air temperatures measured at sea are not likely to be taken **2m** above the sea surface, but at some other height depending on whether readings are taken by buoy or ship.

In the 1441 UTC Feb. 4th 1996 NOAA infrared satellite image, Figure 6.3.1.1 cloud is shown over Eire's south-west coastline. Therefore, 2m air temperature records from here at

1500 UTC Feb. 4th were useful in determining the amplitude of air temperature rise which could occur during a period of cloud build-up over Devon. Unfortunately, hourly air temperature data from South West Ireland was not available from Feb. 4th and 5th, except from 1200 UTC Feb. 4th, 0000 UTC and 1200 UTC Feb. 5th. Data were, however available from all 33 Devon road weather stations and a small portion used in Figures 6.3.4.2a and b showed the relationship between increasing cloud cover with rise in air temperature at Stopgate Cross and Haldon Hill. The reason for choosing these stations was due to their ability to record air temperature to a precision greater than half a degree.

Figures 6.3.4.2a and b can be used to construct algorithms for air temperature as functions of cloud cover. Both show, that despite cloud increases to 8 oktas by 0100 UTC Nov. 5th, the air temperature only rose to 2.5 °C. This was a rather muted rise considering that there are occasions in mid-winter when air temperatures at Haldon Hill and Stopgate Cross can reach 10 °C under cloudy conditions.

The restrained warmings were due to the stable cold air block over the North Sea. However, from 1500 UTC Feb. 4th to 0800 UTC Feb. 5th, influence of this blocking anticyclone on Devon's meteorology declined, though only slightly, which allowed milder air from the Atlantic to ascend and pass over the cool air at the surface. Slow air flow prevented any large scale mixing of warm and cold air from occurring. Thus a suitable algorithm, must take into account any influences of cold anticyclonic air which may be situated up to several hundred kilometres east of Devon. Table 6.3.4.2, below shows the simplest algorithms derived for the air temperature.

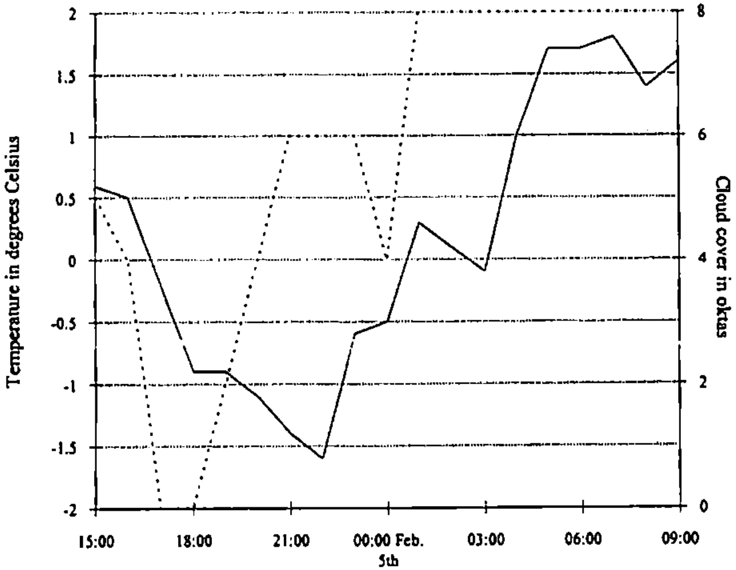

a. Stopgate Cross

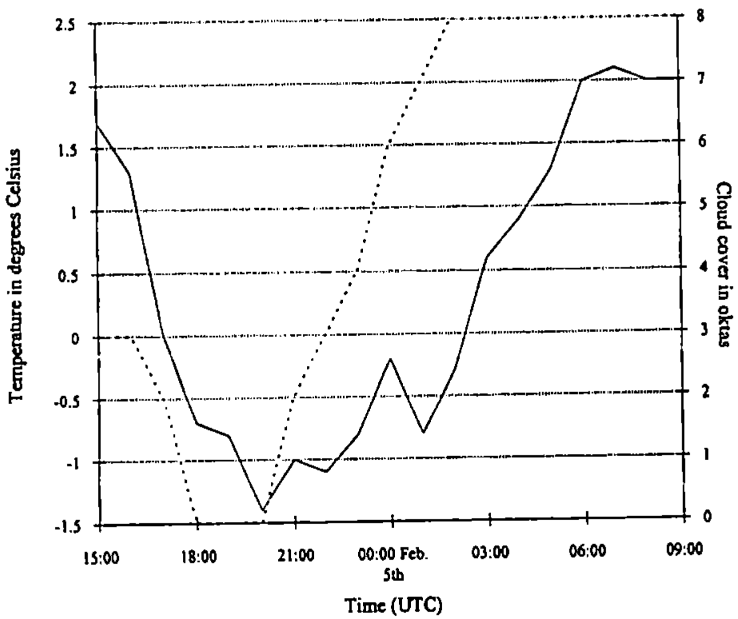

b. Haldon Hill

Observed air temperature

Observed cloud cover (right hand scale)

Figure 6.3.4.2 Conditions from 1500 UTC Feb. 4th to 0900 UTC Feb. 5th 1996.

Table 6.3.4.2 Simple proposed air temperature prediction algorithms using cloud cover changes.

Cloud cover tendency	Air temperature prediction algorithm
Cloud increase between 1900 and 0000 UTC	At Stopgate Cross:- Increase air temp 1 deg. C per hour, after a 2 hour time delay, At Haldon Hill:- Increase air temp 0.6 deg. C per hour, after a 2 hour delay.
Constant cloud amount of over 5 oktas	No air temperature change
Cloud clearance of 1 okta per hour from 3 oktas to clear between 1200 and 0000 UTC	At Stopgate Cross:- Decrease air temp by 1 deg. C per hour, At Haldon Hill:- Decrease air temp by 2 deg. C per hour.
Cloud clearance of 1 okta per hour between 0000 and 0600 UTC	Decrease air temp by 1 deg. C per hour (both stations)

Algorithms such as those above become complicated in quests for greater success in air temperature prediction. The above only work under very specific conditions e.g. light surface and medium level winds, with an eastward moving Atlantic depression moving into an anticyclone. Their application is needed because of cold and warm air advection which affected Roadsurf's energy balance. Stronger winds would have promoted warming effects due to mixing. Also, in an absence of anticyclonic weather east of Devon, the atmosphere at surface level would already have been warmer than during November 4th and 5th 1995.

It would have been interesting to probe the effects of cloud cover increase in already unsettled, mild conditions. However, the small likelihood of danger from ice or frost occurring in such a situation in Devon rendered such an exercise needless.

In this particular case study, no significant warm sector was present. If a warm sector type of system *had* moved into Devon, air temperatures would have risen by at least 2 deg. C per hour whilst its leading warm front introduced the warm sector, probably requiring a completely different algorithm. In such a situation, fixed air temperatures as originally used in Roadsurf, would have produced huge errors.

Furthermore, heavy precipitation as might also occur, rapidly cools the air, sometimes by as much as 0.5 deg. C, especially during rainfall rates of more than 10 mm per hour, due to evaporative cooling. Such cooling is usually brief and air temperatures normally regain their preceding values within 30 minutes. It only causes a minor disturbance to Roadsurf. However, it does cause problems to road maintenance operations if the lowest 100 metres of atmosphere above the surface is close to 0°C. Sleet can change readily to snow during short periods of intense precipitation. Any previous salt spreads become ineffective due to washoff by the sleet, increasing the likelihood of snow accumulation causing potential traffic chaos.

c.) Cloud cover prediction

It is usually not complicated to forecast cloud cover for this type of scenario if a cloud band has already been identified on satellite imagery.

Due to the retrospective nature of the February 4th/5th case study, infrared NOAA satellite images were already available from 1441 UTC Feb. 4th, 0254 UTC Feb. 5th and 0700 UTC Feb.5th (Figures 6.3.1.1a to c). Furthermore, a set of Meteosat 'D2' infrared images (Figures 6.3.1.2a to d) was also available which allowed back tracking of the cloud band and subsequent determination of cloud cover at any individual location. This is obviously impossible to do during an operational situation, so forward tracking is required instead to predict the cloud track. This would have to be done by:-

1) Deriving velocity of cloud movement from preceding images over a specified period of duration depending on image availability,

or 2) Calculating velocities of mid and upper level atmospheric flow and assuming relationships between cloud displacement and wind at these levels.

Method 1:-

The 'cross-correlations' technique of tracking cloud in satellite imagery is easiest to use (see literature survey). Infrared imagery from NOAA satellites showed cloud cover clearer than from Meteosat satellites for resolution reasons. Another benefit of using NOAA imagery is due to the following fact. Meteosat satellites due to their geosynchronous orbit are always situated above the equator and hence have an oblique view of mid latitudes (i.e. England). This results in an illusion of cloud appearing where it does not actually exist. For example, cloud directly above North Devon, may appear in Meteosat images as being above the Bristol Channel instead. NOAA does not have this problem since its orbits are polar, and pass directly overhead.

Meteosat images however, are easier to use for cloud tracking than NOAA's because intervals between successive Meteosat images are small.

Researching cloud track velocities from preceding cloud band movement, it is possible to make a good track and velocity forecast of the cloud band, from which cloud cover in oktas can be estimated.

The NOAA images from Feb. 4th and 5th (Figures 6.3.1.1a to c) show the advancing forward line of the cloud band from 1441 UTC Feb. 4th to 0700 UTC Feb. 5th. In this particular case study, it was simple, especially in the 1441 UTC and 0700 UTC images, to identify this boundary and its displacement. It can be seen however, that ahead of the main thick cloud situated immediately west of 10° West, south-west of Eire, there was a second forward cloud edge between 5 and 7° West at 50° North. It was difficult to determine the amount of cloud which this more easterly cloud edge would introduce into Devon. Furthermore, forced lifting of incoming moist air by the Cornish peninsula made the first cloud edge diffuse as shown by the 0254 UTC Feb. 5th NOAA image.

In an operational environment, a large assumption must be made regarding whether a cloud band will continue to move at the same velocity over land during its passage across the

Eastern Atlantic. A blocking anticyclone over the North Sea will usually slow the approach of an Atlantic sourced cloud band and sometimes even stop it. If this *is* the case and it is not realised, a poor forecast of cloud build-up will result in further hours of unexpected clear sky conditions during which the surface might cool enough to freeze.

Method 2:-

Less favourable than the first method, since more data are required. It is also more complicated, involving some mathematics and can be time consuming.

This method has a series of processes, each of which must be carried out in the following order:-

i) Height determination of existing cloud.

ii) Flow determination at cloud level,

iii) Determination of relationship between flow at cloud level and velocity of cloud movement.

iv) Calculation of present cloud movement and subsequent movement prediction.

The level of existing cloud can be easily be found to within 50 millibars using radiosonde ascents or much less accurately using, satellite image brightness. Atmospheric flow at cloud level can also be found using radiosonde wind data. Unfortunately, radiosonde ascents are routinely carried out at only one location in South West England (Camborne in Cornwall), and not at all over the Atlantic Ocean from where the cloud was approaching, where radiosonde data would have been most valuable. Atmospheric characteristics such as air flow vary greatly between cloudy and clear sky regions ahead of a cloud band, so ascents taken ahead are limited in their usefulness.

Determining flow at individual heights can alternatively be done using geopotential height analyses. These show direction of cloud movement, providing the cloud height is known or can be estimated from satellite imagery. Calculation of flow from these charts involves using the geostrophic equation which, although simple, can be laborious.

In this scenario of a front approaching from the Atlantic, upper level charts are usually good indicators of possible changes in air temperature near surface level. The wind veers with height, associated with warm advection whenever warm or occluded fronts are approaching and so fronts are sloped with their forward edge at upper levels.

Analyses of 850, 700 and 300 mb geopotential height at 1200 UTC Feb. 4th (Figures 6.3.4.3a and b) show remarkably different patterns between levels. Height contours of 850 mb show a signature of the surface anticyclone, but height contours of 700 and 300 mb show an upper level jet stream 200 to 400 km west of Eire which became established above Devon soon after 1200 UTC Feb. 4th. Analyses from twenty-four hours later, 1200 UTC Feb. 5th (Figures 6.3.4.4a and b) show active jet streams at all three atmospheric levels investigated, even at 850 mb. Tables 6.3.4.3i and ii present a summary of wind speed and direction at the three levels.

Table 6.3.4.3 Flow velocities derived from geopotential height analyses of 850, 700 and 300 mb levels and surface pressure at three locations.

i.) 1200 UTC Feb. 4th 1996

	Eastern* Atlantic	Devon	Central England†
300mb	40 ms^{-1} ➘	10 ms^{-1} ➘	10 ms^{-1} ➘
700mb	20 ms^{-1} ➚	<5 ms^{-1} var.	<5 ms^{-1} ⬋
850mb	10 ms^{-1} ➚	<5 ms^{-1} var.	5 ms^{-1} ⬋
Surface	10 ms^{-1} ➚	<5 ms^{-1} var.	<5 ms^{-1} var.

ii.) 1200 UTC Feb. 5th 1996

	Eastern* Atlantic	Devon	Central England†
300mb	45 ms^{-1} ➔	15 ms^{-1} ➔	10 ms^{-1} ➘
700mb	20 ms^{-1} ➔	10 ms^{-1} ➚	5 ms^{-1} ➚
850mb	20 ms^{-1} ➔	10 ms^{-1} ➚	10 ms^{-1} ⬆
Surface	15 ms^{-1} ➔	20 ms^{-1} ➚	15 ms^{-1} ➚

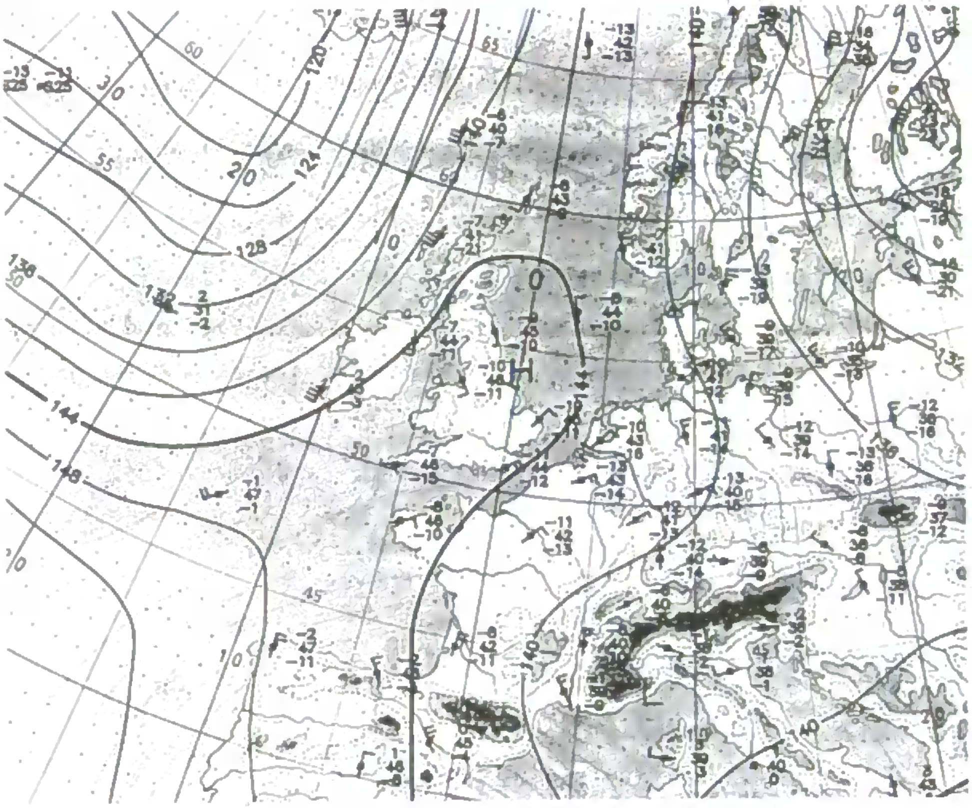

a. 850 mb level

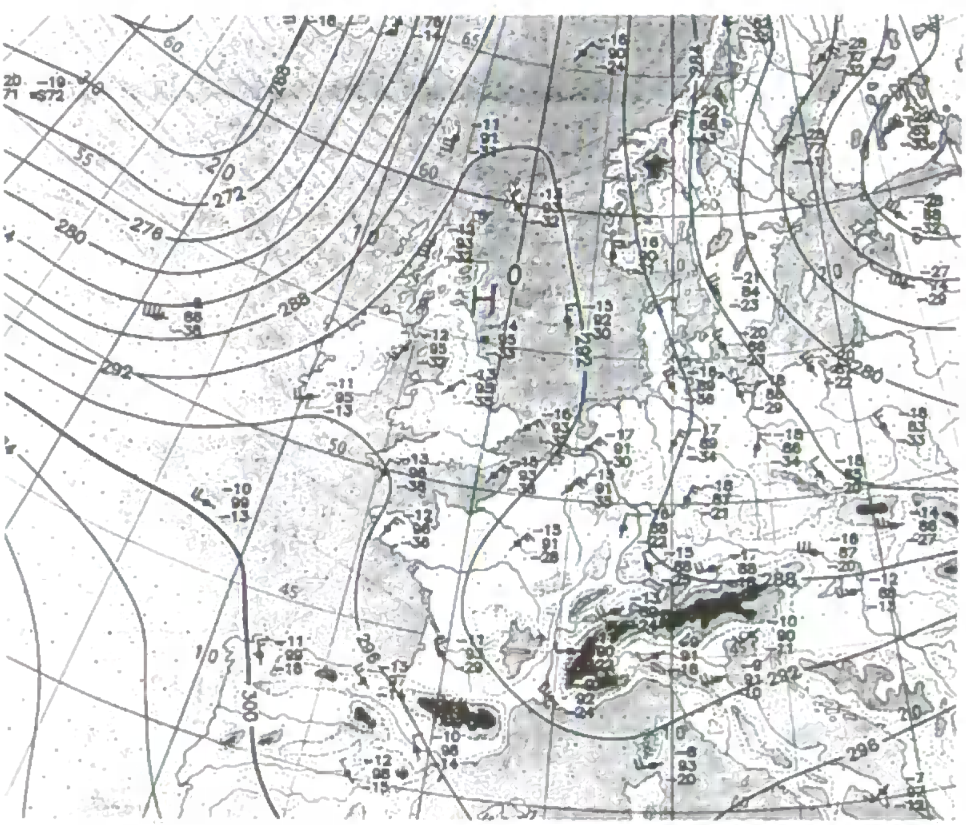

b. 700 mb level

Figure 6.3.4.3 European Meteorological Bulletin geopotential height analyses from 1200 UTC Feb. 4th 1996
(Charts from 0000 UTC Feb. 4th were not available)

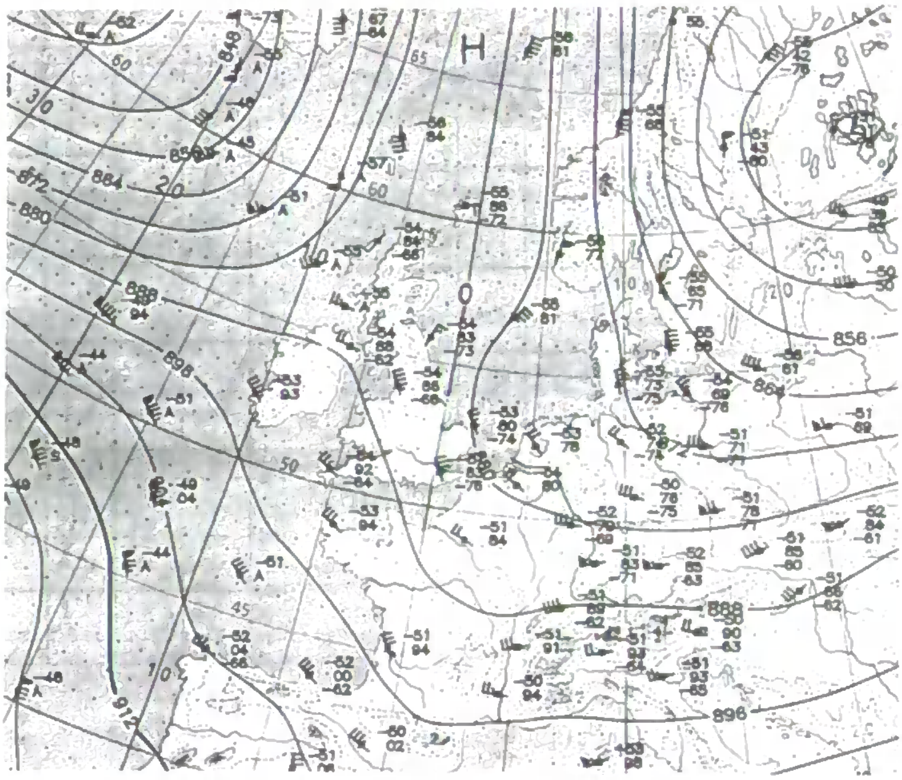

c 300 mb level

Figure 6.3.4.3 European Meteorological Bulletin geopotential analyses from 1200 UTC Feb. 4th
(Charts from 0000 UTC Feb. 4th were not available)

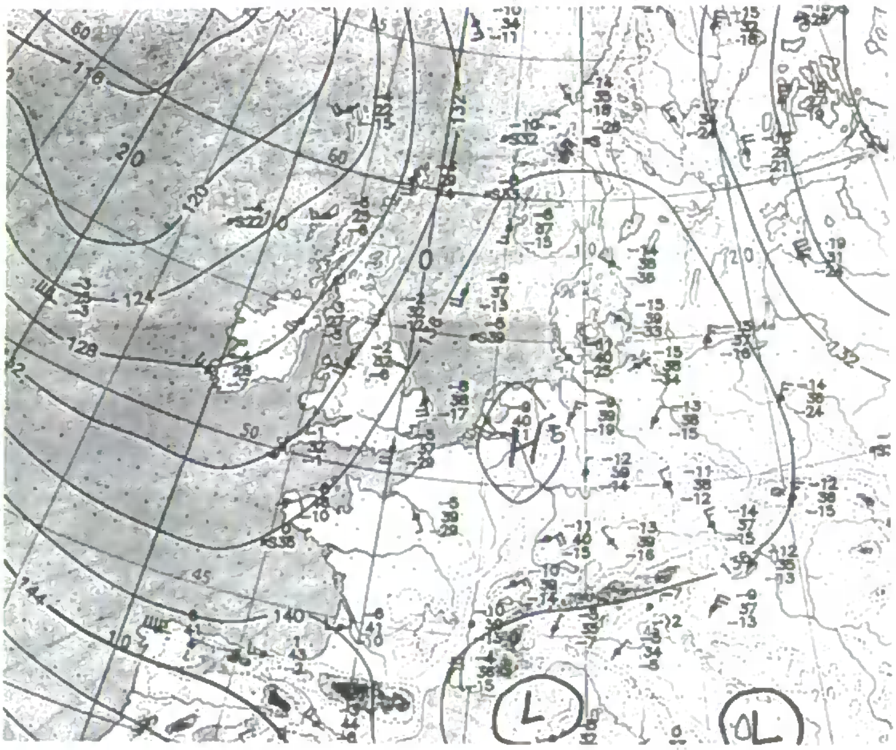

a. 850 mb level

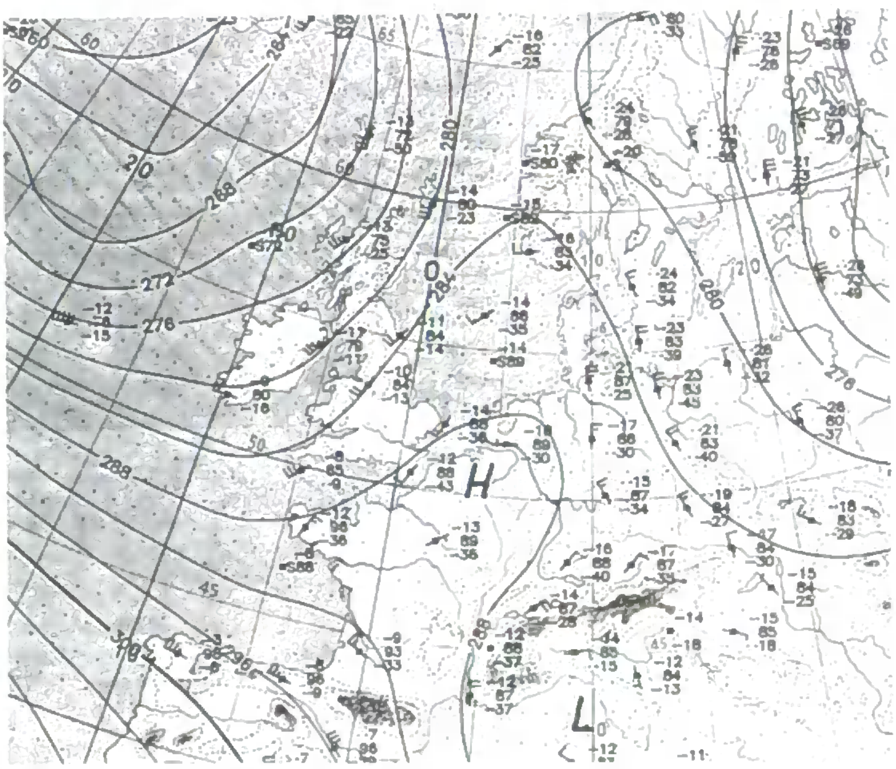

b. 700 mb level

Figure 6.3.4.4 European Meteorological Bulletin geopotential height analyses from 1200 UTC Feb. 5th 1996
(Charts from 0000 UTC Feb. 5th were not available)

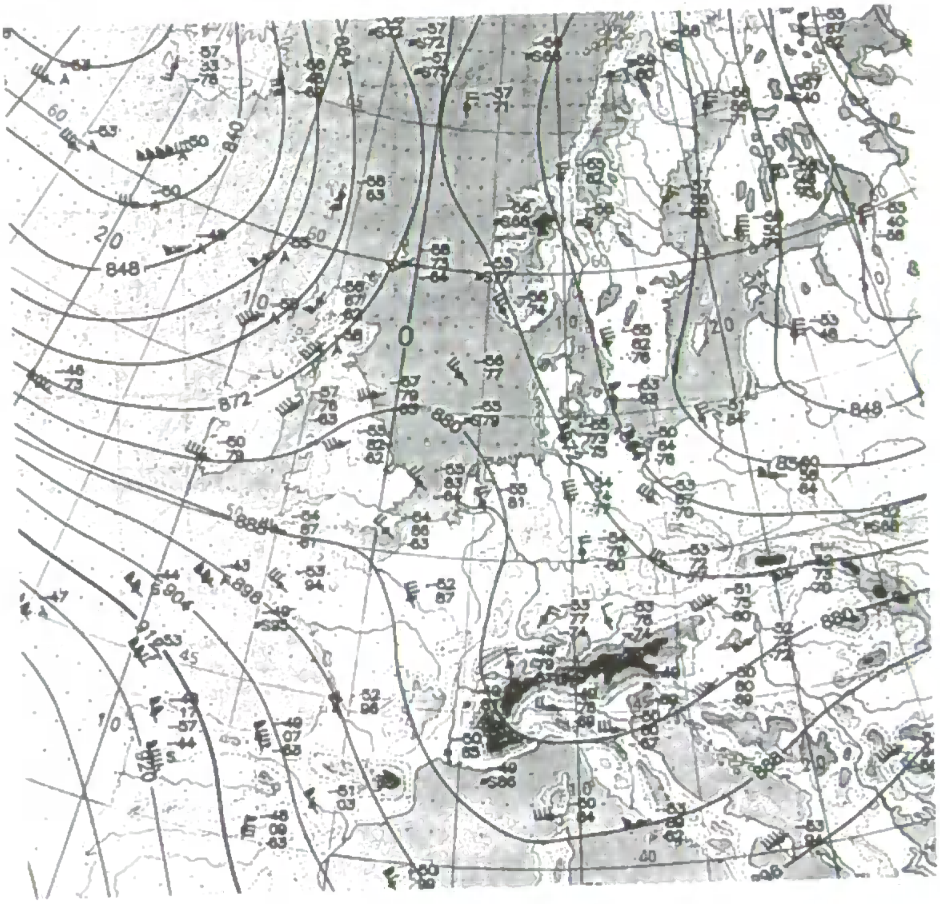

c 300 mb level

Figure 6.3.4.4 European Meteorological Bulletin geopotential height analyses from 1200 UTC Feb. 5th 1996
(Charts from 0000 UTC Feb. 5th were not available)

Notes for Tables 6.3.4.3i and ii.

*: region 50° to 55° N, 10° to 20° W

†: region 51° to 53° N, 0° to 3° W

var.: variable

There are strong relationships between atmospheric flow and cloud velocity as investigated in Chapter 1 (literature survey). A cloud track can then be produced from which cloud cover at individual locations can be estimated.

6.3.5 Algorithm summary

Scenario:-

Frontal cloud moving eastward from the Atlantic into very cold anticyclonic air over Eastern England during January or February.

Algorithm:-

1. Predict mean 2m air temperature for forecast period (1200 UTC onwards) for periods of 6 hours duration, using observations and knowledge of local climate as detailed by Mclean, 1994.

2. Estimate height, track and speed of cloud using observations from a period of at least 6 hours preceding start of forecast.

3. Produce cover forecast in oktas of cloud above a chosen site.

4. Calculate 2m air flow from latest surface air pressure analysis using the **geostrophic wind equation** (6.2.5.2) and compare with weather station observations. Estimate air flow for duration of forecast period, taking exposure into account. Changes in air flow are greatest during passing of the frontal zone.

5. Run Roadsurf using predicted cloud cover, 2m air temperature and wind speed to produce a graph of surface temperature for the chosen site, from which frost onset time and minimum surface temperature can be obtained.

6.4 December 5th and 6th 1995

Scenario:- Frontal cloud moving westwards into Devon from Dorset and Somerset before dissipating, giving an illusion of eastward movement.

6.4.1 Synoptic conditions and cloud cover of December 5th and 6th 1995.

Figures 6.4.1.1a and b show that a blocking anticyclone above Scandinavia dominated Northern Europe throughout Dec. 5th and 6th 1995. Consequently surface flow over Devon was from an easterly origin, though less than $4ms^{-1}$ throughout.

Large areas of low level stratus cloud covered Southwest England between 1200 UTC Dec. 5th and 0900 UTC Dec. 6th, shown clearly by Figures 6.4.1.2a to d. Despite frequent dissipation and formation in situ, its general movement was westwards.

Precipitation occurred at Stopgate Cross but not at Bratton Down, Haldon Hill and Tuelldown. From road weather station data, road surfaces at Bratton Down, Haldon Hill and Stopgate Cross were recorded as being wet, though at Bratton Down, this wetness was most likely due to lying grit and salt. A dry surface was reported at Tuelldown.

6.4.2 Initial Roadsurf predictions.

The initial input parameters for Roadsurf are shown in Table 6.4.2.1. A lack of NOAA satellite imagery over Devon between 2000 and 2359 UTC Dec. 5th due to their polar orbiting nature, and less than adequate coverage between 1400 and 1900 UTC, was a problem. Usefulness of Meteosat imagery was particularly limited since most cloud that did exist above Devon only did so at low altitudes and thus was difficult to detect due to poor resolution.

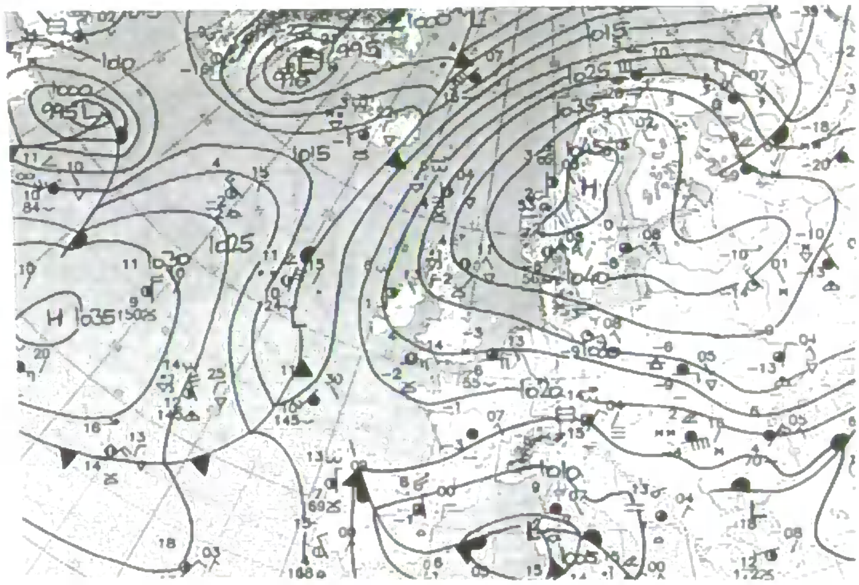

a. 1200 UTC Dec. 5th

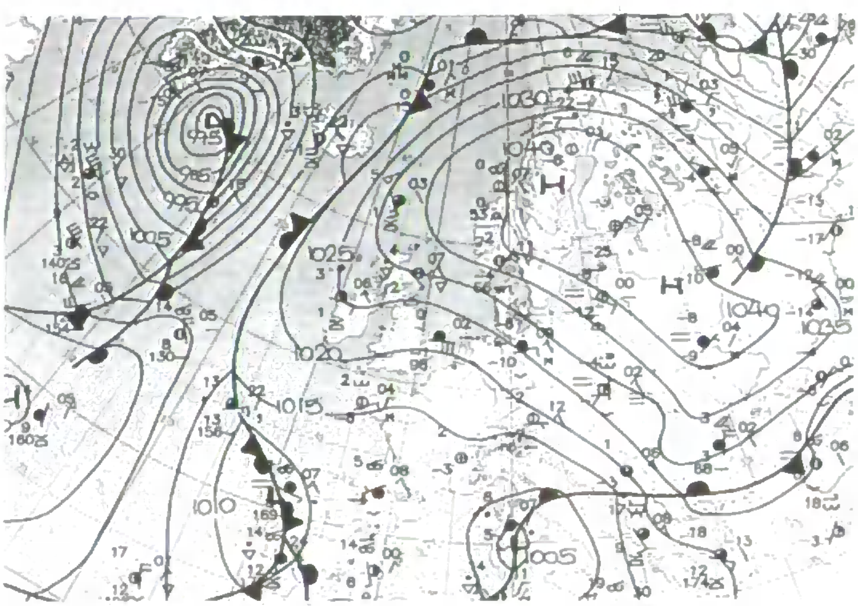

b. 1200 UTC Dec. 6th

Figure 6.4.1.1 European Meteorological Bulletin surface analyses from Dec. 5th and 6th 1995

a. 0800 UTC Dec. 5th 1995

b. 1357 UTC Dec. 5th 1995

c. 0211 UTC Dec. 6th 1995

d. 0352 UTC Dec. 6th 1995

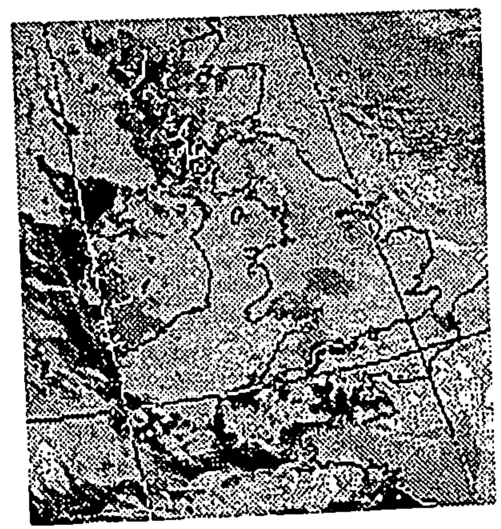

e. 0745 UTC Dec. 6th 1995

Figure 6.4.1.2 NOAA infrared satellite images from Dec. 5th and 6th 1995

Table 6.4.2.1 Major Roadsurf inputs for runs from 1200 UTC Dec. 5th to 0900 UTC Dec. 6th 1995.

Parameter (times in UTC)	Bratton Down	Stopgate Cross	Haldon Hill	Tuelldown
Cloud cover:				
1200-1459	6/Low	6/Low	8/Low	2/Low
1500-1759	*Clear*	*3/Low*	*Clear*	*Clear*
1800-2059	*5/Low*	*8/Low*	*5/Low*	*3/Low*
2100-2359	*5/Low*	*1/Low*	*7/Low*	*5/Low*
0000-0259	5/Low	8/Low	3/Low	1/Low
0300-0559	8/Low	8/Low	8/Low	3/Low
0600-0859	8/Low	Clear	5/Low	8/Low
Air temperature/°C				
1200-1759	0.2	0.4	1.0	2.3
1800-2359	-2.2	-2.5	-2.2	-0.8
0000-0559	-3.6	-3.7	-3.9	-3.1
0600-0859	-2.9	-3.2	-3.3	-2.5
Ts at 1200 Dec. 5th /°C	2.4	1.0	4.2	5.5
Td at 1200 Dec. 5th /°C	2.7	3.0	4.5	4.5
Tcl at 1200 Dec. 5th /°C	3.0	4.9	4.8	3.5
2m wind speed/ms^{-1}				
1200-1759	0.5	0.5	0.5	3.5
1800-2359	0.5	0.5	0.5	3.5
0000-0559	1.5	1.0	1.5	3.5
0600-0859	2.0	1.5	2.0	3.5
DWB/ deg. C	1.9	0.6	0.6	2.3
Surface state	Wet (SRHF=1)	Wet (SRHF=1)	Wet (SRHF=1)	Dry (SRHF=0)

Notes:

Ts: road surface temperature,

Td: 'd' layer temperature (immediately below surface),

Tcl: 'cl' layer temperature (immediately below 'd' layer),

DWB: depression of wet bulb temperature, Periods before 2359 are Dec. **5th**,

Periods after 0000 are Dec. **6th**.

SRHF: parameter used in model to depict surface wetness, observed by road surface sensor at station (1 for wet surfaces, 0 for dry).

Italicalised text indicates probable cloud amounts ascertained using observed temperature data between 1800 UTC and 2359 UTC Dec. 5th due to lack of suitable satellite imagery.

Table 6.4.2.2 Roadsurf results from 1200 UTC Dec. 5th to 0900 UTC Dec. 6th 1995.

Station	Surface freezing onset time			Minimum surface temperature		
	Actual /UTC	Prediction /UTC	Error	Actual /°C	Prediction /°C	Error /deg.C
Bratton Down	1620	1700	40 min late	-3.5	-4.2	-0.7
Stopgate Cross	1625	1835	2hrs 10min late	-3.5	-5.6	-2.1
Haldon Hill	1810	1825	15 min late	-3.7	-4.4	-0.7
Tuelldown	1900	1855	5 min early	-2.5	-4.1	-1.6

Table 6.4.2.2 shows excellent performance by Roadsurf in predicting frost onset times at Tuelldown and Haldon Hill. A forty minute error in prediction at Bratton Down was also adequate. Unfortunately, success did not occur in frost prediction at Stopgate Cross where surface freezing was unacceptably predicted 2 hours late. This was due to an underestimation of cloud cover between 1500 and 1800 UTC Dec. 5th. Consequently, Roadsurf exhibited a warm bias in surface temperature predictions between 1200 UTC and 2000 UTC Dec. 5th. The high influence of cloud cover on Roadsurf can be seen from Figure 6.4.2.1b between 0500 UTC and 0800 UTC Dec. 6th, when the sky briefly cleared. Roadsurf overestimated radiative cooling during this period which directly produced an anomalously low minimum surface temperature prediction.

Due to the absence of suitable satellite imagery between 1400 UTC and 2300 UTC Dec. 5th, cloud had to be ascertained by studying trends in observed air and surface temperature between 1600 UTC Dec. 5th and 0200 UTC Dec. 6th. Two hour delays between significant temperature fluctuations and hypothetical changes of cloud cover were therefore artificially introduced in an attempt to mimic a natural timelag which occurs between cloud increase/decrease and temperature. The natural timelag varies in duration depending on scenario and time of night, so occasions when a two hour lag was unsuitable were likely. This exercise had the benefit however, of showing flaws in the Roadsurf code not responding adequately to cloud cover increase. At Bratton Down from 1800 UTC to 2359 UTC Dec. 5th, using cloud ascertained from air and surface temperature observations and assumed accurate to within 2 oktas, Roadsurf underestimated the suppression of surface cooling caused by the assumed 6 oktas of cloud. An increased difference between observed and Roadsurf predicted surface temperature is shown in Figure 6.4.2.1a.

Further periods when Roadsurf failed to respond under similar phenomena occurred between:-

i) 2000 and 2200 UTC Dec. 5th at Haldon Hill (see Figure 6.4.2.1c),

ii) 0100 and 0300 UTC Dec. 6th at Haldon Hill (see Figure 6.4.2.1c),

iii) 2200 and 2300 UTC Dec. 5th at Tuelldown (see Figure 6.4.2.1d).

These flaws can be explained by comparing observed surface temperatures with those of the air. After 2300 UTC Dec. 5th at all four stations, the air became cooler than the road surface. Increasing cloud cover after 2200 UTC prevented loss of heat from the surface to space. Surface temperature predictions produced by Roadsurf are strongly dependent on air temperature. Thus if no air warming occurs, predicted surface warming by Roadsurf will be small.

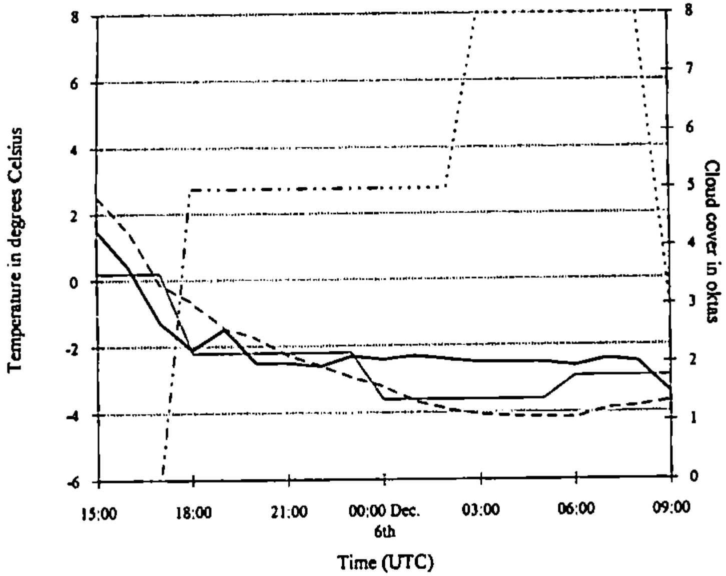

a. Bratton Down

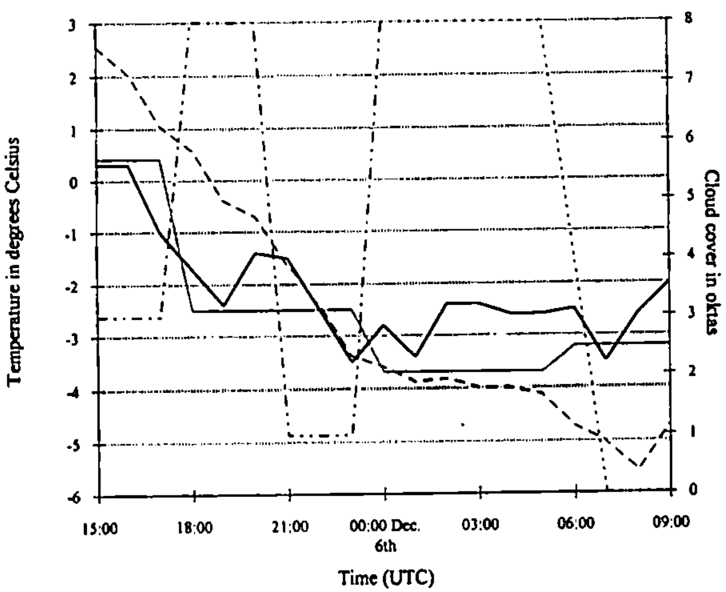

b. Stopgate Cross

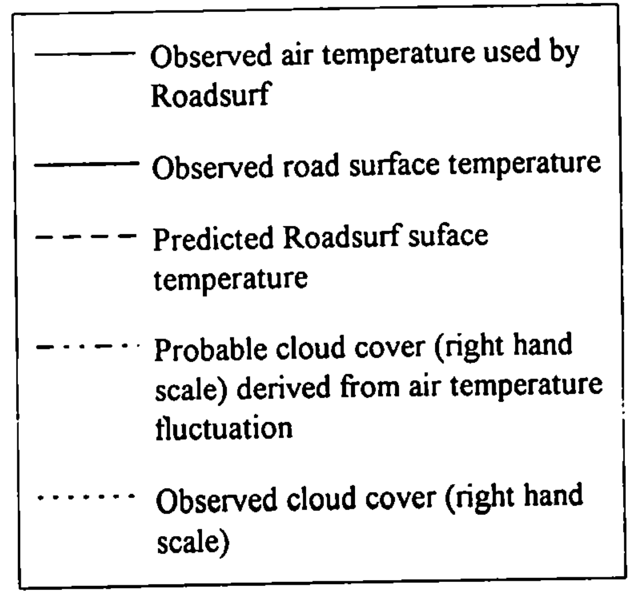

Figure 6.4.2.1 Evolution of conditions from 1500 UTC Dec. 5th to 0900 UTC Dec. 6th 1995.

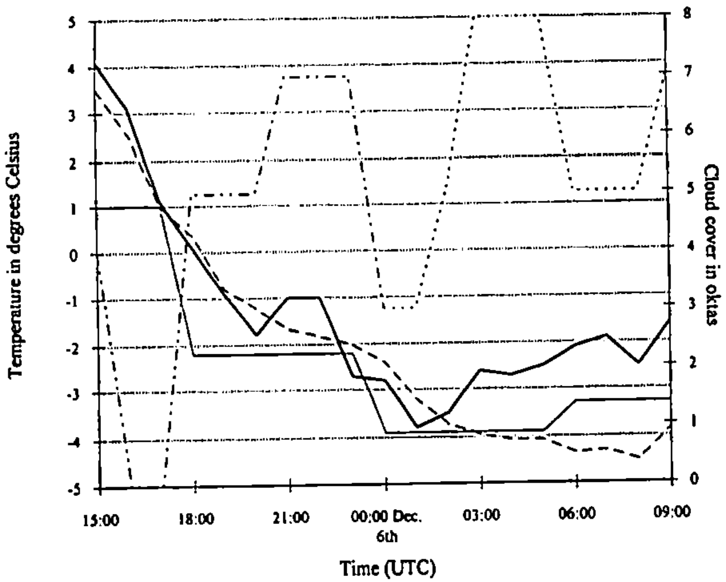

c. Haldon Hill

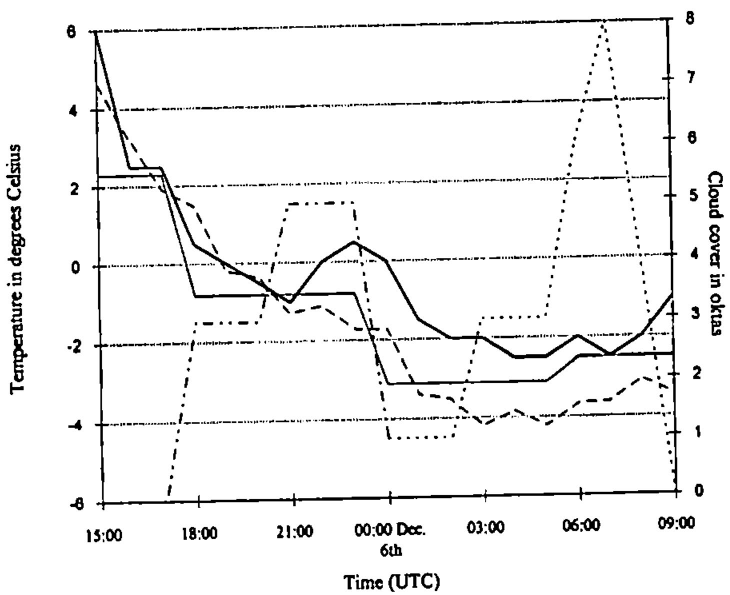

d. Tuelldown

——— Observed air temperature used by Roadsurf

——— Observed road surface temperature

– – – Predicted Roadsurf suface temperature

–·–·· Probable cloud cover (right hand scale) derived from air temperature fluctuation

······· Observed cloud cover (right hand scale)

Figure 6.4.2.1 Evolution of conditions from 1500 UTC Dec. 5th to 0900 UTC Dec. 6th 1995.

Rerunning Roadsurf using air temperatures 1 deg. C artificially warmer was a simple way of solving the problem in this scenario, though such a solution obviously created new errors during occasions when Roadsurf had previously performed successfully.

6.4.3 Algorithm construction

For a scenario of cloud formation and displacement towards the south-west under north-easterly flow, it is necessary to have an algorithm which accounts for cold air advection. The algorithm must emphasise warming effects of cloud cover increase on surface temperature without requiring warmer air temperature inputs. Such an algorithm depends also on wind velocity near the surface and precipitation, if any. Wind speeds were less than 4 ms^{-1} during Dec. 5th and 6th and no precipitation occurred although some surfaces were wet.

Cloud cover in this scenario can be tracked using the cross correlation and plane sailing methods discussed during earlier case studies. For an operational environment, cloud movement during the twelve hours immediately preceding the forecast period can be used produce a cloud forecast for Roadsurf.

Due to cold air advection, it was necessary to modify Roadsurf to repress surface cooling from continued cold air advection whenever moderate cloud increase occurred. This required modified parameterization of processes involving the air temperature.

Roadsurf uses air temperature to compute:-

i) Richardson number of stability,

ii) Sensible heat,

iii) Latent energy

and iv) Emissivity of the sky.

Sensible heat flux

The sensible heat flux, H is given by:- (positive values downward)

$$H^i = EXXO^i * \kappa * (Ta^i + DALR*Za - Ts^i) \qquad 6.4.3.1$$

where,

H = sensible heat flux (Wm^{-2}),

EXXO = parameter related to Richardson number of stability ($kg\ m^{-2}s^{-1}$),

κ = heat capacity ($kJ\ m^{-3}K^{-1}$)

Ta = air temperature (K),

DALR = dry adiabatic lapse rate ($K\ m^{-1}$),

Za = damping depth (m) held constant through Roadsurf operation,

Ts = surface temperature (K)

and superscripts ^{i} indicate time of parameter. E.g. H^1 is sensible heat after one time step (20 minutes)

From 1200 UTC Dec. 5th to 0900 UTC Dec. 6th, the air at 2m was cooler than the surface. Thus according to equation 6.4.3.1, loss of heat from surface to atmosphere would occur, cooling the surface, partly nullifying effects of cloud increase. However, as Figure 6.4.3.1at Bratton Down shows, sensible heat is negligible compared to net radiation loss to the atmosphere, RN. Radiation flux graphs for other stations, although not shown, also exhibited a similar pattern.

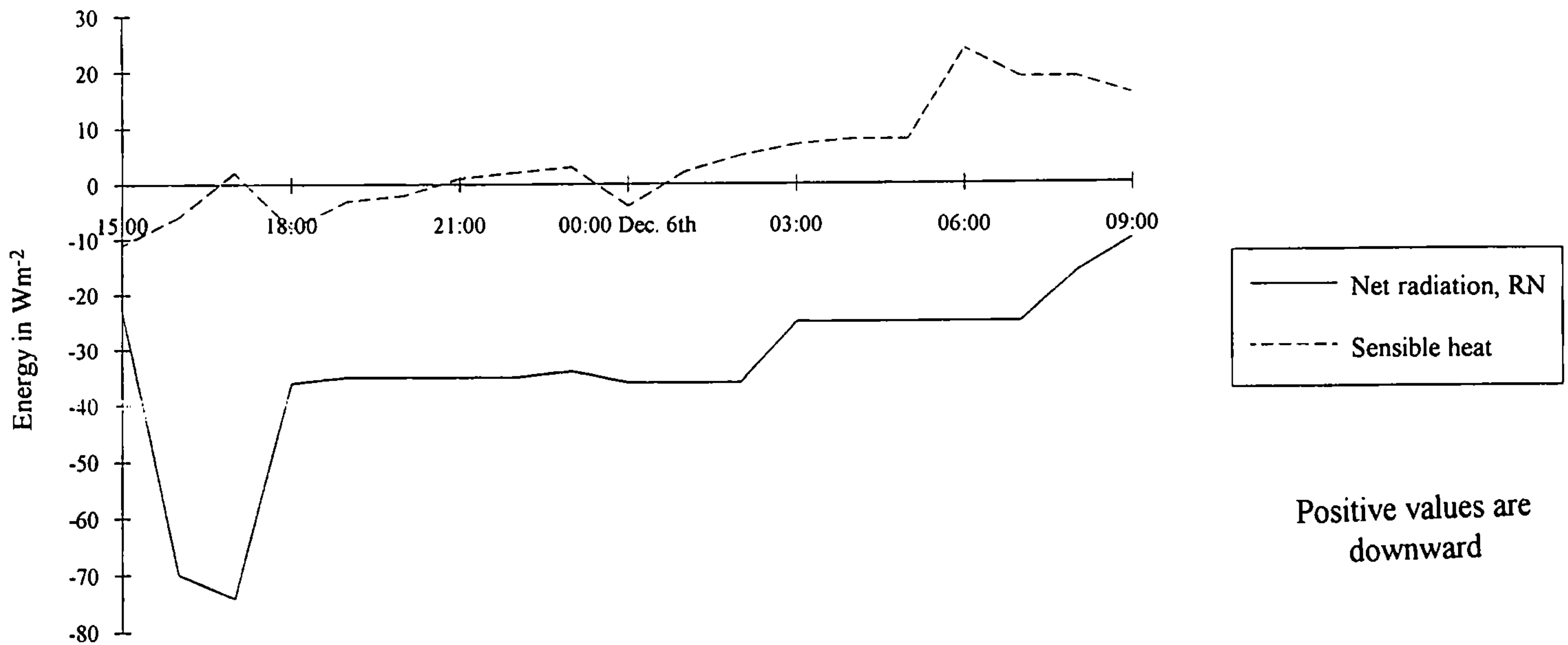

Figure 6.4.3.1 Net radiation and sensible heat fluxes at Bratton Down from 1500 UTC Dec. 5th to 0900 UTC Dec. 6th 1995 from initial Roadsurf run

Net radiation lost to atmosphere

The net radiation loss to the atmosphere is given by:-

$$RN = (1-\alpha)S - \varepsilon\, \sigma T_S^4\ KCLOUD \qquad \textbf{6.4.3.2}$$

where,

RN= net radiation (Wm^{-2})

α = albedo

S = solar radiation (Wm^{-2})

σ = Stefan Boltzmann constant

T_S = surface temperature (K)

KCLOUD = cloud cover dependent factor.

ε = combined emissivity of surface and sky

$$= 0.18 + 0.25 \times 10^{-0.126v} \qquad \textbf{6.4.4.3}$$

where v is the vapour pressure.

During previous case studies, fixed wet bulb depressions were used throughout Roadsurf runs.

Updated wet bulb depressions from observations were then used. Unfortunately, as Figure 6.4.3.2 shows, Roadsurf still failed to respond adequately to cloud cover build-up.

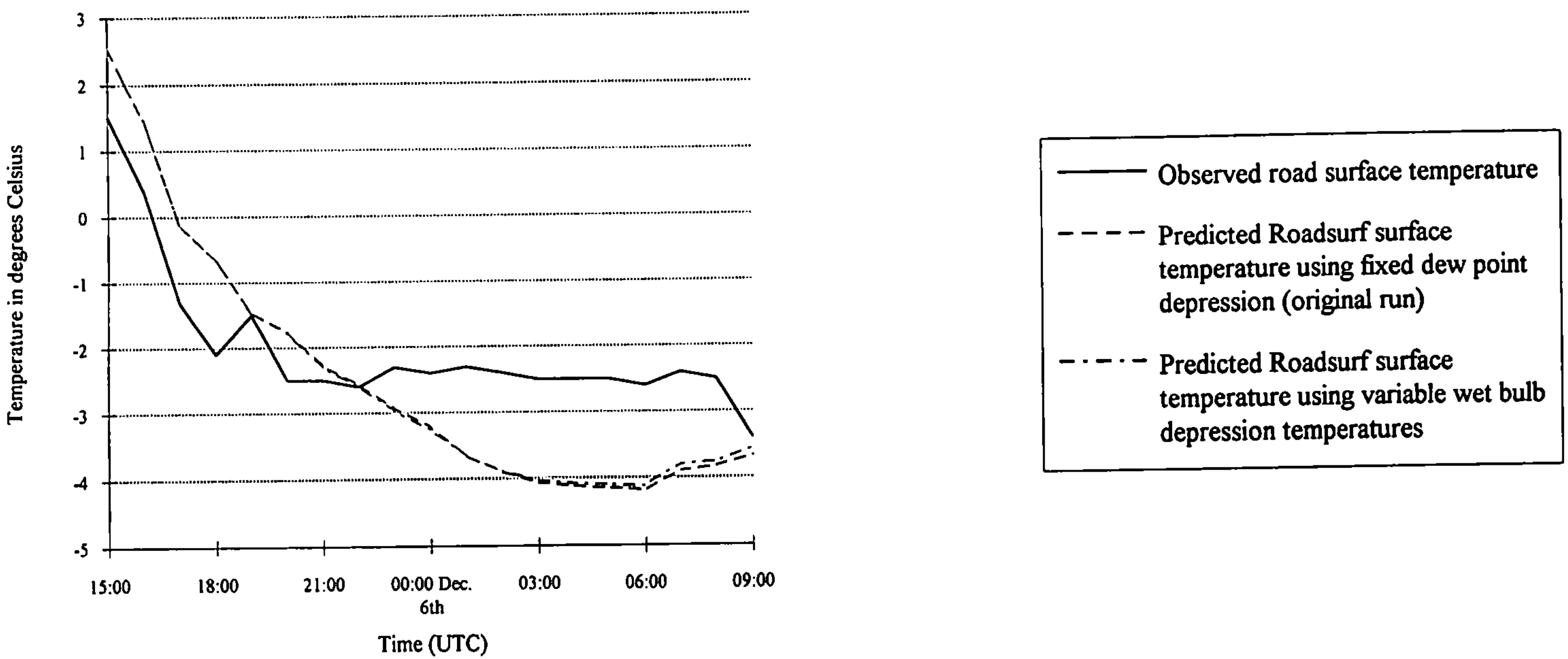

Figure 6.4.3.2 Roadsurf performance at Bratton Down showing affect of dew point depressions on prediction from 1500 UTC Dec. 5th to 0900 UTC Dec. 6th 1995

Air temperature modification

The easiest method of forcing Roadsurf to produce surface temperature predictions to within 2 deg. C of observations was to modify the air temperature inputs. It was decided to fix these parameters at values attained at the start of cloud build-ups (Table 6.4.3.1). Already successful predictions before 1800 UTC Dec. 5th at three stations indicated that this algorithm was necessary only after sunset.

Table 6.4.3.1 Modified air temperature inputs.

Station	Air temperature inputs (/°C) between times shown. All times in UTC			
	Dec. 5th		Dec. 6th	
	1200-1759	1800-2359	0000-0559	0600-1200
Bratton Down	0.2	**-1.3**	**-1.3**	**-1.3**
Stopgate Cross	**-0.8**	**-3.0**	**-3.0**	**-3.8**
Haldon Hill	1.0	**-1.2**	**-1.2**	**-1.2**
Tuelldown	2.3	**1.0**	**-1.5**	**-1.5**

Bold entries indicate air temperature inputs at least 0.5 deg. C removed from observations (i.e. model inputs from original Roadsurf runs of this case study).

Figures 6.4.3.3a and c as well as Table 6.4.3.2 show very successful predictions at Bratton Down and Haldon Hill using the air temperature algorithm. At both locations, predictions were within a single degree of observations for over 90% of the period 1200 UTC Dec. 5th to 0900 UTC Dec. 6th. These results were a good improvement over those obtained without the air temperature algorithm in use. Predictions for post 0000 UTC Dec. 6th using the algorithm at Tuelldown, Figure 6.4.3.3d, were disappointing. Little improvement in general 24 hour prediction had occurred and prediction of frost onset time attained an error of 90 minutes compared to a 5 minute error when not using the algorithm.

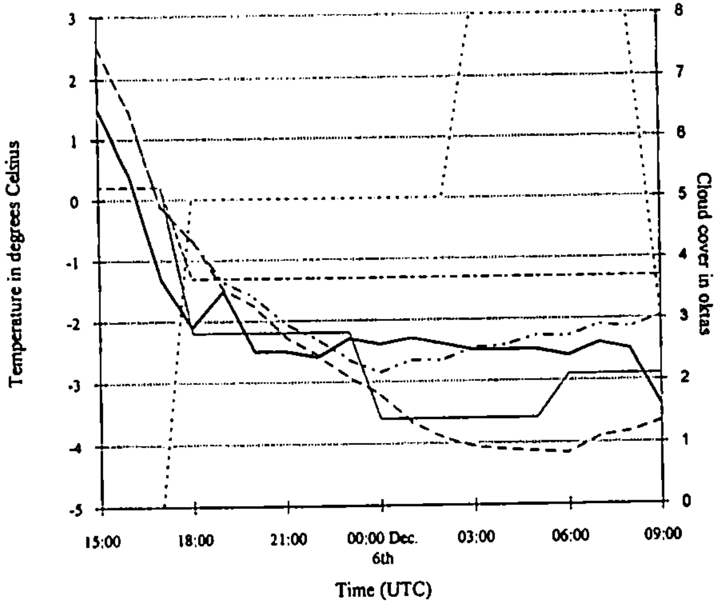

a. Bratton Down

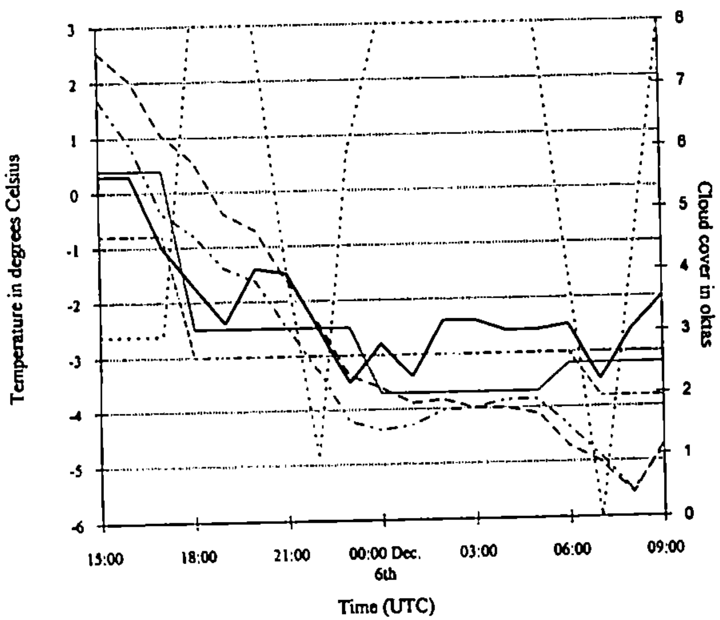

b. Stopgate Cross

Air temperature used by Roadsurf in original run

Modified air temperature used in 'algorithm' run of Roadsurf

Observed road surface temperature

Predicted Roadsurf surface temperature from original run

Predicted Roadsurf surface temperature using modified air temperatures from algorithm

Cloud cover (right hand scale) used by Roadsurf

Figure 6.4.3.3 Roadsurf performance from 1500 UTC Dec. 5th to 0900 UTC Dec. 6th 1995.

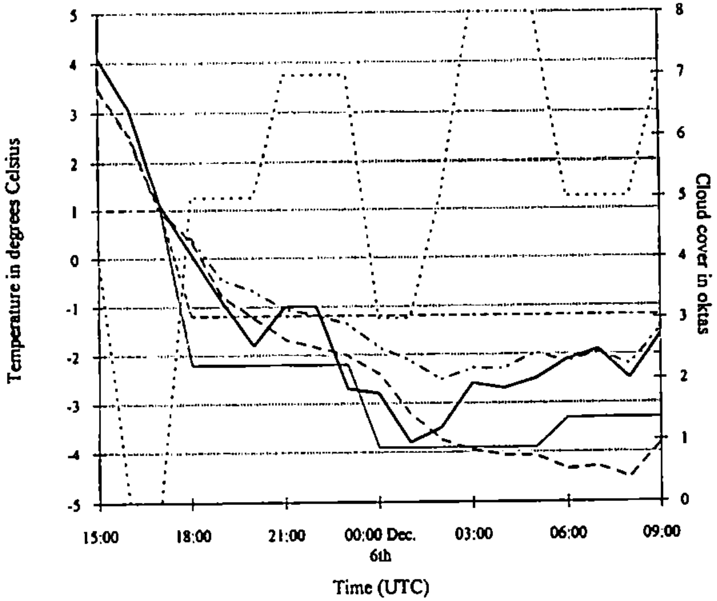

c. Haldon Hill

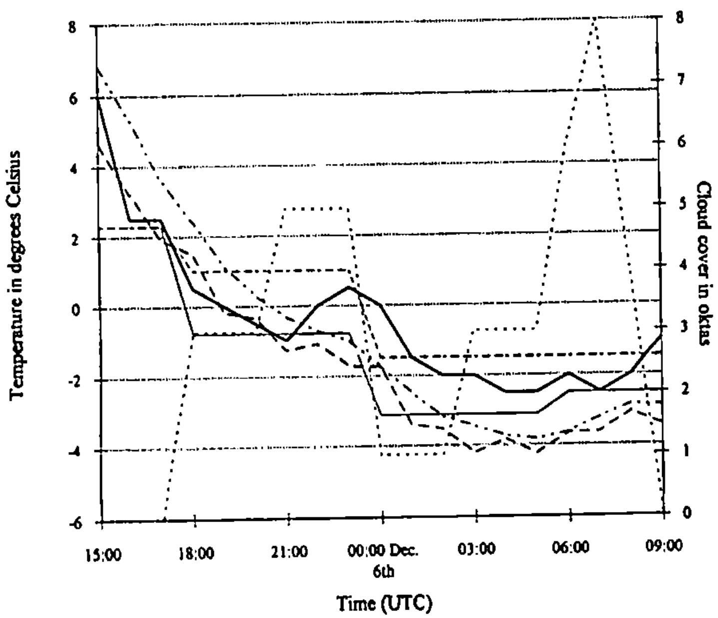

d. Tuelldown

Air temperature used by Roadsurf in original run

Modified air temperature used in 'algorithm' run of Roadsurf

Observed road surface temperature

Predicted Roadsurf surface temperature from original run

Predicted Roadsurf surface temperature using modified air temperatures from algorithm

Cloud cover (right hand scale) used by Roadsurf

Figure 6.4.3.3 Roadsurf performance from 1500 UTC Dec. 5th to 0900 UTC Dec. 6th 1995.

The algorithm produced mixed results at Stopgate Cross (Figure 6.4.3.3b). Significant improvements in frost onset prediction occurred compared to the original model run, but there was no improvement in minimum predicted temperature.

Table 6.4.3.2 Roadsurf results between 1200 UTC Dec. 5th and 0900 UTC Dec. 6th 1995 using air temperature algorithm.

Station	Surface freezing onset time			Minimum surface temperature		
	Actual /UTC	Prediction /UTC	Error	Actual /°C	Prediction /°C	Error /deg.C
Bratton Down	1620	1700	40 mins late	-3.5	-2.8	+0.7
Stopgate Cross	1625	1645	20 mins late	-3.5	-5.5	-2.0
Haldon Hill	1810	1830	20 mins late	-3.7	-2.5	+1.2
Tuelldown	1900	2030	1hr 30 mins late	-2.5	-3.8	-1.3

The pros and cons of the air temperature algorithm, although successful at Haldon Hill and Bratton Down, must be considered carefully in an operational situation. Differences between the results shown in Figures 6.4.3.3a to d show a big problem in attempting to predict surface temperatures in Devon: variability in site characteristics. Relief appeared not to affect algorithm suitability (see Table 6.4.3.3) though directional exposure *did*.

Obviously sites exposed to the east or north-east experienced greater cold air advection during Dec. 5th and 6th. Wind observations were only available from Haldon Hill for this particular occasion rendering such a study unfeasible. However, parameters shown in Table 6.4.3.3(Mclean, 1994) show that successful trials of the algorithm occurred at sites with a coastal proximity.

Table 6.4.3.3 Properties of four Devon sites. (Mclean, 1994)

Site	Exposure	Height above mean sea level (m)	Location
Bratton Down	Open	320	Coastal
Stopgate Cross	Open	253	Inland
Haldon Hill	Partly closed	219	Coastal
Tuelldown	Partly closed	205	Inland

In attempting to produce general predictions for whole forecast periods, care should be taken not to overlook the original and most important aim:- the accuracy of predicted frost onset time.

The air temperature algorithm should not be used in operational circumstances if it is suspected of reducing the accuracy of predicted surface freezing time, even if the algorithm is likely to improve surface temperature predictions generally throughout a model run. There are exceptions to this rule, for instance whenever precipitation might occur due to cloud build-up from the east. An accurate surface temperature prediction curve would indicate likelihood of snow settling and freezing rain.

6.4.4 Algorithm summary

For the following scenario, the process below should be used to produce reliable forecasts of the likelihood of icy conditions for a road surface in Devon.

Scenario:-

Frontal cloud moving westwards into Devon from Dorset and Somerset before dissipating, giving an illusion of eastward movement. Cold air advection occurring due to east or northeast surface flow over Devon.

Algorithm:-

1. Ascertain general cloud movement to produce cloud forecast for Devon. Most important period is of cloud cover change.

2. Estimate surface geostrophic wind for forecast period from charts of surface pressure available over the Internet (see Appendix 4) using the **geostrophic wind equation** (6.2.5.2)

3. In the event of east or northeasterly 2m air flow, air temperature input for Roadsurf for the forecast period should be estimated only up to start of cloud build-up for coastal regions. Thereafter, air temperature should be held constant except during clear sky occasions.

4. Run Roadsurf using parameters from stages **1.**,**2.** and **3.** Frost onset times from Roadsurf are likely to be predicted up to an hour late, so modify predicted time to an hour earlier. An earlier than predicted frost onset time is more beneficial in an operational situation, particularly if precipitation is nil.

5. Re-run Roadsurf during forecast period using observations as they become available. Remember to keep air temperature input fixed during cloud increase as in stage **3**.

6.5 February 6th/7th 1996

Scenario:- Frontal cloud moving eastwards into anticyclonic cold air over Eastern England

6.5.1 Summary of cloud cover and synoptic conditions of February 6th/7th 1996.

Figures 6.5.1.1a and b show that a weak occluded front moved eastwards over Eastern England and into the North Sea between 1200 UTC Feb. 6th and 1200 UTC Feb. 7th.

A surface low pressure system 500 ±50 km west of Eire moved south-eastward with two associated fronts, one cold and one warm which introduced extensive medium level cloud into Devon from 2200 UTC Feb. 6th, shown by NOAA infrared satellite imagery in Figures 6.5.1.2a to e, though this time varied by an hour depending on location within Devon. Sporadic, mostly light precipitation occurred after 0500 UTC Feb. 7th at Roborough, West Country Inn and Whiddon Down, but not at Ashmill and Stopgate Cross. According to sensors, roads were wet throughout Feb. 6th and 7th due to salt deposits from gritting operations.

Table 6.5.1.1 Flow at 2m from sensors at three Devon County Council road weather stations from 1200 UTC Feb. 6th 1996.

	Sourton Cross	Haldon Hill	Ashmill
1200 to 1759 UTC Feb. 6th	3.9 ms^{-1} ↘	4.4 ms^{-1} ↘	3.9 ms^{-1} ←
1800 to 2359 UTC Feb. 6th	no data available	2.6 ms^{-1} ↘	1.0 ms^{-1} ↙
0000 to 0559 UTC Feb. 7th	3.2 ms^{-1} ↖	1.2 ms^{-1} variable	0.9 ms^{-1} ↓
0600 to 1159 UTC Feb. 7th	8.5 ms^{-1} ←	3.5 ms^{-1} ↖	4.8 ms^{-1} ↙

From Table 6.5.1.1, the 2 metre air flow at 0000 UTC Feb. 7th was light with a direction dependent on location relative to the low pressure centre. The centre passed through Devon between 0000 and 1200 UTC Feb. 7th shown in Figure 6.5.1.1

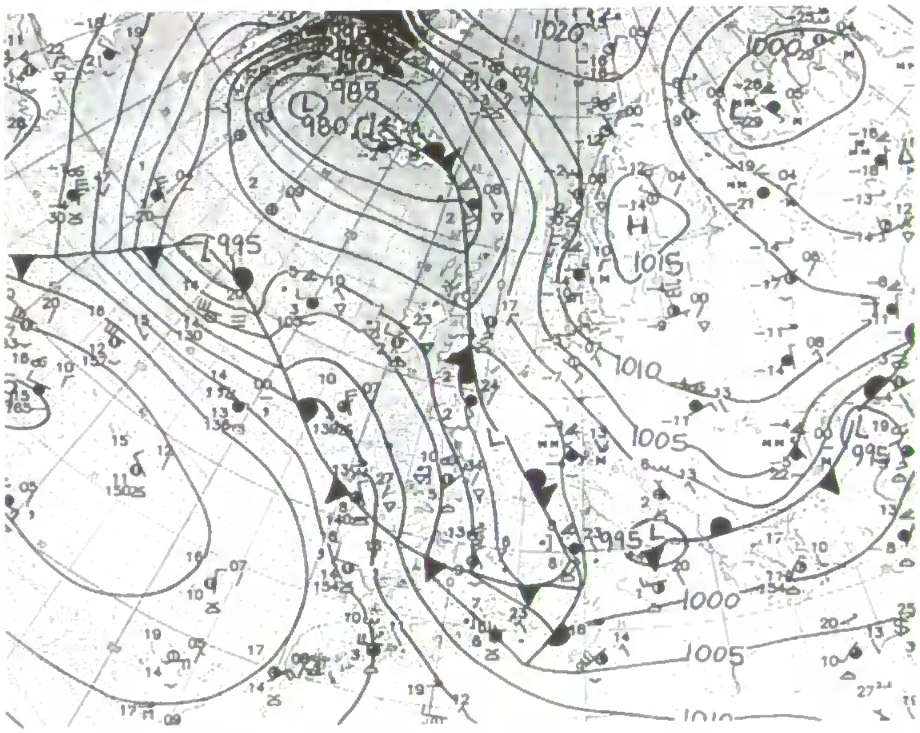

a. 1200 UTC Feb. 6th 1996

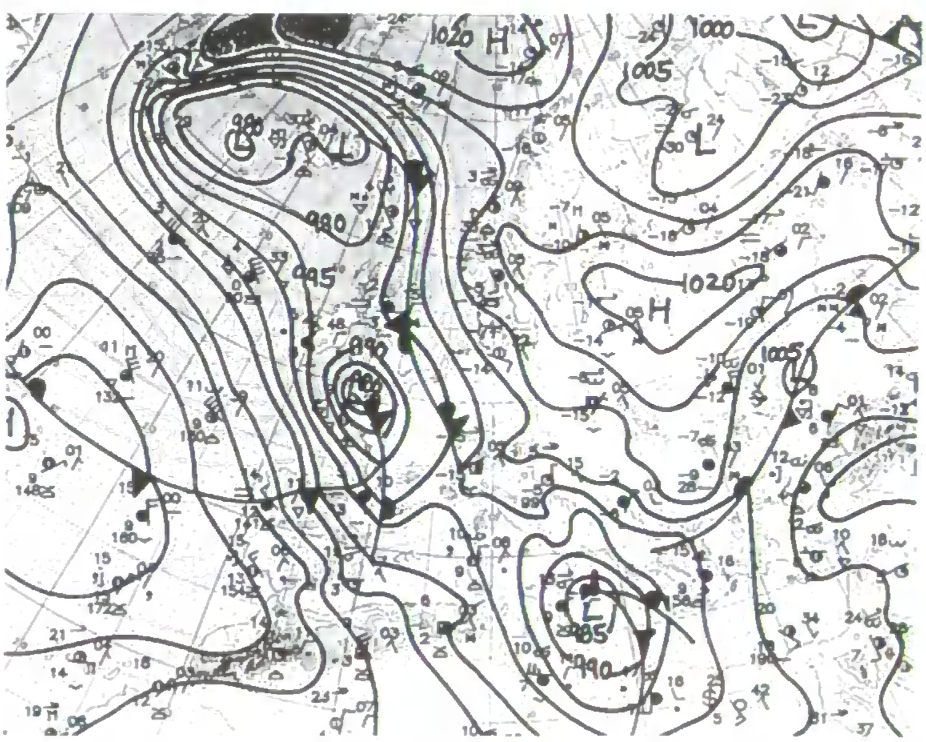

b. 1200 UTC Feb. 7th 1996

Figure 6.5.1.1 European Meteorological Bulletin surface analyses

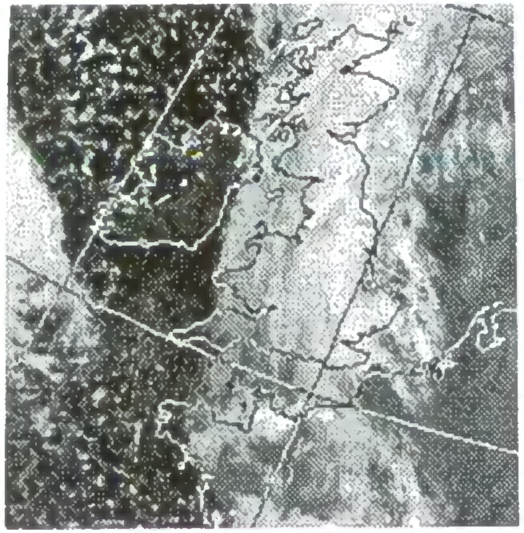

a. 1238 UTC Feb. 6th 1996

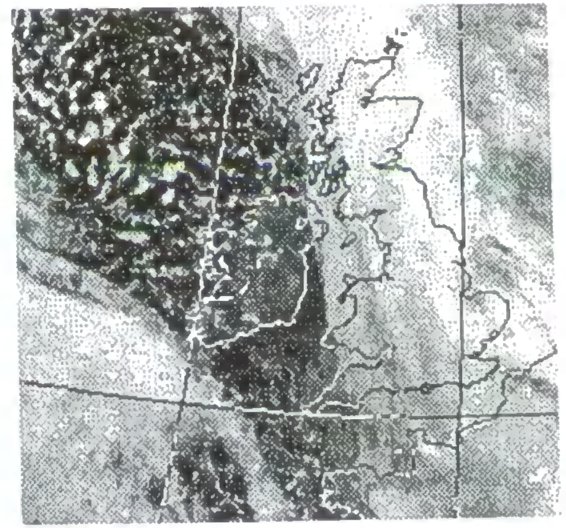

b. 1419 UTC Feb. 6th 1996

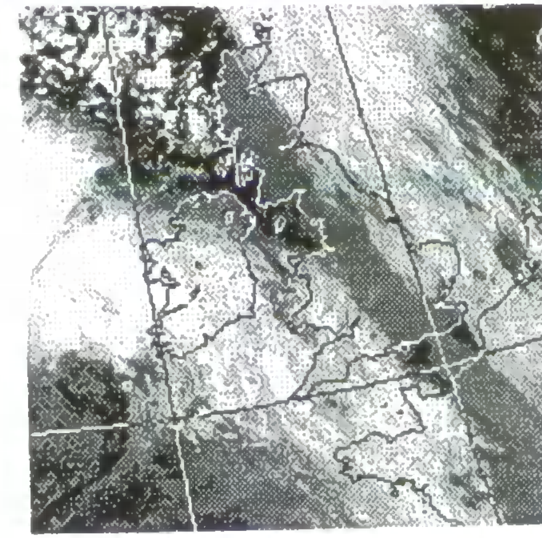

c. 0233 UTC Feb. 7th 1996

d. 0413 UTC Feb. 7th 1996

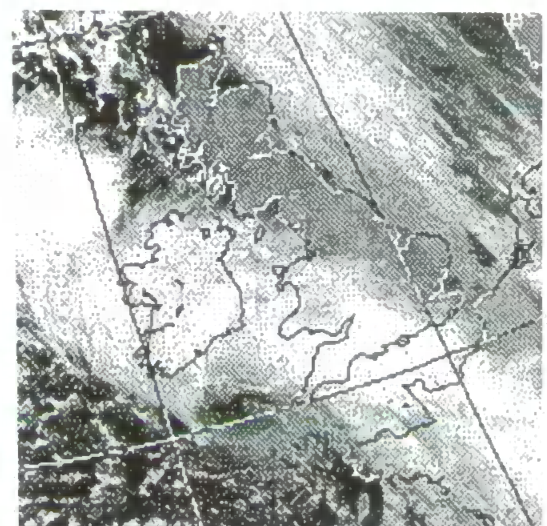

e. 0813 UTC Feb. 7th 1996

Figure 6.5.1.2 NOAA infrared satellite images from Feb. 6th and 7th 1996

6.5.2 Initial Roadsurf predictions.

Roborough, Sourton Cross, Haldon Hill, Ashmill and Stopgate Cross were chosen to be the forecast stations due to their even spread across Devon, in a hope that effects on temperature due to cloud movement could be easily observed. Table 6.5.2.1 shows input parameters for Roadsurf for the initial set of runs, whose results are shown by Table 6.5.2.2 and Figures 6.5.2.1.

Table 6.5.2.1 Major inputs for Roadsurf between 1200 UTC Feb. 6th and 1200 UTC Feb. 7th 1996

Parameter (Times in UTC)	Roborough	Sourton Cross	Haldon Hill	Ashmill	Stopgate Cross
Air temperature /°C					
1200-1759 Feb. 6th	4.9	3.0	2.7	2.9	0.4
1800-2359 Feb. 6th	2.6	2.0	2.0	1.0	1.4
0000-0559 Feb. 7th	1.8	2.1	1.2	-0.8	0.8
0600-1159 Feb. 7th	2.6	1.6	2.1	1.9	0.7
Ts at 1200 Feb. 6th /°C	4.5	3.0	4.0	4.0	2.1
Td at 1200 Feb. 6th /°C	3.7	2.8	3.5	3.5	2.0
Tcl at 1200 Feb. 6th /°C	3.0	2.7	2.7	2.7	1.8
Windspeed /ms^{-1}					
1200-1759 Feb. 6th	4.0	4.0	4.4	4.0	4.4
1800-2359 Feb. 6th	1.0	2.1	2.7	1.0	2.7
0000-0559 Feb. 7th	0.9	3.2	0.7	0.9	0.7
0600-1159 Feb. 7th	4.8	8.5	3.3	4.8	3.3
DWB/ deg. C	2.0	2.2	0.8	0.9	0.6
Surface state	Wet (SRHF=1.0) at all stations				
Cloud cover in oktas					
1200-1459 Feb. 6th	1/8 Low	1 Low	Clear	Clear	Clear
1500-1759 Feb. 6th	Clear	Clear	Clear	Clear	Clear
1800-2059 Feb. 6th	6/8 Low	6/8 Low	2/8 Low	Clear	Clear
2100-2359 Feb. 6th	8/8 Med	8/8 Med	5/8 Med	3/8 Med	3/8 Med
0000-0259 Feb. 7th	8/8 Med	8/8 Med	8/8 Med	8/8 Med	8/8 Med

Notes for table :-

Ts: road surface temperature,

Td: 'd' layer temperature (immediately below surface),

Tcl: 'cl' layer temperature (immediately below 'd' layer),

Low: low level cloud,

Med: medium level cloud,

DWB: depression of wet bulb temperature,

SRHF: parameter used in model to depict surface wetness, observed by road surface sensor at station (1 for wet surfaces, 0 for dry),

Cloud cover between 0259 and 1200 UTC Feb. 7th was set as 8 oktas, medium level.

Table 6.5.2.2 Specific Roadsurf predictions from initial run between 1200 UTC Feb. 6th and 1200 UTC Feb. 7th 1996.

Station	Frost onset time			Minimum temperature		
	Prediction /UTC	Actual /UTC	Error	Prediction /°C	Actual /°C	Error /deg.C
Roborough	2240	none	-	-1.7	+1.6	+3.3
Sourton Cross	2300	1900	4hrs 00min late	0.00	-1.5	-1.5
Haldon Hill	2030	1935	55min late	-1.9	-1.5	+0.4
Ashmill	1840	1930	50min early	-3.5	-2.6	+0.9
Stopgate Cross	1555	1900	3hrs 5min early	-2.5	-3.0	-0.5

Roadsurf predicted frost onset times at Sourton and Stopgate Cross (Table 6.5.2.2) 4 hours too late and 3 hours too early at the two stations respectively, inadequate in operational situations. At Roborough, frost was forecast for 2240 UTC Feb. 6th, which never occurred! The large variations in predicted frost onset times between Sourton and Stopgate Cross were due to the differing cloud input into Roadsurf shown in Table 6.5.2.1. Cloud increase at Sourton presumed to occur between 1700 and 1900 UTC was 3 to 4

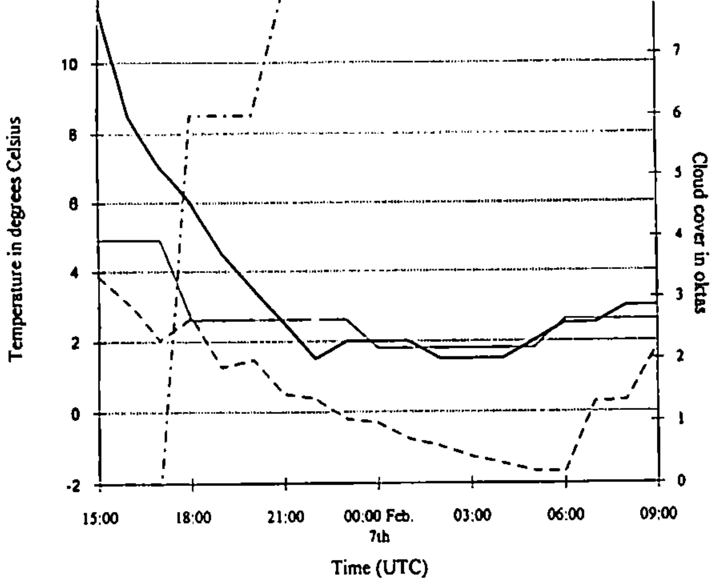

a. Roborough

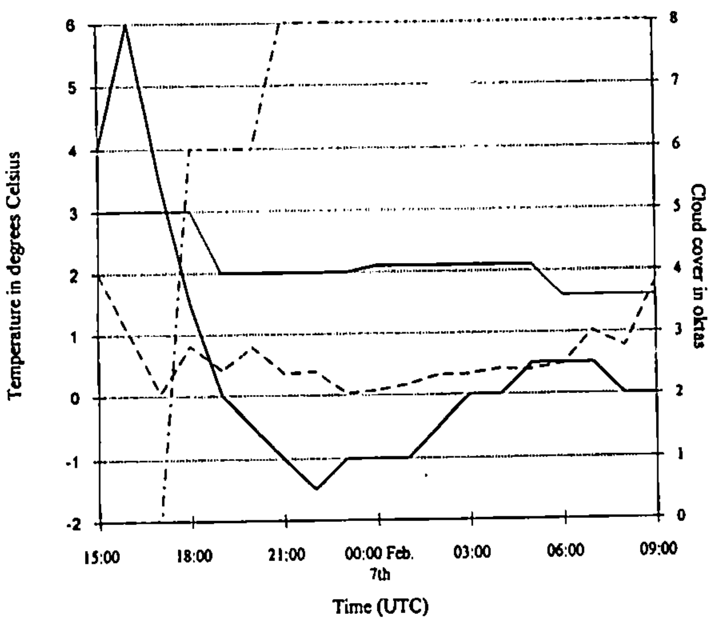

b. Sourton Cross

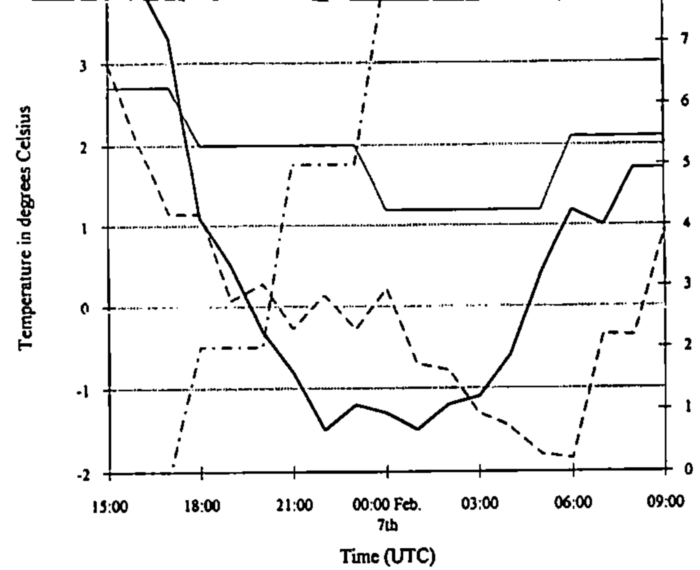

c. Haldon Hill

Observed air temperature used by Roadsurf

Observed road surface temperature

Predicted Roadsurf surface temperature

Observed cloud cover (right hand scale)

Probable cloud cover (right hand scale) derived by back tracking cloud movement from post 0000 UTC Feb. 7th satellite imagery

Figure 6.5.2.1 Evolution of conditions from 1500 UTC Feb. 6th to 0900 UTC Feb. 7th 1996

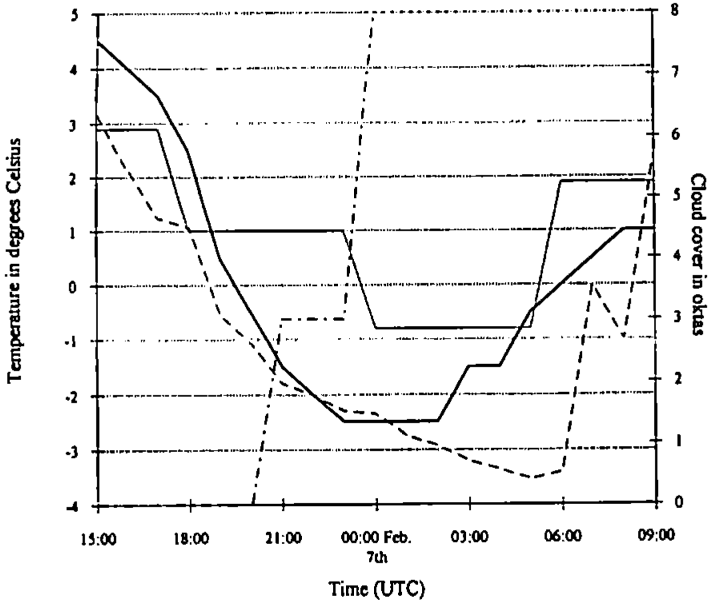

d. Ashmill

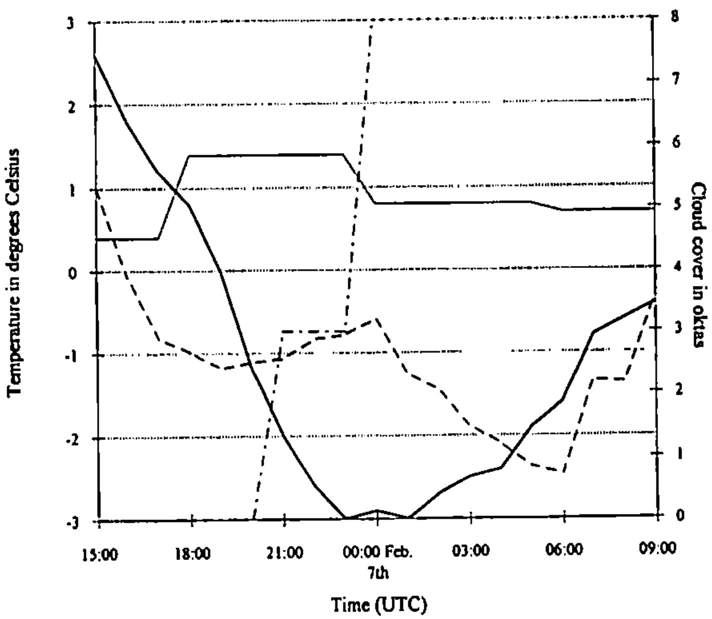

e. Stopgate Cross

Observed air temperature used by Roadsurf

Observed road surface temperature

Predicted Roadsurf surface temperature

Observed cloud cover (right hand scale)

Probable cloud cover (right hand scale) derived by back tracking cloud movement from post 0000 UTC Feb. 7th satellite imagery

Figure 6.5.2.1 Evolution of conditions from 1500 UTC Feb. 6th to 0900 UTC Feb. 7th 1996 hours earlier than a similar cloud increase at Stopgate Cross. Unfortunately, NOAA satellite imagery was only available from 1400 UTC Feb. 6th, 0200 UTC Feb. 7th and 0400 UTC imagery. Cloud cover from 1600 UTC to 2359 UTC Feb. 6th had to be ascertained by back tracking a warm front straddling Southwest England using the NOAA infrared imagery of 0233 UTC and 0413 UTC Feb. 7th. This process did not pose any significant problems since the front had a well defined front edge at 0233 UTC Feb. 7th.

Roadsurf predictions for Ashmill were however surprising. Cloud parameters used by Roadsurf were identical to those used for Stopgate Cross but only a 50 minute error occurred in frost onset prediction, 150 minutes shorter than at Stopgate Cross. This was probably due to a difference in exposure between the two stations which was also true for Haldon Hill and Sourton Cross which are partly closed and open respectively. Roadsurf frost onset time predictions before 2200 UTC for partly closed sites were more accurate than for sites which are open.

Thus Roadsurf appeared to have certain prediction problems unique to Stopgate Cross due to factors other than inaccurate cloud cover. It is significant that of the road surfaces at the five locations studied, Stopgate Cross was coolest at the start of the forecast period (1200 UTC Feb. 6th). This lower initial temperature was responsible for the early frost onset time at Stopgate Cross.

Even though Roadsurf poorly predicted the frost onset time for Stopgate Cross, it *did* manage to predict minimum surface temperature to within 0.5 deg C of the observed value.

Notable Roadsurf performances shown best by Figures 6.5.2.1a to e:-

i. Colder surface temperature predictions than observed at Roborough and Stopgate Cross after 0200 UTC Feb. 7th.

ii. Occasions of opposite trends between predicted and observed surface temperature. For example a predicted cooling from 0000 UTC Feb. 7th at Haldon Hill whereas observations showed surface warming. Roadsurf performance during this phenomenon at Haldon Hill was thus unacceptable.

Unfortunately, as in some other case studies, a lack of NOAA satellite imagery from certain periods of a model run increased inaccuracy of cloud cover inputs, distorting model output.

Backtracking however, of cloud from NOAA imagery at 0233 UTC and 0413 UTC Feb. 7th was not difficult at first since the cloud's forward edge was well defined. Misjudgements in timing of cloud build-up would have occurred if cloud movement was not constant throughout the tracked period of 1200 UTC to 2359 UTC Feb. 6th.

Use of geopotential height charts for flow determination.

Analyses of geopotential height at 850 and 500 millibars at 1200 UTC Feb. 6th (Figures 6.5.2.2a and b) show north-westerly flow at both levels but from the cloud track, cloud was assumed to have been moving from a purely westerly direction, *not* north-westerly. Thus a northerly component in cloud movement at 850 and 500 mb might have also occured.

Furthermore, radiosonde data above Camborne, Cornwall at 1200 UTC Feb. 6th (Figure 6.5.2.3a) reported north-westerly winds of 20 ms^{-1} at 850 mb. The observed wind at 850 mb twenty-four hours later (Figure 6.5.2.3b) had veered easterly and moderated to 5 ms^{-1}. Hence eastward movement across England of cloud cover would have slowed, so inaccuracies in cloud inputs used in Roadsurf in this case study were increasingly large the earlier the time.

The unfortunate results from this case study show errors which can arise during cloud tracking exercises, be it back tracking retrospectively or forward tracking.

A reassessment of cloud cover at each site was needed.

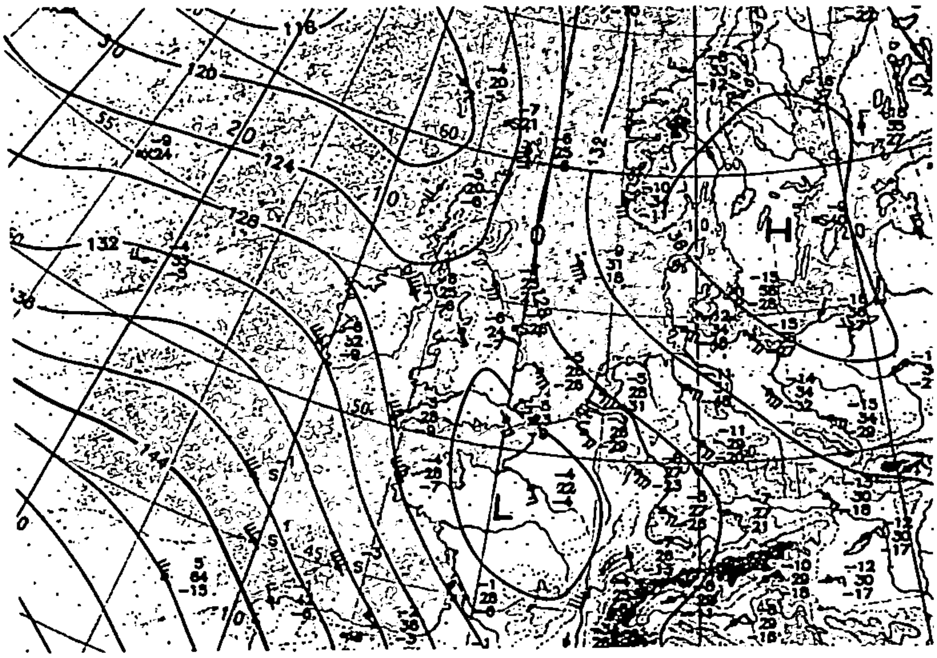

a. 850 mb level

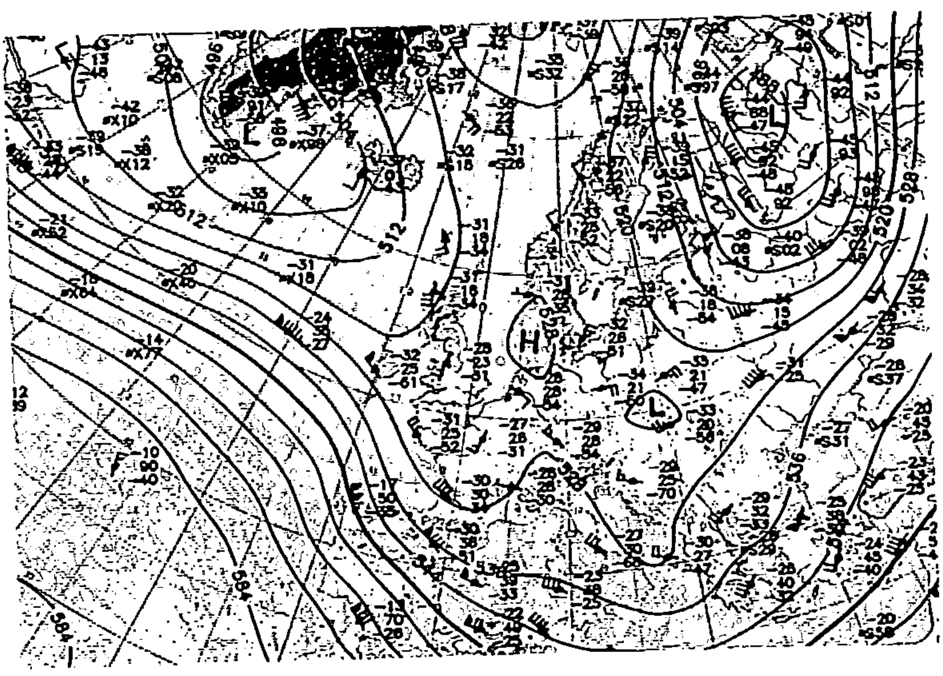

b. 500 mb level

Figure 6.5.2.2 European Meteorological Bulletin geopotential height analyses from 1200 UTC Feb. 6th 1996

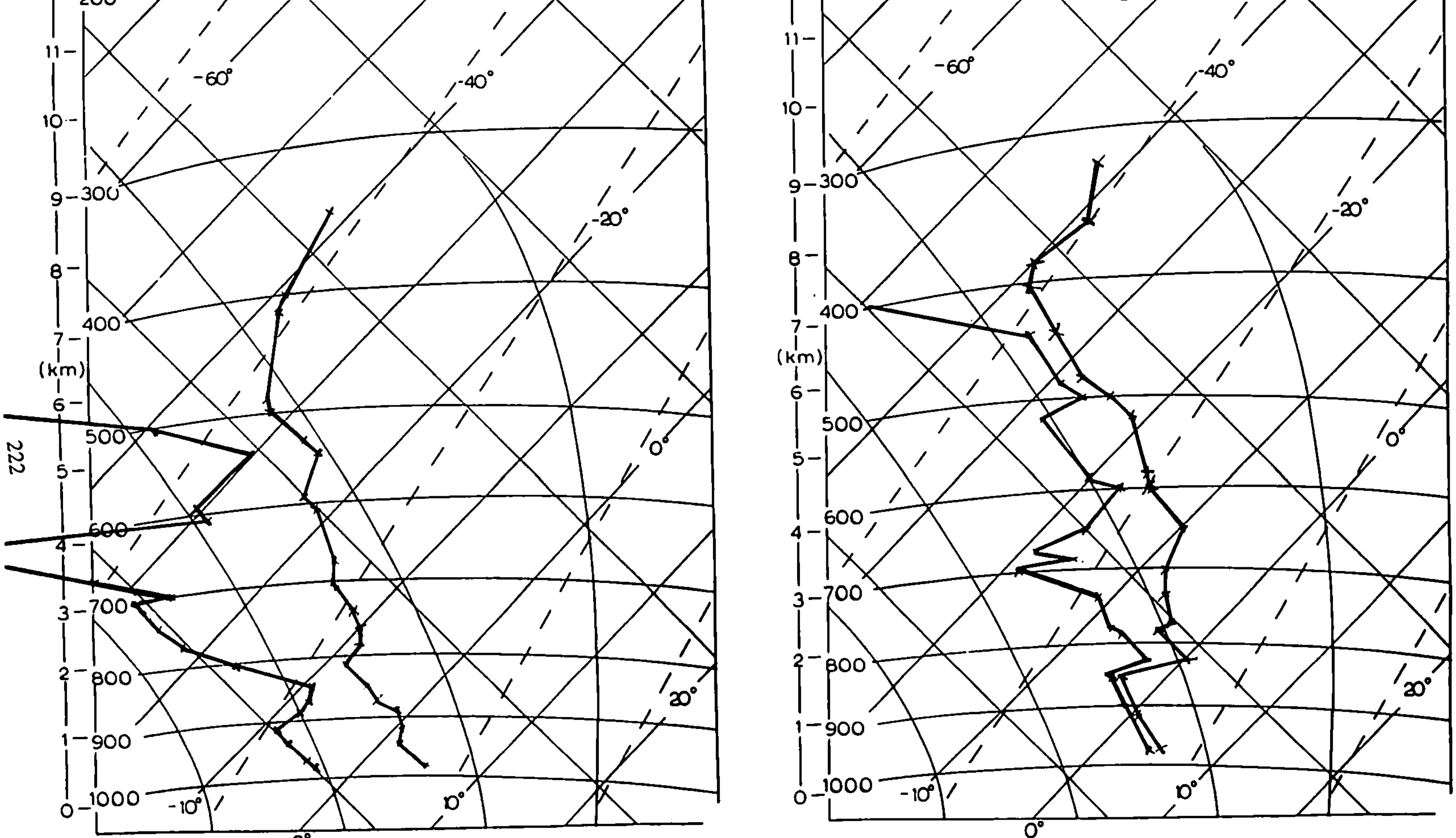

a. 1200 UTC Feb. 6th 1996

b. 1200 UTC Feb. 7th 1996

Figure 6.5.2.3 Radiosonde ascents over Camborne, Cornwall.

6.5.3 Reassessment of cloud

Table 6.5.3.1a and b show large differences between flow speeds obtained from radiosonde data and those calculated using geopotential height and surface analyses at 1200 UTC Feb. 6th and 7th. This is partly due to the fact that radiosonde data were from Camborne at 5°W 51°N whereas wind velocities from the analyses were from 10°W 50°N. The **geopotential height** analyses show significantly faster geostrophic flow (calculated using Equation 6.2.5.1) at 500 mb at 1200 UTC Feb. 6th than at 1200 UTC Feb. 7th, indicating that movement of cloud at this level would probably have slowed as it passed over England.

Table 6.5.3.1a Observed flow at 1200 UTC Feb. 6th 1996

From radiosonde ascent at Camborne			From gph and surface analyses, at 10°W 50°N		
Level	Wind speed / ms^{-1}	Wind direction	Level	Geostrophic wind speed / ms^{-1}	Wind direction
500 mb	5	→	500 mb	25	↘
850 mb	20	↘	850 mb	20	↘
surface	10	↘	surface	10	↘

Table 6.5.3.1b Observed flow at 1200 UTC Feb. 7th 1996

From radiosonde ascent at Camborne			From gph and surface analyses, at 10°W 50°N		
Level	Wind speed / ms^{-1}	Wind direction	Level	Geostrophic wind speed / ms^{-1}	Wind direction
500 mb	10	↓	500 mb	10	↘
850 mb	5	←	850 mb	25	↘
surface	15	←	surface	25	↘*

Note:

gph = geopotential height,

* = wind direction at 1200 UTC Feb. 7th at surface level was not ↘ over the **whole** of Cornwall due to depression centre situated over the county at the time.

Radiosonde data were only available from 1200 UTC Feb. 6th and 7th. The 1200 UTC Feb. 7th ascent showed likely conditions for cloud from the surface to 850 mb, and from 550 mb to 450 mb. The presence of two layers would cause problems for Roadsurf since the lower cloud has the greatest influence on the thermal radiation emitted from the Earth's surface. Roadsurf was ran on an assumption that the only cloud present was of medium level determined from NOAA satellite imagery.

Since air flow velocity at 500 mb was different to that at 850 mb, it can be assumed that cloud at these two levels would have moved **relative to one another**.

Roadsurf was re-run using the revised cloud in Table 6.5.3.2 with results shown by Figures 6.5.3.1a to e.

Table 6.5.3.2 Revised cloud used for 1200 UTC Feb. 6th to 1200 UTC Feb. 7th 1996 Roadsurf re-run.

<table>
<tr><th>Parameter
(Times in UTC)</th><th>Roborough</th><th>Sourton Cross</th><th>Haldon Hill</th><th>Ashmill</th><th>Stopgate
Cross</th></tr>
<tr><td>1200-1459 Feb. 6th</td><td>4/8 Med</td><td rowspan="4">Same as
in
previous
run</td><td>6/8 Med</td><td rowspan="4">Same
as
Haldon
Hill</td><td>8/8 Med</td></tr>
<tr><td>1500-1759 Feb. 6th</td><td>4/8 Med</td><td>4/8 Med</td><td>7/8 Med</td></tr>
<tr><td>1800-2059 Feb. 6th</td><td>8/8 Med</td><td>5/8 Med</td><td>5/8 Med</td></tr>
<tr><td>2100-2359 Feb. 6th</td><td>8/8 Low</td><td>8/8 Low</td><td>7/8 Low</td></tr>
<tr><td>0000-0259 Feb. 7th</td><td colspan="5" rowspan="4">Same as in previous runs of this case study date for all stations
between 0000 and 1200 UTC Feb. 7th 1996</td></tr>
<tr><td>0300-0559 Feb. 7th</td></tr>
<tr><td>0600-0859 Feb. 7th</td></tr>
<tr><td>0900-1159 Feb. 7th</td></tr>
</table>

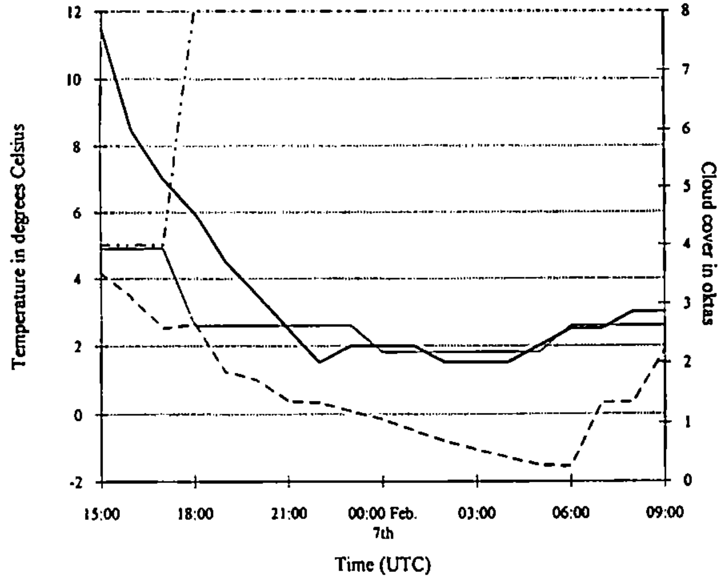

a. Roborough

- Observed air temperature used by Roadsurf
- Observed road surface temperature
- Predicted Roadsurf surface temperature using revised and observed cloud
- Observed cloud cover (right hand scale)
- Revised cloud cover (right hand scale) resulting from multi level flow discussion

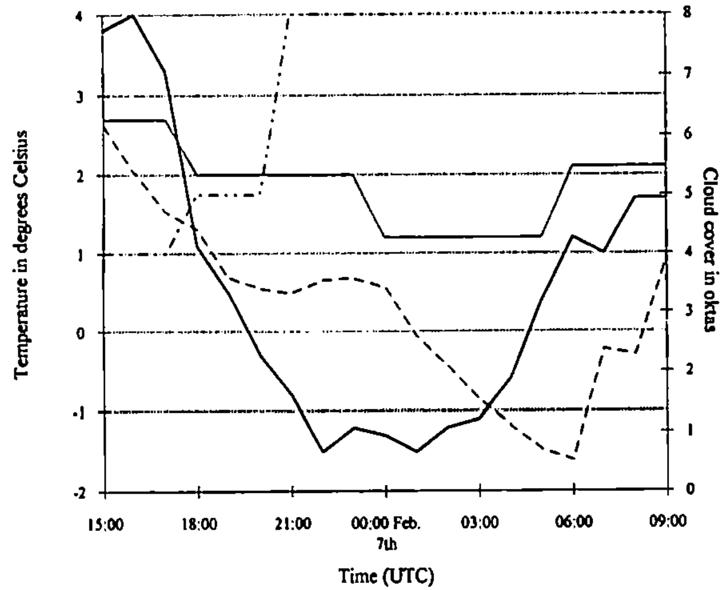

c. Haldon Hill

Figure 6.5.3.1 Evolution of conditions from 1500 UTC Feb. 6th to 0900 UTC Feb. 7th 1996.
(Using revised cloud cover for Roadsurf).

(No Sourton Cross graph since cloud cover was not revised at this location)

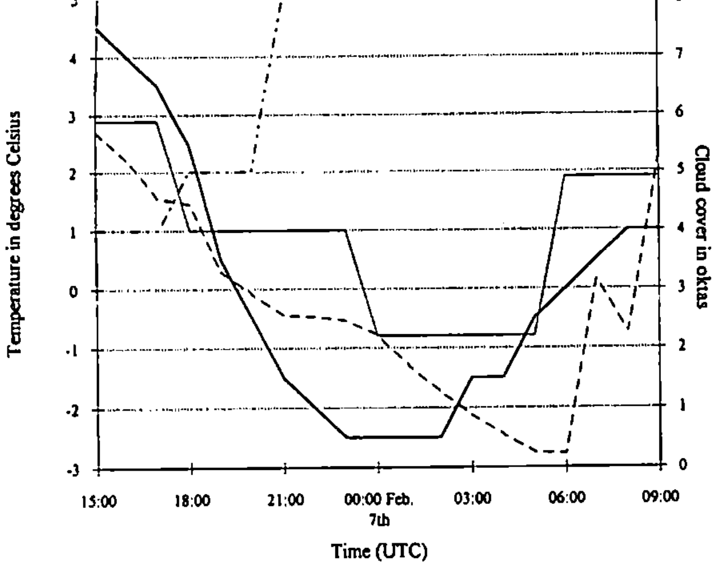

d. Ashmill

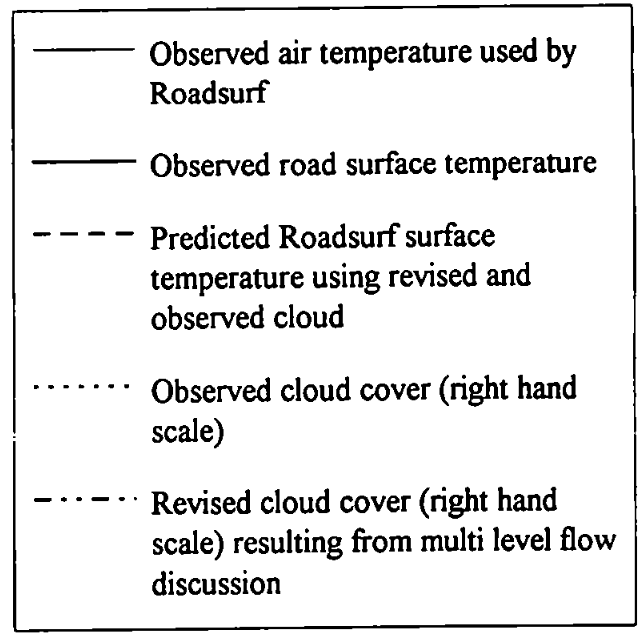

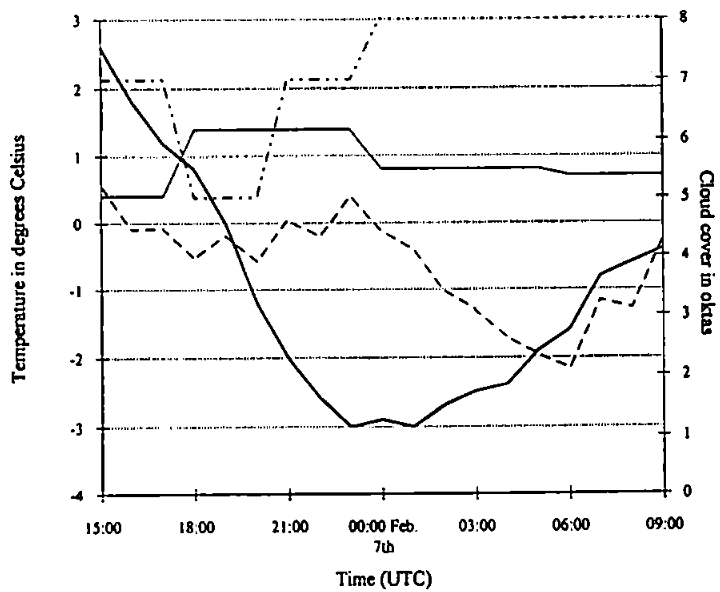

e. Stopgate Cross

Figure 6 .5.3.1 Evolution of conditions from 1500 UTC Feb. 6th to 0900 UTC Feb. 7th 1996. (Using revised cloud cover for Roadsurf).

The re-run produced slightly improved frost onset time predictions at Ashmill and Stopgate Cross, but general surface temperature predictions were still disappointing, with no significant improvement compared to previous runs. This was due to negative air temperature tendencies which occurred for 5 hours before 0000 UTC Feb. 7th. Roadsurf exhibited a timelag of too long a duration between start of air warming due to cloud and/or warm air advection, and termination of surface cooling. Hence any air temperature fall resulted in surface cooling which continued for a further six hours. The effect from this phenomenon was greater than suppression of surface cooling caused by cloud cover formation. Because of this timelag, warm air advection at Roborough, Haldon Hill and Ashmill after 0200 UTC Feb. 7th was not apparent in surface temperature fields until 0600 UTC (Figures 6.5.3.1a, c and d). In an algorithm for this scenario, the lag must be shortened.

Reasons for lag.

As already discussed elsewhere in this thesis, Roadsurf relies on accurate air temperature inputs to operate successfully. However, in all runs, these inputs have always been held constant for 6 hour intervals and for runs of Feb. 6th and 7th, were of air temperatures averaged over 6 hour periods. Thus atmospheric warming and cooling at 2m, similar in magnitude and occurring within the same 6 hour period, for example 0000 to 0600 UTC, would have been smoothed by the averaging process. Hence if a cooler than previous air temperature is introduced to Roadsurf at the beginning of a 6 hour period, cooling at the surface is likely to occur which will continue until the following updated air temperature input 6 hours later. This possibly caused the apparent timelag of five hours discussed above. Use of hourly updated inputs of air temperature would hopefully improve prediction accuracy. This is not feasible in an operational situation since the air temperature itself must also be predicted. Inputting air temperatures every hour is also time consuming when it needs to be done for several sites.

6.5.4 Roadsurf modification, to predict air temperature

A new method of air temperature input into Roadsurf was proposed:-

1) Input initial observed air temperature,
2) Input expected (or observed if model run is retrospective) **trends** into Roadsurf.

Roadsurf would therefore be able to calculate air temperatures itself using the trends added by the user. Necessary modifications were thus made to Roadsurf producing a new version of the model:- Roadsurf 2.

General performance of Roadsurf 2 using the air temperature trends shown in Table 6.5.4.1 was an improvement over that of its predecessor at Ashmill and Sourton Cross but was still generally unacceptable at Stopgate Cross, Roborough and Haldon Hill (see Table 6.5.4.2). A timelag still occurred between air temperature and predicted surface temperature, 4 hours longer than that shown by *observations* of surface temperature. Surface temperature response to changes in cloud cover was still too late as Figures 6.5.4.1a, c and e clearly show.

Table 6.5.4.1 Air temperature trends used by Roadsurf 2 from 1200 UTC Feb. 6th to 1159 UTC Feb. 7th 1996.

	Air temperature trends used: (deg. C change per hour)			
	1200-1759 UTC Feb. 6th	1800-2359 UTC Feb. 6th	0000-0559 UTC Feb. 7th	0600-1159 UTC Feb. 7th
Roborough	+0.08	-0.50	+0.25	-0.25
Sourton Cross	+0.16	-0.16	0.00	-0.13
Haldon Hill	-0.02	-0.35	+0.43	+0.35
Ashmill	+0.16	-1.00	+0.75	-0.13
Stopgate Cross	+0.28	-0.22	0.00	+0.08

Table 6.5.4.2 Specific Roadsurf 2 results from 1200 UTC Feb. 6th to 1200 UTC Feb. 7th 1996.

Station	Frost onset time			Minimum temperature		
	Prediction /UTC	Actual /UTC	Error	Prediction /°C	Actual /°C	Error /deg.C
Roborough	2225	none	none	-2.2	+1.6	-3.8
Sourton Cross	2045	1900	1hr 45 mins late	-0.5	-1.5	+1.0
Haldon Hill	2230	1935	2hr 55 mins late	-1.8	-1.5	-0.3
Ashmill	2120	1930	1hr 50 mins late	-2.2	-2.6	+0.4
Stopgate Cross	2140	1900	2hr 40 mins late	-2.5	-3.0	+0.5

Table 6.5.4.3 Timelag between change in trend of observed and predicted surface temperature between 0000 and 0600 UTC Feb. 7th 1996.

Station	Timelag
Roborough	2 hours
Sourton Cross	1 hour
Haldon Hill	5 hours
Ashmill	1 hour
Stopgate Cross	5 hours

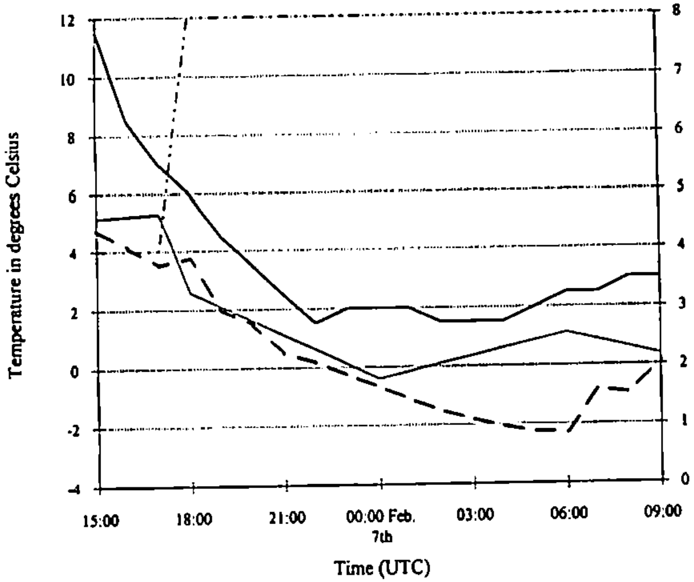

a. Roborough

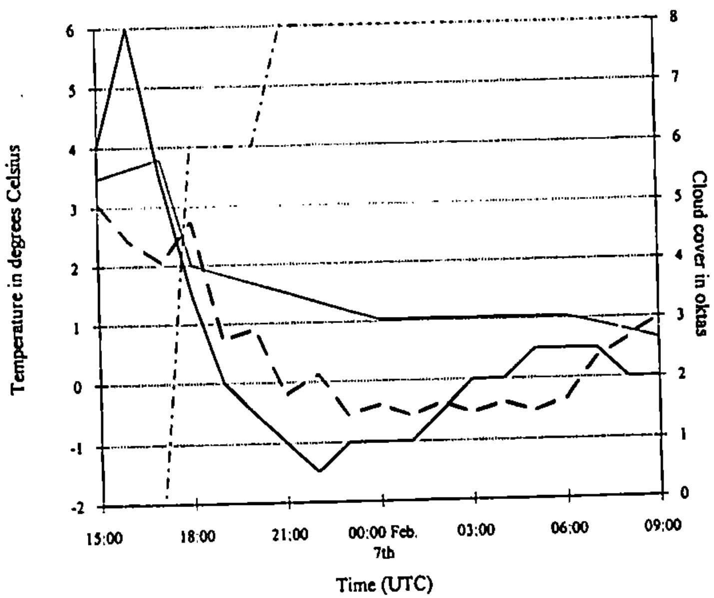

b. Sourton Cross

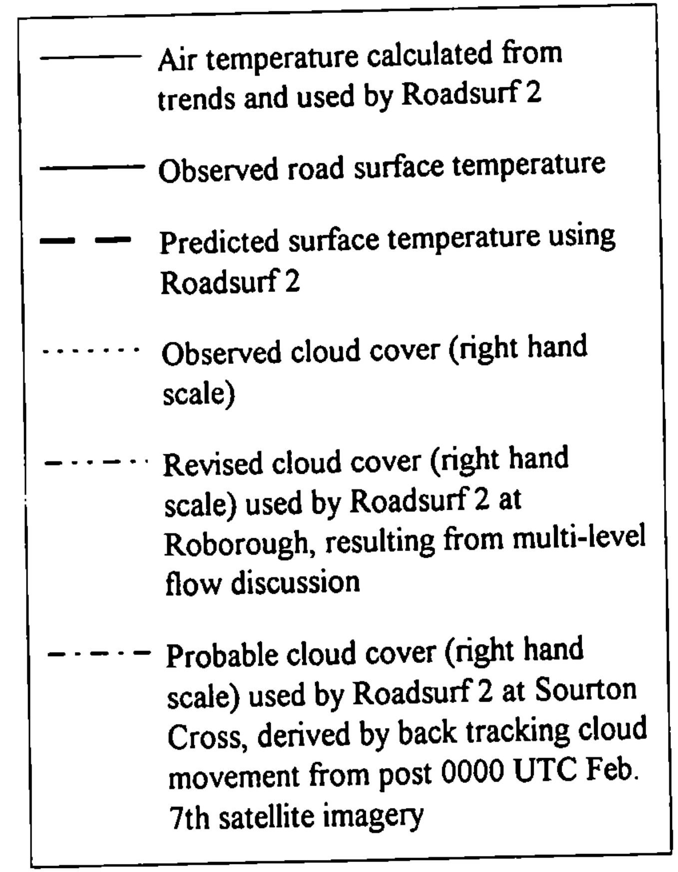

Figure 6.5.4.1 Evolution of conditions from 1500 UTC Feb. 6th to 0900 UTC Feb. 7th 1996 using Roadsurf 2.

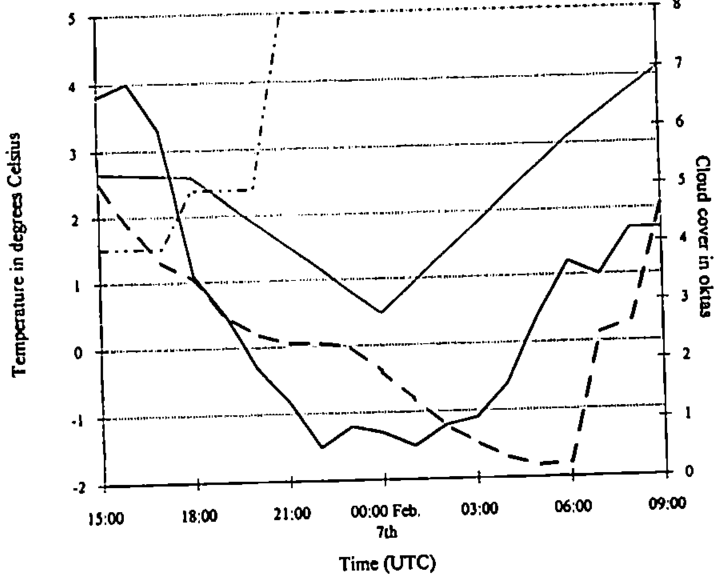

c. Haldon Hill

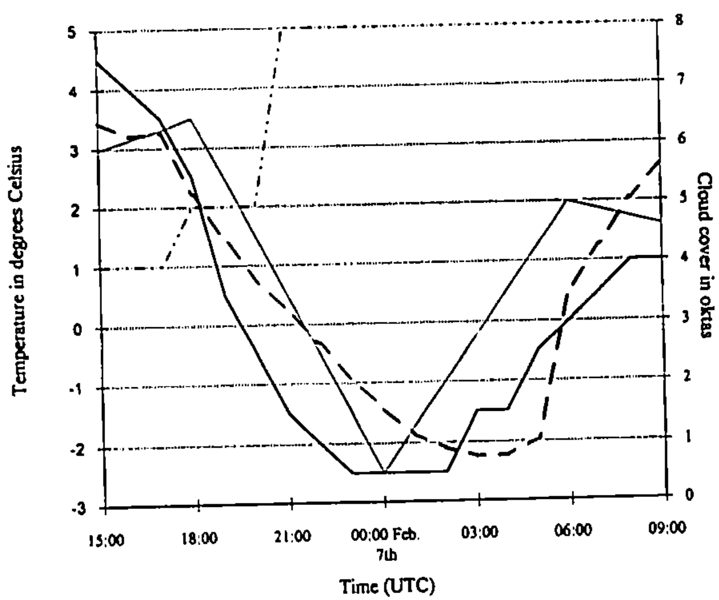

d. Ashmill

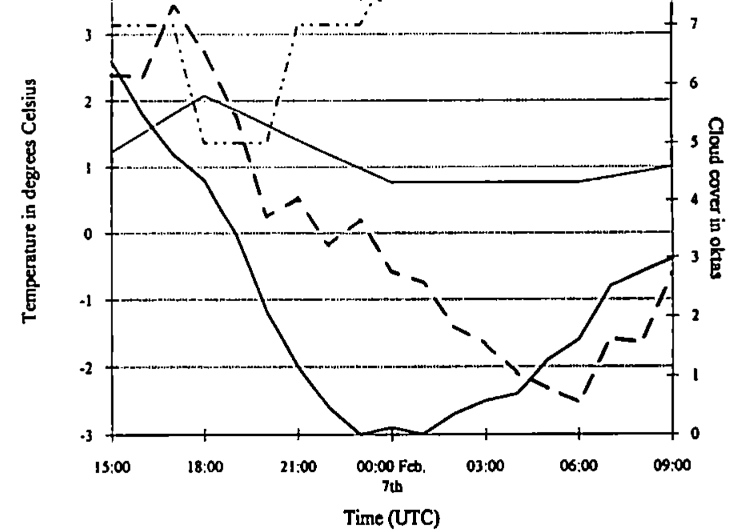

e. Stopgate Cross

Air temperature calculated from trends and used by Roadsurf 2

Observed road surface temperature

Predicted surface temperature using Roadsurf 2

Observed cloud cover (right hand scale) used by Roadsurf 2

Revised cloud cover (right hand scale) used by Roadsurf 2, resulting from multi-level flow discussion

Figure 6.5.4.1 Evolution of conditions from 1500 UTC Feb. 6th to 0900 UTC Feb. 7th 1996 using Roadsurf 2.

A major benefit of using Roadsurf 2 is its use in operational (real time) situations, since it only requires the user to input an initial (observed) air temperature and its trends instead of the requirement to calculate and input individual air temperatures. Good estimates of such trends can be made by a user with a limited meteorological knowledge gained from records.

With the exception at Roborough, Roadsurf 2 did not exhibit a cold bias, even though the surface temperature continued to fall for limited periods of cloud build-up.

The timelag resulted from the radiation lost to space not accurately calculated by the model. If cloud cover was accurate, the KCLOUD parameters used, the use of which is explained earlier in thesis, were not, which in conjunction with the multi-layer nature of cloud, reduced the ability of the Roadsurf models to handle the weather conditions of this particular occasion.

A multi-atmospheric layer version of Roadsurf would need to be developed to overcome the problems encountered in this case study. This would be required since the individual parameterizations of cloud (ALBEDO, DPUS and KCLOUD) have varying dependencies on cloud height.

6.5.5 Mesoscale model performances during February 6th and 7th 1996.

Predicted cloud cover and air temperatures from the UK Meteorological Office mesoscale model were analysed for four Devon sites.

The model encountered similar problems as the Roadsurf models with cloud cover, especially between 2200 UTC Feb. 6th and 0200 Feb. 7th when it predicted 5 okta cloud clearances over 2 hours late (see Figures 6.5.5.1 a to e).

The mesoscale model predicts air temperatures, not surface, though a surface temperature observation at 1200 UTC is an input parameter.

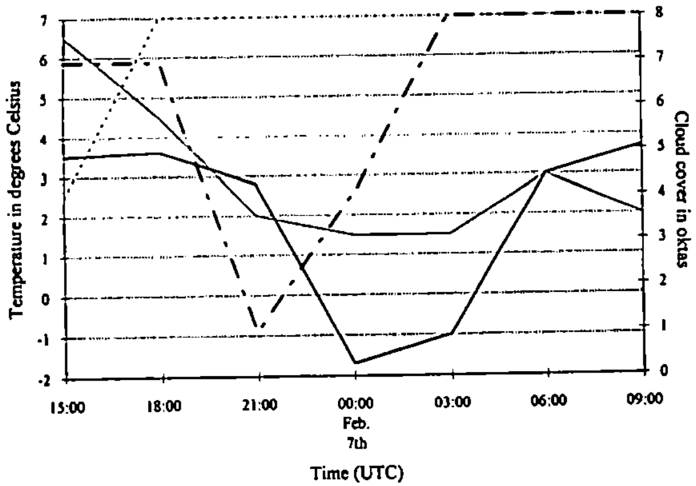

a. Roborough

Predicted air temperature from mesoscale model

Observed air temperature

Predicted cloud cover (right hand scale) from mesoscale model

Actual cloud cover (right hand scale)

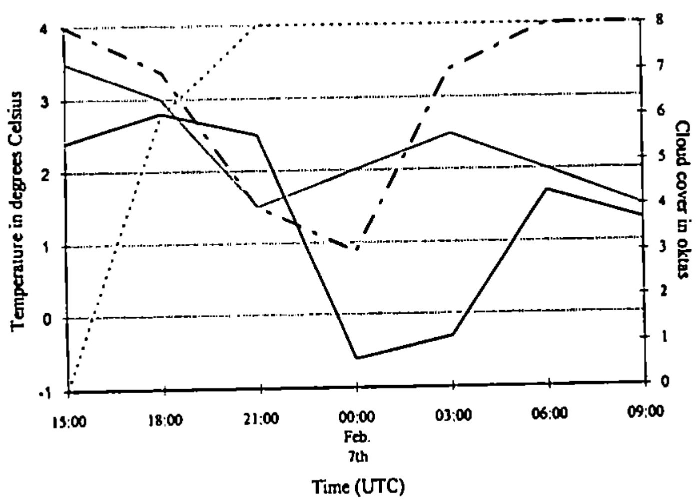

b. Sourton Cross

Figure 6.5.5.1 Observations and mesoscale model predictions from 1500 UTC Feb. 6th to 0900 UTC Feb. 7th 1996.

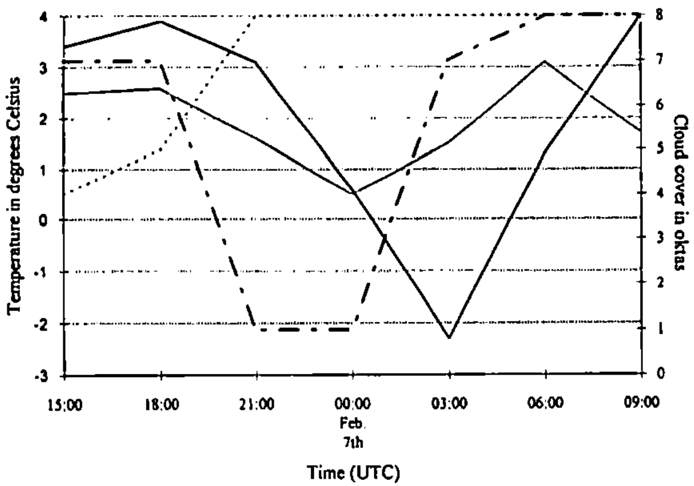

c. Haldon Hill

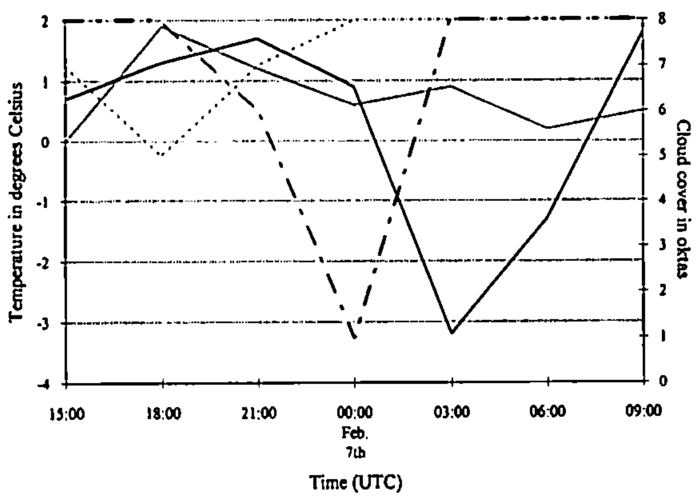

e. Stopgate Cross

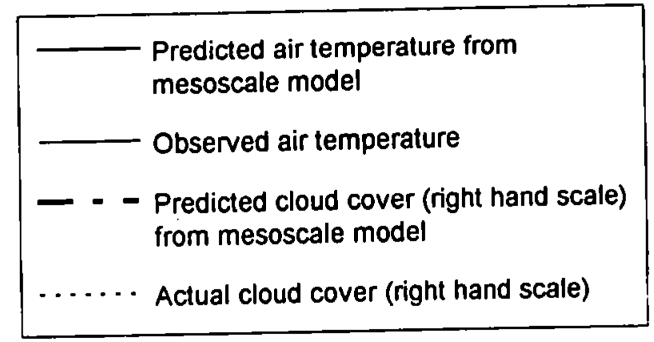

Figure 6.5.5.1 Observations and mesoscale model predictions from 1500 UTC Feb. 6th to 0900 UTC Feb. 7th 1996.

(No graph for Ashmill since mesoscale model is not run at this location)

Clear indicators of the model's performance of air temperature prediction were as follows:-

1) Predictions of air frost at Roborough, Haldon Hill, Sourton Cross and Stopgate Cross which never occurred.

2) Prediction time of air temperature decrease before 0000 UTC Feb. 7th in comparison with observations:-

Roborough: 3 hours late,

Sourton Cross: 3 hours late,

Stopgate Cross and Haldon Hill: no noticeable difference.

3) Prediction time of air temperature **increase** before 0000 UTC Feb. 7th in comparison with observations was 3 hours too early at all 4 stations studied (Roborough, Sourton Cross, Stopgate Cross and Haldon Hill).

The poor air prediction of the mesoscale model between 0000 and 0600 UTC Feb. 7th was due to underestimation of cloud build-up from the west. Consequently, Figures 6.5.5.2a and b show that the mesoscale model tended to predict far greater diurnal ranges of air temperature than observed.

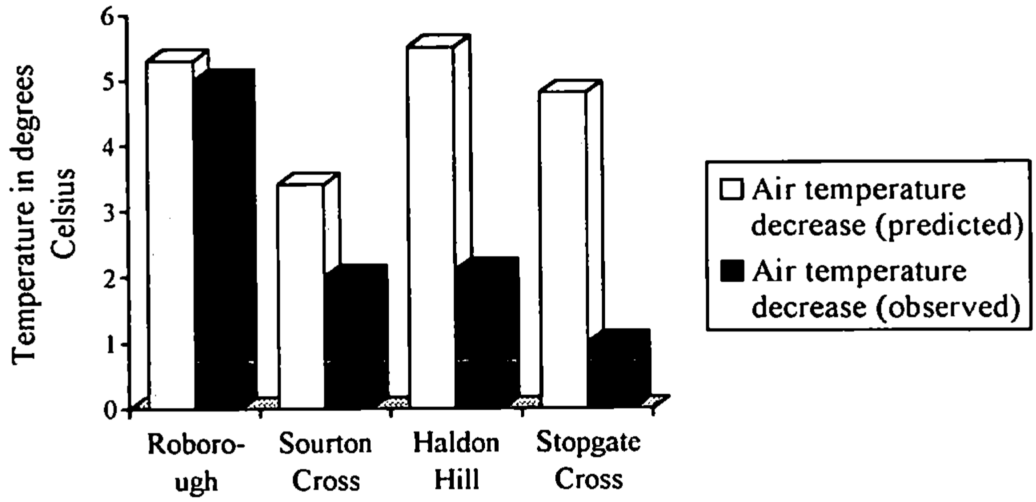

Figure 6.5.5.2a Mesoscale model results during air cooling between 1800 and 2359 UTC Feb. 6th due to cloud dispersement

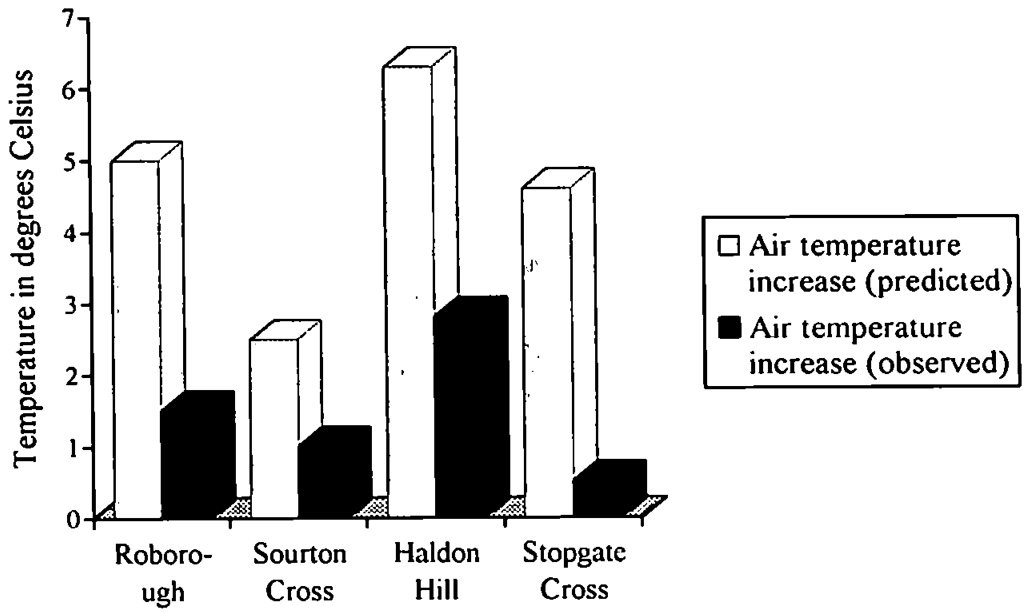

Figure 6.5.5.2b Mesoscale model results during air warming between 0000 and 0600 UTC Feb. 7th associated with cloud increase

The atmospheric thermodynamics of Feb. 6th and 7th were unusual due to deceleration of cloud approaching Devon and its multi-layer structure which rendered the mesoscale and Roadsurf models inaccurate at certain locations.

6.5.6 Algorithm summary

Scenario:-

Frontal cloud moving eastwards over Devon towards anticyclonic cold air over Eastern England.

Algorithm:-

1. Estimate cloud for forecast period using plane sailing method applied to cloud movement during the six hours preceding start of forecast period..

2. Predict air flow, if possible using forecast charts of surface pressure and geopotential height. If forecast charts are not available, charts from observations from the twelve hour period preceding start of forecast period can be used, by continuing any patterns observed whilst bearing in mind, that a front moving eastwards towards a blocking anticyclone over Eastern England will slow. Note possible veering of wind direction with height which would indicate horizontal extent of front, enabling cloud forecast from **1.** to be improved if necessary. As the case study showed, reassessment of cloud cover in this scenario is advised.

3. Estimate air temperature trends for six hourly periods of the forecast based on cloud cover and time of evening. Suitable averages, gleaned from hourly observations from the case study are shown in Table 6.5.6.1

Table 6.5.6.1 Suggested air temperature trends for Devon locations for a scenario of cloud cover increase between 1500 and 2100 UTC with anticyclonic air east of Devon during winter.

Time interval (UTC)	Air temperature trend (deg.C/hr)
1200-1759	+0.13
1800-2359	-0.45
0000-0559	+0.29
0600-1159	-0.17 at locations with less than 4 oktas of cloud, otherwise +0.22

4. Run Roadsurf 2 using the parameters obtained from parts **1.** **2.** and **3.** above. Roadsurf 2 frost onset prediction will probably be between 1 and 3 hours late depending on location and cloud cover increase rate.

It is unlikely that predictions of minimum surface temperature need to be modified.

6.6 Summary and conclusions from this chapter

- Most accurate forecasting methods comprise of a mixture of model and manual predictions. Updating boundary conditions for Roadsurf during an operational situation can be used if Roadsurf is performing badly.

- Variable acceptability of errors in Roadsurf predicted surface temperatures, dependent on predictand:- surface freezing onset time or minimum surface temperature.

Case study summaries:-

Nov. 18th/19th 1995 *Cloud forming in situ under settled anticyclonic conditions with wind speed not more than 1 ms^{-1}.*

- Problems arose due to foliage at Cross Farm, at a sensor which gave observations of a warmer surface than at nearby stations during hours of darkness.

- Changes in cloud cover with time were associated more with changes of air temperature than surface temperature, due to warm air advection towards Devon from the mild Atlantic. The phenomenon is not accounted for by Roadsurf unless observed air temperature inputs are added into the model throughout a run.

- Differences between Roadsurf predictions and observations increased with cloud increases which occurred before 0000 UTC and vice-versa afterwards at Haldon Hill, Roborough, Sourton Cross and Bratton Down. Roadsurf exhibited a cold bias with increasing cloud associated with warm air advection.

• The UK Meteorological Office mesoscale model was unable to accurately forecast cloud for this situation due to the non-frontal nature of the cloud which formed. Thus mesoscale model predictions of air temperature were poor.

Jan. 23rd/24th 1996 *Shallow, non-developing low pressure system situated close to or over Devon during January or February. Blocking high pressure system over Scandinavia. Non precipitating cloud band passing directly above Devon. Surface flow less than 20ms^{-1}, without feed of air from high pressure region.*

• Thorough evaluation of satellite images was required to determine cloud in this situation of multi-layered cloud. Upper level frontal cloud cleared faster than low level cloud which was barely visible in NOAA imagery due to its dark appearance in temperature detecting infrared imagery.

• Cloud clearances shorter than two hours in duration can occur which are not detectable from NOAA images, but which allow a road surface to cool by increased emission of longwave radiation during hours of darkness.

• Surface cooling occurred without air temperature decrease due to horizontal warm air advection.

• For a dry road surface which becomes wet mid-way through a night as a result of light precipitation or humidity, a 'dry' parameterization of surface wetness, as opposed to wet, produced closer surface temperature predictions to observations.

Feb. 4th/5th 1996 *Frontal cloud moving eastward from the Atlantic into very cold anticyclonic air over Eastern England during January or February.*

- Roadsurf was unable to react fast enough to cloud cover increases of more than 2 to 3 oktas per hour when a fixed 1200 UTC wind input was used. 3m flow increased after 1200 UTC Feb. 4th which produced mixing which increased the 3m air temperature which warmed the surface

- Roadsurf performance using air temperature inputs averaged over six hour periods and a variable wind speed was excellent at Stopgate Cross, Haldon Hill and Tuelldown. Minimum surface temperatures were predicted to within 0.8 deg. C of observations and frost onset time is predicted to within an hour at Stopgate Cross and Haldon Hill. This applied only to conditions of increasing cloud associated with air temperature increase caused by mixing and warm air advection from the west. Roadsurf performance at Ashmill was poor due to its valley location which reduced the effects of warm air advection and the station's location slightly north of a warm sector introduced by cloud. Using updated observations as inputs improved model performance.

Dec. 5th/6th 1995 *Frontal cloud moving westwards into Devon from Dorset and Somerset before dissipating, giving an illusion of eastward movement.*

- Large intervals between NOAA passes presented major problems when used to track cloud, especially when the cloud was below 800 mb which reduced ease of detection in Meteosat imagery.

- Roadsurf predicted surface freezing onset time well at Bratton Down, Haldon Hill and Tuelldown but badly at Stopgate Cross.

- Hilltop locations of Stopgate Cross and Haldon Hill prevented surface cooling during short lived clear windows in otherwise cloudy skies.

- Roadsurf underestimated suppression of surface cooling at exposed sites if cloud formed whenever cold air advection occurred and fixed air temperature inputs were used by the model.

- Roadsurf sensitivity to changes in depression of the wet bulb temperature (DWB) was negligible. Using variable DWBs as opposed to fixed values throughout Roadsurf runs at Bratton Down had no effect on surface freezing prediction time and only a 0.1 deg. C increase in minimum predicted surface temperature.

- Fixing Roadsurf air temperature inputs to those attained at start of changes in cloud produced more accurate predictions of surface temperature at coastal locations but not inland.

Feb. 6th/7th 1996 *Frontal cloud moving eastwards into anticyclonic cold air over Eastern England*

- Very strong dependence of rate of surface temperature change on timing of cloud cover occurred. Thus poor Roadsurf predictions of surface freezing time resulted from lack of satellite imagery between 1600 and 2359 UTC despite backtracking of frontal cloud from available 0200 and 0400 UTC images

- Under clear skies before 2200 UTC, Roadsurf predictions were more accurate for partly closed locations rather than those which were fully exposed. The model had a cold bias between 1500 and 2200 UTC during clear skies which produced the largest errors at stations which lose surface heat fastest. Air temperatures at partly closed locations were slightly higher due to microclimatic effects of shelter suppressing heat loss by thermal emission.

- Unacceptably large timelags occurred between changes in air temperature and Roadsurf predicted surface temperature when spot air temperatures (fixed throughout 6 hour periods) were used as inputs. New algorithms which enabled Roadsurf to calculate variable air temperatures from rates of air temperature change with time improved Roadsurf performance at two out of five locations. Algorithm success was independent of topography and coastal proximity but *was* strongly dependent on cloud cover.

- Roadsurf badly handled multiple layers of cloud which moved relative to each other since the model parameterises the thermal and radiative properties of a single cloud layer at any one time.

- The UK Meteorological Office mesoscale model poorly predicted air frost onset time at Roborough, Haldon Hill, Sourton Cross and Stopgate Cross because of the multi-layered cloud and inability of the model to account for microclimatic effects including topography and exposure. Furthermore, the mesoscale model underestimated extent of cloud cover.

Chapter 7 Real time tests of algorithms from 1996/97 winter

7.1 Introduction

The algorithms devised from the 1995/96 winter case studies were tested with data from the following winter, 1996/97. Unfortunately, the two winters were largely dissimilar so scenarios which occurred in the first, were rare in the 2nd. Although surface pressure patterns on occasions were similar, those of cloud cover change were not. Cold events *did* occur between October 1996 and April 1997 but a lack of frontal cloud during them rendered most unsuitable for algorithm tests. In particular a blocking anticyclone over Scotland produced a severe cold spell from December 25th 1996 to January 3rd 1997, but a clear sky predominated throughout.

One particular event of the winter, March 5th/6th 1997 was perfect for constructing an additional scenario type:- that of a well defined rapid cloud clearance from the west.

7.2 November 18th/19th 1996

November 18th/19th 1996 presented a potentially similar case to Scenario 3 of Chapter 6 (see algorithm summaries at end of that chapter) of frontal cloud moving eastwards over Devon.

The algorithm devised from the February 4th/5th case study in Chapter 6 was tested by applying it to conditions of November 18th/19th 1996. Certain aspects of the algorithm were modified as a result and are explained during the discussion in section 7.2.3.

Due to technical problems, the tests had to be carried out retrospectively. This had the increased benefit of satellite image availability from November 18th *and* 19th. However, use of such imagery from the forecast period would have partly defeated the object, so imagery from after the start of forecast period (1200 UTC Nov. 18th) was deliberately ignored until the discussion.

7.2.1 General conditions

Following an earlier passage of a depression into Germany from England, a weak ridge of high pressure had built over Eastern England between 0000 UTC and 1200 UTC Nov. 18th. It was certainly not as dominant as the original anticyclone over Eastern England from which the algorithm which gave rise to Scenario 3 was developed (Feb. 4th/5th 1996). However the ridge, shown by the 1200 UTC Nov. 18th surface analysis in Figure 7.2.1.1 was an extension of a large anticyclone 200 km west of France and Spain.

Very cold air over Eastern England is a symptom of Scenario 3 and although no pool of very cold air occurred there during Nov. 18th 1996, northerly winds and initially clear skies suggested a similar scenario.

7.2.2 Estimating variables for Roadsurf

Cloud cover

From Figures 7.2.1.2a, to c and the plane sailing method (Chapter 2), the cloud movements shown in Table 7.2.2.1 were used to produce a cloud forecast for the period 1300 UTC Nov. 18th to 0900 UTC Nov. 19th as shown in Table 7.2.2.2.

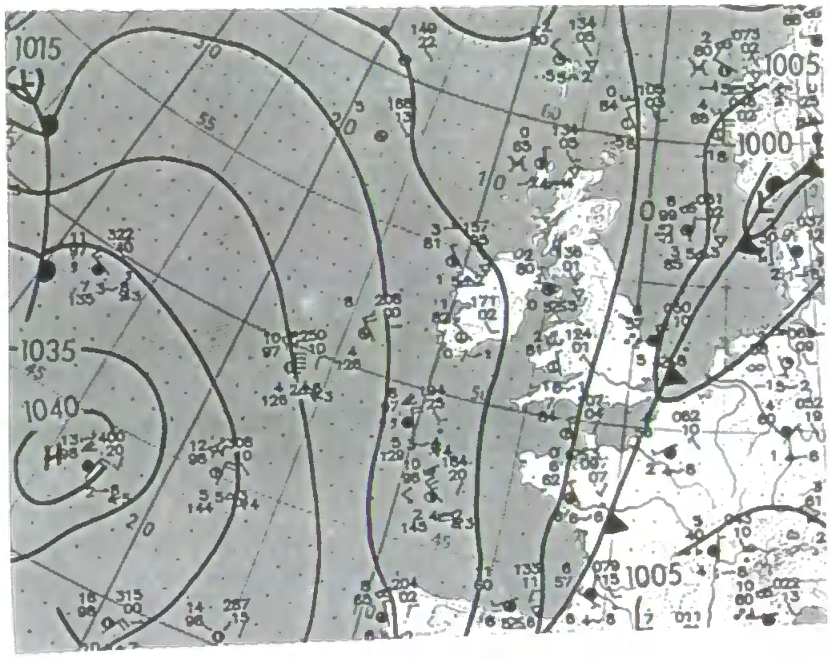

a. 0000 UTC

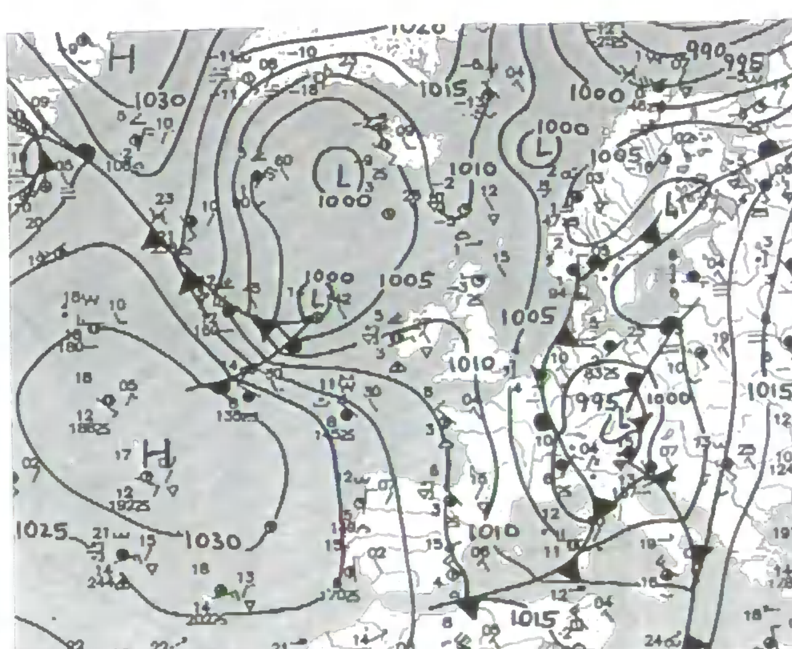

b. 1200 UTC

Figure 7.2.1.1 European Meteorological Bulletin surface analyses from November 18th 1996

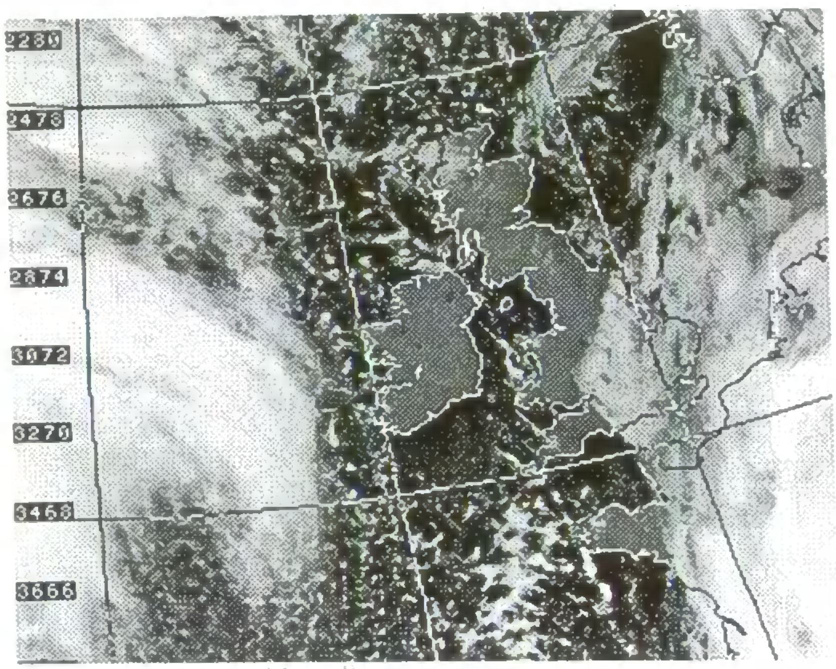

a. 0251 UTC

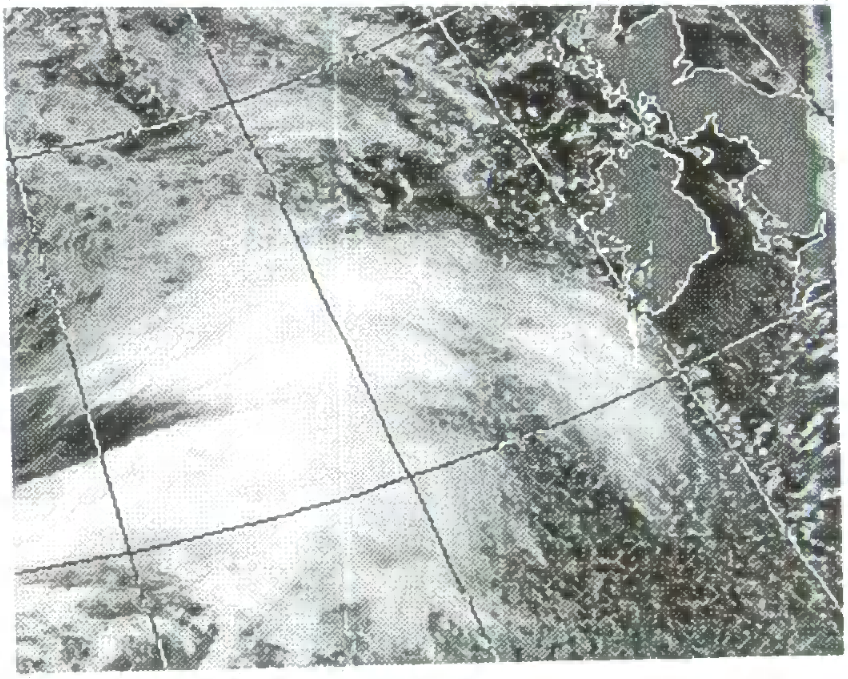

b. 0432 UTC

Figure 7.2.1.2 NOAA infrared satellite images from November 18th 1996

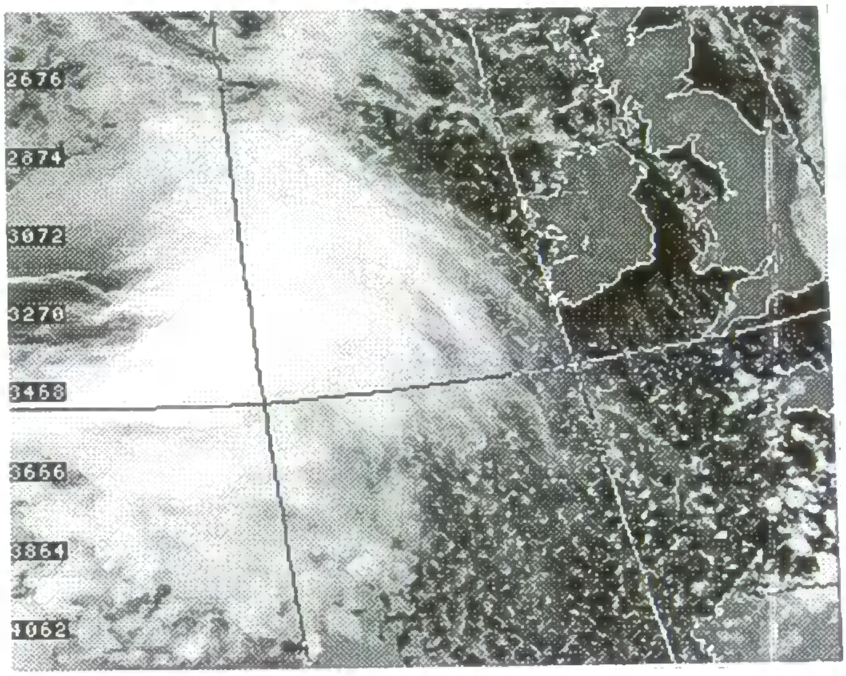

c. 0753 UTC

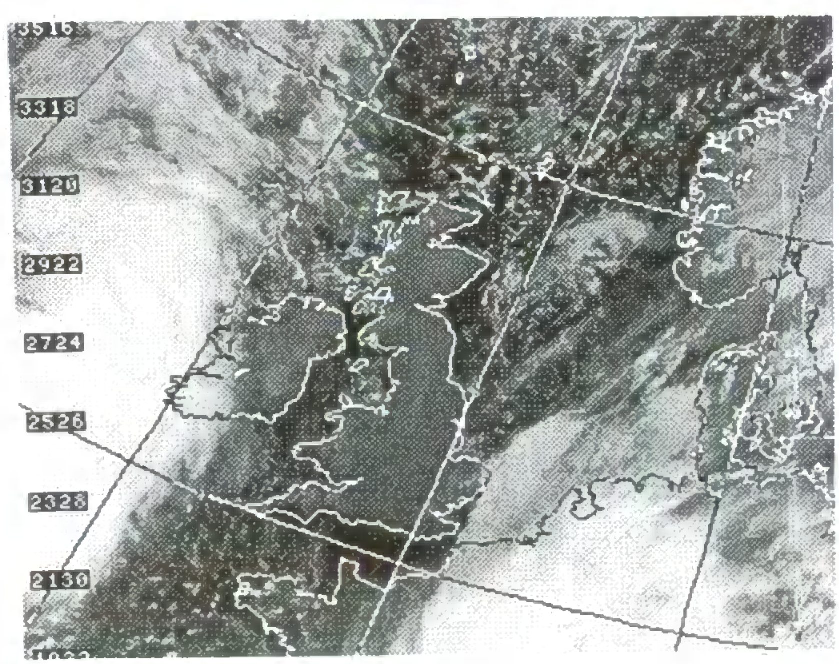

d. 1246 UTC

Figure 7.2.1.2 NOAA infrared satellite images from November 18th 1996

Table 7.2.2.1 Cloud movement and extent between 0432 UTC and 1246 UTC Nov. 18th 1996 ascertained from Figures 7.2.1.2a,b and c

Feature	Observation
Easternmost tip of thick cloud southwest of Ireland at 10°W 56°N at 0432 UTC.	Between 0432 and 1246 UTC, movement was 750 km eastwards at 93 km hr^{-1} to 7.8°W 56°N
N/S extent of cloud along 20°W longitude	At 0432: 1400 km (46°N to 58°N) At 0753: 1600 km (44°N to 58°N) At 1246: cloud off image
N/S extent of cloud along 10°W longitude	At 0432: 0 km At 0753: 300 km (47°N to 50.5°N) At 1246: 1100 km (45°N to 55°N)
E/W extent of cloud along 55°N **latitude**	At 0432: 1300 km (33°W to 15°W) At 0753: 700 km of thick cloud (22°W to 14°W) 1100 km of low cloud (29°W to 14°W) At 1246: cloud off image

Table 7.2.2.2 Cloud forecast from 1300 UTC Nov. 18th to 0900 UTC Nov. 19th 1996

Time period (UTC)	Cloud cover (in oktas) and level
1300 to 1459 Nov. 18th	2 low
1500 to 1759	3 medium
1800 to 2059	8 medium
2100 to 2359	8 medium
0000 to 0259 Nov. 19th	8 medium
0300 to 0559	6 medium
0600 to 0859	6 medium

Surface wind

Observed geostrophic flow over Devon from the 1200 UTC Nov. 18th surface analysis, using geostrophic equation 1 from Chapter 6 was a northwesterly 7.7 ± 2 ms^{-1}, whilst an observation from Brest (Northwest France) was 5 ms^{-1}. These were considered close enough to reliably indicate that flow could be calculated from surface pressure analyses. A wind forecast in Table 7.2.2.3 was constructed based on geostrophic wind calculated along 50°N, west of Ireland, in the path of the depression shown in Figure 7.2.1.1. Roadsurf, however uses surface flow, which due to friction, approximates to 70 percent of the geostrophic flow over land. The third column of Table 7.2.2.3 thus has the predicted wind velocities required by Roadsurf.

Table 7.2.2.3 Predicted flow from 1200 UTC Nov. 18th to 0900 UTC Nov. 19th 1996

Time period (UTC)	Geostrophic velocity	Geostrophic velocity less 30%
1200 to 1759 Nov. 18th	2 ms^{-1} NW	1.4 ms^{-1} NW
1800 to 2359 Nov. 18th	8 ms^{-1} W	5.6 ms^{-1} W
0000 to 0559 Nov. 19th	10 ms^{-1} NW	7.0 ms^{-1} NW
0600 to 0900 Nov. 19th	10 ms^{-1} NW	7.0 ms^{-1} NW

Air temperature

Table 7.2.2.4 shows observations from three stations for the 12 hours before the start of the forecast period starting at 1200 UTC Nov. 18th. The same stations were used as in the case study from which the scenario algorithm was constructed (Feb. 4th/5th 1996) except Ashmill whose Nov. 18th 1996 data were unavailable. Ashmill data presented many irregularities in the Feb. 4th/5th 1996 study which rendered the algorithm's accuracy haphazard at the station. In conjunction with Table 7.2.2.5 which shows data from the similar scenario of Feb. 4th/5th 1996 (see Chapter 6.5), Table 7.2.2.6 of forecast 2m air temperature was constructed.

Table 7.2.2.4 Mean 2m air temperatures at three locations from 0000 UTC to 1200 UTC Nov. 18th 1996 between times shown.

Location	Temperature /°C
Stopgate Cross	0000 and 0600 UTC: 1.3
	0600 and 1200 UTC: 1.9
Haldon Hill	0000 and 0600 UTC: 2.5
	0600 and 1200 UTC: 3.0
Tuelldown	0000 and 0600 UTC: 2.3
	0600 and 1200 UTC: 2.3

Table 7.2.2.5 Mean air temperatures used as Roadsurf inputs for case study 3 of Chapter 6 (Feb. 4th/5th 1996).

(Times in UTC, temperatures in °C)	Stopgate Cross	Haldon Hill	Tuelldown	Ashmill
1100-1759 Feb. 4th	0.2	1.1	2.6	2.6
1800-2359 Feb. 4th	-1.0	-1.0	-1.3	-3.2
0000-0559 Feb. 5th	0.6	0.3	0.5	-0.7
0600-1159 Feb. 5th	1.5	2.0	2.2	2.1

Table 7.2.2.6 Forecast of mean air temperatures for three locations for 1200 UTC Nov. 18th to 1200 UTC Nov. 19th 1996.

(Times in UTC, temperatures in °C)	Stopgate Cross	Haldon Hill	Tuelldown
1100-1759 Nov. 18th	2.5	4.0	3.5
1800-2359 Nov. 18th	3.0	5.0	5.0
0000-0559 Nov. 19th	4.0	5.0	5.0
0600-1159 Nov. 19th	3.0	4.5	4.0

In the Feb. 4th/5th case study, Roadsurf produced more accurate predictions of surface freezing when using mean (averaged over six hour periods) rather than spot air temperatures. Thus it was hoped that the same would occur for this Nov. 18th/19th 1996 case study.

Table 7.2.2.7 Other 1200 UTC Nov. 18th 1996 parameters

Location	Surface temperature / °C	Dewpoint depression (DWD) / deg. C	Depth (30cm) temperature /°C
Stopgate Cross	8.6	1.2	not known - use Clyst Honiton ob: 5.5
Haldon Hill	11.0	1.6	6.8
Tuelldown	5.7	1.1	6.5

7.2.3 Roadsurf predictions

Data from Tables 7.2.2.2, 7.2.2.3, 7.2.2.6 and 7.2.2.7 were used to produce a Roadsurf forecast for the period 1200 UTC Nov. 18th to 1200 UTC Nov. 19th. Unfortunately Roadsurf became unstable after 0000 UTC Nov. 19th due to the windspeed of 7 ms^{-1}. Such a speed caused the sensible heat flux to oscillate as a result of the centred time differencing equations within Roadsurf (see Chapter 4).

Roadsurf was rerun using the modified wind speeds shown in Table 7.2.3.1. Figure 7.2.3.1 shows the main predictions and observations obtained.

Table 7.2.3.1 Modified windspeeds used by Roadsurf from 1200 UTC Nov. 18th to 0900 UTC Nov. 19th 1996

Time period (UTC)	Velocity / ms^{-1}
1200 to 1759 UTC Nov. 18th	2
1800 to 2359 UTC Nov. 18th	2
0000 to 0559 UTC Nov. 19th	4
0600 to 0900 UTC Nov. 19th	4

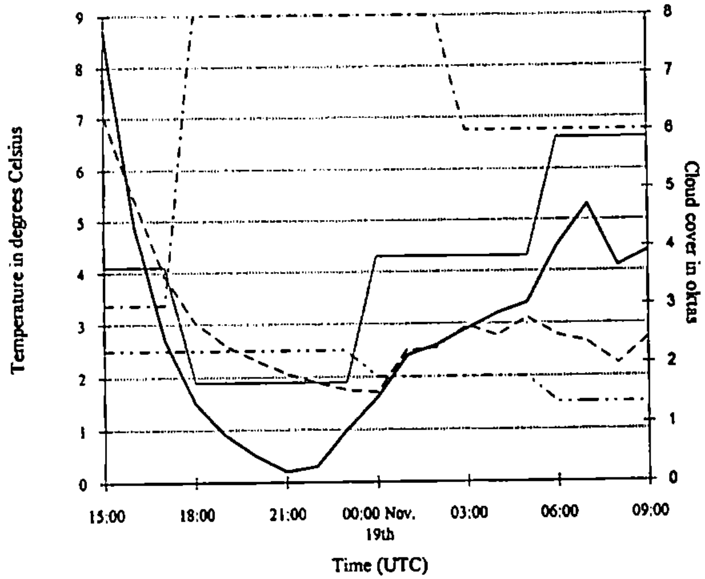

a. Stopgate Cross

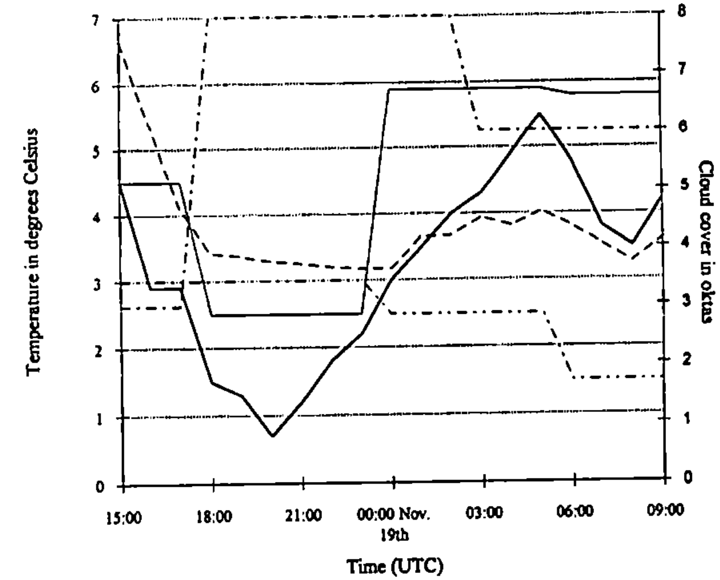

c. Tuelldown

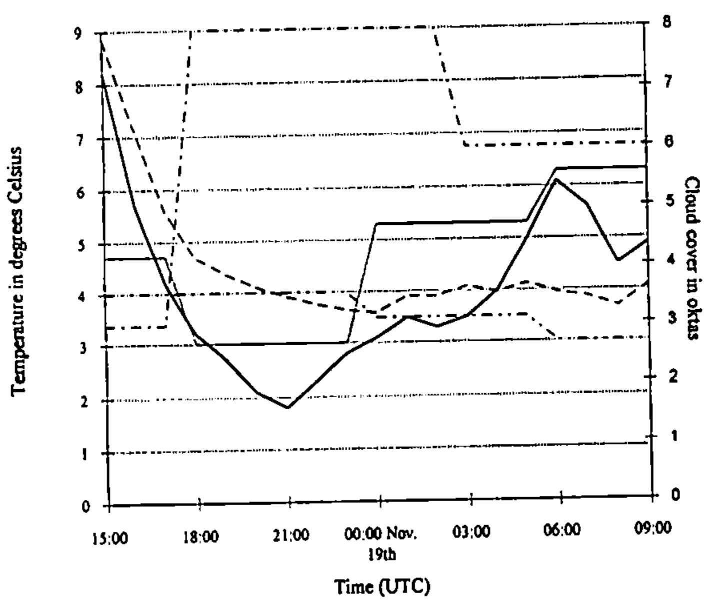

b. Haldon Hill

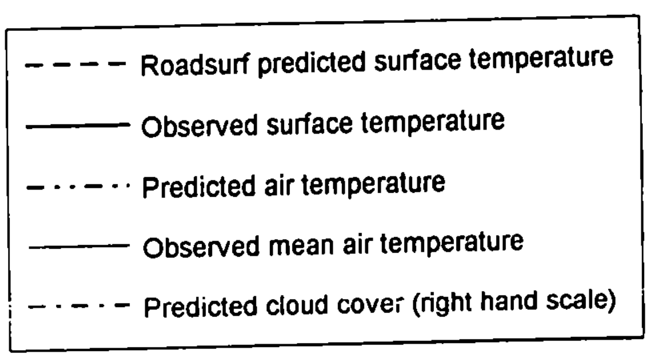

Figure 7.2.3.1 First Roadsurf predictions and evolution of conditions from 1500 UTC Nov. 18th to 0900 UTC Nov. 19th 1996

Figures 7.2.3.1a to c show excellent Roadsurf performance between 0000 UTC and 0400 UTC Nov. 19th with negligible differences between predicted and observed surface temperature. Surface cooling at 0600 UTC caused by cloud clearing was predicted well by Roadsurf at all three stations and to within 1 deg. C at Tuelldown and Haldon Hill.

Unfortunately Roadsurf's attempt to predict minimum surface temperature (Table 7.2.3.2) was unsuccessful.

Table 7.2.3.2 Minimum surface temperature between 1200 UTC Nov. 18th and 0900 UTC Nov. 19th 1996

	Predicted minimum surface temp. / °C	Observed minimum RST / °C	Error in min. prediction / deg. C
Stopgate Cross	1.7 at 0000 UTC	0.2 at 2100 UTC	1.5, 3 hours late
Haldon Hill	3.6 at 0000 UTC	1.8 at 2100 UTC	1.8, 3 hours late
Tuelldown	3.2 at 2200 UTC	0.7 at 2000 UTC	2.5, 2 hours late

An alternative method of preventing Roadsurf from oscillating during strong winds was to increase the time filter factor (tff), explained in Chapter 4. Increasing this quantity smoothes out erroneous temperature predictions produced by the centred time differencing equations used by Roadsurf, preventing any sprurious predictions from being recycled.

Roadsurf was rerun using a increased tff of 0.3 (previously 0.1) and the expected wind speeds of Table 7.2.2.3.

Unfortunately no improvement was obtained (Figures 7.2.3.2.a to c). At Tuelldown, predictions were even worse then previously. The filter factor was strong enough to prevent Roadsurf oscillating out of control , but had a suppressing effect on surface cooling especially between 1600 and 1900 UTC Nov. 18th. Rates of predicted temperature change were softened compared to observations. Thus the following modifiation to the algorithm for this scenario is neccessary:-

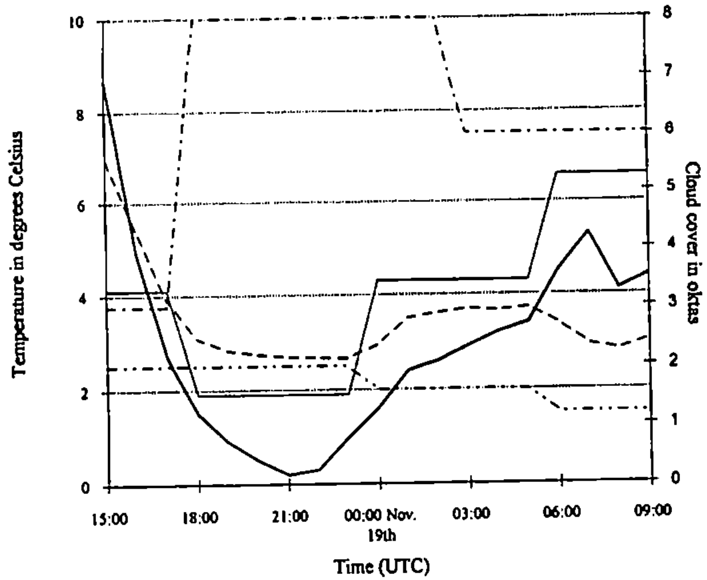

a. Stopgate Cross

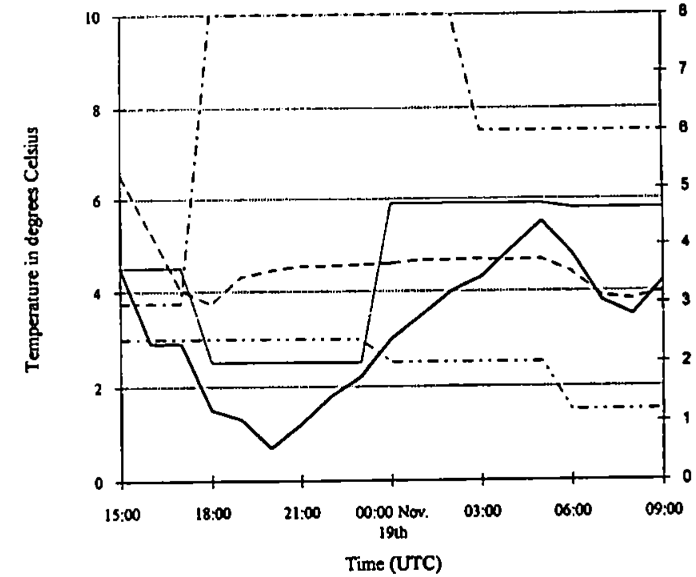

c. Tuelldown

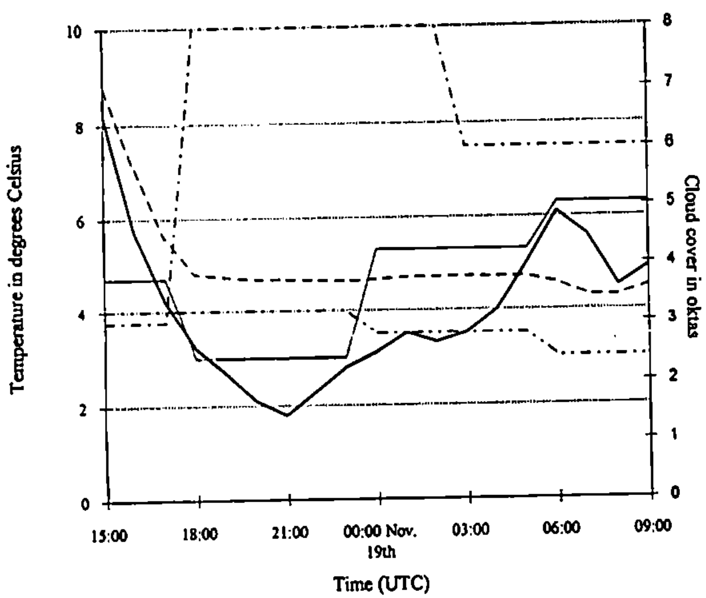

b. Haldon Hill

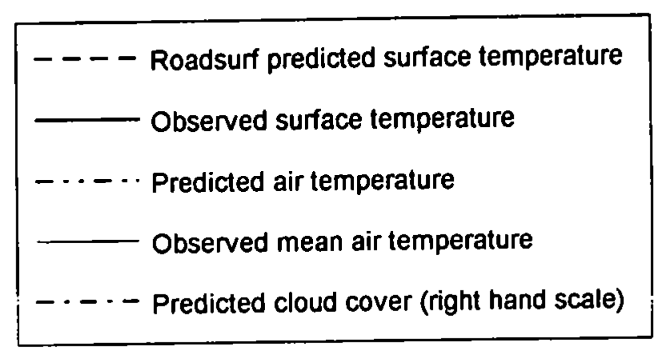

Figure 7.2.3.2 Roadsurf predictions and observations from 1500 UTC Nov. 18th to 0900 UTC Nov. 19th 1996.

Roadsurf used a 'time filter factor', tff of 0.3 and the forecast windspeeds of Table 7.2.1.3

If a sharp fall in surface temperature is expected with winds stronger than 8 ms^{-1}, put tff=0.1 and use 4 ms^{-1} as maximum mean wind speed.

Errors in the above two sets of runs were due to the cloud predictions of Table 7.2.2.2. The NOAA satellite images in Figures 7.2.3.3a to e show a later cloud cover increase than that predicted. Roadsurf thus under-estimated significant surface cooling between 1800 UTC and 2200 UTC Nov. 18th. Cloud movement obviously slowed as it neared Britain. This could have been forseen as a result of the weak ridge of high pressure over Southwest England ahead of the approaching surface depression.

A further reason for the underestimation was due to the *lack* of radiative and evaporative cooling in Roadsurf of the constant flux layer immediately above the surface due to cloud cover input. As Figure 7.2.3.4 shows, wind speed was predicted to increase between 1700 and 2100 UTC Nov. 18th at a higher rate than observed at 28m. This could have also been forseen (but was not) as a result of the ridge of high pressure. The 'observed surface wind' curve in Figure 7.2.3.4 was calculated using Equation 7.2.3.1, based on the observations from the Plymouth University weather station 28m above surface level. Equation 7.2.3.1 (Panofsky, 1977) adjusts the 28m wind to what would have been expected at 3m.

$$U_1 = U_2(Z_1/Z_2)^{0.19} \qquad 7.2.3.1$$

where:-

U_1 = wind speed at height Z_1

U_2 = wind speed at height Z_2

Z_1 = 3m,

Z_2 = 28m.

The absence of radiative cooling was due to the strengthening surface wind between 1900 and 2200 UTC Nov. 18th causing mixing as the surface depression approached Devon.

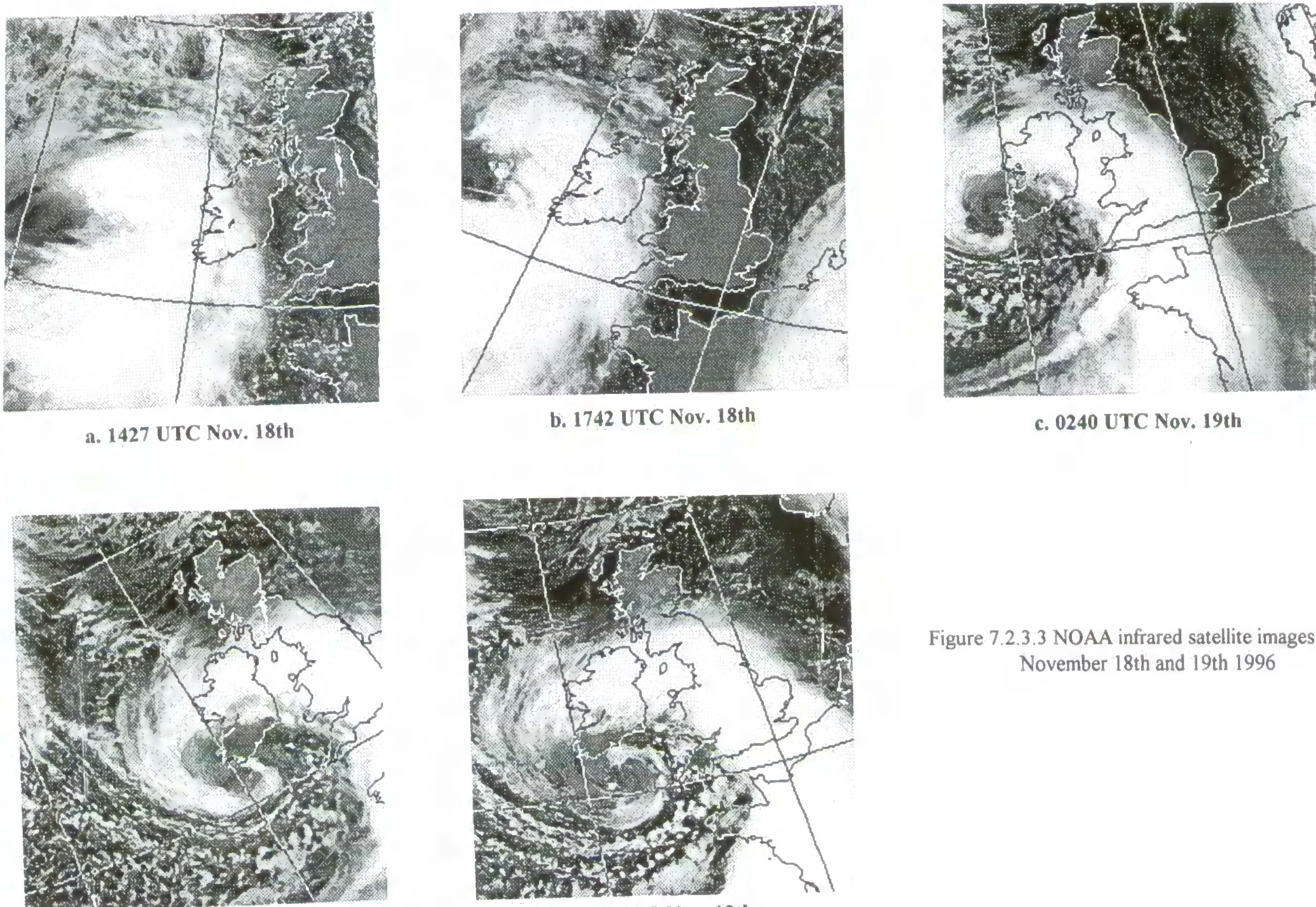

a. 1427 UTC Nov. 18th

b. 1742 UTC Nov. 18th

c. 0240 UTC Nov. 19th

d. 0421 UTC Nov. 19th

e. 0731 UTC Nov. 19th

Figure 7.2.3.3 NOAA infrared satellite images from November 18th and 19th 1996

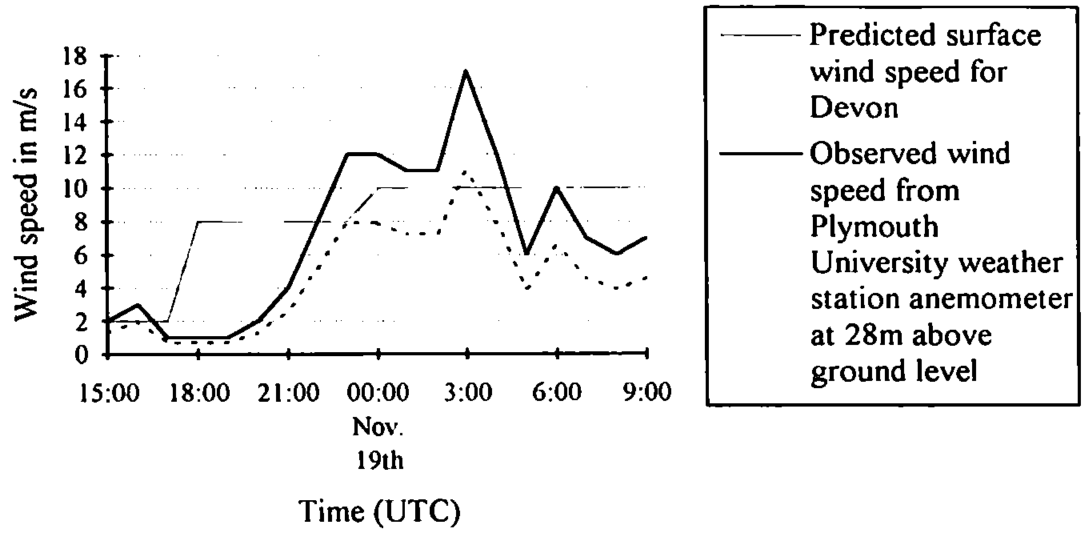

Figure 7.2.3.4 Predicted and observed mean wind speeds over 1 hour periods from 1200 UTC Nov. 18th to 0900 UTC Nov. 19th 1996

A final rerun of Roadsurf for Nov. 18th/19th 1996, using *observations* of air temperature, cloud cover and humidity produced sufficiently accurate minimum surface temperature predictions (see Table 7.2.3.3), though its timing continued to be rather poor. In the winter maintenance context, a predicted minimum temperature within 1 deg. C of 0°C would be enough to put salting crews on alert.

General performance was also an improvement (see Figures 7.2.3.5a to c) over previous runs. The modified wind speeds of Table 7.2.2.1 were used as an alternative to observed values shown in Figure 7.2.3.4 to ensure model stability.

Table 7.2.3.3 Minimum surface temperature between 1200 UTC Nov. 18th and 0900 UTC Nov. 19th 1996 from Roadsurf, using *observations* of air temperature, cloud cover and humidity.

	Predicted minimum surface temp. / °C	Observed minimum RST / °C	Error in min. prediction / deg. C
Stopgate Cross	1.0 at 2300 UTC	0.2 at 2100 UTC	0.8, 2 hours late
Haldon Hill	2.2 at 0000 UTC	1.8 at 2100 UTC	0.4, 3 hours late
Tuelldown	1.4 at 2300 UTC	0.7 at 2000 UTC	0.7, 3 hours late

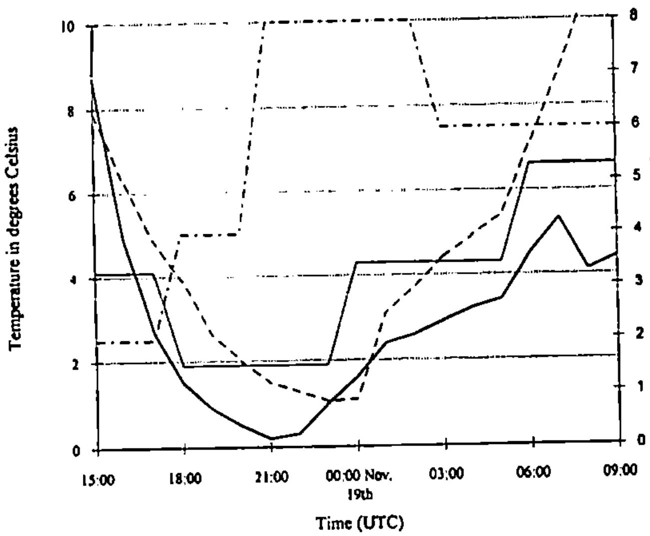

a. Stopgate Cross

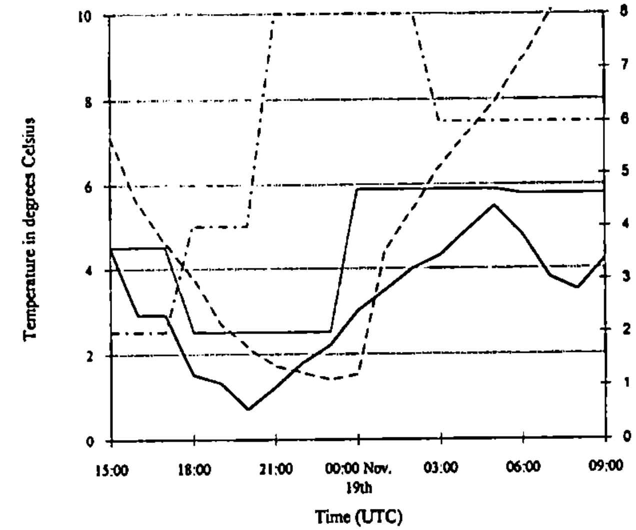

c. Tuelldown

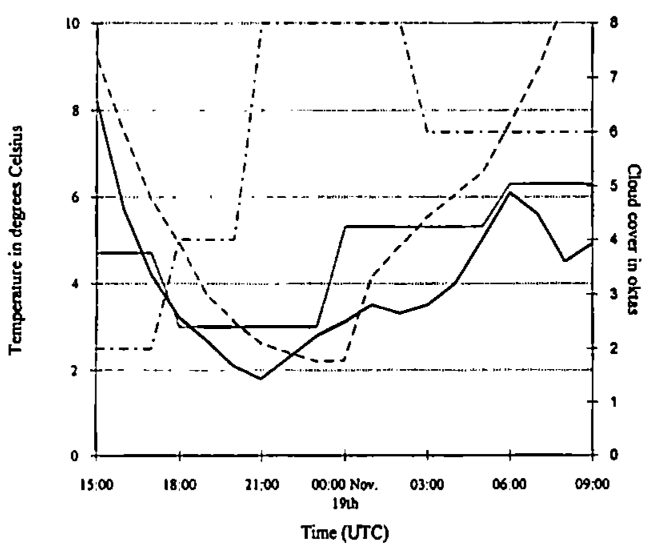

b. Haldon Hill

Roadsurf predicted surface temperature

Observed surface temperature

Observed mean air temperature

Observed cloud cover (right hand scale)

Figure 7.2.3.5 Evolution of conditions from 1500 UTC Nov. 18th to 0900 UTC Nov. 19th 1996

For these re-runs, Roadsurf used observed air temperatures, cloud cover and the wind speeds of Table 7.2.3.1.

7.2.4 Conclusions

As a conclusion for this case study, the algorithm for Scenario 3 of chapter 6 needs to be changed to the following, to take into account any problems of strong winds and changing cloud movement:- (changes to original algorithm are in *italics*)

Scenario:-

Frontal cloud moving eastward from the Atlantic into very cold anticyclonic air over Eastern England during January or February.

Algorithm:-

1. Predict mean 2m air temperature for forecast period (1200 UTC onwards) for periods of 6 hours duration, using observations and knowledge of local climate as detailed by McLean, 1994.

2. Estimate height, track and speed of cloud using observations from a period of at least 6 hours preceding start of forecast. *Afford special attention to features which will slow cloud movement, for example ridges of high pressure over Southwest England.*

3. Produce cloud cover forecast in oktas above a chosen site.

4. Calculate 2m flow from latest surface air pressure analysis using **geostrophic equation 1**. Reduce geostrophic flow by 30% to account for land/air friction or by 20% over water and compare with weather station observations. Estimate surface air flow for duration of forecast period, taking exposure into account. Changes in air flow are greatest during passage of the frontal zone. *If air flow is expected to be faster than 5 ms^{-1}, one of the following options must be selected to ensure Roadsurf remains stable:-*

a. If 2m air temperature is expected to fall rapidly - for example due to radiative cooling, use modified wind speeds of 4 ms^{-1} maximum.

b. Alternatively, increase the 'time filter factor', tff to 0.3 or 0.4. The higher value is most powerful in preventing instability, but softens rapid changes in surface temperature. Not suitable if rapid air and surface temperature changes are expected.

5. Run Roadsurf using predicted cloud cover, 2m air temperature and chosen wind speeds to produce a graph of surface temperature for the chosen site, from which frost onset time and minimum surface temperature can be obtained.

7.3 March 5th/6th 1997

7.3.1 Summary of cloud cover and synoptic conditions of March 5/6th 1997.

The evening of March 5th presented an event very different from those featured in Chapter 6: that of an overnight cloud clearance. Figures 7.3.1.1a to h of the NOAA images shows a cold front which moved southeastward during daylight hours of March 5th. Polar maritime air behind the front was of a showery nature, shown by a vast area (over a million sq. km) of cumulus cloud tops south of Iceland in the satellite imagery.

Surface pressure analyses (Figures 7.3.1.2a and b) from March 5th/6th show anticyclonic air over Southwest Europe, a deep depression of central pressure 950 mb close to Iceland and the cold front between the two. Surface pressure increased across Britain during March 5th as a result of the Icelandic depression filling and the Spanish anticyclone enlarging to encompass France, western England and southern Eire.

7.3.2 Initial Roadsurf predictions.

Roadsurf was run using the inputs of Table 7.3.2.1. Since the run was retrospective, it was possible to use cloud observations from NOAA infrared satellite imagery.

Table 7.3.2.1 Inputs required by Roadsurf for 1200 UTC March 5th to 0900 UTC March 6th 1997 runs (Taken from observations).

Parameter (Times in UTC)	Halwell Camp	Waldon Bridge	Bratton Down
Cloud cover:- (in oktas)			
1200 to 1459 March 5th	8 oktas (medium)		
1500 to 1759 March 5th	8 oktas (medium)	Same	Same
1800 to 2059 March 5th	8 oktas (medium)	as	as
2100 to 2359 March 5th	4 oktas (low)	Halwell	Halwell
0000 to 0259 March 6th	1 okta (low)	Camp	Camp
0300 to 0559 March 6th	clear		
0600 to 0859 March 6th	4 oktas (low)	4 oktas (low)	2 oktas (low)

Table 7.3.2.1 continued:-

2m air temperature /°C			
1200-1759 March 5th	9.5	10.6	8.5
1800-2359 March 5th	8.5	7.0	5.6
0000-0559 March 6th	5.2	3.1	3.7
0600-1159 March 6th	4.4	3.3	3.9
Ts at 1200 Mar. 5th /°C	10.1	10.3	8.8
Td at 1200 Mar. 5th /°C	8.6	9.3	8.0
Tcl at 1200 Mar.5th /°C	7.1	8.2	7.2
Surface wind speed from Culdrose:- (in ms^{-1})			
1200-1759 March 5th	3.0	Same	Same
1800-2359 March 5th	3.0	as	as
0000-0559 March 6th	2.0	Halwell	Halwell
0600-1159 March 6th	2.0	Camp	Camp
Surface DWB:- (deg. C)			
1200-1759 March 5th	0.1	0.3	0.0
1800-2359 March 5th	0.5	0.3	0.0
0000-0559 March 6th	0.5	0.1	0.2
0600-1159 March 6th	0.6	0.2	1.5
Surface state at 1200 March 5th	dry, SRHF=0.0	dry, SRHF=0.0	dry, SRHF=0.0

Note: Halwell Camp and Waldon Bridge were new stations for the 1996/97 winter and are shown on the map in Appendix 3. They were meant to replace Totnes Cross and Cross Farm respectively.

No surface freezing was predicted or observed during this case study despite a total cloud clearance. Surface cooling moderated at Halwell Camp (see Figure 7.3.2.1a) after 0000 UTC March 6th and was even reversed at Bratton Down and Waldon Bridge (see Figures 7.3.2.1b and c). The rise in surface temperature at these two locations did not occur at the same time, which indicated that the most likely reason for the warming events after midnight was isolated cloud. Unfortunately the 0138 UTC and 0319 UTC satellite images do not show this suspected cloud due to resolution constraints.

a. 0712 UTC

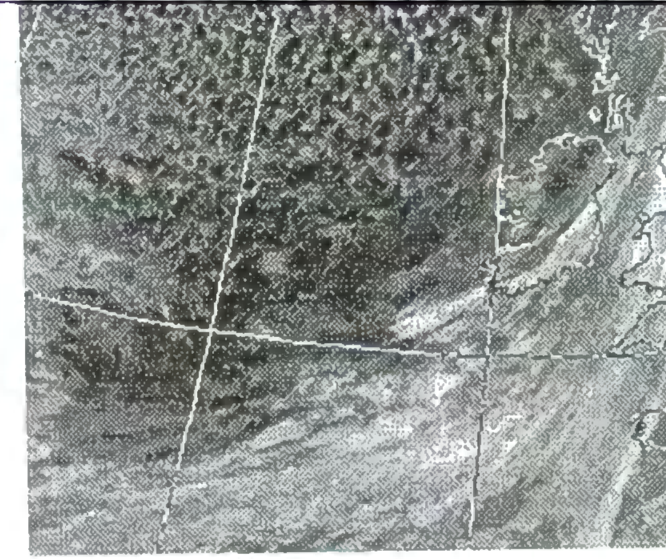

c. 1506 UTC

b. 1324 UTC

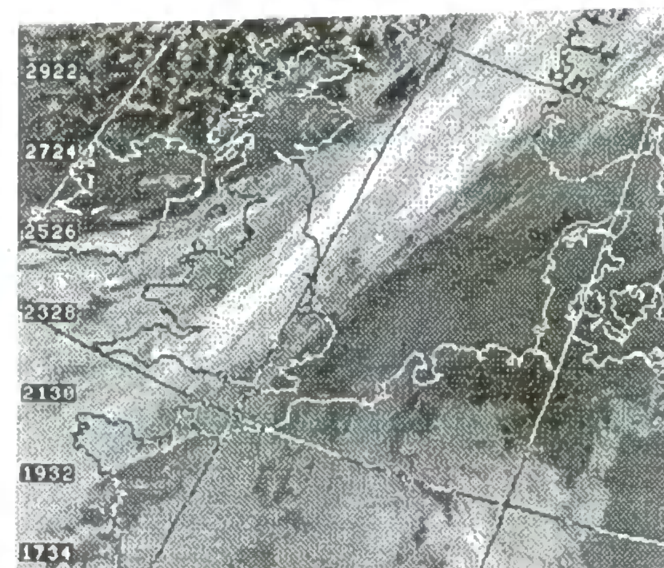

d. 1702 UTC

Figure 7.3.1.1 NOAA infrared imagery
from March 5th 1997

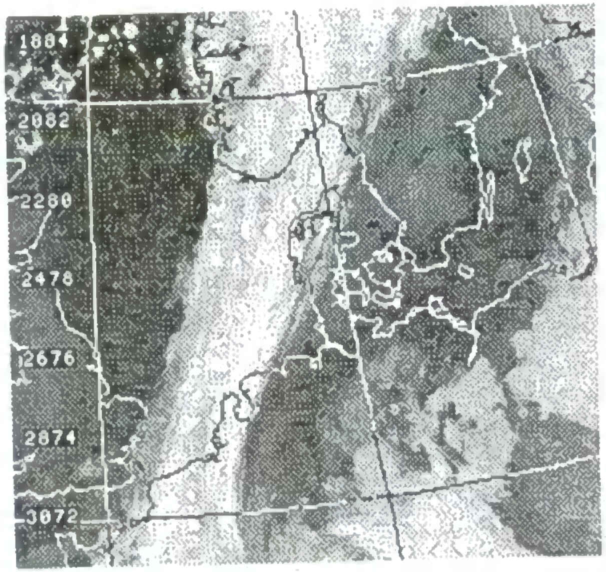

e. 0138 UTC

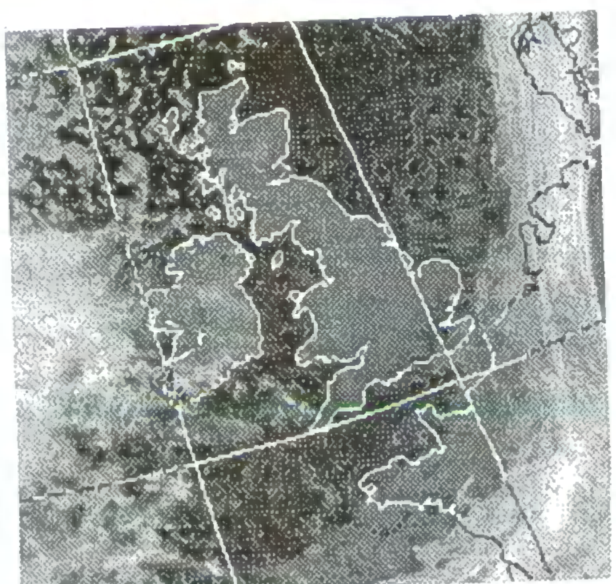

f. 0319 UTC

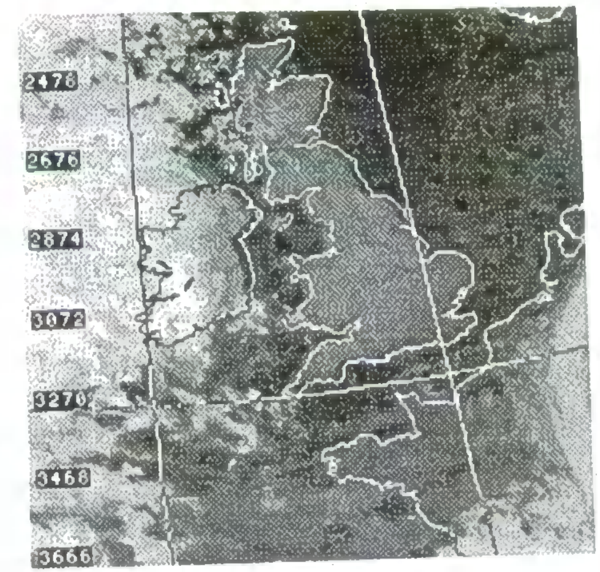

g. 0650 UTC

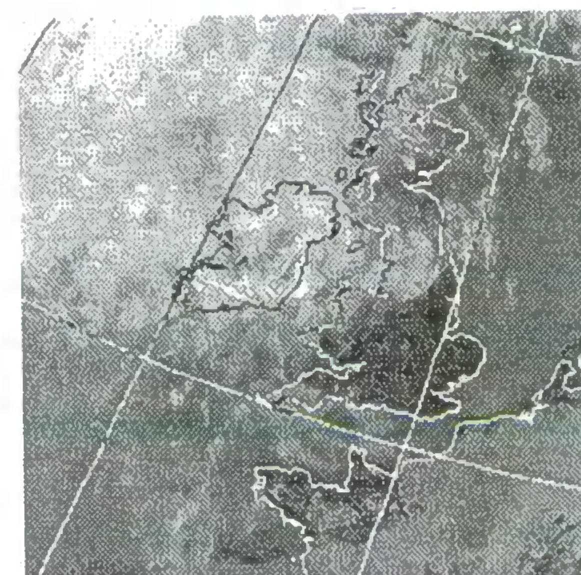

h. 1313 UTC

Figure 7.3.1.1 NOAA infrared imagery
from March 6th 1997

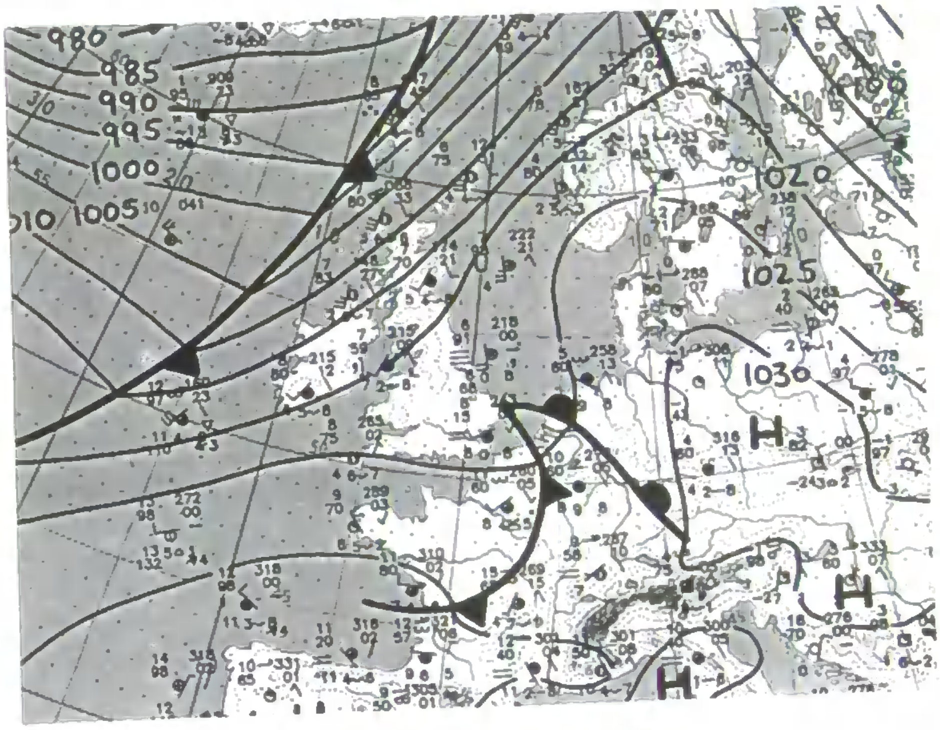

a. 0000 UTC March 5th

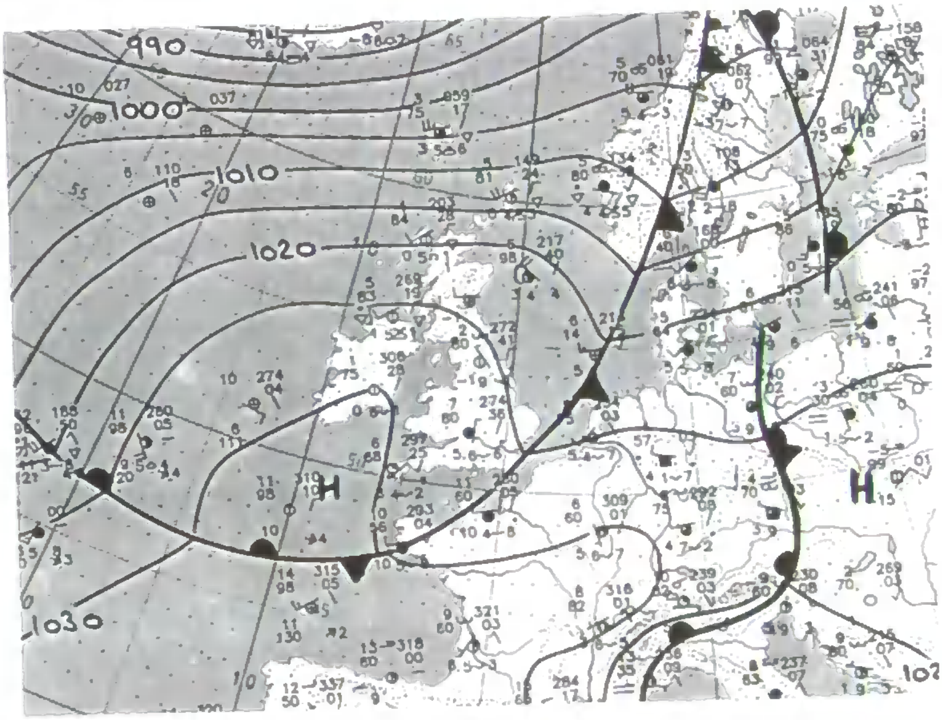

b. 0000 UTC March 6th

Figure 7.3.1.2 European Meteorological Bulletin surface analyses from March 5th and 6th 1997

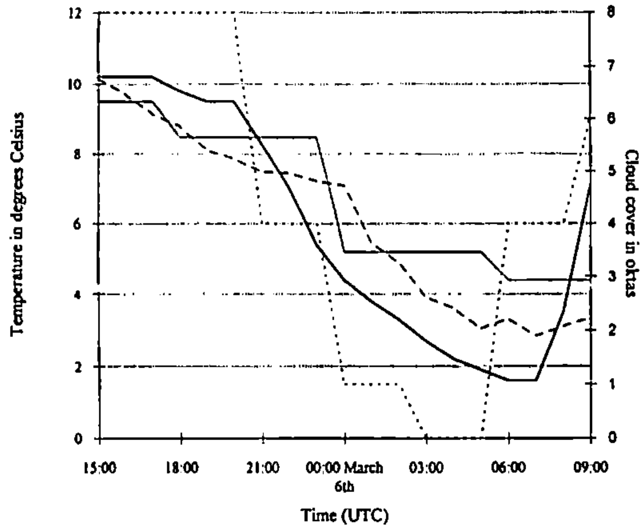

a. Halwell Camp

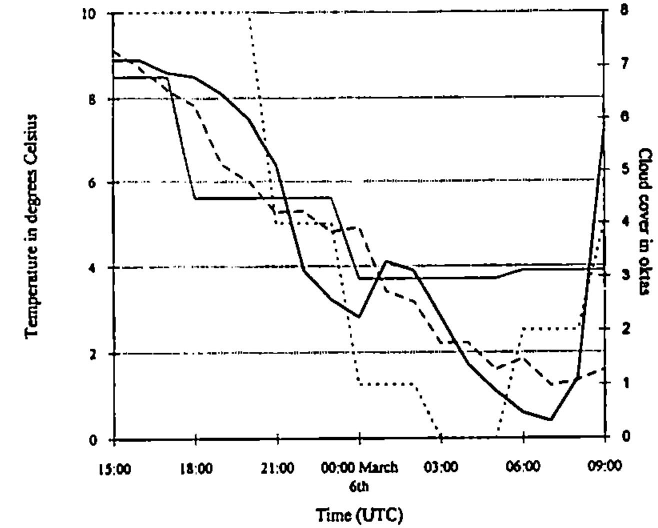

c. Bratton Down

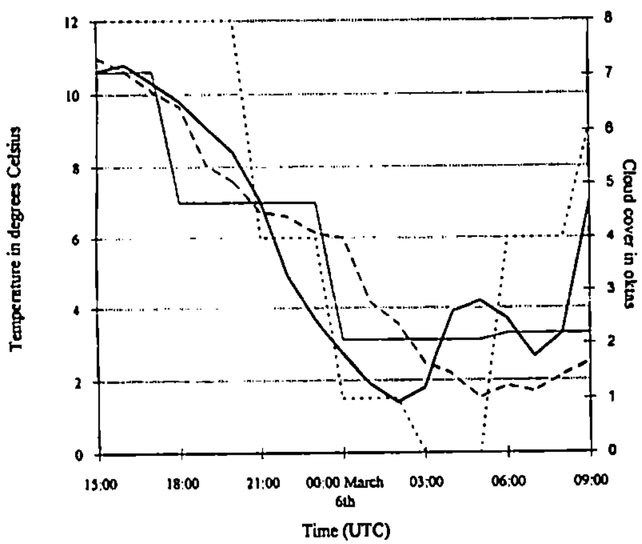

b. Waldon Bridge

- - - - Roadsurf predicted surface temperature
—— Observed surface temperature
—— Observed air temperature (averaged over 6 hour periods)
· · · · · · Observed cloud cover (right hand scale)

Figure 7.3.2.1 Roadsurf predictions and evolution of conditions from 1500 UTC March 5th to 0900 UTC March 6th 1997

The inputted cloud had mixed results on predicted minimum surface temperature as Table 7.3.2.2 shows. Halwell Camp and Bratton Down predictions were on time but the least error occurred rather surprisingly at the latter station despite the temporary surface warming between 0000 and 0200 UTC March 6th. Minimum temperature prediction at Waldon Bridge was 3 hours too late because the temporary rise in surface temperature coincided with the three hour period before dawn, during which minimum temperature *normally* occurs.

Table 7.3.2.2 Minimum surface temperature statistics from March 5th/6th 1997

	Predicted	Observed	Error in prediction
Halwell Camp	2.8 °C at 0700	1.6 °C at 0700	1.2 deg. C, on time
Waldon Bridge	1.5 °C at 0500	1.4 °C at 0200	0.1 deg. C, 3 hours late
Bratton Down	1.2 °C at 0700	0.4 °C at 0700	0.8 deg. C, on time

7.3.3 Algorithm construction

Cloud prediction

Individual cloud is difficult to take into account when developing an algorithm to predict frost onset time and minimum temperature. If the pre-midnight cooling had continued at Bratton Down and Waldon Bridge, freezing would have been highly likely. Predicting individual clouds which might occur 12 to 24 hours into a forecast period is not feasible. The effects from the suspected cloud situations from between 0300 UTC and 0500 UTC March 6th at Halwell Camp and Waldon Bridge could not have been foreseen. As data from Waldon Bridge showed (see Table 7.3.2.2 and Figure 7.3.2.1b), the timing of cloud on minimum temperature was highly important.

For safety reasons in this scenario, it is more advantageous to assume that no cloud will occur after the main frontal band has cleared unless there are strong reasons why cloud might occur (for example a developing band of cumulus). Roadsurf would inevitably exhibit a cool bias if cloud were to occur after the frontal clearance, but predicted temperatures under conditions likely to cause freezing (and thus of highest importance) should therefore be sufficiently accurate.

In this scenario, for an algorithm to be successful, an accurate forecast of frontal cloud clearance is essential. Such a forecast should be produced from tracking the frontal cloud edge for at least 6 hours before start of forecast, to determine when its back edge will cross Devon. All changes in cloud speed should be noted, especially any acceleration of cloud movement since this will advance frost onset time, if frost was likely. A possibility of back edge cloud becoming diffuse is also a major source of error because it gives an appearance of faster movement. Furthermore, thinning cloud depth within a frontal cloud band is possible and, if overlooked, will result in unexpected localised radiative cooling.

Hourly radiosonde ascents from stations within the frontal cloud are most useful for determining cloud depth variations but their expense rules them impractical. Regions of darker cloud pixels in satellite images can be tracked to partly ascertain if cloud thinning occurred before start of forecast.

Due to the vertical gradient of cold fronts, it was thought possible that geostrophic flow from upper level charts could be used to indicate changes in cloud velocity at the front's back edge. Geostrophic wind speeds calculated from Figures 7.3.3.1a and b were thus compared with displacement speeds of the back edge of the frontal cloud shown in Figure 7.3.3.2. The velocities are shown in Tables 7.3.3.1 and 7.3.3.2.

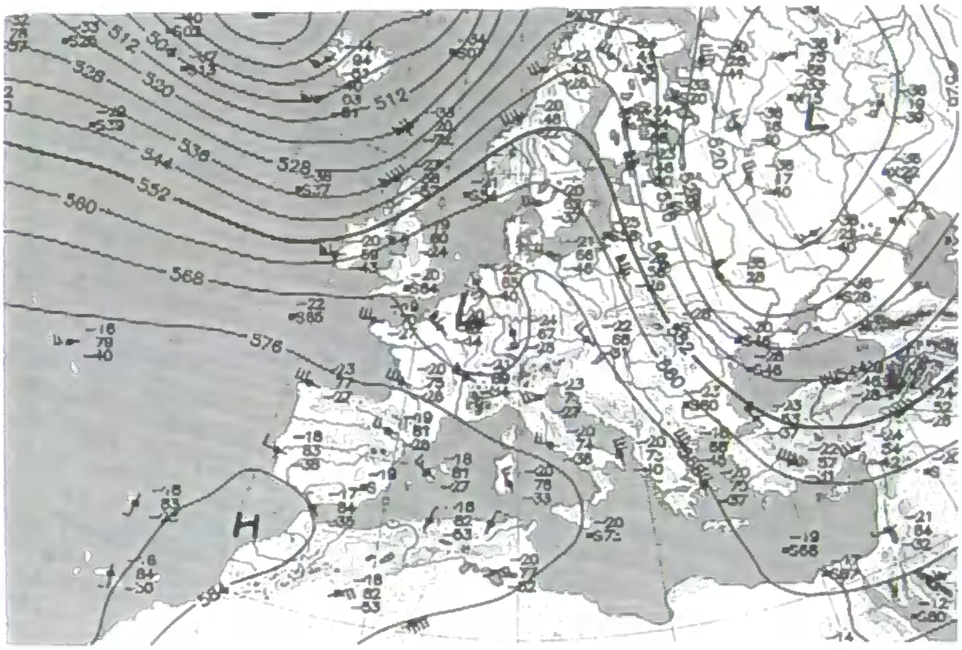

a. 500mb level

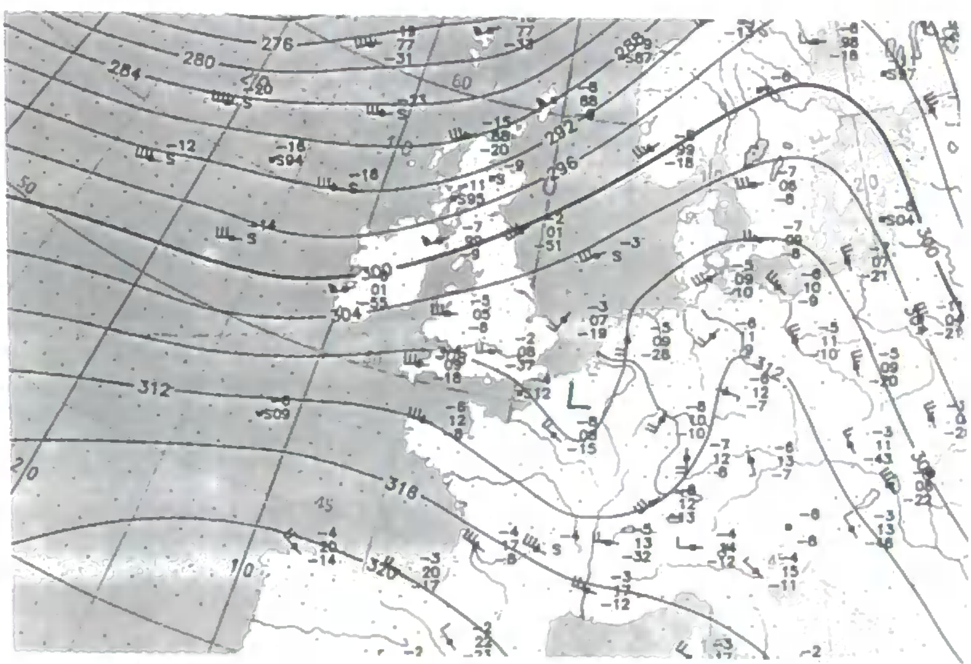

b. 700 mb level

Figure 7.3.3.1 European Meteorological Bulletin geopotential height analyses from 1200 UTC March 5th 1997

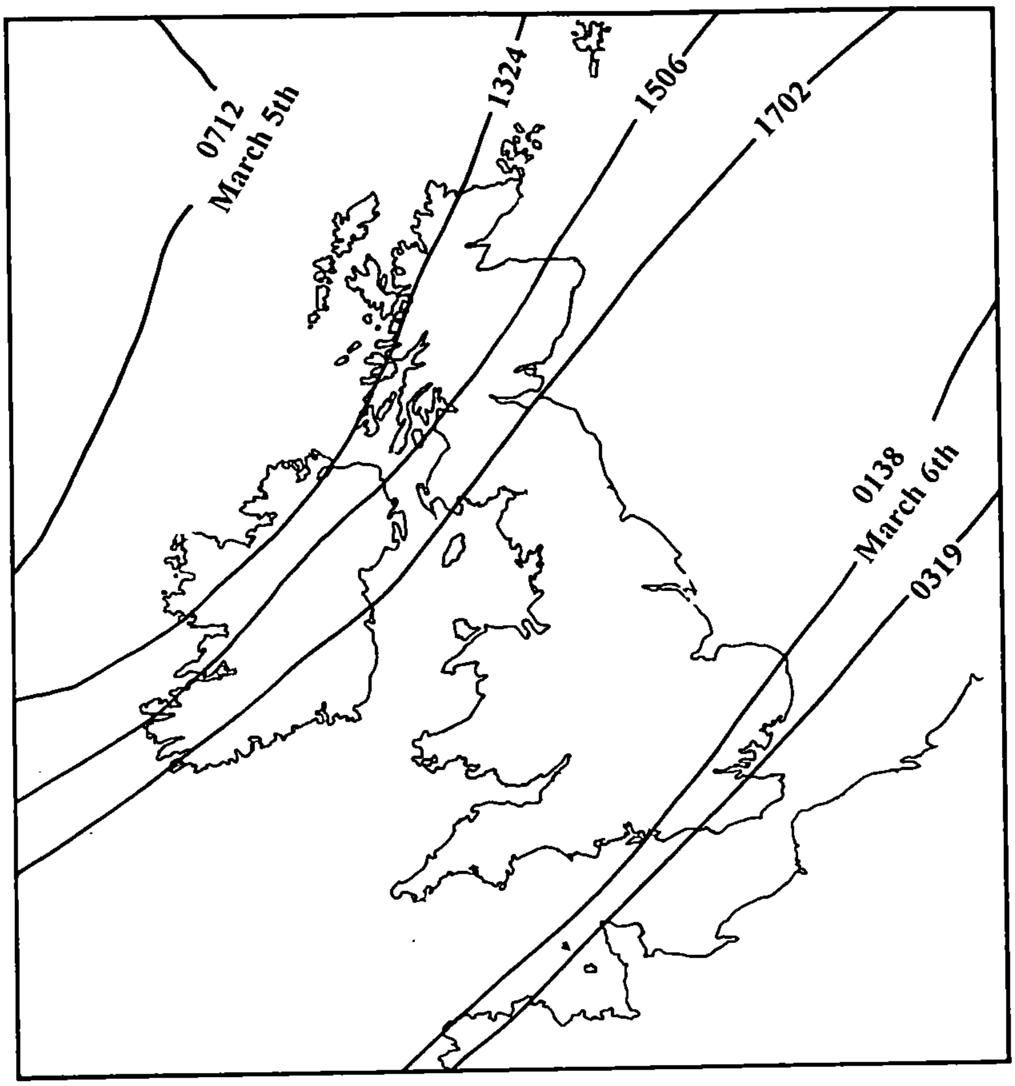

Figure 7.3.3.2 Back edge of southeastward moving cloud during March 5th and 6th 1997 at times shown.

(All times in UTC)

Table 7.3.3.1 Flow at 500 mb at 1200 UTC March 5th 1997

	Calculated geostrophic flow	Flow observed by ascent
Flow at 500 mb level		
West coast of Eire Scotland	42 ms^{-1} WSW 45 ms^{-1} SW	30 ms^{-1} WSW (Shannon) 45 ms^{-1} SW (Stornoway)
Flow at 700 mb level		
50° to 55° N along 10° W Devon 55° to 60° N along 8° W (location of cloud edge at 1200 UTC)	25 ms^{-1} WSW 15 ms^{-1} W 21 ms^{-1} SW	25 ms^{-1} SW (Shannon) 15 ms^{-1} W (St Mawgan) 15 ms^{-1} SW (Stornoway)

Table 7.3.3.2 Displacement of back edge of cold front cloud during March 5th/6th 1997

	Total displacement	Speed of cloud back edge
0712 UTC to 1324 UTC		
(cloud west of Scotland)	430 km from west	19.3 ms^{-1}
(cloud west of N. Ireland)	240 km from northwest	10.8 ms^{-1}
1324 UTC to 1702 UTC		
(over Scotland)	245 km from west	18.8 ms^{-1}
(over Eire)	125 km from northwest	9.7 ms^{-1}
1506 UTC to 0138 UTC		
(over England)	550 km from northwest	14.5 ms^{-1}
0138 UTC to 0319 UTC		
(over English Channel)	36 km from northwest	5.9 ms^{-1}

Flow speed at 700mb was closer in magnitude to cloud movement than at 500mb, but it was not possible to detect any change in speed at the front's back edge. Consequently it would be unwise to use upper level geopotential height charts to determine increases or decreases in cloud speed at the back edge of a front. Flow **direction** at 500mb and 700mb *did* however veer behind the front. Thus there is a good indicator in upper level charts of geopotential height of a cold front's back edge position, though the precision of such an indicator is too small to be of use in pinpointing the location of the associated cloud to within 100 km.

Air temperature prediction

Since the clearing front will introduce polar air with mostly clear skies, the accuracy of an air temperature forecast is obviously dependent on the predicted cloud. Table 7.3.3.3 of observed air temperature decrease rate averaged over six hour periods from March 5/6th gives a good guide to what would hopefully happen if the scenario was to be reoccur.

Table 7.3.3.3 Air temperature decrease rates averaged over six hour periods from 1200 UTC March 5th to 1200 UTC March 6th.

Periods (UTC)	Air temperature decrease rate between periods in first column (deg.C per 6 hours)		
	Halwell Camp	Waldon Bridge	Bratton Down
1200-1800 and 1800-0000	1.0	3.6	2.9
1800-0000 & 0000-0600	3.3	3.9	1.9
0000-0600 and 0600-1200	0.8	-0.2 (suspected cloud between 0200 and 0500 UTC March 6th)	-0.2 (suspected cloud between 0000 and 0200 UTC March 6th)

Note:-

1200-1800 UTC: March 5th

1800-0000 UTC: March 5th

0000-0600 UTC: March 6th

0600-1200 UTC: March 6th

In an operational situation the average 1200-1800 UTC air temperature would have to be estimated. Average air temperature predictions for the periods 1800 to 0000, 0000 to 0600 and 0600 to 1200 UTC can be calculated using the set of rules in Table 7.3.3.4:-

Table 7.3.3.4 Algorithm for estimating air temperature for scenario of cloud clearance from west or northwest.

	Algorithm to estimate air temperature
Between 1800 and 0800 UTC after frontal cloud clearance	If isolated cloud is expected between 0000 and 0300, then air temperature fall is expected to be 2.0 deg. C between 1800-0000 and 0000-0600 UTC periods If isolated cloud is expected between 0300 and 0600, then air temperature is expected to become constant If clear sky is expected, then air temperature is expected to fall by 3.0 deg. C between 1800-0000 and 0000-0600 UTC period
After 0800 UTC	Solar radiation will increase air temperature, though predictions for this far ahead ('T+18' to 'T+24') are not likely to be sufficiently accurate

If surface flow is likely to be faster than 3 ms^{-1} (see below), mixing will suppress air cooling. In this situation, from the algorithm of Table 7.3.3.4, Roadsurf will yield a cold bias in road surface temperature prediction. It is advisable to halve all expected air temperature changes if this is the case, though only if confidence in the wind forecast is high.

Wind prediction

Table 7.3.3.5 shows the wind speed used by Roadsurf during March 5th/6th. The values were estimated using calculated geostrophic flow from the 1200 March 5th and 0000 UTC March 6th surface pressure analyses and observations from Culdrose. Unfortunately wind data from individual road weather stations was not available. This was not necessarily a hindrance however since it was clear from the surface pressure charts that wind speeds were no more than 3.0 ms^{-1}.

In an algorithm, the winds of Table 7.3.3.5 can be used if the pressure gradient during a future occurrence if this scenario is not likely to increase with the passing front over Devon. The slack pressure gradient during March 5th/6th was due to the close proximity of the high pressure.

The wind direction must also be westerly, north-westerly or northerly between 1200 and 0600 UTC.

Table 7.3.3.5 Surface wind speed, averaged over six hour periods used by Roadsurf from March 5th/6th 1997.

Period (UTC)	Wind speed (ms^{-1}) and direction
1200-1800 March 5th	3.0 westerly
1800-0000 March 5th	3.0 westerly
0000-0600 March 6th	2.0 northerly
0600-1200 March 6th	2.0 variable

7.3.4 Algorithm summary

For the following scenario, the process below should be used to produce reliable forecasts of the likelihood of icy conditions for a road surface in Devon.

Scenario:-

Cold front passing over Devon before 0000 UTC in winter, introducing mostly clear skies with possible isolated cloud.

Algorithm:-

1. Ascertain movement of back edge of frontal cloud using sequential NOAA satellite images for six hour period before midday (start of forecast).

2. Using **1**, predict time of cloud clearance over Devon. A maximum error of 3 hours is permissible. Particular attention must be made to potential cloud edge thinning and acceleration. Cloud at the back edge will be at a higher level than the rest of the front due to frontal slope, thus forecast charts of upper level geostrophic flow will give a guide to the likely speed of the cloud's back edge as it passes over Devon. Such charts are readily available over the Internet (see Appendix 4) and indicate accelerating/decelerating flow, which will affect cloud at that level.

3. Assume clear skies after initial cloud clearance unless there is strong evidence of cumulus developing within the polar air stream behind the cold front. It is not possible to predict times of isolated cloud which might occur over Devon.

4. Estimate wind for forecast period by comparing latest (or predicted) surface pressure analysis with those of March 5th and 6th 1997 (Figures 7.3.1.2a and b). If contour spacings are similar and a low/high pressure dipole exists between Iceland and Spain, the wind speeds of Table 7.3.3.5 can be used. Alternatively, forecasts of surface geostrophic flow can be obtained from Internet web pages mentioned in Appendix 4, using the geostrophic Equations **1** and **2** in Chapter 6. Reducing these speeds by 30% to compensate for average surface roughness will give surface wind forecasts.

5. Estimate air temperature for 1200 to 1800 UTC and apply rules of Table 7.3.3.4 to obtain air temperatures for after 1800 UTC. Halve all air temperature decreases if wind is likely to be faster than 3 ms^{-1}.

6. Depression of the wet bulb temperature (DWBs) will increase after cold front clearance, so use rules in Table 7.3.4.1.

7. Run Roadsurf using the inputs obtained from the previous 6 steps, and note computed surface freezing predictions and minimum surface temperature.

8. Re-run Roadsurf during forecast period, using updated inputs if front clearance is suspected to occur earlier than originally envisaged.

Table 7.3.4.1 Suggested predictions of the wet bulb depression for a winter scenario of a cold front clearance. (Taken from observations during March 5th and 6th 1997.)

Cloud state	Depression of the wet bulb (DWB) / deg.C
Within cold front (overcast cloud)	0.1
After cloud clearance (clear skies)	0.5
Within isolated cloud (less than 5 oktas)	0.3
After 0600 UTC with clear skies	1.0

7.4 Summaries of the case studies in this chapter

Nov. 18/19th 1996 *Frontal cloud from west of Eire and Sole moving towards England and Wales*

- Instability in Roadsurf code occurred whenever wind speeds increased to over 7 ms^{-1}. The instability resulted from oscillations in the model parameterisation of the sensible heat flux. Changes to the algorithm developed from Scenario 3 of Chapter 6 were required to handle this problem.

- Cloud movement slowed as it approached England which allowed surface cooling in Devon to unexpectedly continue. This was due to a weak ridge of high pressure over Southwest England.

- Roadsurf furthermore underestimated the cooling before cloud increase, due to stronger wind speed inputs used by the model than those observed at 2m. The ridge of high pressure over Southwest England was responsible.

March 5/6th 1997 *Cold front passing over Devon prior to 0000 UTC, introducing mostly clear skies with isolated cloud.*

- Roadsurf predicted minimum surface temperature well for this situation unless temporary isolated cloud occurred within 3 hours of dawn. Temporary surface warming caused by mixing or warm air advection associated with individual cloud was not accounted for by Roadsurf. Individual cloud formation which may occur after a front has cleared can not be predicted. It is safer to assume clear skies will predominate in this case.

- Accurate timing of predicted cloud clearance and likely air temperature change is essential for Roadsurf to perform sufficiently well.

Chapter 8 Discussions

Discussions relating to the cloud tracking in Chapter 3

Despite the apparent simplicity of the cloud track exercise carried out in Chapter 3, assumptions had to be made which are not always valid. Using analyses of surface pressure and geopotential height to determine wind flow increases errors due to inaccuracies in contour drawing. Furthermore, an ageostrophic component of wind flow is usually present, especially at the surface. This component was assumed small (<2 ms^{-1}) in the two case studies covered in Chapter 3 since the Rossby number, dependent on curvature was estimated to be less than 0.1 over Devon. There is a likelihood that during some occasions, the isobars in the surface pressure analyses were excessively smoothed to an extent that Rossby numbers derived using isobar curvature were smaller in magnitude than their true values. A larger Rossby number is a consequence of an increased pressure gradient force which increases the ageostrophic component of flow. This partly explains differences between measured flow and calculated flow using the geostrophic equation. Surface flow is also impeded to a varying extent by topography and surface roughness.

Cloud tracked in Chapter 3 was estimated to be at one of three levels:- low, medium and high, corresponding to 850, 500 and 200 mb to reduce errors which easily arise from tracking multi-layered cloud. Though this had a positive aspect, it is still apparent that there were wide margins of error in cloud track measurements. Ascent in unstable air lifts saturated air from low levels which condenses into clouds at medium levels which gives an illusion to the satellite viewer of movement of cloud which was previously already at medium levels. This is relevant since ascent is predominant in frontal regions, where cloud tracking appears easiest to undertake. Conversely, descending unsaturated air from upper to medium levels may evaporate medium level cloud, which would also give false representations of medium level cloud movement whenever the descent rate is variable. Hence tracking of vertical velocity peaks with time might be expected to yield results showing frontal displacement.

The choice of using Meteosat rather than NOAA imagery can be difficult to make. Meteosat images were used in the Chapter 3 studies because NOAA imagery was unavailable. Meteosat output usually has the benefit of hourly images which is much more regular than with NOAA satellites. This fact reduces errors and facilitates improved cloud tracking, but is not essential. Resolution of NOAA images is much better than with Meteosat. Furthermore, satellite viewer obliquity to the Earth's surface is less of a problem with NOAA orbiters which reduces errors arising from tracking cloud relative to fixed surface markers such as coastlines. This was borne in mind and it was decided that NOAA images were more suitable for most types of cloud tracking, particularly of low level cloud. Meteosat images are useful for extra information and especially for occasions when intervals between NOAA passes were over 3 hours.

Discussions relating to the sensitivity tests in Chapter 5

Although Roadsurf produced invaluable information about the consequences of erroneous cloud forecasts, there were flaws in the model predictions due to the simplicity of certain inputs and parameterisations. Fixed air temperatures and wind speed throughout all sensitivity tests could well have moderated predictions of surface temperature compared to observations for tests of increasing cloud, It was felt necessary to keep the air temperatures and wind speed factors parameters fixed to research the effects of cloud increase solely as a result of varying fractions of thermal radiation lost from the surface to space and solar radiation reaching the surface. Of course in real life, air temperature and wind speed usually varies with time, especially during cloud cover change.

Roadsurf was not developed for a specific site, hence there are some sites where the modelling of cloud effects on surface temperature would yield results dissimilar to those obtained in real life. The surface and ground composition in the model was of a standard road of rolled asphalt and concrete. Extra tests using a model system consisting entirely of asphalt and then entirely of concrete showed differences of <0.5 deg. C in minimum predicted surface temperature under clear skies.

Discussions relating to the case studies in Chapters 6 and 7

For the case studies of Chapters 6 and 7, it was necessary to determine which dates would be most suitable for the case studies to be undertaken. The two main determining factors of whether to pursue a case study for a particular date were:-

1) Likelihood of surface freezing:- If surface freezing was not likely to occur, the date was rejected.

2) Likelihood of cloud cover change:- If cloud cover was not likely to change during the 24 hours of a case study, the date was rejected.

A further determining factor can arise due to data availability though this was generally not a problem during the 1995/96 and 1996/97 winters. Absence of data availability in real time during the 1996/97 winter was a problem since it was originally envisaged to undertake the case studies of this winter as they occurred and not retrospectively. Even though all case studies were carried out retrospectively, large intervals between successive NOAA images reduced the accuracy of cloud track measurements for certain dates.

As well as determining which dates were best for the case studies, it was also necessary to decide which sites would be suitable for such studies. With frontal cloud, it was best to use data from sites spread across Devon to clearly detect changes in surface and air temperature associated with changes in cloud cover. This was especially taken into consideration for the Feb. 4/5th 1996, Feb. 6/7th 1996 and March 5/6th 1997 case studies.

Stations equipped to measure 'depth' temperatures below the surface were considered to be good study locations since Roadsurf requires depth observations to function accurately. There were six suitably equipped stations:- Bratton Down, Sourton Cross, Cross Farm, Roborough, Haldon Hill and Stopgate Cross. A further reason for favouring these sites for use in the studies was due to analyses of mesoscale model data which was only available for these stations.

Inconsistencies in Roadsurf's ability to predict surface temperature were clear throughout the case studies in Chapters 6 and 7. As well as effects of cloud on surface temperature prediction, several other factors presented problems with modelling temperatures in Devon. Roadsurf was unable to accurately handle warm air advection associated with cloud which was more influential at coastal sites than inland. However, the strength of the warm air advection was considerably dependent on wind direction and time of winter. The coastal influence on warm air advection is usually more prevalent during November when the sea surface temperature around Devon is 11 to 12 ° C than during late February when the sea surface is 3 to 4 deg. C cooler. Coastal influence on road surface temperature is also highly dependent on wind speed. During calm conditions, the effect on surface temperature from advection of warm air from above the sea during mid-winter is negligible whereas it can become a significant factor with stronger winds. Furthermore, close coastal proximity increases low level humidity during onshore winds which presents problems to Roadsurf's parameterization of latent energy. As mentioned in Chapter 1, topography and exposure are responsible for wide variations of surface temperature across Devon. Although Roadsurf partly accounts for effects from these two influences by using air temperature and wind speed inputs, their effects still introduced inaccuracies to Roadsurf predictions in the case studies of Chapters 6 and 7. Differences between physical processes at sites of varying topography are partly responsible for these inaccuracies. For example, cold air drainage at Culver Bottom at the bottom of a deep and narrow valley is possible under partly clear skies allowing road surface cooling. But Whiddon Down, less than 20 km north-west of Culver Bottom would have experienced less cold conditions as a result of its open hilltop location where low level atmospheric mixing and an absence of cold air drainage would have reduced surface cooling.

Roadsurf is unfortunately unable to predict temperature change due to cold air drainage, hence if a warm bias is exhibited in surface temperature predictions, for example at Whiddon Down, the model would perform better at Culver Bottom. McLean (1994) separated all Devon road weather stations into groups based on range of temperature which frequently occurs at each station. 'Extreme' stations included those where cold air drainage is most prevalent during clear skies. During these conditions, open stations usually experience warmer conditions. The opposite occurs during cloudy skies when so called 'damped' stations are coolest, for example Bratton Down, Stopgate Cross and Sourton Cross; all three of which are exposed and have hilltop locations. This is especially likely with cold air advection under cloud whenever easterly or northerly winds occur during the winter. Exposure is responsible for the surface cooling whereas valley sites are sheltered during these conditions and hence milder. Locations on leeward sides of hills are also sheltered from cold air advection and hence slightly less cold. Thus Roadsurf would undoubtedly benefit from additional algorithms dependent on topography and exposure. Topography can furthermore cause localised cloud as a result of convection and forced lifting of saturated air. Convective cloud however is less likely during hours of darkness than daylight.

Apart from the natural effects on surface temperature already discussed, man made factors are also influential on road surface temperature prediction. The largest of these is due to traffic. Friction between car tyres and tarmac generates heat which can increase RST by as much a 2 deg. C on busy roads. Simultaneously, exhaust fumes warm the 3m air temperature. These factors were completely ignored by Roadsurf during all case studies of Chapters 6 and 7 since traffic during the most important forecast window (overnight) was assumed to be light. Large vehicles such as lorries and buses cause mixing of the constant flux layer of the atmosphere immediately above the surface, advecting air from the verge, neighbouring lanes and fields. This factor was also ignored since it was assumed not to occur continuously during hours of darkness.

Bridges above highways suppress surface cooling by reducing thermal emission of heat to space to such an extent, that road surfaces can be as much as 2 deg. C warmer underneath parapets. Roadsurf can not predict accurate road surface temperatures for these locations. There is little need to modify the model to account for this since the bridges only form a very small part of the road network. Care of course should be taken to ensure that road weather station instruments are not effected by nearby bridges.

Chapter 9 Conclusions and recommendations

This research investigated two diverse subject areas of meteorology:- cloud tracking and energy balance modelling, which were later combined to construct algorithms to enable accurate cloud dependent forecasts of road surface temperature. This should enable Devon County Council to improve their winter road maintenance plan, making savings when salting and gritting are not required and improving their effectiveness when ice is likely. The surrounding environment should benefit as well from less over-salting.

9.1 Conclusions from the cloud tracking

Positive results of cloud tracking using the plane sailing method were observed from the case studies in Chapter 3 relating cloud movement to geostrophic flow at 500 and 200 mb. Occasional difficulties in determining suitable cloud tracers occurred, especially with short lived features. It is thus recommended that all cloud tracers have a lifetime of at least three hours.

It was concluded using radiosonde ascents in the February 9th 1994 case study, that infrared satellite imagery occasionally over emphasised the thickness of low level cloud. Furthermore it appeared that conventional observations of cloud by humans at surface level were still the most accurate method of determining the fraction of sky covered by cloud. The February 9th 1994 case study also showed that thick cloud *can* exist in stable air, though this is usually unlikely.

Displacement of cloud north of Spain on February 16th highlighted a potential cloud tracking problem of false illusion of cloud movement caused by cloud which dispersed and reformed nearby. This same case study also concluded that the brightness of cloud pixels in infrared satellite images was related linearly to cloud top height, though the relationship was weak and difficult to detect unless deliberately large ranges of image brightness were compared to cloud top height.

9.2 Conclusions from the Roadsurf sensitivity tests

The transformation from Surftemp (developed by Outcalt, 1971) into Roadsurf was successful. New time differencing mathematical methods of prediction in Roadsurf performed better and accurately forecast timelags similar to those in real-life. Detailed conclusions from the sensitivity tests performed using Roadsurf in Chapter 5 have been placed at the end of that chapter (section 5.3). The timing of changes in cloud cover was found to be highly influential on predicted frost onset time. On some occasions, timing was even more influential than duration of constant cloud amounts.

9.3 Conclusions from 1995/96 winter (Chapter 6) case studies

It was concluded from Chapter 6, that acceptability of expected Roadsurf forecast was dependent on predicted rate of surface temperature change. The most accurate forecasts are predicted using a mixture of conventional human and modelling operations.

November 18/19th 1995

Siting of station sensors affected change in air and surface temperature. For instance, at Kingsteignton, increases of recorded air and road surface temperature due to advection associated with cloud increase were much smaller than at other road weather stations in Devon due to the sensor's location on a bridge.

An algorithm of simple adjustments to Roadsurf surface temperature output, constructed from this case study required cloud dependent rules, even though cloud parameterisation had already played a part in the original Roadsurf predictions. This was because Roadsurf initially exhibited a warm bias. Observations from 5 stations showed that decreasing rate of cloud corresponded more with decreasing rate of air rather than surface temperature. Warm air advection from Cornwall also influenced observations in Devon.

The UK Meteorological Office mesoscale model air temperature predictions for six sites across Devon were poor due to inaccurate mesoscale model cloud forecasts. The model failed to produce even realistic estimates of minimum air temperature except at Bratton

Down. Failure to take micro-climatic effects into account was a second reason for the model's bad performance.

January 23/24th 1996

This case study highlighted consequences of poor evaluation of satellite imagery particularly strongly. A low, but extensive cloud sheet of similar height and thickness covered much of Britain which appeared at first glance to be clear sky in the infrared images, especially since additional bands of brighter, medium level cloud were occasionally present. Evaluating this low cloud as clear sky produced bad surface freezing onset time forecasts with 5 hour errors.

Examination of surface wetness effects on predictions concluded that with a situation of a dry road which became wet in the middle of the night, a 'dry' parameterization of the surface for the **entire** night produced closer surface temperature predictions to observations than if the road was classified as 'wet'. Roadsurf would have exhibited a strong cold bias if the road was deemed as being wet due to evaporation. Furthermore, there was a tendency of Roadsurf to become unstable at Haldon Hill when using a wet parameterization with the other conditions present during Jan. 23rd and 24th 1996.

For the algorithm derived from this case study, a fixed parameterization of 3m air flow was adequate and no special modifications to Roadsurf predictions were required as long as model inputs and cloud forecasts were sufficiently accurate.

February 4/5th 1996

Roadsurf did not react fast enough to cloud increases of more than 2 to 3 oktas per hour during Feb. 4th 1996 which initially gave badly predicted rates of surface temperature change. This was due to Roadsurf using a wind, observed at 1200 UTC and fixed throughout the model run, whereas real life observations showed an increasing wind speed. This caused low level mixing of air which warmed the surface. Re-runs of Roadsurf with variable wind speeds performed better. Parameterising cloud cover slightly differently by reducing KCLOUD, a cloud dependent parameter which controls the thermal radiation also improved predictions but results of further tests deemed this modification to be unnecessary. Utilising mean air temperatures as inputs for Roadsurf instead of spot air temperatures at six hour intervals improved model output still further.

The main requirement for an algorithm applicable during a re-occurrence of the conditions of Feb. 4/5th 1996 is a need to have good estimations of the arrival time of Atlantic depressions and especially of its associated cloud bands. Weak troughs ahead of the major fronts are also highly influential on temperature predictions. Analysis of air and surface temperatures from South East Eire is recommended once cloud has reached that region, as an indication of the magnitude of warming which could later occur over Devon due to cloud increase. From the Feb. 4/5th study, it was concluded that a cloud dependent algorithm is an adequate method of predicting air temperature inputs for Roadsurf. Cloud prediction by forward tracking cloud using cross correlation was considered to be the easiest and quickest method, though possible deceleration of cloud approaching stable air as part of an anticyclone over the North Sea had to be anticipated. Cloud cover prediction by comparing geostrophic flow at upper levels to cloud movement showed signs of success, but is too time consuming for an operational situation.

December 5/6th 1995

During Dec. 5th and 6th, with a scenario of south-westward cloud movement within north-easterly flow, cold air advection occurred which increased errors in general temperature predictions by Roadsurf. It was found necessary to modify air temperature inputs required by Roadsurf for coastal locations to repress surface cooling from continued cold air advection whenever moderate cloud increase occurred.

It was pointed out that even if general Roadsurf performance improved when using altered air temperature inputs, they should not be used if predicted surface freezing onset time is likely to become inaccurate.

February 6/7th 1996

Poor determination of cloud cover and its movement using cross correlation were responsible during Feb. 6th and 7th for unacceptable errors in surface freezing onset times predicted by Roadsurf. Cloud movement ascertained from NOAA images appeared to be westerly at 1200 UTC Feb. 6th at medium levels whereas geostrophic flow at 850 and 500 mb was north-westerly. The wind at these levels eased and at 850 mb, veered to an easterly direction by 1200 UTC Feb. 7th which indicated that cloud movement would have slowed during the morning of Feb. 7th.

A thorough reassessment of cloud cover, using radiosonde ascents revealed an occurrence of two cloud layers, moving relative to each other which complicated Roadsurf cloud parameterization. Predicted surface temperatures from a Roadsurf re-run using the re-assessed cloud were still unacceptable. Attempts to reduce large time lags caused by air temperature inputs which were fixed for six hour periods, using air temperature tendency were successful at Stopgate Cross, Roborough and Haldon Hill. Large lags, it was concluded were an additional cause of poor Roadsurf performance.

The UK Meteorological Office mesoscale model failed to forecast realistic air temperature due to it underestimating cloud cover.

9.4 Conclusions from the 1996/97 winter (Chapter 7) case studies

November 18/19th 1996

It was concluded from tests of the algorithm derived from the Feb. 4/5th 1996 case study of Chapter 6 that Roadsurf becomes unstable when wind speeds of over 7 ms^{-1} occur with the conditions present during Nov. 18th and 19th 1996. Wet road surfaces were partly responsible. Stability was found to be improved by increasing a 'time filter factor' as explained in section 7.2.3 or by using modified wind speeds.

Roadsurf, even when stable, performed poorly in the tests due to later cloud increase than expected since cloud movement slowed as it approached high pressure. Hence, special attention must be paid to influences of anticyclones on cloud movement.

The algorithm for the scenario was modified (section 7.2.4) due to the findings from this case study.

March 5/6th 1997

Accurate forecasting (± 2 hours) of frontal cloud clearance was found to be essential for the scenario of this case study:- that of a cold front clearing Devon and introducing a showery, polar airstream from the west or north-west during a winter's night.

Geostrophic flow was strongly related to direction of cloud movement, whilst veering of wind, shown clearly as kinks in contours in geopotential height analyses of 500 and 700mb, indicated medium and upper level positions of the front. Horizontal acceleration and deceleration of the cloud's back edge could not be determined by studying geostrophic flow velocity during the scenario of March 5/6th 1997.

Roadsurf performed well in this case study. Temporary warmings due to isolated cloud did not adversely reduce the accuracy of Roadsurf minimum predicted surface temperatures unless warmings occurred within 2 hours of dawn. Isolated cloud, suspected of occurring between 0000 and 0600 UTC March 6th could not be detected in NOAA infrared satellite images from the same six hour period due to their short lifetimes. Predicting individual clouds is not possible, especially twelve hours ahead. For road safety reasons, it is wise to assume that after frontal cloud clearance, the sky will be cloud free, even though this would possibly give Roadsurf a cold bias if cloud were to occur.

9.5 Algorithm summary

The following algorithm for the scenarios listed below should give successful forecasts of surface freezing onset time and minimum temperature in an operational environment during winter months for Devon roads.

Decide which scenario type is occurring and use relevant algorithm below:-

i. Cloud forming in situ under settled anticyclonic conditions. **Use Algorithm 1**

ii. Situations in which *all* the following are present:- shallow non-developing low pressure system situated close to or over Devon, blocking anticyclone over Scandinavia, non-precipitating cloud band passing directly above Devon, surface flow less than 20 ms^{-1} without feed of air from anticyclone. **Use Algorithm 2**

iii. Frontal cloud moving eastward from the Atlantic into very cold anticyclonic air over Eastern England. **Use Algorithm 3**

iv. Situations of frontal cloud moving westwards into Devon from Dorset and Somerset before dissipating, giving an illusion of eastward movement whilst cold air advection occurs due to east or north-east surface flow over Devon. **Use Algorithm 4**

v. Frontal cloud moving eastwards over Devon towards anticyclonic cold air over Eastern England. **Use Algorithm 5**

vi. Cold front passing over Devon before 0000 UTC, introducing mostly clear skies with possible isolated cloud. **Use Algorithm 6**

Algorithm 1:-

1. At a chosen station, determine surface flow for start of forecast period using latest possible observation. Under the scenario, changes in wind velocity are likely to be negligible for the 24 hours from start of forecast.

2. Estimate cloud cover for forecast period using satellite imagery from the same period, but 24 hours earlier to ascertain likelihood of formation and dissipation in situ.

3. Estimate air temperature for forecast period split into three hour intervals. A little knowledge of average air temperature fluctuation for this type of scenario is invaluable. Observations from the previous night can be reliable *only* if the scenario and cloud pattern are both expected to remain unchanged.

Text forecasts are widely available from the Internet (see Appendix 4) of expected minimum air temperature from which three hourly approximate predictions can be calculated.

4. Run Roadsurf for the chosen station and apply to the surface temperature predictions, the operations specified in Table 6.1.4.1 for the station nearest to chosen station.

Algorithm 2:-

1. Determine flow at 850 and 500 millibars using 1200 UTC geopotential height analyses and **geostrophic equation 2** (see Page 294).

2. Estimate likely cloud track for the following 18 hours.

3. Ascertain the height of cloud being tracked.

4. From the track prediction, estimate cloud cover prediction in oktas for a chosen site for the duration of forecast window (usually up to 0900 UTC following day) at 3 hourly intervals.

5. Run Roadsurf using initial observations, cloud height and cover prediction as input variables.

6. Plot graph of surface temperature for forecast period and note the expected frost onset time and minimum surface temperature for the chosen site.

Algorithm 3:-

1. Predict mean 2m air temperature for forecast period (1200 UTC onwards) for periods of 6 hours duration, using observations and knowledge of local climate as detailed by McLean, 1994.

2. Estimate height, track and speed of cloud using observations from a period of at least 6 hours preceding start of forecast. Afford special attention to features which will slow cloud movement, for example ridges of high pressure over Southwest England.

3. Produce cloud cover forecast in oktas above a chosen site.

4. Calculate 2m flow from latest surface air pressure analysis using **geostrophic equation 1** (see page 294) . Reduce geostrophic flow by 30% to account for land/air friction or by 20% over water and compare with weather station observations. Estimate surface air flow for duration of forecast period, taking exposure into account. Changes in air flow are greatest during passage of the frontal zone. If air flow is expected to be faster than 5 ms^{-1}, one of the following options must be selected to ensure Roadsurf remains stable:-

a. If 2m air temperature is expected to fall rapidly - for example due to radiative cooling, use modified wind speeds of 4 ms^{-1} maximum.

b. Alternatively, increase the 'time filter factor', tff to 0.3 or 0.4. The higher value is most powerful in preventing instability, but softens rapid changes in surface temperature. Not suitable if rapid air and surface temperature changes are expected.

5. Run Roadsurf using predicted cloud cover, 2m air temperature and chosen wind speeds to produce a graph of surface temperature for the chosen site, from which frost onset time and minimum surface temperature can be obtained.

Algorithm 4:-

1. Ascertain general cloud movement to produce cloud forecast for Devon. Most important period is of cloud cover change.

2. Estimate surface wind for forecast period from charts of surface pressure available over the Internet (see Appendix 4) using **geostrophic equation 1** (see page 294)

3. In the event of east or north-easterly 2m air flow, air temperature input for Roadsurf for the forecast period should be estimated only up to start of cloud build-up for coastal regions. Thereafter, air temperature should be held constant except during clear sky occasions.

4. Run Roadsurf using parameters from stages **1.**,**2.** and **3.** Frost onset times from Roadsurf are likely to be predicted up to an hour late, so modify predicted time to an hour earlier. An earlier than predicted frost onset time is more beneficial in an operational situation, particularly if precipitation is nil.

5. Re-run Roadsurf during forecast period using observations as they become available. Remember to keep air temperature input fixed during cloud increase as in stage **3**.

Algorithm 5:-

1. Estimate cloud for forecast period using plane sailing method applied to cloud movement during the six hours preceding start of forecast period.

2. Predict the wind using **geostrophic equations 1** and **2** (see page 294) from forecast charts of surface pressure and geopotential height from the Internet (see Appendix 4). If forecast charts are not available, charts from observations from the twelve hour period preceding start of forecast period can be used, by continuing any patterns observed whilst bearing in mid, that a front moving eastwards towards a blocking anticyclone over Eastern England will slow. Note possible veering of wind direction with height which would indicate horizontal extent of front, enabling cloud forecast from **1.** to be improved if necessary. Reassessment of cloud cover is advised if predicted flow and cloud movement direction differ.

3. Estimate air temperature trends for six hourly periods of the forecast based on cloud cover and time of evening. Suitable averages, gleaned from hourly observations from the case study are shown in Table 9.5.5.1.

4. Run Roadsurf 2 using the parameters obtained from parts **1. 2.** and **3.** above. Roadsurf 2 frost onset prediction will probably be between 1 and 3 hours late depending on location and cloud cover increase rate.

It is unlikely that predictions of minimum surface temperature need to be modified.

Table 9.5.5.1 Suggested air temperature trends for Devon locations for a scenario of cloud cover increase between 1500 UTC and 2100 UTC with anticyclonic air east of Devon during winter.

Time interval (UTC)	Air temperature trend (deg.C/hr)
1200-1759	+0.13
1800-2359	-0.45
0000-0559	+0.29
0600-1159	-0.17 at locations with less than 4 oktas of cloud, otherwise +0.22

Algorithm 6:-

1. Ascertain movement of back edge of frontal cloud using sequential NOAA satellite images for six hour period before midday (start of forecast).

2. Using **1**, predict time of cloud clearance over Devon. A maximum error of 3 hours is permissible. Particular attention must be made to potential cloud edge thinning and acceleration. Cloud at the back edge will be at a higher level than the rest of the front due to frontal slope, thus forecast charts of upper level geostrophic flow will give a guide to the likely speed of the cloud's back edge as it passes over Devon. Such charts are readily available over the Internet (see Appendix 4) and indicate accelerating/decelerating flow, which will affect cloud at that level.

3. Assume clear skies after initial cloud clearance unless there is strong evidence of cumulus developing within the polar air stream behind the cold front. It is not possible to predict times of isolated cloud which might occur over Devon.

4. Estimate wind for forecast period by comparing latest (or predicted) surface pressure analysis with those of March 5th and 6th 1997 (Figures 7.3.1.2a and b). If contour spacings are similar and a low/high pressure dipole exists between Iceland and Spain, the wind speeds of Table 7.3.3.5 can be used. Alternatively, forecasts of surface geostrophic flow can be obtained from Internet web pages mentioned in Appendix 4, using **geostrophic equations 1** and **2** (see page 294). Reducing these speeds by 30% to compensate for average surface roughness will give surface wind forecasts.

5. Estimate air temperature for 1200 to 1800 UTC and apply rules of Table 7.3.3.4 to obtain air temperatures for after 1800 UTC. Halve all air temperature decreases if wind is likely to be faster than 3 ms^{-1}.

6. Depression of the wet bulb temperature (DWBs) will increase after cold front clearance, so use rules in Table 9.5.6.1

7. Run Roadsurf using the inputs obtained from the previous 6 steps, and note computed surface freezing predictions and minimum surface temperature.

8. Re-run Roadsurf during forecast period, using updated inputs if front clearance is suspected to occur earlier than originally envisaged.

Table 9.5.6.1 Suggested predictions of the wet bulb depression for a winter scenario of a cold front clearance. (Taken from observations during March 5th and 6th 1997.)

Cloud state	Depression of the wet bulb (DWB) / deg.C
Within cold front (overcast cloud)	0.1
After cloud clearance (clear skies)	0.5
Within isolated cloud (less than 5 oktas)	0.3
After 0600 UTC with clear skies	1.0

The following two equations are for use with the algorithms mentioned above.

Geostrophic equation 1

For use with analyses or forecasts of surface pressure only:-

$$\mathbf{V}_g = - \frac{1}{\rho 2\Omega \sin\phi} \frac{\partial p}{\partial \mathbf{n}}$$

where,

$\mathbf{V}_g$= geostrophic wind in vector form (ms^{-1})

$\partial p/\partial \mathbf{n}$= pressure gradient (Pa m^{-1})

ρ= air density at surface (1.25 kg m^{-3})

ϕ= latitude (51° North)

and Ω= angular velocity of the Earth (7.29×10^{-5} rad s^{-1}).

Geostrophic equation 2

For use with geopotential height charts only:-

$$\mathbf{V}_g = - \frac{g}{2\Omega \sin\phi} \frac{\partial z}{\partial \mathbf{n}}$$

where,

$\partial z/\partial \mathbf{n}$= rate of change of height with horizontal distance perpendicular to geopotential height contours

g= acceleration due to gravity (9.8 ms^{-2}).

References

Anderson, R.K. (1969) Exercise in estimating high-level winds. *Satellite Meteorology.* Bureau of Meteorology, Australia. 35-36

Baker, W.E (1993) Wind measurements expected with the laser atmospheric wind sounder. *NOAA/National Meteorological Center technical note.* Washington DC. 5.5 169-174

Barrett, E.C (1974) Climatology from satellites, Meuthen and Co. Ltd. Ch.5 124-130

Bedient, H.A., Collins, W.G. and Dent, G. (1967) An operational tropical analysis system. *Monthly Weather Review*, **95** 942-949

Bogren, J., Gustavsson, T and Lindqvist, S. (1992) A description of a local climatological model used to predict temperature variations along stretches of road. *Meteorological Magazine,* **121** no. 1440 157-164

Browning, K. A and Roberts, N. M (1994) Structure of a frontal cyclone. *Quarterly Journal of the Royal Meteorological Society* **120** pp1535-1557

Carlson, T. N (1991) Mid-latitude weather systems, Allen and Unwin. pp364-375

Cooley, J.W. and Tukey, J.W. (1965) An algorithm for the machine computation of complex Fourier series. *Mathematical Computation* **19** 297-301

Drescher, A. (1988) The tandem satellite concept for cloud spectroscopy and wind derivation. *Weltraumforsch* **12**, 127-128

Eigenwillig, N. and Fischer, H. (1982) Determination of mid-tropospheric wind vectors by tracking pure water vapour structures in METEOSAT water vapour image sequences. *Bulletin of the American Meteorological Society* **63**, no.1, 44-57

Erickson, C.O. (1964) Satellite photographs of convective clouds and their relation to the vertical wind shear. *Monthly Weather Review* **92**, no. 6, 283-296

Herman, L.D. (1990) Validation of cloud motion vectors from AVHRR images. *Paper from the 12th Conference on Weather Analysis and Forecasting*, American Meteorological Society Oct. 2-6 1989 465-468

Herman, L.D (1993) High frequency satellite cloud motion at high latitudes. System design and applications branch, *AMS conference papers* 1993 no14.5 465-468

Hinsman, D.E (1993) WMO Space Activities: Standardization of techniques for cloud track wind observations. *Advanced Space Research* **14**, no. 3, 119-125

Hubert, L.F. and Whitney, L.F. (1971) Wind estimation from geostationary satellite pictures. *Monthly Weather Review* **99**, 665-672

Hubert, L.F. (1979) Wind derivation from geostationary satellites. *WMO Technical note* **166** 33-45

Jacobs, W. and Raatz, W. E (1996) Forecasting road-surface temperatures for different site characteristics. *Meteorological Applications* **3** 243-256

Kastner, M., Fischer, H. and Bolle, H.J. (1979) Wind determination from Nimbus 5 observations in the 6.3μm water vapour band. *Journal of Applied Meteorology* **19**, no. 4 409-417

Leese, J.A., Novak, C.S. and Clark, B.B. (1970) An automated technique for obtaining cloud motion from geosynchronous satellite data using cross correlation. *Journal of Applied Meteorology* **10**, no. 2 118-132

McIntosh, D. H and Thom, A. S (1983) Essentials of Meteorology, Wykeham Publications. London. 84-90

McLean, P. J. (1994) The effect of synoptic scale weather and topography on road surface temperatures in Devon. Unpublished PhD thesis, University of Plymouth.

McLean, P. J. and Wood, N. L. H. (1995) The use of sequential satellite images in forecasting road-surface temperatures. *Meteorological Applications* **2**, 149-157

Menzel, W.P., Smith, W.L. and Stewart, T.R. (1982) Improved cloud motion wind vector and altitude assignment using VAS. *Journal of Applied Meteorology* **22**, 377-385

Merrill, R.T., Menzel, P., Baker, W., Lynch, J. and Legg, E. (1991) A report on the recent demonstration of NOAA's upgraded capability to derive cloud motion satellite winds. *Bulletin of the American Meteorological Society* **72**, no. 3, 372-376

Merritt, E.S. and Rogers, C.W.C. (1965) Meteorological satellite studies of mid-latitude atmospheric circulation. Aracon Geophysics co., *Final report of Contract No. 62306-1584*

Outcalt, S.I (1971) A numerical surface climate simulator. *Geographical Analysis Research Notes*, P. 379

Panofsky, H.A. and Brier, G.W. (1965) Some applications of statistics to meteorology. Pennsylvania State University Press, 224

Panofsky, H. A. (1977) Wind structures in strong winds below 150m. *Wind Engineering* **1**, 91-103

Perry, A. (1997) Regional Climates of the British Isles - South-West England and the Channel Islands (edited by Wheeler, D and Mayes, J.). *Routledge Publishing,* 47-66

Ratsey, S. (1975) The climate at Slapton Ley', *Field Studies,* 4 191-206

Reuter, H. (1951) Forecasting minimum temperatures. *Tellus, Stockholm,* **3** 141-147

Schmetz, J., Holmlund, K., Hoffman, J., Strauss, B., Mason, B., Gaertner, V., Koch, A. and Van de Berg, L. (1992) Operational cloud-motion winds from Meteosat infrared images. *Journal of Applied Meteorology* **32** 1206-1223

Shao, J., Swanson, J. C., Patterson, R., Lister, P. J. and McDonald, A. N. (1997) Variation of winter road surface temperature due to topography and application of Thermal Mapping. *Meteorological Applications* **4** 131-137

Steranka, J., Lewis, J.A. and vincent, V. (1972) Application of Nimbus 4 THIR 6.7μm observations to regional and global moisture and wind field analyses. *Journal of Applied Meteorology* **12** no3, 386-395

Thornes, J. E. (1972) An objective aid for estimating the night minimum temperature of a concrete road surface. *Meteorological Magazine* **101** 13-25

Thornes, J. E. (1983) Retrospective forecasting of road surface temperatures for a site on the M4 motorway, England. *Atmosphere-Road Surface Interaction Study Group. University of Birmingham, England.* Working Paper no. 8

Thornes, J.E. and Shao, J. (1991) Spectral analysis and sensitivity tests for a numerical road surface temperature prediction model. *Meteorological Magazine* **120** no. 1428 117-124

Thornes, J.E. and Shao, J. (1992) Objective method for improving the operational performance of a road ice prediction model using interpolated mesoscale output and a templet for correcting systematic error. *Meteorological Magazine* **121** no. 1442 197-204

Turner, J. and Warren, D.E. (1989) Cloud track winds in the polar regions from sequences of AVHRR images. *International Journal of Remote Sensing* **10** nos. 4 and 5 695-703

Wade, G., Lau, K. S. and Wood, N.L.H. (1992) Clustering applied to cloud wind determination. *International Journal of Remote Sensing* **13** no.16 3135-3155

Wood, N.L.H (1977) An evaluation of the surface energy balance model for giving equilibrium surface temperature. *Working Paper No. 3, Atmosphere-Road Surface Interaction Study Group*, University College, London.

Wood, N.L.H (1978) A model for the receipt of solar radiation at the Earth's surface. *Working Paper No. 4, Atmosphere-Road Surface Interaction Study Group*, University College, London.

Appendix 1

Location of stations mentioned in the European Meteorological Bulletin ascents and redrawn tephigrams of Chapter 3

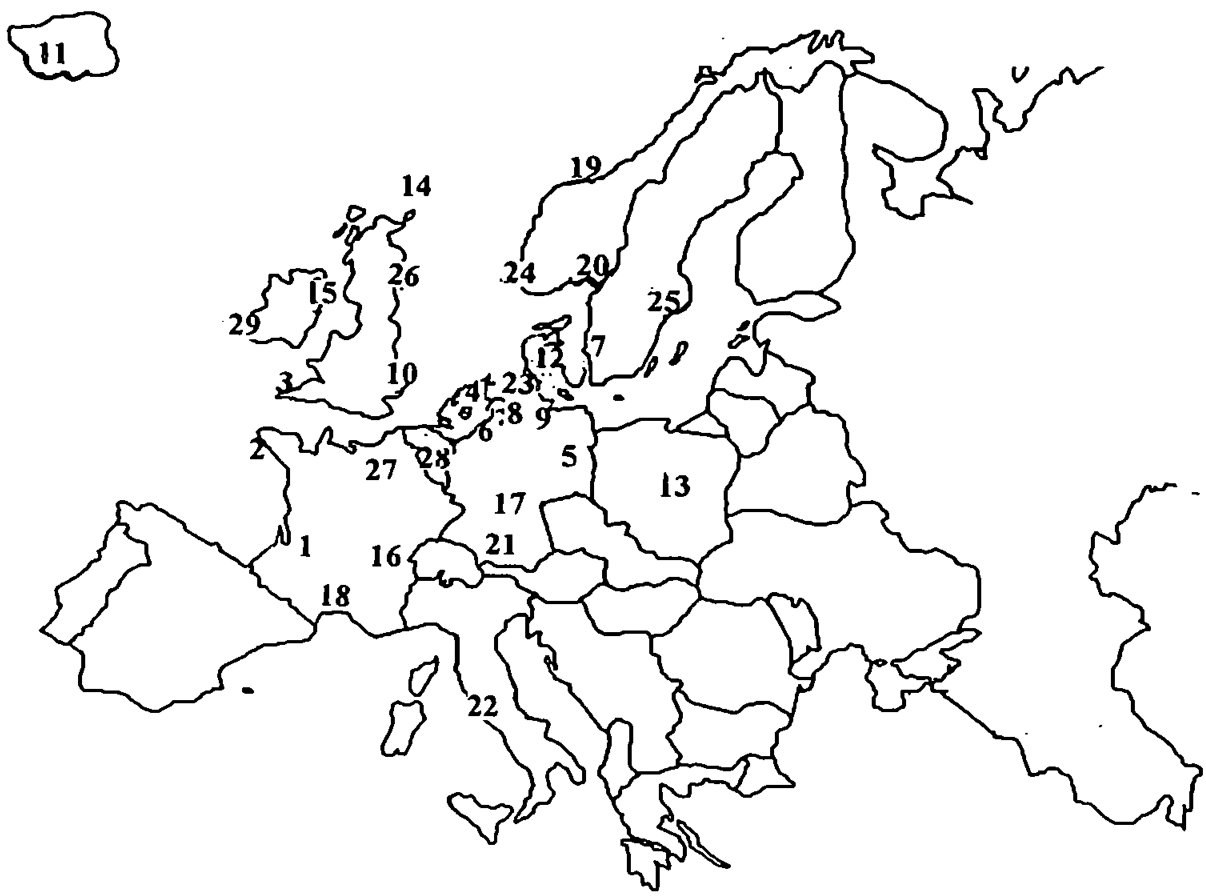

1. Bordeaux
2. Brest
3. Camborne
4. De Bilt
5. Dresden
6. Essen
7. Goteborg
8. Greifswald
9. Hannover
10. Hemsby
11. Keflavik
12. Kobenhavn
13. Legionowo
14. Lerwick
15. Longkesh
16. Lyon
17. Munchen
18. Nimes
19. Orland
20. Oslo
21. Payerne
22. Roma
23. Schleswig
24. Stavanger
25. Stockholm
26. Shanwell
27. Trappes
28. Uccle
29. Valentia

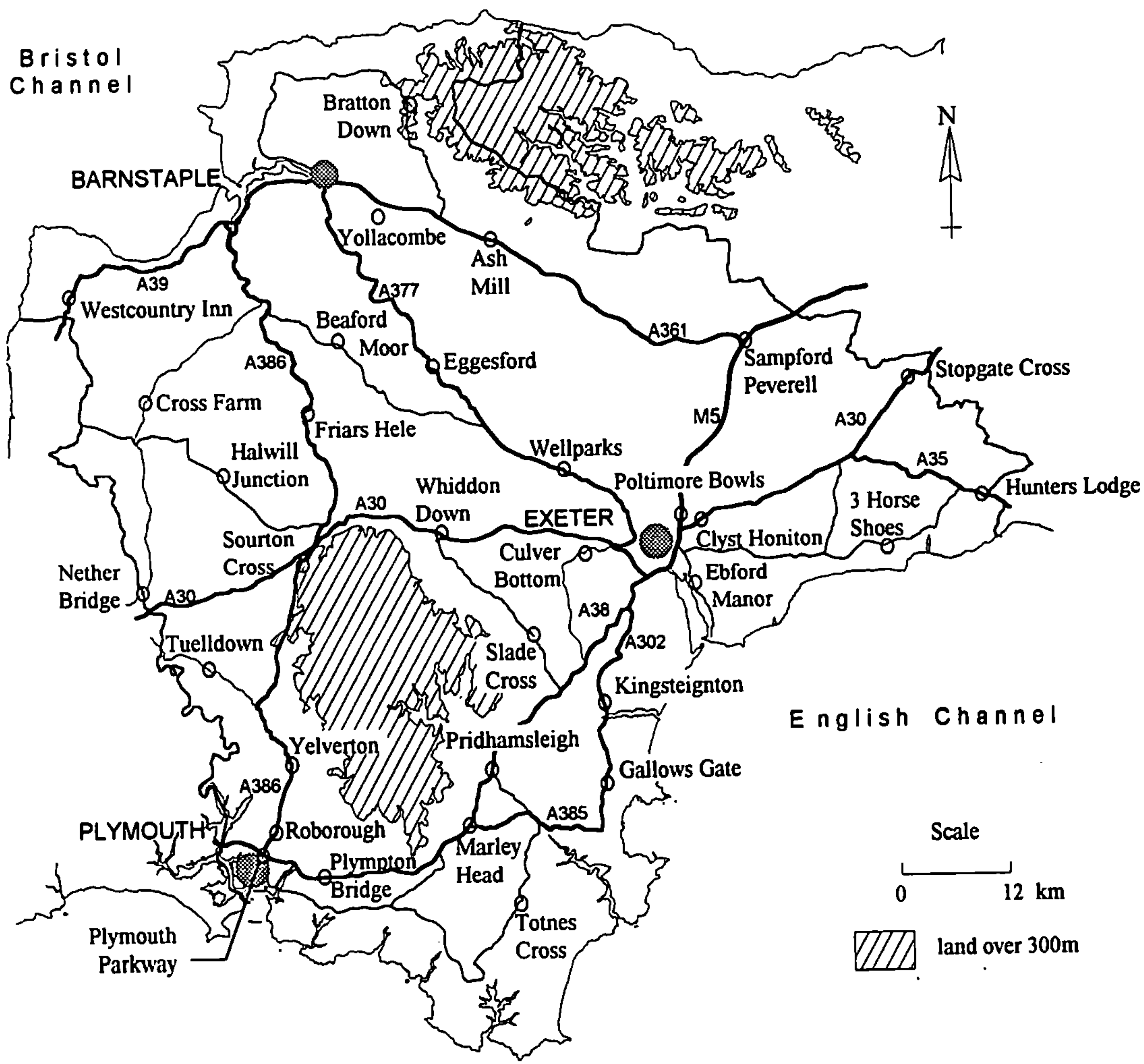

Appendix 2

Automatic road weather station locations in Devon (1995/96 winter)

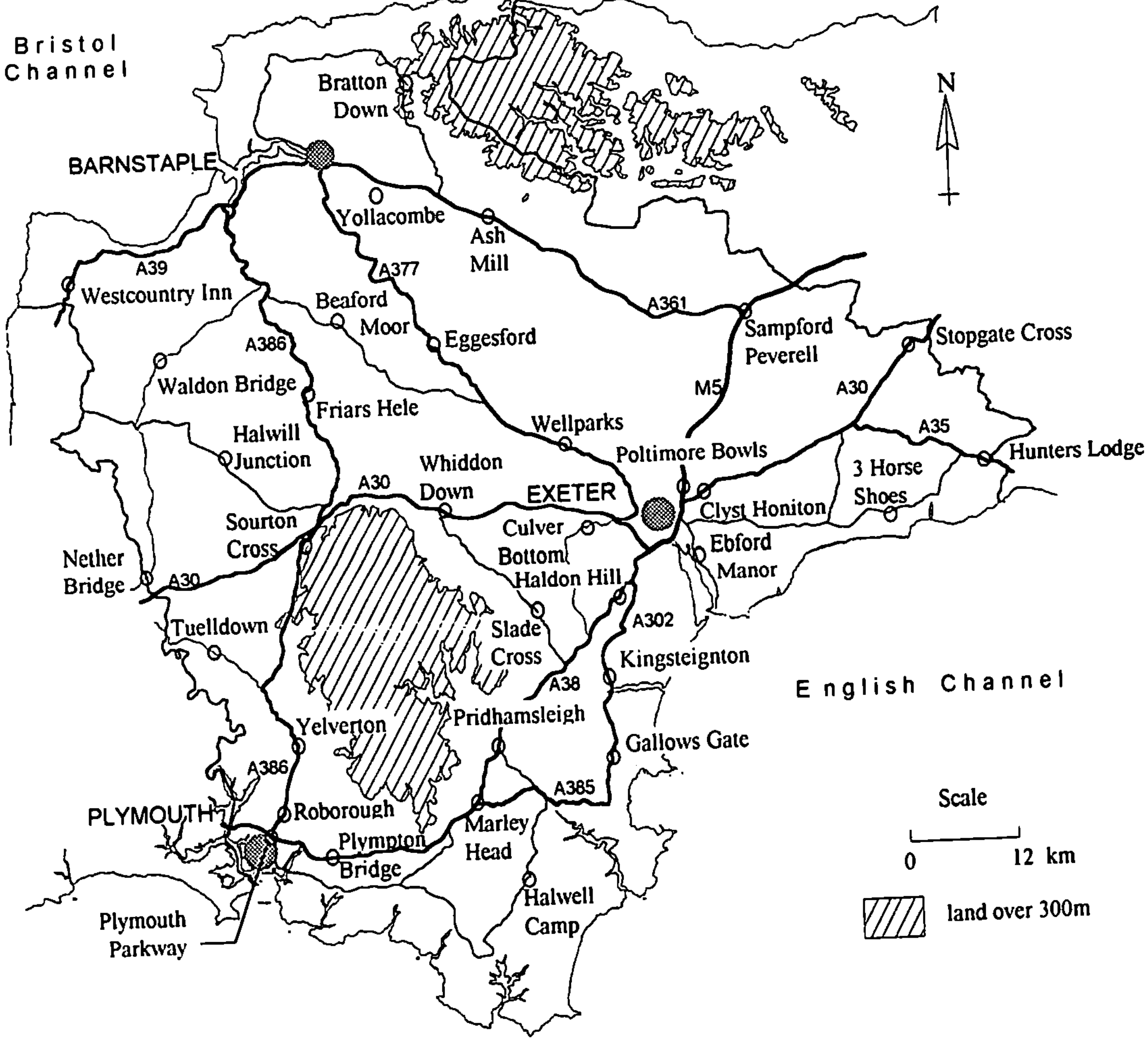

Appendix 3

Automatic road weather station locations in Devon (1996/97 winter)